



Universidade do Estado do Rio de Janeiro

Centro de Tecnologia e Ciências

Faculdade de Geologia

Lucas Eduardo de Abreu Barbosa Araujo

**O Complexo Juiz de Fora no Sul do Rio de Janeiro: Geocronologia,
Petrogênese, Evolução Tectônica e sua relação com o Orógeno Minas-Bahia**

Rio de Janeiro

2020

Lucas Eduardo de Abreu Barbosa Araujo

**O Complexo Juiz de Fora no Sul do Rio de Janeiro: Geocronologia, Petrogênese,
Evolução Tectônica e sua relação com o Orógeno Minas-Bahia**

Dissertação apresentada, como requisito parcial para
obtenção do título de Mestre, ao Programa de Pós-
Graduação em Geociências, da Universidade do
Estado do Rio de Janeiro. Área de concentração:
Geociências.

Orientadora: Prof.^a Dra. Monica da Costa Lavalle Heilbron

Coorientador: Prof. Dr. Wilson Teixeira

Rio de Janeiro

2020

CATALOGAÇÃO NA FONTE
UERJ / REDE SIRIUS / BIBLIOTECA CTC/C

A663

Araujo, Lucas Eduardo de Abreu Barbosa.

O Complexo Juiz de Fora no Sul do Rio de Janeiro: Geocronologia, Petrogênese, Evolução Tectônica e sua relação com o Orógeno Minas-Bahia / Lucas Eduardo de Abreu Barbosa Araujo. – 2020.

160f.: il.

Orientadora: Monica da Costa Lavalle Heilbron.

Coorientador Wilson Teixeira.

Dissertação (Mestrado) – Universidade do Estado do Rio de Janeiro, Faculdade de Geologia.

1. Geocronologia – Teses. 2. Petrologia – Rio de Janeiro (Estado) – Teses. 3. Granulito – Rio de Janeiro (Estado) – Teses. 4. Geologia isotópica – Rio de Janeiro (Estado) – Teses. 5. Geoquímica – Rio de Janeiro (Estado) – Teses. I. Heilbron, Monica. II. Teixeira, Wilson. III. Universidade do Estado do Rio de Janeiro. Faculdade de Geologia. IV. Título.

CDU 550.93:552(815.3)

Bibliotecária responsável: Taciane Ferreira da Silva / CRB-7: 6337

Autorizo, apenas para fins acadêmicos e científicos, a reprodução total ou parcial desta dissertação, desde que citada a fonte.

Assinatura

Data

Lucas Eduardo de Abreu Barbosa Araujo

**O Complexo Juiz de Fora no Sul do Rio de Janeiro: Geocronologia, Petrogênese,
Evolução Tectônica e sua relação com o Orógeno Minas-Bahia**

Dissertação apresentada, como requisito parcial para obtenção do título de Mestre, ao Programa de Pós-Graduação em Geociências, da Universidade do Estado do Rio de Janeiro. Área de concentração: Geociências.

Aprovada em 30 de março de 2020.

Orientadora: Prof.^a Dra. Monica da Costa Lavalle Heilbron

Faculdade de Geologia – UERJ

Coorientador: Prof. Dr. Wilson Teixeira

Universidade de São Paulo

Banca Examinadora:

Prof. Dr. Elton Dantas

Universidade de Brasília

Prof. Dr. Claudio de Morisson Valeriano

Faculdade de Geologia – UERJ

Prof. Dr. Miguel Tupinambá

Faculdade de Geologia – UERJ

Rio de Janeiro

2020

DEDICATÓRIA

Dedico essa dissertação ao meu avô Jorge e ao meu padrasto Edson, ambos falecidos, que foram fundamentais para eu alcançar o ensino superior.

AGRADECIMENTOS

Agradeço primeiramente à toda minha família, em especial a minha mãe Gisele, por nossa relação de cumplicidade de sempre, minha vó Circe, por ter me dado todo o amor e carinho de sempre. Gostaria de agradecer ao meu Pai Henrique, à toda hospedagem e suporte em São Paulo. Gostaria de agradecer à minha namorada Pâmela Richetti, que sempre entendeu e me motivou a dar meu melhor, mesmo que tivesse que escrever na casa dela. Meus amigos de UERJ, graduação, Albert Sabin, cursinho, colégio. muito obrigado a todos vocês!

Gostaria de agradecer aos meus colegas de grupo de pesquisa: Henrique Bruno, Felipe Corrales, João Paulo Giro, Matheus Castro e Gabriel Paravidini, por todo apoio e suporte dos últimos 2 anos. Henrique, pelo suporte geoquímico, Garça e JP pela companhia. Já o Gabriel ficou 24 horas rodando minhas análises em São Paulo. Só amigo faz isso. O Matheus, me ajudou no campo a coletar toneladas de amostras para a datação, que sozinho não conseguiria.

Gostaria de agradecer aos meus amigos de São Paulo, Tiago Valim e Marina Seraine, que me ofereceram hospedagem em meio à análise SHRIMP, e a todos aqueles que me também hospedaram em São Paulo para as matérias que realizei: Baby, Brity e Xena, muito obrigado! Gostaria de agradecer à Marcela Chinen pelo abrigo em Ouro Preto, mesmo ela não estando em casa, para a análise de Hf. A todos meus amigos geológicos de todo Brasil, que sempre vieram com palavras de incentivo em meio a minha ausência e desestímulo.

Venho aqui agradecer também todas as mães dos meus alunos, que sempre entenderam o meu compromisso e muitas vezes foram flexíveis para que eu pudesse me dedicar também nessa dissertação de mestrado.

Quero saudar também todos os técnicos dos laboratórios da UERJ, da USP e da UFOP que me ajudaram muito agilizando lâminas, mounts, análises etc. Quero agradecer à Cida Soares, auxiliar financeira da minha orientadora, que sempre me ajudou nos perrengues financeiros de análises, diárias etc. Gostaria de agradecer ao Bobô, o motorista da UERJ, que sempre colocou a gente na boa no campo.

Gostaria de agradecer à minha orientadora Monica Heilbron, pela inspiração e carisma, ao meu co-orientador Wilson Teixeira, pelas reuniões de alto nível de aprendizado, pelos puxões de orelha que me fizeram melhorar. Muito obrigado a todos os professores que fizeram parte da minha trajetória até aqui. À Diana Ragatky, pela primeira oportunidade no ramo acadêmico.

É que tem mais chão nos meus olhos do que cansaço nas minhas pernas, mais esperança nos meus passos do que tristeza nos meus ombros, mais estrada no meu coração do que medo na minha cabeça.

Cora Coralina

RESUMO

ARAUJO, Lucas Eduardo de Abreu Barbosa. *O Complexo Juiz de Fora no Sul do Rio de Janeiro: Geocronologia, Petrogênese, Evolução Tectônica e sua relação com o Orógeno Minas-Bahia.* 2020. 160f. Dissertação (Mestrado em Geociências) – Faculdade de Geologia, Universidade do Estado do Rio de Janeiro, Rio de Janeiro, 2020.

O Complexo Juiz de Fora (CJF) é uma das unidades do embasamento do Terreno Ocidental da Faixa Ribeira Central, interpretado como parte da borda retrabalhada do paleocontinente São Francisco. O CJF compreende rochas metamorfisadas em fácies granulito com variadas composições geoquímicas, fábricas deformacionais e idades que denotam o seu caráter policíclico. Esse trabalho apresenta novas idades de U-Pb (SHRIMP) e dados isotópicos de Lu-Hf (LA-ICPMS) em zircão, além de dados isotópicos de Sm-Nd e Sr (TIMS) em rocha total e geoquímicos dos ortogranulitos do Complexo Juiz de Fora, localizados no Sul do estado do Rio de Janeiro. O objetivo desse estudo é caracterizar a evolução paleoproterozoica dessa unidade, bem como a fonte dos magmas precursores dos seus protólitos. Seis amostras, selecionadas por suas composições geoquímicas, foram objeto de análises U-Pb e Lu-Hf. O granulito enderbítico toleítico apresenta idade de 2.44 Ga. Três granulitos charnoenderbiticos com assinaturas de TTG e sanukitóides apresentam idades entre 2.20 e 2.18 Ga. Um granulito máfico apresenta idade de 2.13 Ga. Um granulito charnockítico leucocrático possui idade de 1.78 Ga. Bordas metamórficas ao redor de núcleos magmáticos apresentam idades de 600 a 580 Ma, confirmando o metamorfismo Neoproterozoico associado à faixa Ribeira. Grãos de zircão herdado datados de 2.53 a 2.38 Ga foram encontrados em duas amostras. Os resultados isotópicos mostram que o magmatismo sideriano (2.45-2.38 Ga?) é moderadamente juvenil ($\epsilon_{\text{Nd}_{(t)}}$ de -0.1 à +3.2; $\epsilon_{\text{Hf}_{(t)}}$ de -8 a +3). O magmatismo riaciano (2.20-2.18 Ga?) é moderadamente juvenil à evoluído ($\epsilon_{\text{Nd}_{(t)}}$ de -0.6 à -4,8; $\epsilon_{\text{Hf}_{(t)}}$ de -11.7 a +0.2). Ambos episódios magmáticos apresentam fontes juvenis siderianas e crustais arqueanas ($T_{\text{DM Nd}}$: 2.62-2.31 Ga; $T_{\text{DM Hf}}$ 3.25 a 2.49 Ga) com os magmas riacianos apresentando maior contribuição crustal em sua gênese. Há predominância de fontes juvenis ($T_{\text{DM Nd}}$) paleoproterozoicas para o Complexo Juiz de Fora. A contribuição crustal arqueana ocorre em menor escala. A evolução geológica do CJF começa no Sideriano (2.45 – 2.38 Ga?) com a cristalização de dioritos toleíticos em um episódio de arco primitivo. Os granodioritos riacianos representam o segundo estágio heterogêneo do arco Juiz de Fora entre 2.2 e 2.18 Ga. Um terceiro episódio magmático de arco é interpretado pela ocorrência de gabros toleíticos (IAT) com assinatura moderadamente juvenil e contaminação crustal pelos outros dois eventos magmáticos. A colisão dos Complexos Juiz de Fora e Mantiqueira é atribuída por grãos e bordas metamórficas de idade 2035 ± 30 Ma nesse granulito máfico. Após cratonização, um episódio magmático intraplaca datado de 1.78 Ga pode ser correlacionado com a suíte Borrachudos. O metamorfismo em fácies granulito (600-580 Ma) acoplado com a deformação está registrado em quase todas as amostras estudadas. Esse estudo é importante para reconstruções paleogeográficas do Sul do Cráton São Francisco por causa da descoberta de rochas siderianas de arco no CJF e do metamorfismo paleoproterozoico. A orogênese acrecionalária Minas parece ser diacrônica e os episódios magmáticos do Complexo Juiz de Fora e Cinturão Mineiro durante o Sideriano e Riaciano muito similares, com a ocorrência de plútôns TTG e sanukitóides em ambos.

Palavras-chave: Arcos juvenis paleoproterozoicos. Rochas siderianas. Tafrogênese Estateriana.

ABSTRACT

ARAUJO, Lucas Eduardo de Abreu Barbosa. *The Juiz de Fora Complex at Rio de Janeiro: Geochronology, Petrogenesis, Tectonic Evolution and its relationship with Minas-Bahia orogeny.* 2020. 160f. Dissertação (Mestrado em Geociências) – Faculdade de Geologia, Universidade do Estado do Rio de Janeiro, Rio de Janeiro, 2020.

The Juiz de Fora Complex (JFC) is one of the basement units of the Occidental Terrane in the Central Ribeira belt, regarded as part of the reworked border of the São Francisco paleocontinent. The JFC comprises metamorphosed rocks in granulite facies with varied geochemical compositions, deformational fabrics and ages that refer its polycyclic character. This work presents new zircon U-Pb (SHRIMP) ages and Lu-Hf (LA-ICPMS) data, besides whole-rock Sr and Sm-Nd (TIMS) isotopic and elementary data from JFC orthogranulites, located on Southwest Rio de Janeiro state. The main goal of this study is to constrain the Paleoproterozoic Evolution of this unit, as well as, magma sources of its protholiths. Six samples, chosen by their element compositions, were selected for U-Pb and Lu-Hf analysis. The tholeiitic enderbitic granulite present age of ca. 2.44 Ga. Three charno-enderbitic protoliths with TTG and sanukitoid signatures yielded crystallization ages from ca. 2.2 to 2.18 Ga. A mafic granulite has age of ca. 2.13 Ga. One sample of the high-K leucocratic charnockitic group yielded a crystallization age of ca. 1.78 Ga. Metamorphic rims around the magmatic cores present ages from 600 to 580 Ma confirming the Neoproterozoic overprint, related to Ribeira Belt. Inherited zircon crystals from ca. 2.53 to 2.38 Ga were identified in two samples. The isotopic data show that arc related Siderian magmatism (2.45-2.38 Ga?) is juvenile to moderately juvenile ϵ Nd(t) from -0.1 to +3.2; ϵ Hf(t) from -8 to +3). The arc-related Rhyacian magmatism is heterogeneous (ϵ Nd(t) from -0.6 to -4.8; ϵ Hf(t) from -11.7 to +0.2). Both magmatic episodes present juvenile siderian and crustal archean sources (TDM Nd: 2.62 to 2.31 Ga; TDM Hf 3.25 to 2.49 Ga) with rhyacian magmas showing major crustal contribution on its genesis. There is a predominance of Paleoproterozoic juvenile sources (Nd T_{DM}) for Juiz de Fora Complex. The minor Archean crustal contribuition occurs in minor scale. The envisaged geological evolution from JFC starts at Siderian (ca. 2.45-2.38 Ga?) with crystallization of the arc-related tholleitic diorite marking the initial stage of arc development. The granodioritic protholiths represent a heterogeneous stage of Juiz de Fora arc between ca. 2.20 and 2.18 Ga. The third arc-related magmatic episode is constrained by a tholeiitic gabbro (IAT) with moderately juvenile signature and crustal contamination by two previous magmatic events. The collision between Juiz de Fora and Mantiqueira Complexes is attributed by metamorphic rims and grains dated at ca. 2035±30 Ma on this mafic granulite. After the cratonization, a Statherian (1.78 Ga) episode of intra-plate magmatism was detected and correlates to the Borrachudos Suite. During the Brasiliano orogeny, 600-580 Ma granulite facies metamorphism, coupled with deformation, is recorded in the studied samples. This study is important for paleogeographic reconstructions on the southern São Francisco Craton because of the discovery of more Siderian rocks in the JFC and by Paleoproterozoic metamorphism. The Minas Accretionary Orogen seems to be diachronic and the magmatic episodes from Juiz de Fora Complex and Mineiro Belt very similar, with occurrence of TTG and sanukitoid plutons on both units.

Keywords: Juvenile Paleoproterozoic Arcs. Siderian rocks. Statherian Taphrogenesis.

LISTA DE FIGURAS

Figura 1 –	Mapa tectônico regional com destaque para o Complexo Juiz de Fora (verde).....	14
Figura 2 –	Mapa geográfico com o acesso à área de estudo (em vermelho; IBGE, 1976) e as folhas topográficas 1:50.000 IBGE que fazem parte dela.....	17
Figura 3 –	Mapa simplificado do paleocontinente São Francisco com os terrenos de seu embasamento arqueano à paleoproterozoico aflorantes no cráton ou nos seus arredores.....	30
Figura 4 –	Fotos em escala de afloramento (a), de amostra de mão (b) e assinatura ETR do granulito charnockítico leucocrático (amostra RPM-570).....	44
Figura 5 –	Diagrama Wetherill Concordia com cálculo de idade concordante e media ponderada de idades $^{206}\text{Pb}/^{207}\text{Pb}$ para o granulito charnockítico leucocrático (RPM-570) do CJF na área de estudo.....	45
Figura 6 –	Prancha com todos os grãos de zircão da amostra RPM-570 utilizados para cálculo de idade concordante de cristalização e análises Hf pontuais, além de algumas informações petrogenéticas dos sistemas Sm-Nd e Sr-Sr com a idade de cristalização U-Pb obtida para essa amostra.....	45
Figura 7 –	Correlação dos parâmetros petrogenéticos εHf e $T_{\text{DM}} \text{ Hf}$ com a amostra estateriana da área de estudo (RPM-570) com anfibolitos e metariolitos relativos ao magmatismo intraplaca do Bloco Guanhães (1.74 Ga).....	46

LISTA DE ABREVIATURAS E SIGLAS

CJF	Complexo Juiz de Fora
CSF	Cráton São Francisco
UERJ	Universidade do Estado do Rio de Janeiro
UFOP	Universidade Federal de Ouro Preto
USP	Universidade de São Paulo
LAGIR	Laboratório de Geologia Isotópica e Isótopos Radiogênicos
LGPA	Laratório Geológico de Preparação de Amostras

LISTA DE SÍMBOLOS

- % Porcentagem
± Mais ou menos
 ε Épsilon (Parâmetro petrogenético de Nd e Hf)
 ρ Rhô – Erro de correlação geocronológico (sistema U-Pb)

SUMÁRIO

	INTRODUÇÃO	13
1	OBJETIVOS	15
2	APRESENTAÇÃO DA DISSERTAÇÃO E LOCALIZAÇÃO DA ÁREA DE ESTUDO.....	16
2.1	Apresentação da dissertação.....	16
2.2	Localização da área de estudo.....	17
3	MATERIAIS E MÉTODOS.....	19
3.1	Revisão Bibliográfica.....	19
3.2	Bases de dados e mapas integrados.....	19
3.3	Trabalhos de campo.....	20
3.4	Petrografia.....	20
3.5	Preparação das amostras para análises geocronológicas e geoquímicas.....	21
3.5.1	<u>Geocronologia U-Pb.....</u>	21
3.5.2	<u>Geoquímica elementar e isotópica (Sm-Nd e Sr).....</u>	23
3.6	Geoquímica elementar.....	23
3.7	Geocronologia U-Pb (SHRIMP).....	24
3.8	Geoquímica isotópica Sm-Nd e Sr.....	25
3.9	Análises isotópicas Lu-Hf.....	26
3.10	Tratamento e integração de dados.....	27
4	SÍNTESE BIBLIOGRÁFICA E O ESTADO DA ARTE DO COMPLEXO JUIZ DE FORA.....	28
4.1	Evolução do embasamento do Cráton São Francisco.....	28
4.2	A crosta paleoproterozoica da paleoplaca São Francisco.....	29
4.2.1	<u>Orógenos Paleoproterozoicos no Cráton do São Francisco.....</u>	31
4.2.2	<u>Manifestações magmáticas paleoproterozoicas em blocos arqueanos do Cráton São Francisco.....</u>	32
4.2.3	<u>Porções do orógeno paleoproterozoico nas faixas neoproterozóicas.....</u>	33
4.3	Estado da Arte do Complexo Juiz de Fora.....	35
4.3.1	<u>Denominações e correlatos.....</u>	35
4.3.2	<u>Geoquímica Elementar.....</u>	36
4.3.3	<u>Geocronologia isotópica (U-Pb) – Idades de cristalização.....</u>	37

4.3.4	<u>Geoquímica isotópica (Sm-Nd, Lu-Hf)</u>	38
4.3.5	<u>Modelos geotectônicos</u>	38
4.3.6	<u>Evolução tectono-metamórfica</u>	39
5	RESULTADOS	41
5.1	Introdução	41
5.2	Artigo publicado na <i>Brazilian Journal of Geology</i>	41
5.3	Pré-publicação na <i>Precambrian Research</i>	42
5.4	Granito anorogênico no Complexo Juiz de Fora	42
	CONSIDERAÇÕES FINAIS	47
	REFERÊNCIAS	50
	APÊNDICE A – Lithogeochemical and Nd-Sr isotope data of the orthogranulites of the Juiz de Fora complex, SE-Brazil: insights from a hidden Rhyacian Orogen within the Ribeira belt (Artigo Científico).....	68
	APÊNDICE B – Crustal evolution of the Juiz de Fora Complex: A Siderian to Rhyacian juvenile arc and its tectonic implications for Minas-Bahia orogeny and correlations with the Western Central Africa belt (Artigo Científico).....	88
	APÊNDICE C – Tabelas geocronológicas (U-Pb) e geoquímicas isotópicas (Lu-Hf) em zircão do granulito leucocrático representatante do magmatismo intraplaca estateriano.....	159

INTRODUÇÃO

A região de estudo situa-se no Sul do Rio de Janeiro, entre as cidades de Nossa Senhora do Amparo e Valença (RJ). Está inserida no contexto tectônico da Faixa Ribeira (Heilbron *et al.* 2004a), que foi formada pela múltipla colisão de microplacas e arcos no período que se estende desde o Neoproterozoico ao Cambriano (ca. 605 a 510 Ma).

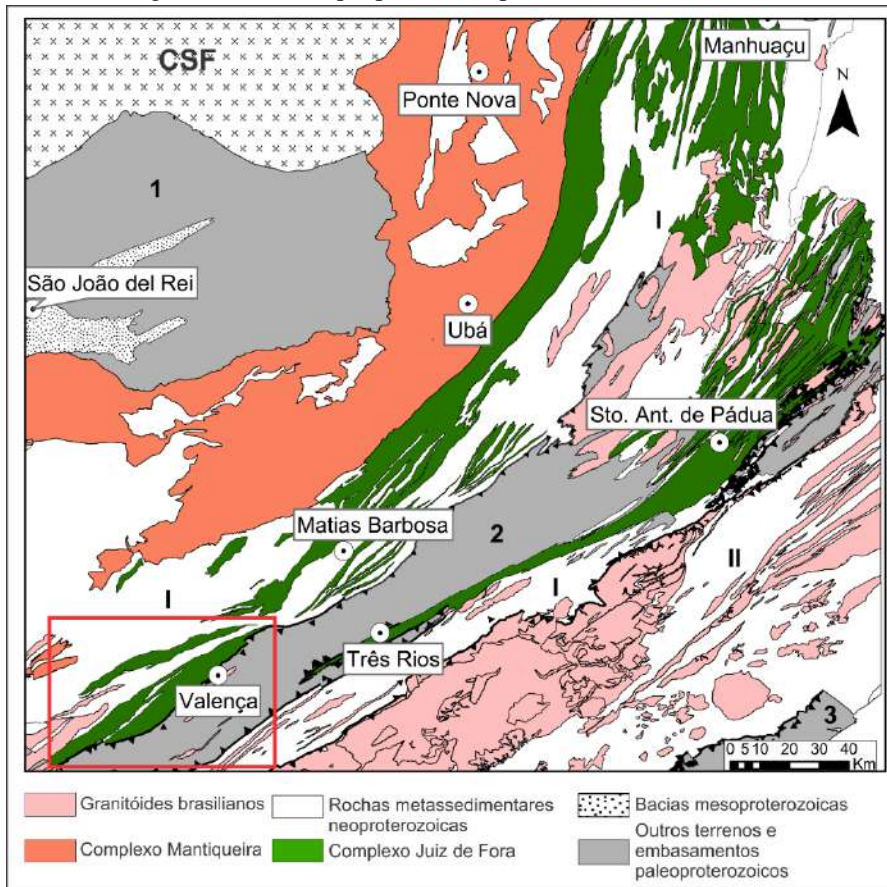
O Complexo Juiz de Fora (CJF - Figura 1), objeto de estudo, é composto de rochas ortoderivadas metamorfisadas em fácies granulito que constituem uma das unidades do embasamento Paleoproterozóico do paleocontinente do São Francisco (Heilbron *et al.* 2004a). A heterogeneidade dessa unidade litoestratigráfica é marcante (Duarte *et al.* 1997; Heilbron *et al.*, 1988), já que nela afloram granitóides cálcio-alcalinos (com diferentes teores de K₂O) com assinaturas de arco e rochas básicas com assinaturas geoquímica para ambientes convergente de arco magmático (IAT), divergente (E-MORB, N-MORB) e intraplaca (WPB). A complexidade de ambientes tectônicos encontrados em uma só unidade cartografada, bem como sua ampla distribuição regional pela Faixa Ribeira, justificam o adensamento de informações geocronológicas na área de estudo, até mesmo para a realização de correlações mais robustas com outros terrenos paleoproterozoicos da Orogênese Minas-Bahia. Ademais, o metamorfismo granulítico atuante na área mascara as relações de contato e tende a homogeneizar as paragêneses metamórficas dos diferentes grupos geoquímicos de ortogranulitos da área, o que dificulta a distinção, principalmente dos litotipos básicos, em campo. As relações de campo, petrografia, geoquímica elementar e isotópica em rocha total (Nd e Sr) podem auxiliar na distinção entre diferentes tipos de rochas dentro do Complexo Juiz de Fora e definição de protólitos desses ortogranulitos. Já a geocronologia U-Pb de alta precisão (SHRIMP) é ferramenta fundamental para a distinção temporal desses protólitos, desde que haja uma sistemática de classificação geoquímica elementar e isotópica prévia para essas rochas.

As unidades de embasamento riaciano adjacentes ao Complexo Juiz de Fora como o Cinturão Mineiro e o Complexo Mantiqueira apresentam metamorfismo de alto grau na transição entre o Riaciano e o Orosiriano (Cutts *et al.* 2018; Silva *et al.* 2002). No Complexo Juiz de Fora, o metamorfismo granulítico está registrado apenas no evento metamórfico neoproterozoico (Orogenia brasiliiana). A técnica U-Pb (SHRIMP), por se tratar de alta resolução espacial, pode, em bordas de zircão ou grãos metamórficos, trazer informações quanto aos eventos metamórficos que as rochas do Complexo Juiz de Fora sofreram.

Além disso, interpretações tectônicas prévias colocam o Complexo Juiz de Fora como um arco intraoceânico no Paleoproterozoico (Heilbron *et al.* 2010, Noce *et al.* 2007). O caráter juvenil ou evoluído do Complexo Juiz de Fora na área de estudo poderá ser testado com as análises geoquímicas isotópicas (Sm-Nd em rocha total e Lu-Hf em zircão). As fontes e a residência crustal do magma precursor desse arco serão investigadas nesse estudo.

A paleogeografia do Complexo Juiz de Fora e sua correlação geológica regional com outros terrenos de embasamento paleoproterozoico nos arredores do Cráton São Francisco, que integram o Cinturão Minas-Bahia (Alkmim & Teixeira, 2017) será discutida nesse estudo. Além disso, correlações entre os registros geológicos da parte brasileira com as contrapartes oeste africanas do Cráton do Congo também serão debatidas nessa dissertação.

Figura 1 - Mapa tectônico regional com destaque para o Complexo Juiz de Fora (verde)



Legenda: Embasamento paleoproterozoico (cinza): 1- Cinturão Mineiro; 2- Complexo Mantiqueira; 3- Terreno Central da Faixa Ribeira (Complexo Quirino – embasamento); 4- Terreno Cabo Frio (Complexo Região dos Lagos – embasamento). Rochas Metassedimentares neoproterozoicas: I- Megassequência Andrelândia; II- Domínio Costeiro do Terreno Oriental da Faixa Ribeira.

Fonte: Araujo *et al.* (2019), modificado pelo autor, 2020.

1 OBJETIVOS

Dentro do quadro exposto acima, pretende-se caracterizar os eventos magmáticos e suas assinaturas geoquímicas do Complexo Juiz de Fora, bem como elaborar a completa evolução geológica para rochas de diferentes assinaturas geoquímicas aflorantes na área de estudo por meio de ferramentas geoquímicas elementares e isotópicas (Sr, Nd e Hf) bem como geocronológicas (U-Pb SHRIMP) e de novos dados de geoquímica isotópica dos ortogranulitos. A distribuição temporal dos eventos magmáticos que ocorrem no Complexo Juiz de Fora (CJF), bem como a caracterização isotópica das fontes dos protólitos destes ortogranulitos, ajudarão na calibração do modelo evolutivo dessa importante unidade regional.

A comparação das características geocronológicas e isotópicas entre o CJF e outras unidades de embasamento que integram o Cinturão Minas-Bahia (Alkmim & Teixeira, 2017) faz parte do escopo da investigação. Os registros geológicos entre os ciclos orogênicos paleoproterozoicos no paleocontinente São Francisco-Congo também é objetivo importante dessa dissertação.

2 APRESENTAÇÃO DA DISSERTAÇÃO E LOCALIZAÇÃO DA ÁREA DE ESTUDO

2.1 Apresentação da dissertação

O presente trabalho contempla os resultados obtidos na pesquisa realizada entre as cidades de Valença (RJ) e Nossa Senhora do Amparo (RJ) em um terreno metamórfico de alto grau localizada na Faixa Ribeira. O objeto de estudo são os ortogranulitos do Complexo Juiz de Fora, nos quais foram submetidos a análises petrográficas, geoquímica elementares e isotópicas em rocha total (Nd e Sr) bem como à análises geocronológicas (U-Pb) e isotópicas (Lu-Hf) em zircão para melhor caracterização dessas rochas.

O trabalho tem como foco a aquisição e interpretação de novos dados geoquímicos e geocronológicos na área de estudo, de modo a colaborar com a evolução do conhecimento científico do Complexo Juiz de Fora em escala local e regional.

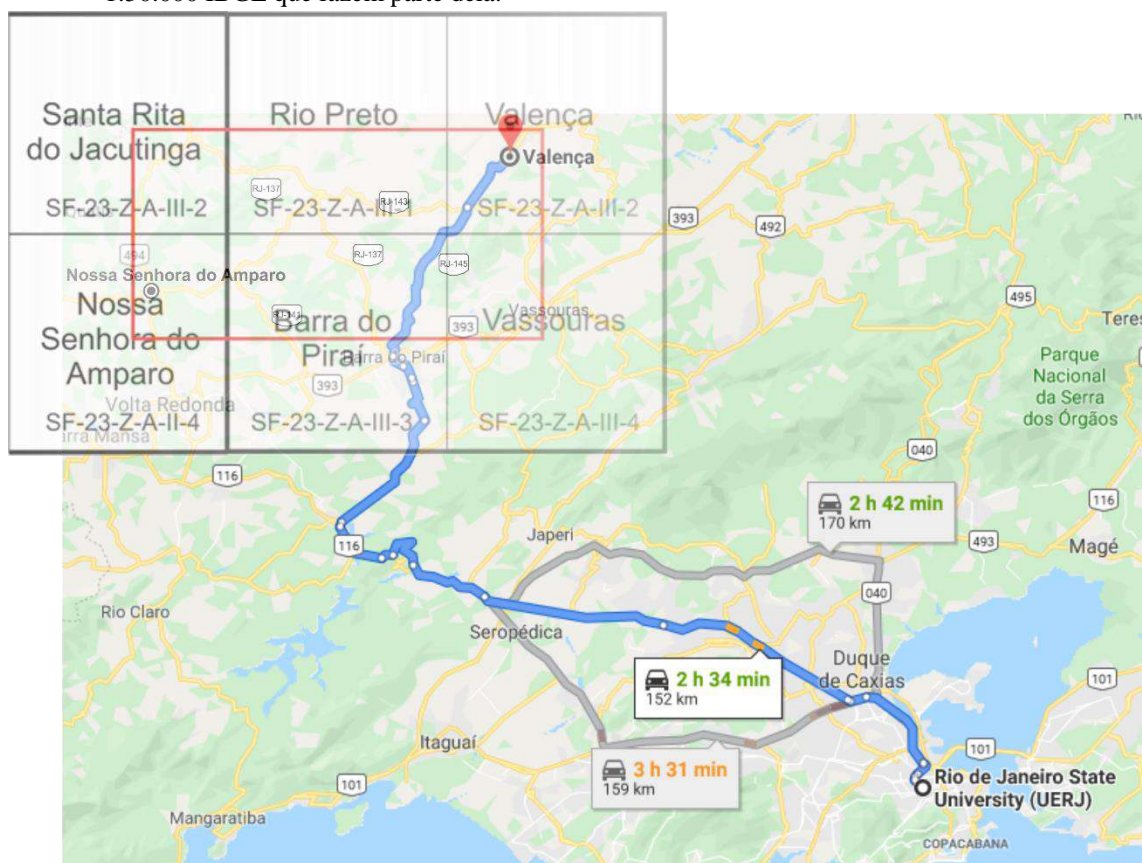
Essa dissertação pretende contribuir com o tema abordado a partir da aplicação de sua sistemática de trabalho, que contemplou análises geoquímicas elementares e isotópicas (Sm-Nd) antes da coleta geocronológica de seis amostras do Complexo Juiz de Fora, visando o registro de diferentes episódios magmáticos na unidade. Além disso, os novos dados obtidos trazem à tona a discussão de eventos tectonotermais, correlações geoquímicas e isotópicas e geocronológicas do embasamento paleoproterozoico do Cráton São Francisco e seus arredores.

O documento é dividido em 6 capítulos e segue o padrão de dissertação argumentativa associada com artigos científicos. O capítulo dos resultados (Capítulo 5) é composta pelo artigo “*Lithogeochemistry and Nd-Sr isotope constrains of orthogranulites of the Juiz de Fora complex, SE-Brazil: insights on a hidden Rhyacian Orogen within the Neoproterozoic Ribeira belt*”, publicado recentemente na revista *Brazilian Journal of Geology*. Além dele o manuscrito que reporta as idades e parâmetros petrogenéticos do Complexo Juiz de Fora se encontra como manuscrito a ser submetido à revista *Precambrian Research*. A última sessão dos resultados reporta os dados de um granito anorogênico encontrado no Complexo Juiz de Fora.

2.2 Localização da área de estudo

A área de estudo situa-se entre o 4º distrito de Barra Mansa (RJ) (Nossa Senhora do Amparo) e o município de Valença (RJ), a nordeste da cidade de Resende (RJ). É limitada pelos meridianos 43°30' e 44°15'e pelos paralelos 22°15' e 23°15'. Entre essas cidades, o maior município é mesmo o de Valença, com população aproximada de 76 mil habitantes (IBGE, 2004). Pela distribuição alongada na direção NE-SW, a área de estudo abrange 4 folhas topográficas do IBGE na escala 1:50.000: Folha Nossa Senhora do Amparo (SF-23-Z-A-II-4), Folha Rio Preto (SF-23-Z-A-III-1), Folha Valença (SF-23-Z-A-III-2), e Folha Barra do Piraí (SF-23-Z-A-III-3), ilustradas na Figura 2.

Figura 2 – Mapa geográfico com o acesso à área de estudo (em vermelho; IBGE, 1976) e as folhas topográficas 1:50.000 IBGE que fazem parte dela.



Fonte: O autor, 2020.

Os acessos à área de estudo se dão por meio de várias rodovias. Partindo do Rio de Janeiro, utiliza-se a Rodovia Presidente Dutra (BR-116) até a altura da cidade de Piraí, no Km 237, quando o percurso deve prosseguir pela Rodovia Alberto Santos Dumont (RJ-145) até a

cidade de Valença (RJ), extremo leste da área. Outra opção é seguir pela Rodovia Presidente Dutra (BR-116), e entrar na saída do Km 265, acessando a Rodovia Lúcio Meira (BR-393) até a cidade de Volta Redonda. De lá, se pega a rodovia Julio Caruso (RJ-153) até a cidade de Nossa Senhora do Amparo, extremo oeste da área. Existe uma rodovia que corta a área de estudo toda, com percurso aproximadamente W-E, que é a Estrada Quatis-Amparo (RJ-143). Outras duas rodovias estaduais importantes são a Rodovia Camrobert Rocha Faria (RJ-141) e a RJ-137, que são rodovias transversais (N-S) à Estrada Quatis-Amparo e que também permitem acesso à algumas localidades da área de estudo, como São José do Rio Turvo e Conservatória, respectivamente.

3 MATERIAIS E MÉTODOS

3.1 Revisão Bibliográfica

A revisão bibliográfica foi uma das primeiras atividades a serem desenvolvidas ao longo da dissertação. A leitura de artigos científicos de cunho regional sobre o Complexo Juiz de Fora e outros que abordassem as metodologias U-Pb, Lu-Hf, Sm-Nd e Rb-Sr nos embasamentos arqueano à paleoproterozoico foram privilegiados. Além disso, trabalhos científicos que se tratava de interpretação e tratamento de dados de U-Pb e Lu-Hf foram fundamentais para a redução dos dados e todo o tratamento feito com as amostras a serem datadas.

Nessa etapa foi realizada a compilação de dados bibliográficos sobre o Complexo Juiz de Fora e outros embasamentos no que diz respeito à geocronologia U-Pb e geoquímica isotópica Sm-Nd e Lu-Hf dessas unidades.

3.2 Bases de dados e mapas integrados

A base de dados geográficos foi as cartas topográficas do IBGE (escala 1:50.000) com destaque para as cartas: Folha Nossa Senhora do Amparo (SF-23-Z-A-II-4), Folha Rio Preto (SF-23-Z-A-III-1), Folha Valença (SF-23-Z-A-III-2), e Folha Barra do Piraí (SF-23-Z-A-III-3).

A base de dados geológicas veio do projeto PRONAGEO (2007) entre a CPRM e a UERJ. Mapas geológicos geoprocessados foram obtidos no Laboratório de Estudos Tectônicos (LET-UERJ). Além disso, mapas geológicos na escala de 1:50.000 das mesmas cartas supracitadas foram utilizadas em campo para localização de afloramentos.

3.3 Trabalhos de campo

O mapeamento geológico das folhas topográficas 1:50.000 em que a área de estudo está inserida foi feito pelo grupo TEKTOS (UERJ) em parceria com o Serviço Geológico do Brasil (CPRM) no projeto PRONAGEO entre os anos de 2003 e 2007. O “Mapa Geológico e de Recursos Minerais do Rio de Janeiro” foi publicado em 2017 e todas as informações geológicas foram utilizadas para os trabalhos de campos da Monografia de Graduação e de mestrado do presente autor.

O trabalho de campo da Monografia foi realizado entre as cidades de Nossa Senhora do Amparo (RJ) e Valença (RJ) em maio de 2017 e consistiu na coleta de amostras para petrografia, geoquímica elementar e isotópica. Nessa campanha de campo também foram revisitados alguns contatos do Complexo Juiz de Fora, bem como foi coletado uma amostra para estudos geocronológicos (amostra RP-LM-04).

O trabalho de campo foi realizado na mesma área de estudo da Monografia de Graduação, em 4 dias. Ele consistiu na coleta de amostras com objetivo principal de datação U-Pb de cada rocha. O critério mais utilizado para a coleta foram as classificações dos grupos geoquímicos pré-estabelecidas durante a monografia da graduação, buscando abrangência de todos agrupamentos, bem como faciologias e composições isotópicas. Além disso, foi levado em consideração se o afloramento em que tal rocha ocorria poderia receber uma amostragem em maior volume. A coleta de amostras no trabalho de campo seguiu os procedimentos do “Guia de procedimentos para amostragem e Seleção de métodos geocronológicos aplicados ao mapeamento regional” (Silva, 2006), com atenção na quantidade de amostra coletada e com o devido cuidado de se evitar leucossomas, bandamentos, etc.

3.4 Petrografia

A maioria das amostras coletadas já possuíam lâmina petrográfica, mas algumas lâminas foram realizadas depois da etapa de campo. Elas foram elaboradas no Laboratório Geológico de Preparação das Amostras (LGPA-UERJ). Todas elas possuem ortopiroxênio metamórfico e, portanto, são granulitos. Sua classificação petrográficas (Streckeisen, 1976) encontra-se no item 6.3 e informações detalhadas são reportadas em Araujo *et al.* (2019).

3.5 Preparação das amostras para análises geocronológicas e geoquímicas

3.5.1 Geocronologia U-Pb

A preparação de amostras para a datação U-Pb (SHRIMP) foi realizada no Laboratório Geológico de Preparação de amostras (LGPA) na UERJ, com sugestão de incorporação da peneiragem das amostras no decorrer do processo de preparação das amostras, segundo as normas do Laboratório de Processamento de Materiais do IGC-USP. A preparação consistiu na diminuição do volume e redução da granulometria da amostra até as alíquotas mais finas serem levadas à separação densimétrica (por meio de líquidos e da mesa vibratória) e eletrodinâmica (FrantzTM) dos seus minerais até a concentração de grãos de zircão. Cada etapa da preparação de amostras será descrita brevemente abaixo.

O primeiro procedimento realizado na preparação de amostras foi a lavagem e a secagem em banho de luz das seis amostras que vieram do trabalho de campo. O processo de diminuição do volume e granulometria das amostras começa com a passagem no britador de mandíbulas, sempre seguido por peneiramento de 30 mesh (30#). A alíquota mais fina segue para o moinho de discos seguido de peneiramento de, 60 mesh (60#). O material mais fino foi posteriormente peneirado em peneiras de 100#, com exceção da amostra de rocha básica que também teve peneiramento em 230#, tendo, portanto, duas frações, uma entre 100 e 230# e outra menor que 230#.

As amostras peneiradas foram levadas à mesa vibratória de Wifley com angulação de 10°, na qual o despejo da amostra na mesa com água corrente faz com que os minerais se segreguem por sua densidade. Os minerais das amostras são separados em três recipientes: o de rejeito, os leves e os pesados (concentrado). Os dois primeiros são descartados, e o último aproveitado para as etapas seguintes. Além disso, foi realizada pipetação no rastro de minerais pesados da mesa vibratória, com o intuito de obter mais facilmente os cristais de zircão por ele ser um mineral pesado. Portanto, para cada amostra, obteve-se duas alíquotas da mesa vibratória: a pipetada e a concentrada, que foram posteriormente emersas no álcool e postas no banho de luz.

As alíquotas pipetadas das amostras foram então levadas para o primeiro separador densimétrico líquido (Bromofórmio, de densidade 2,89 g/cm³), no qual os minerais pesados

fluem para baixo por gravidade e os minerais leves como quartzo e plagioclásio tendem a ficar retidos na superfície do líquido.

A alíquota pesada foi então passada no ímã de mão, para retirar a magnetita da amostra e posteriormente, levada no separador eletromagnético FrantzTM, no qual por meio de uma corrente elétrica os minerais que atraíveis se separam dos menos atraíveis. A primeira corrente utilizada foi a de 0,2 A, fração na qual a maioria dos minerais atraíveis são ilmenitas. A fração não atraível é passada de novo, em procedimentos sucessivos de aumento de corrente elétrica até chegar a 1,5 A. Idealmente, os grãos de zircão ígneos são os não magnéticos, portanto os menos atraíveis. As frações atraíveis nesse processo são identificadas e guardadas. Na fração de 0,4 A, normalmente são atraíveis monazitas e ilmenitas residuais. Nas frações de 0,5, 0,75, 1,0 e 1,5 A, retiram-se respectivamente granadas, titanitas e rutilos da amostra.

A alíquota não atraível à corrente de 1,5 A é então levada à outro líquido denso, o Iodeto de Metileno (densidade de 3,35 g/cm³). Esse líquido separa muito bem a apatita (densidade 3,15-3,20 g/cm³) dos outros minerais pesados. A apatita costuma ser não atraível pela corrente de 1,5 A no Frantz,. A alíquota leve é então guardada e a fração pesada é o material que deverá haver muitos grãos de zircão, já que ele possui densidade de 4,6 g/cm³, densidade bem maior que o Iodeto.

A amostra básica BP-CM-151 teve que ter seu concentrado reprocessado, já que a alíquota pipetada não estava em quantidade suficiente para os técnicos da USP selecionarem os grãos de zircão para catação e posterior preparação dos mounts. Os procedimentos de catação dos grãos foram realizados no laboratório SHRIMP-IIe (USP) pelos técnicos do local.

O processo de catação dos grãos de zircão foi feito em lupa binocular selecionando em torno de 80 à 100 grãos para todas as amostras, exceto para a amostra básica (BP-CM-151) que foram catados por volta de 60 grãos. A seleção dos grãos é feita baseada em características físicas tais como morfologia, transparência, cor e presença de fraturas e inclusões nos grãos. Os grãos são extraídos do concentrado com uma pinça e colocados em uma placa de Petri com álcool. A preparação dos mounts começa com a colagem dos grãos de zircão (um a um) em fita dupla face fixada em uma placa de vidro antes de serem colocados num disco de epóxi e serem cortados, lixados e polidos. O polimento é realizado até expor a metade dos grãos e deixar a superfície do mount bem plana. Após isso, é realizada a limpeza do mount é limpo com éter de petróleo (30°-70°) P.A.-ACS. O último procedimento da preparação do mount é a metalização em ouro de todo o mount.

Vale lembrar que durante a preparação do mount para a metodologia SHRIMP (U-Pb) é necessária a incorporação de padrões de cristais de zircão conhecidos (idades e razões

isotópicas). No caso do laboratório Geocronológico de Alta Precisão (SHRIMP-IIe) da USP, o padrão utilizado é o TEMORA-2.

3.5.2 Geoquímica elementar e isotópica (Sm-Nd e Sr)

A preparação de amostras para análises geoquímicas foi também realizada no LGPA-UERJ. A lavagem e secagem das amostras vindas do trabalho de campo é o primeiro procedimento feito no laboratório. Depois, a britagem manual com um martelo é feita nas amostras embaladas em um saco plásticos sobre uma bigorna. Essa técnica é utilizada para a diminuição da granulometria das amostras até o tamanho de pequenas partículas. Posteriormente, é feito o quarteamento das amostras para que elas tenham uma homogeneidade granulométrica e representem de fato a composição da rocha total. Essas alíquotas são levadas no moinho de bolas, no qual são pulverizadas automaticamente por volta de 10 a 15 minutos, até chegarem à fração silte. O pó é armazenado em dois tubinhos de 10g, que são lacrados e enviados para os laboratórios fazerem as análises geoquímicas pertinentes.

3.6 Geoquímica elementar

As análises litogeoquímicas tiveram o intuito de caracterizar a assinatura geoquímica das rochas por sua série e sub-série magmática. Os tubos de 10g de cada amostra foram enviados para o Activation Laboratories (Actlabs), localizado no Canadá, para análise química através dos métodos FUS-ICP/ICP-OES e FUS-MS, para análise dos elementos químicos maiores, elementos-traços, elementos terras raras, incluindo U, Th, Hf, Ta e Pb. No primeiro procedimento, uma amostra oxidada é dissolvida em um fluido de borato e posteriormente diluída em ácido nítrico aquoso, quando, posteriormente a ICP-OES (Espectrometria de emissão óptica com plasma) é executada para quantificar os vários elementos presentes na solução resultante. Nesta análise é detectada a radiação eletromagnética emitida pelos átomos ou íons na região do espectro visível e ultravioleta. No segundo método, a quantificação dos elementos é feita por espectrometria de massa (MS), que permite obter informações sobre a composição

atômica e molecular do material, a partir da relação massa-carga iônica (Klein & Dutrow, 2012).

3.7 Geocronologia U-Pb (SHRIMP)

O SHRIMP tem um diâmetro de laser mais pontual se comparado com a técnica LA-ICPMS o que aumenta a resolução temporal da análise. Essa metodologia é recomendada para terrenos retrabalhados já que cristais de zircão desse terreno podem registrar diversos eventos tectonotermais que só serão descobertos com análises pontuais no mesmo cristal.

O mount preparado e descrito no item 4.5 seguiu para análise de catodoluminescência (CL) utilizando o Microscópio Eletrônico de Varredura (MEV) no equipamento VPSEM FEI Quanta 250 localizado no Laboratório Geocronológico de Alta Precisão (SHRIM-IIe) da Universidade de São Paulo. As análises foram realizadas em fevereiro de 2019. O procedimento de catodoluminescência consiste num feixe de luz que atinge a superfície do cristal até uma certa profundidade de $20\mu\text{m}$, imageando assim o interior dos cristais de zircão. Adicionalmente foi realizado o imageamento com luz refletida para permitir a melhor descrição das formas e hábitos do zircão. A escolha dos spots para a análise foi feita baseada na análise destas imagens.

A análise geocronológica dos cristais de zircão foi executada no espectrômetro de alta resolução e sensibilidade do laboratório SHRIMP-IIe (USP). A metodologia é baseada na ionização do spot a ser datado no cristal de zircão por feixe de elétrons de oxigênio. O espectrômetro elimina as razões interferentes e lê os isótopos de U e Pb por meio de seus diversos detectores. O cálculo da idade de cada grão é feito por meio das concentrações de cada isótopo e razões obtidas por comparações com padrões.

A partir de análise criteriosa das imagens de CL, os sítios (spots) análise geocronológica foram previamente selecionados. Focou-se em feições como zoneamento oscilatório para idades de cristalização, núcleos de xenocristais para testes de zircão herdado, bem como bordas homogêneas para idades de eventos metamórficos. A aquisição não é automática. O operador deve posicionar o laser no local certo do spot para poder atirar na amostra e obter os resultados. Uma norma estabelecida para o bom funcionamento da máquina é a obtenção sistematizada de uma idade do padrão TEMORA2 à cada 4 spots obtidos nas amostras. Outro parâmetro muito importante na aquisição dos dados é a observação do valor de Pb^{204} no detector. Há valores específicos adotados pelo laboratório para amostras de diferentes idades (Paleoproterozoico:

até 15%; Neoproterozoico: até 10%). Quando os valores de chumbo comum estão acima desses valores, deve-se abortar a análise para não comprometer o bom funcionamento do espectrômetro. Após a aquisição, a redução dos dados resultou nas planilhas finais de dados com as razões dos isótopos de U, Th e Pb, suas idades e grau de interrelação entre erros. Os erros reportados estaticamente são 1σ .

3.8 Geoquímica isotópica Sm-Nd e Sr

As análises geoquímicas isotópicas foram processadas no Laboratório de Geocronologia e Isótopos radiogênicos (LAGIR) da UERJ. O pó das amostras é submetido ao processo de diluição isotópica em ácidos e soluções específicas durante tempo controlado.

Os procedimentos químicos foram feitos em salas limpas usando a destilação específica de ácidos Milli-Q® water e PA Merck® (Cardoso *et al.* 2019). Do tudo de 10g de amostra pulverizada (item 4.5), entre 25 e 50 mg foram submetidos à digestão em recipientes Savillex® em placas quentes, após à adição de quantidades proporcionais de solução dupla do traçador ^{149}Sm - ^{150}Nd . Uma mistura do concentrado de ácidos (HF and HNO₃ 6N) foi aplicada por três dias, seguida por digestão com ácido HCl 6N por 2 dias. A separação do Sr e ETR usou troca catiônica seguindo técnicas convencionais com colunas Teflon preenchidas com resina Biorad® AG50W-X8 (100-200 mesh) em meio de HCl. Para a separação química de Sm e Nd, uma coluna secundária foi usada com resina Eichrom LN-B-25S (50-100 µm). Após a evaporação, Sm, Nd e Sr foram separadamente carregados em filamentos de Re previamente degaseificados em mounts duplos, utilizando o ácido H₃PO₄ como ativador da ionização. As razões isotópicas ($^{147}\text{Sm}/^{144}\text{Nd}$, $^{143}\text{Nd}/^{144}\text{Nd}$ e $^{87}\text{Sr}/^{86}\text{Sr}$) foram medidas no espectrômetro de massa de ionização termal (técnica: TIMS; marca- ThermoScientific TRITON). Ele possui um arranjo de oito coletores Faraday no modo estático. As razões isotópicas medidas são reportadas com erros padrões absolutos (2σ) abaixo de 10^{-5} . Elas foram normalizadas respectivamente para a razão da constante natural de $^{146}\text{Nd}/^{144}\text{Nd} = 0,7219$, $^{147}\text{Sm}/^{152}\text{Sm} = 0,5608$ e $^{88}\text{Sr}/^{86}\text{Sr} = 8,3762$. A razão média $^{143}\text{Nd}/^{144}\text{Nd}$ ratio de repetidas medidas do JNd-1 (Tanaka *et al.* 2000) foi $0,512098 \pm 0,000006$ ($n = 322$). A razão média de $^{87}\text{Sr}/^{86}\text{Sr}$ do padrão NBS-987 (Wise & Waters, 2007) foi $0,710239 \pm 0,000008$ ($n = 158$). Repetidas análises de materiais de referência vindos do Serviço Geológico dos Estados Unidos (BCR e AVG) mostraram razões $^{147}\text{Sm}/^{144}\text{Nd}$

com reproducibilidade dentro de 1% (Valeriano *et al.* 2008). As idades modelos de Nd (T_{DM}) foram calculadas usando o modelo de manto empobrecido de DePaolo (1981).

3.9 Análises isotópicas Lu-Hf

A análise geoquímica isotópica de Lu-Hf em zircão foi realizada no Laboratório de Geoquímica Isotópica da UFOP por meio da metodologia LA-ICP-MS na máquina Neptune. A análise foi realizada em junho de 2019. Para as análises isotópicas de Lu-Hf foram escolhidos os cristais de zircão referentes à cristalização magmática que apresentasse maior concordância ou estivesse dentro do range de discordância (-5% < D < +5%). Primeiro, marca-se manualmente os spots de Hf dentro dos grãos de zircão nas imagens digitalizadas do mount.

É aconselhável colocar um quarto do spot dentro da área previamente datada pela metodologia U-Pb a fim de obter parâmetros petrogenéticos relacionados àquela idade geológica.

A aquisição dos dados de Lu-Hf ao contrário da metodologia U-Pb é automática. Os padrões utilizados foram o BB com idade de 560 Ma e razão $^{176}\text{Hf}/^{177}\text{Hf}=0.2816713$ (Santos *et al.* 2017), Mudtank com idade 732 Ma e $^{176}\text{Hf}/^{177}\text{Hf}=0.282504$, GJ-1 com idade 602 Ma e $^{176}\text{Hf}/^{177}\text{Hf}=0.2820000$ e Plesovice com idade de 337 Ma e $^{176}\text{Hf}/^{177}\text{Hf}=0.2820000$. A análise começa com 15 análises entre os padrões visando a calibração do espectrômetro de massa, para depois fazer 30 análises pontuais nos zircões selecionados (Amostras BP-LM-12, VA-LM-07B e RPM-570). Após isso, mais 12 tiros foram dados nos padrões para mais 45 análises em nossas amostras (Amostras BP-LM-13, RP-LM-04 e BP-CM-151). A aquisição de dados se encerrou com mais 12 análises entre padrões e brancos.

As amostras que receberam mais análises de Lu-Hf em seus spots foram as amostras BP-CM-151 e a RP-LM-04 com 15 e 20 análises cada, respectivamente. As amostras restantes receberam 10 análises cada.

3.10 Tratamento e integração de dados

O tratamento dos dados geoquímicos foi feito no software *GCDKit* versão 4.1, com o intuito de construir diagramas geoquímicos, aplicados à classificação dos grupos de rochas, além da plotagem em diagramas tectônicos. Para as análises de geoquímica isotópica (Sm-Nd, Lu-Hf e Sr), os parâmetros petrogenéticos ($\varepsilon_{\text{Nd}_{(t)}}$, $T_{\text{DM Nd}}$, $^{87}\text{Sr}/^{86}\text{Sr(i)}$, $\varepsilon_{\text{Hf}_{(t)}}$ e $T_{\text{DM Hf}}$) foram obtidos por meio de cálculos feitos cálculos no programa *Excel*. Idades modelos ($T_{\text{DM Nd}}$) foram calculadas usando o modelo de manto empobrecido (DePaolo, 1981). As idades modelos de $T_{\text{DM Hf}}$ foram calculadas através do modelo de duplo-estágio em cristais de zircão, utilizando as razões do manto empobrecido de Dhuime *et al.* (2011).

As análises geocronológicas (U-Pb) foram tratadas conforme o teor de Pb comum (<0.5%), grau de discordância com “range” de 5% de margem de erro (-5% < D + 5%). Grãos de zircão com valores fora deste parâmetro não foram considerados para o cálculo de idades concordantes de sua amostra. Contudo, algumas amostras possuem grãos de zircão com alta discordância, sendo necessário o uso de discórdias para o cálculo de idades de cristalização e metamorfismo (Interceptos superior e inferior, respectivamente). Outro parâmetro utilizado no tratamento dos dados foi a correlação de erros entre as idades individuais. Posteriormente, utilizou-se o software *Isotplot 4.15* para a confecção de diagramas Wetherill-Concordia para as amostras, bem como cálculo de idades concordantes e idades de interceptos superiores e inferiores da Discordia.

Mapas geológicos de campo foram confeccionados com software *ArcGis* versão 10.1. A integração de dados geoquímicos foi realizada por meio de diagramas e gráficos que foram confeccionados no software *Corel Draw* versão x5.

4 SÍNTESE BIBLIOGRÁFICA E O ESTADO DA ARTE DO COMPLEXO JUIZ DE FORA

4.1 Evolução do embasamento do Cráton São Francisco

O Cráton São Francisco é uma importante entidade geológica da Plataforma Sulamericana. Ele é uma pequena extensão do proto Cratón do Congo, no que se trata dos embasamentos arqueanos e paleoproterozoicos (Trompette, 1994). A sua definição como cráton está condicionada à sua estabilidade tectônica durante o Neoproterozoico (Almeida, 1977), período dos grandes ciclos orogênicos (Brasiliiano-PanAfricano) que culminaram na amalgamação do Gondwana Ocidental. O último evento tectônico que teve papel na construção do proto-craton foi o evento Transamazônico, também chamado de Eburneano na parte africana (2.3-1.9 Ga) no qual episódios orogênicos afetaram os núcleos arqueanos (Bloco Jequié, Gavião e Guanhães) e produziram a crosta continental). Nesse período na parte norte do Cráton São Francisco, o bloco Jequié sofreu a acresção de rochas de arco datadas de 2.19 Ga, formando o orógeno Itabuna-Salvador Curaçá (Oliveira *et al.* 2010). No Sul do Cráton, entre 2.1 e 2.0 Ga, os núcleos arqueanos do cráton (ex. granitoides Campo Belo, Bonfim, Bação e Belo Horizonte) bem como as sequências supracrustais greenstone belts (Ex. Rio das Velhas) sofreram metamorfismo regional decorrente da acresção do Cinturão Mineiro, Mantiqueira e Juiz de Fora. Esse evento é chamado localmente de Orogenia acrecionalária Minas (Teixeira *et al.* 2015).

O núcleo arqueano da parte sul do Cráton São Francisco é representado por greenstone belts e complexos metamórficos com rochas gnáissicas de assinatura TTG (Lana *et al.* 2013, Noce *et al.* 1998).

Esses granitoides arqueanos na transição do Arqueano ao Paleoproterozoico serviram de áreas fonte para a deposição do Supergrupo Minas (2.58-2.05 Ga). Um conjunto de cinco sequências compõe esse Supergrupo e elas refletem diferentes momentos da bacia e da evolução do Cráton São Francisco. São eles:

- a) Grupos Tamanduá/Caraça – sedimentos aluviais à marinhos com idade de deposição mínima de 2580 ± 7 Ma (Hartmann *et al.* 2006)

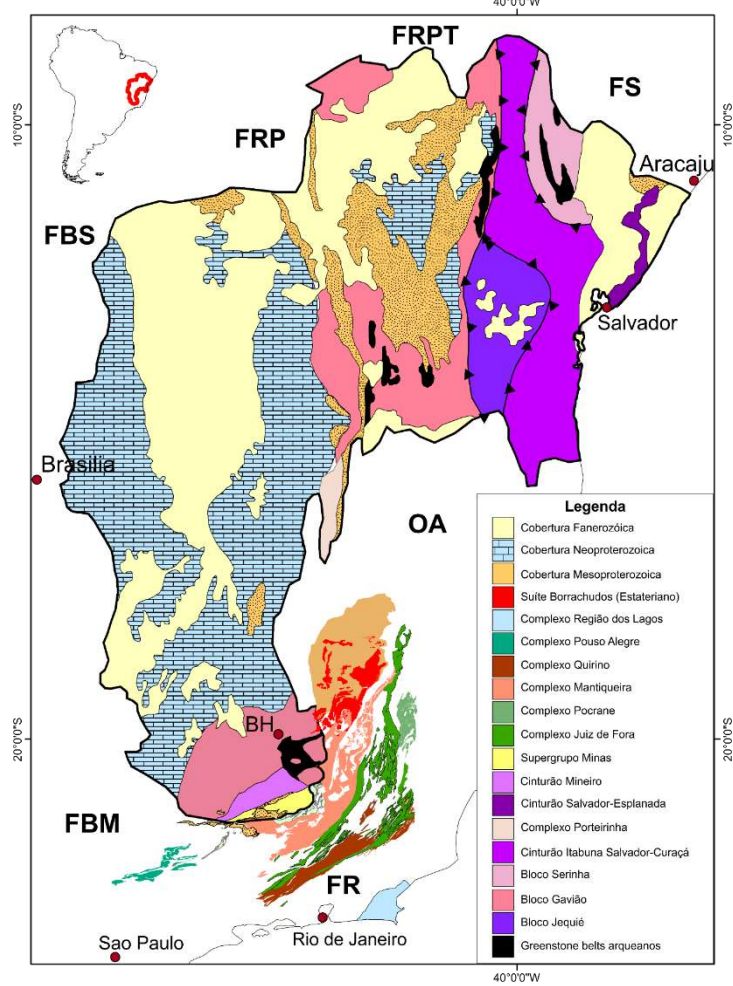
- b) Grupo Itabira – sedimentos marinhos à marinhos rasos, com destaque para os BIF's da formação Cauê (2453 ± 18 Ma - Cassino (2014)) e os mármore dolomíticos da Formação Gandarela (2419 ± 19 Ma – Babinski *et al.* 1995);
- c) Grupo Piracicaba – sedimentos deltaicos recobertos por pelitos marinhos, arenitos e folhelhos escuros (Heilbron *et al.* 2017 e referências dentro). A base dessa sequência tem deposição mínima de 2680 ± 24 Ma (Mendes *et al.* 2014);
- d) Grupo Sabará – depósitos turbidíticos de leque submarino (2125 ± 4 Ma – Machado *et al.* 1996a), em um regime compressivo com áreas fontes sendo granitoides do Cinturão Mineiro e embasamentos Riacianos da Faixa Ribeira e Araçuaí (Complexo Mantiqueira e Complexo Juiz de Fora);
- e) Grupo Itacolomi – depósitos aluviais, sin-orogênicos (2058 ± 9 Ma: Alkmin *et al.* 2014).

4.2 A crosta paleoproterozoica da paleoplaca São Francisco

Os orógenos paleoproterozoicos podem estar inseridos dentro do cráton São Francisco (ex. Cinturão Mineiro e Cinturão Itabuna-Salvador-Curaçá) ou podem ser retrabalhados pela orogênese Brasiliiana e estarem inseridos (coordenadas atuais) como embasamentos das faixas marginais ao cráton São Francisco (ex. Complexo Mantiqueira, Complexo Juiz de Fora, Complexo Quirino, Complexo Região dos Lagos – Faixa Ribeira). Além disso, blocos arqueanos do cráton São Francisco (ex. paleoplaca Gavião, bloco Porteirinha) apresentam também episódios magmáticos relativos à orogênese paleoproterozoica entre o Cráton São Francisco e Congo.

Os Complexos Mantiqueira, Juiz de Fora, Quirino e Região dos Lagos em conjunto com o Cinturão Mineiro e o Cinturão Itabuna-Curaçá-Salvador fazem parte de um sistema orogênico regional riaciano-orosiriano denominado Cinturão Minas-Bahia (Alkmim e Teixeira, 2017). O mapa da figura 3 apresenta a compartimentação tectônica para o paleocontinente São Francisco.

Figura 3 – Mapa simplificado do paleocontinente São Francisco com os terrenos de seu embasamento arqueano à paleoproterozoico aflorantes no cráton ou nos seus arredores.



Legenda: Faixas neoproterozoicas marginais: FR- Faixa Ribeira; FBM- Faixa Brasília Meridional; FBS – Faixa Brasília Setentrional; FRP- Faixa Rio Preto; OA-Orógeno Araçuaí; FRPT- Faixa Riacho do Pontal; FS- Faixa Sergipana.

Fonte: Modificado de Alkmin *et al.* (1993) pelo autor (2020).

Degler *et al.* (2018) estudaram terrenos de embasamentos de idade paleoproterozoica do Sudeste do Brasil com base em geocronologia e geoquímica isotópica (Sm-Nd, Lu-Hf) pode separar as frentes orogênicas riacianas-orosirianas em três, por localidade e caráter geoquímico:

- W-ROOS:** Sistema Orogênico Riaciano-Orosiriano Oeste – composto pelo Cinturão Mineiro, Complexo Mantiqueira, granitoides do Complexo Porteirinha e do Cinturão Itabuna-Salvador-Curaçá;
- E-ROOS:** Sistema Orogênico Riaciano-Orosiriano Leste – composto pelos Complexos Quirino e Região dos Lagos e a parte leste do Domínio Orogênico Bahia. Fazem parte desse sistema também os embasamentos do cráton do Congo e Angola;

- c) **JU-ROOS:** Sistema Orogênico Riaciano-Orosiriano Juvenil – composto pelos Complexos Juiz de Fora, Pocrane e o Complexo Buerarema.

4.2.1 Orógenos Paleoproterozoicos no Cráton do São Francisco

Nesse tópico serão descritas as unidades de embasamento que possuem idades de seus episódios magmáticos e dinâmicas relacionados ao ciclo orogênico riaciano-orosiriano. Com isso, os Complexos que serão descritos abaixo só possuem idades metamórficas paleoproterozoicas de suas rochas e estão inseridas dentro do Cráton São Francisco.

O Cinturão Mineiro faz parte do extremo sul do Cráton São Francisco. É um domínio geológico que aflora diversos plútões de idades entre o Sideriano (2.47 Ga) e o Riaciano (2.12 Ga), sequências vulcanossedimentares associadas. O Cinturão Mineiro é afetado pela deformação e metamorfismo (fácies anfibolito) decorrente da orogenia acrecional Minas (Teixeira *et al.* 2015). Seus plútões são relacionados à subducção, mas mostram diferenças em suas assinaturas geoquímicas conforme seu tempo de alojamento na crosta. Os plútões siderianos e os do início do Riaciano têm características TTG e são juvenis (ex. Cassiterita, Lagoa Dourada, Resende Costa – Barbosa *et al.* 2018, Seixas *et al.* 2012, Teixeira *et al.* 2015, Ávila *et al.* 2014), podendo refletir um ambiente de subducção raso e quente. Já os plutões do Riaciano são mais evoluídos e apresentam características cálcio-alcalinas (Ex. Alto Maranhão, Ritápolis – Seixas *et al.* 2013, Barbosa *et al.* 2015) que podem significar um aumento no ângulo de subducção para gerar esses plútões. Eles são as principais áreas fontes das sequências vulcanosedimentares, datadas entre 2.35 e 2.10 Ga (Teixeira *et al.* 2012, Teixeira *et al.* 2015), que se depositaram em contexto de arco intraoceânico (Teixeira *et al.* 2015). No Cinturão Mineiro também aflora rochas do Supergrupo Minas.

O Cinturão Itabuna-Salvador-Curaçá foi formado pela colisão dos blocos arqueanos: bloco homônimo ao cinturão formado (Itabuna-Salvador-Curaçá), Serrinha, Gavião, Jequié (Peucat *et al.* 2011). Esse cinturão tem orientação praticamente N-S se localizando no Norte do Cráton entre os blocos Gavião, Jequié e Serrinha. Seu embasamento é composto por granulitos charnockíticos neoarqueanos (2.8-2.7 – Silva *et al.* 2002). Episódios magmáticos posteriores como suíte tonalíticas e charnockíticas Riacianas (2.25 Ga e 2.1 Ga) ocorrem (D’el-Rey Silva *et al.* 2007; Silva *et al.* 2002; Barbosa *et al.* 2008). Ocorre ainda plútões sin a tardi-colisionais alcalinos sieníticos em 2.08 Ga (ex. Itiuba - Oliveira *et al.* 2004a, b; Conceição *et al.* 2003).

Todo esse conjunto de rochas foi metamorfizado em fácies granulito no fim do Riaciano (2.07 Ga – Oliveira *et al.* 2010; Peucat *et al.* 2011) com a colisão dos blocos arqueanos supracitados.

O domínio orogênico do Leste da Bahia, antigamente conhecido como Cinturão Salvador Esplanada, possui ortognaisses graníticos a tonalíticos cálcio-alcalinos migmatizados, com seus protólitos datados em 2.9 Ga (Silva *et al.* 2002). Há também anfibolitos e corpos graníticos com tendência alcalina no Cinturão (Delgado *et al.* 2002). Esses plútuns graníticos datam de 2064 Ma e marcam o episódio tardi-pós colisional (Souza-Oliveira *et al.* 2014) correlacionável ao Cinturão Itabuna-Salvador-Curaçá.

O Complexo Ibicaraí-Buerarema aflora localmente no Cinturão Itabuna-Salvador-Curaçá, não estando, portanto, representado na escala do mapa da figura 3. Ele é constituído por ortogranulitos de composição variada e foi previamente proposto por Arcanjo (1997). O Complexo Buerarema, como definido por Silva *et al.* (2002), é também referido como os granulitos tonalitos-trondjemitos com enclaves máficos apresentando granada (granulitos TT1 – Peucat *et al.* 2011). Esses granulitos tem seus protólitos interpretados como de arco magmático e datados entre 2191 e 2069 Ma (Silva *et al.*, 2002a, Silva, 2006, Peucat *et al.*, 2011). Seu caráter juvenil é atestado pela ausência de zircões herdados e assinaturas petrogenéticas (Sm-Nd) pouco evoluída (Peucat *et al.* 2011).

4.2.2 Manifestações magmáticas paleoproterozoicas em blocos arqueanos do Cráton São Francisco

Essas manifestações magmáticas também encontram-se dentro do cráton São Francisco, mas intrudem os blocos arqueanos pré-existentes (ex. Bloco Gavião, Bloco Serrinha e Complexo Porteirinha). Os plútuns paleoproterozoicos encontrados nesses blocos arqueanos tem relação com a evolução tectônica do Cinturão Minas-Bahia, com plútuns pré, sin a pós-colisionais datados ao longo do Paleoproterozoico.

Os blocos Gavião e Serrinha tiveram suas margens continentais arqueanas intrudidas por magmatismo cálcio-alcalino (estágio pré-colisional de arco– Barbosa *et al.* 2017) durante o Riaciano (bloco Gavião: 2320 a 2125 Ma – Santos Pinto *et al.* 1998; Guimarães, 2005; bloco Serrinha: 2165 a 2127 Ma – Rios *et al.* 2000). No fim do Riaciano, por volta de 2100 Ma, ocorreu a colagem desses blocos e a ocorrência de magmatismo granítico sin-colisional, (Teixeira, 2005; Rios *et al.* 2000). Por fim, com o colapso orogênico do Cinturão Itabuna-

Salvador-Curaçá, o bloco Gavião registra episódios magmáticos representados por plútuns alcalinos entre 2050 e 1969 Ma (Rosa, 1999; Rudowski, 1989; Cruz *et al.* 2016).

O Complexo Porteirinha se localiza na parte leste do cráton São Francisco, ocorrendo como um dos embasamentos da Faixa Araçuaí. Nele afloram gnaisses de idades variadas. O Complexo Porteirinha possui gnaisses paleoarqueanos com assinaturas TTG (3371 ± 6 Ma – Silva *et al.* 2016) metamorfizados no Mesoarqueano (3145 ± 24 Ma) e retrabalhado pela orogênese Brasiliiana (698 ± 85 Ma – Silva *et al.* 2016). Esse Complexo representa assim, uma extensão do núcleo arqueano cráton São Francisco, retrabalhado no Neoproterozoico. Além disso, plútuns neoarqueanos, riacianos e orosirianos são observados intrudindo o Complexo TTG supracitado (Silva *et al.* 2016). Exemplos são o plúton Riaciano (2140 ± 14 Ma – Silva *et al.* 2016), um leucogranito gnaisse de natureza sin-colisional (ex. Córrego Tinguí) e o plúton Paciência (2039 ± 8 Ma), este último fazendo parte de uma suíte alcalina pós-colisional.

4.2.3 Porções do orógeno paleoproterozoico nas faixas neoproterozóicas

Algumas unidades paleoproterozoicas relacionadas à orogênese paleoproterozoica encontram-se fora do cráton São Francisco, sendo submetidas à retrabalhamento Neoproterozoico e aflorando, portanto, nas faixas móveis marginais ao cráton São Francisco (Ribeira, Araçuaí e Brasília). Estas unidades são representadas pelos Complexos Mantiqueira, Juiz de Fora (objeto do presente estudo), Quirino, Região dos Lagos.

O Complexo Mantiqueira ocorre à sul do Sul do Cráton São Francisco, como embasamento da Faixa Ribeira e Araçuaí (Noce *et al.* 2007; Silva *et al.* 2002; Heilbron *et al.* 2010). Mais especificamente, é o embasamento da escama de empurrão superior (Domínio Andrelândia), no Terreno Ocidental da Faixa Ribeira, que corresponde à margem retrabalhada do cráton São Francisco (Heilbron *et al.* 2010). Afloram nesse complexo ortognaisses contendo camadas de anfibolitos e lentes de metaultramáficas (Heilbron *et al.* 2017; Noce *et al.* 2007). Seus protólitos são do Riaciano (Heilbron *et al.* 1998, 2010; Noce *et al.* 2007; Duarte *et al.* 2000, 2004). Ele é interpretado como um arco de margem continental ativa paleoproterozoica com assinatura crustal arqueana (substrato arqueano de 2700-2600 Ma: Heilbron *et al.* 2017) por conta de grãos de zircão herdados (Heilbron *et al.*, 2010) e parâmetros petrogenéticos Sm-Nd (Noce *et al.* 2007). O Complexo Mantiqueira registra um evento metamórfico de alto grau no fim do Riaciano/ Orosiriano (ca. 2080 – 1940 Ma) (Jordt-Evangelista *et al.*, 1994; Heilbron

et al., 2010; Barbosa *et al.*, 2004; Cutts *et al.*, 2018) e metamorfismo de fácies anfibolito no Brasiliano (Silva *et al.*, 2002; Duarte *et al.*, 2005; Noce *et al.*, 2007; Heilbron *et al.*, 2010; Cutts *et al.*, 2018).

O Complexo Quirino faz parte do embasamento do Terreno Paraíba do Sul da Faixa Ribeira Central (Heilbron *et al.* 2004a). Se trata de hornblenda-biotita gnaisses tonalíticos com enclaves maficos e ultramáficos (Machado *et al.* 1996). Seus protólitos, classificados em duas séries cálcio-alcalinas (médio e Alto K) são datados entre 2185 ± 8 Ma e 2169 ± 3 Ma (Valladares *et al.* 2002), possuindo cristais de zircão herdado meso- a neoarqueanos (2900-2800 Ma – Valladares *et al.* 1997; Machado *et al.* 1996). Os parâmetros petrogenéticos de Nd desse embasamento remete a fontes juvenis no paleoproterozoico e fusão de crosta arqueana como mecanismo petrogenéticos para a gênese dos protólitos do Complexo Quirino (Valladares *et al.* 2002). O Complexo Quirino foi metamorfizado em fácies anfibolito no Neoproterozoico (Valladares *et al.* 2002).

O Complexo Região dos Lagos é o embasamento do Domínio Tectônico Cabo Frio, que representa um terreno amalgamado na construção da Faixa Ribeira Central (Schmitt *et al.* 2004). Esse complexo possui ortognaisses tonalíticos à sienograníticos com enclaves microgranulares maficos bem como camadas de anfibolitos, diques e outras rochas maficas (Schmitt *et al.* 2008). O Complexo Região dos Lagos tem seus protolitos datados entre 2000 e 1960 Ma (Zimbres *et al.* 1990; Schmitt *et al.* 2004; Fonseca, 1993; Schmitt *et al.* 2008) e registra seu evento metamórfico em fácies anfibolito no eo-Cambriano entre 530 e 525 Ma (Schmitt *et al.* 2002).

O Complexo Pocrane faz parte do embasamento da Faixa Araçuaí. Sua constituição litológica é representada por ortognaisses bandados, laminados e migmatizados com intercalação de anfibolitos e rochas metassedimentares (Novo, 2013). Os protólitos desses ortognaisses são datados entre 2184 e 2068 Ma (Degler *et al.* 2018) e seu metamorfismo em fácies anfibolito é brasiliano (609 ± 3 Ma – Degler *et al.* 2018). Ele foi interpretado como um equivalente em difente nível crustal (crosta média) do Complexo Juiz de Fora no paleoproterozoico (Degler *et al.* 2018).

O Complexo Juiz de Fora faz parte das unidades dos embasamentos do Terreno Ocidental da Faixa Ribeira, assim como o Complexo Mantiqueira. Se encontra no domínio Juiz de Fora, a escama de empurrão basal do Terreno Ocidental, formada na orogênese brasiliana. É também reconhecido como uma unidade do embasamento da Faixa Araçuaí (Noce *et al.* 2007). O complexo engloba rochas ortogranulíticas paleoproterozoicas (<1,8 Ga) que se encontram intercaladas tectonicamente com rochas metassedimentares da parte distal do grupo

Andrelândia. Seus protólitos tem idades variando de 2400 a 1650 Ma (Heilbron *et al.* 2010; Noce *et al.* 2007; Degler *et al.* 2018; Kuribara *et al.* 2019). A superposição brasiliiana, está representada pelo metamorfismo de fácies granulito associado a intensa deformação e milonitização dos protólitos (Heilbron *et al.* 2010; Noce *et al.* 2007; Degler *et al.* 2018; Kuribara *et al.* 2019).

4.3 Estado da Arte do Complexo Juiz de Fora

O Complexo Juiz de Fora aflora entre cidades do Sul do Rio de Janeiro ao Leste de Minas Gerais, passando pelo Oeste do Espírito Santo. É, portanto, uma unidade litológica importante da Faixa Ribeira, por sua distribuição regional ampla e por ser peça chave de correlação com o embasamento da Faixa Araçuaí. Porém, seu conhecimento geológico evoluiu muito durante os últimos 60 anos e mudanças no sentido de sua classificação, interpretação tectônica e geoquímica foram promovidas mediante o avanço de técnicas geocronológicas. Será abordada aqui uma breve síntese do Complexo Juiz de Fora.

4.2.4 Denominações e correlatos

A definição do Complexo Juiz de Fora mudou muito, sendo primeiramente definida como Série Juiz de Fora para protolitos sedimentares (Ebert, 1955, 1957) e depois integrada com a série Paraíba do Sul (Ebert, 1968). Tentativas de subdivisões a partir de análises geoquímicas e texturais (Oliveira, 1983) não se sucederam. A série Valença que abarcava granulitos semelhantes à Série Juiz de Fora foi desmembrada e sua parte de gnaisses e migmatitos com intercalações supracrustais foi correlacionada à Série Paraíba de Sul (Machado, 1984, 1986). Figueiredo *et al.* (1989, 1990), Campos Neto e Figueiredo (1990), Figueiredo (1990), Figueiredo & Campos-Neto (1993) descreveram o Complexo Juiz de Fora, no norte fluminense, como sendo composto por ortogranulitos migmatíticos com gnaisses e migmatitos cinzentos subordinados. Diatexitos graníticos peraluminosos (tipo-S) também faziam parte do complexo. Heilbron (1993, 1995) utilizou a designação Complexo Juiz de Fora para englobar ortognaisses e metabasitos com paragêneses da fácie granulito, que localmente

mostram evidências de evento metamórfico retrógrado, com formação de hornblenda e biotita a partir de piroxênios. Os metassedimentos intercalados tectonicamente com os ortogranulitos foram correlacionados com as unidades distais da Megassequência Andrelândia. A denominação Complexo Juiz de Fora ficou restrita então, às unidades ortoderivadas integrantes do embasamento (idade $> 1,8$ Ga). Neste trabalho essa última classificação será adotada. Rochas metabásicas com idades estaterianas já foram descritas no Complexo Juiz de Fora, mas são intrusivas em escala não mapeáveis para serem submetidas à nomenclatura.

A suíte Caparaó é composta por granulitos charnockíticos que afloram em uma janela do embasamento do Orógeno Araçuaí com intercalação tectônica com paragnaisse de alto grau (Silva *et al.* 2002). Possui também algumas intercalações de granulitos máficos. Seus protólitos datam de 2195 ± 15 Ma e seu metamorfismo em fácies granulito é brasiliano (587 ± 9 Ma – Silva *et al.* 2002). Junto com o Complexo Pocrane, eles foram correlacionados ao Complexo Juiz de Fora. A suíte Caparaó no mesmo nível crustal inferior, enquanto o Complexo Pocrane em crosta média (Degler *et al.* 2018).

4.2.5 Geoquímica Elementar

Heilbron (1993, 1995) individualizou duas suítes básicas (uma toleítica e outra transicional) e três suítes cálcio-alcalinas (de alto, médio e baixo K) para os ortogranulitos do Complexo Juiz de Fora, na região entre Rio Preto e Valença (RJ). Posteriormente, incorporando os dados de Duarte *et al.* (1997) e Heilbron *et al.* (1988), os autores apresentaram uma subdivisão geoquímica simplificada em quatro conjuntos: duas suítes cálcio-alcalinas e duas suítes de rochas básicas. As duas primeiras, com assinatura de arcos magmáticos cordilheiranos e granitos colisionais, indicando ambiente tectônico compressivo. Já a suíte básica alcalina apresentou assinatura de ambiente intraplaca, enquanto a segunda, toleítica, mais heterogênea e formada por rochas básicas com assinaturas que variam de E-MORB (basalto oceânico enriquecido em elementos incompatíveis) a toleiítos de arco (IAT).

Valente (1999) e Duarte *et al.* (2001b, 2002) concluíram que, as rochas básicas toleíticas possuem distintas fontes mantélicas (N-MORB, E-MORB e intracontinental) e, que há no mínimo duas suítes cálcio-alcalinas, sendo que uma é heterogênea e não cogenética, enquanto a outra é formada por rochas intermediárias a ácidas cogenéticas evoluídas por processo de cristalização fracionada.

Araujo *et al.* (2019) propuseram para os ortogranulitos félscicos da região entre Valença e Nossa Senhora do Amparo 4 suítes cálcio-alcalinas baseado nos seus padrões de elementos Terras raras aliados à geoquímica isotópica (Sm-Nd, Sr). Além disso, as rochas básicas foram também separadas em 3 suítes toleíticas e 1 alcalina, também por esses parâmetros geoquímicos. As série cálcio-alcalinas foram associadas à ambientes compressivos (pré-colisional à pós-colisional) e duas das séries toleíticas são relacionadas à ambientes distensivos, uma à compressivo e a suíte alcalina à ambiente intraplaca.

4.2.6 Geocronologia isotópica (U-Pb) – Idades de cristalização

Diversos autores dataram os ortogranulitos do Complexo Juiz de Fora por grãos de zircão na metodologia U-Pb. As idades dos protólitos do CJF chegam 2.4 Ga a 1.65 Ga (Noce *et al.* 2007, Heilbron *et al.* 2010; Degler *et al.* 2018; Kuribara *et al.* 2019). A maioria das idades do CJF estão entre 2.20 e 2.05 Ga e se referem aos granulitos intermediários cálcio-alcalinos com assinatura de arco vulcânico do Complexo. Isócronas de referência Rb-Sr revelaram períodos mais velhos (idades entre 2.65 e 2.25 Ga) reforçaram nos ortogranulitos do Complexo Juiz de Fora entre as cidades de Juiz de Fora e Carangola-MG (Delhal *et al.* 1969; Cordani *et al.* 1973). Na cidade de Juiz de Fora foi reportado um granulito enderbitico de idade arqueana (2.98 Ga) com metamorfismo também mesoarqueano (2.8 Ga – Silva *et al.* 2002). A idade de 2.4 Ga se refere à um granulito máfico E-MORB na cidade de Itaperuna-RJ (Heilbron *et al.* 2010), interpretado como fragmento da crosta oceânica. Já as rochas de 1.7-1.65 Ga foram datadas nas cidades de Itaperuna e Valença-RJ (Heilbron *et al.* 2010) e representam idades de granulitos máficos a intermediários de assinatura intra-placa.

Na cidade de Mangaratiba, ortogranulitos outrora incluídos no Complexo Juiz de Fora foram estudados por André *et al.* (2018) e revelaram herança arqueana (2.6 Ga) e idade riaciana (2.1 Ga). As idades radiométricas K-Ar obtidas em piroxênios ou plagioclásios tem range de 1570 à 1220 Ma (Delhal *et al.* 1969; Cordani *et al.* 1973), não tendo nenhuma significância geológica ou podendo ser uma idade de mistura entre a cristalização paleoproterozoica e o metamorfismo brasileiro.

4.2.7 Geoquímica isotópica (Sm-Nd, Lu-Hf)

Os dados do Complexo Juiz de Fora previamente publicados mostram idades modelo T_{DM} Nd Siderianas a Riacianas (2.37 - 2.03 Ga – Degler *et al.* 2018; Fischel *et al.* 1998, André *et al.* 2009) com $\varepsilon_{Nd(t)}$ fracamente negativos, característicos de magmas moderadamente juvenis de fontes fundidas no Paleoproterozoico. Porém, idades modelos arqueanas (2.62-2.53 Ga) reportadas em Ubá-MG (Noce *et al.* 2007) e em Ipiabas-RJ (Araujo *et al.* 2019) indicam contribuição arqueana na gênese dos protólitos do Complexo Juiz de Fora, em coerência portanto as as idades U-Pb em zircões herdados. As idades modelos T_{DM} Hf em zircão mostram resultados entre 3.45 e 2.26 Ga com uma grande concentração nos períodos Sideriano e Racianno (Degler *et al.* 2018; Kuribara *et al.* 2019). Os parâmetros petrogenéticos $\varepsilon_{Hf(t)}$ são quase todos fracamente positivos, o que aponta para uma fonte mantélica paleoproterozoica na gênese das rochas do Complexo Juiz de Fora (Degler *et al.* 2018; Kuribara *et al.* 2019).

Todo o conhecimento geocronológico (U-Pb, Rb-Sr e K-Ar) bem como todos os parâmetros petrogenéticos (Sm-Nd e Lu-Hf) do Complexo Juiz de Fora está sintetizado em Araujo *et al.* (2019).

4.2.8 Modelos geotectônicos

Noce *et al.* (2007) interpretam que o Complexo Juiz de Fora evoluiu em um contexto de arco magmático oceânico, ou em uma crosta continental estirada, entre 2195 e 2084 Ma. Esse arco magmático ocêanico foi interpretado com polaridade de subducção para oeste, para seguir a polaridade do arco Mantiqueira instalado na margem arqueana do Cráton São Francisco no Racianno.

Heilbron *et al.* (2010) sugeriram que o Complexo Juiz de Fora foi originado em um ambiente de arco de ilha intraoceânico, na parte distal da margem arqueana do paleocontinente São Francisco. Ele foi posteriormente acrescionado aos arcos Mantiqueira e Mineiro, durante o evento transamazônico. A polaridade da subducção (de oeste para leste) foi justificada pela distribuição geoquímica das rochas de arco, com rochas de maior teor de K_2O à leste, bem como sua progressiva idade mais nova para leste. Nesta concepção, o Complexo Juiz de Fora, faria

parte (junto com outros complexos de rochas) então, da margem retrabalhada à sul do paleocontinente São Francisco, hoje representado pelo Terreno Ocidental da Faixa Ribeira.

Alternativamente, Kuribara *et al.* (2019) interpretaram que o Complexo Juiz de Fora é um sistema de arcos magmáticos vulcânicos com dois episódios de geração de magma juvenil (Sideriano e Orosiriano). Esses magmas teriam sido gerados por fusão de um microcontinente arqueano (~3.45 Ga). Um outro período de reciclagem crustal foi proposto por Kuribara *et al.* (2019) em um magmatismo de arco continental no final do Neoproterozoico. Cutts *et al.* (2019) discutiram que parece desnecessário criar o modelo geotectônico de um microcontinente arqueano como parte do Complexo Juiz de Fora, já que as idades modelos T_{DM} Hf obtidas por Kuribara *et al.* (2019) podem ser explicadas como sedimentos de áreas fontes arqueanas do cráton (zircão detritico) que foi posteriormente subductado no arco juvenil Sideriano.

4.2.9 Evolução tectono-metamórfica

Segundo Duarte (1988) e Duarte & Heilbron (1999) dois pulsos metamórficos, denominados M1 e M2, afetaram as rochas do Complexo Juiz de Fora. O metamorfismo M1, com pico térmico entre 800° e 895°C, está registrado em todas as rochas do Complexo Juiz de Fora e foi responsável pela formação de paragêneses diagnósticas da fácie granulito (ortopiroxênio + plagioclásio ± clinopiroxênio ± hornblenda), em arranjo granoblástico claramente anterior à formação da foliação milonítica relacionada à Orogênese Brasiliana. Condições de pressão baixa a intermediária, são evidenciadas pela composição química das hornblendas. Segundo os autores, M1 representaria um metamorfismo passivo proveniente de aquecimento e da atuação de fluidos carbônicos liberados durante evento extensional por magma basáltico na base da crosta. Foi proposta uma Trajetória P-T-t anti-horária para M1. Já o evento metamórfico M2, de caráter retrogrado, apresenta contemporaneidade com a deformação principal, pois sua paragênese se desenvolveu na foliação principal. Os cristais de opx e cpx dão lugar a hornblenda, biotita e granada nos ortogranulitos. O retrometamorfismo ocorreria pela entrada de água no sistema previamente desidratado. A contemporaneidade da deformação principal e M2 não está expressa nos paragnisses intercalados, já que estes apresentaram apenas evidências de desidratação. Condições de temperatura e pressão puderam ser aferidas a partir de dados de campo, petrográficos e de química mineral, indicando que M2 evoluiu sob condições de $T > 700^{\circ}$ - 750° C e P entre 6 e 7 kb. Um modelo de empilhamento de

escamas de empurrão mais quentes sobre escamas mais frias foi proposto e com isso, os paragnaisses desisdratariam enquanto os ortogranulitos se hidratariam. Uma trajetória P-T-t horária foi proposta baseada nesse modelo. Posteriormente, com base nas idades U-Pb obtidas, verificou-se que a idade do metamorfismo M1 também era brasiliana.

O metamorfismo granulítico brasiliano é observado em quase todas as análises geocronológicas (U-Pb) do CJF (Silva *et al.* 2002; Machado *et al.* 1996; Noce *et al.* 2007; Heilbron *et al.* 2010; Kuribara *et al.* 2019; Degler *et al.* 2018). Ele apresenta um intervalo temporal entre 620 e 520 Ma, sendo consistente com idades K-Ar em biotitas e anfibólios publicadas (Delhal *et al.* 1969; Cordani *et al.* 1973). Além disso, idades isócronas minerais (600 a 496 Ma) corroboram para o fato do retrabalhamento brasiliano do Complexo (Delhal *et al.* 1969; Cordani *et al.* 1973).

5 RESULTADOS

5.1 Introdução

Os resultados dos dados gerados durante o estudo incluiram novos dados de campo com coleta de amostras para estudos petrográficos, para a obtenção de 28 novas análises de geoquímica elementar e isotópica (Sm-Nd e Sr), além de análises geocronológicas (U-Pb SHRIMP) e de isótopos de Lu-Hf em zircão, obtidas em 6 amostras escolhidas por seus atributos geoquímicos elementares e isotópicos. Os dados referentes à geologia local, às análises geoquímicas e isotópicas de Nd e Sr foram incluídas no artigo científico "Lithogeochemistry and Nd-Sr isotope constrains of orthogranulites of the Juiz de Fora complex, SE-Brazil: insights on a hidden Rhyacian Orogen within the Neoproterozoic Ribeira belt" que foi publicado na revista *Brazilian Journal of Geology* (doi: 10.1590/2317-4889201920190007). Estes resultados estão incluídos no item 5.2, no formato de artigo publicado. Já as análises geocronológicas U-Pb e isotópicas de Lu-Hf, fazem parte do manuscrito à ser submetido para a *Geoscience Frontiers* na edição especial de Evolução Tectônica da América do Sul, sendo reportados adiante no item 5.3. O item 5.4 apresenta os dados geocronológicos (U-Pb) e isotópicos (Lu-Hf) de uma rocha granítica com assinatura totalmente contrastante com o ciclo orogênico Paleoproterozoico bem como suas discussões e correlações regionais.

5.2 Artigo publicado na *Brazilian Journal of Geology*

Os dados geoquímicos e geoquímica isotópica para Sm-Nd e Sr estão apresentados no Apêndice A (p.68), no formato do artigo publicado em 2019 pela *Brazilian Journal of Geology*.

5.3 Pré-publicação na *Precambrian Research*

Estes novos dados estão apresentados, no Apêndice B (p.88), no formato de pré-publicação de um artigo científico. A submissão desse manuscrito está prevista para o final de junho de 2020 para a revista científica *Precambrian Research*.

5.4 Granito anorogênico no Complexo Juiz de Fora

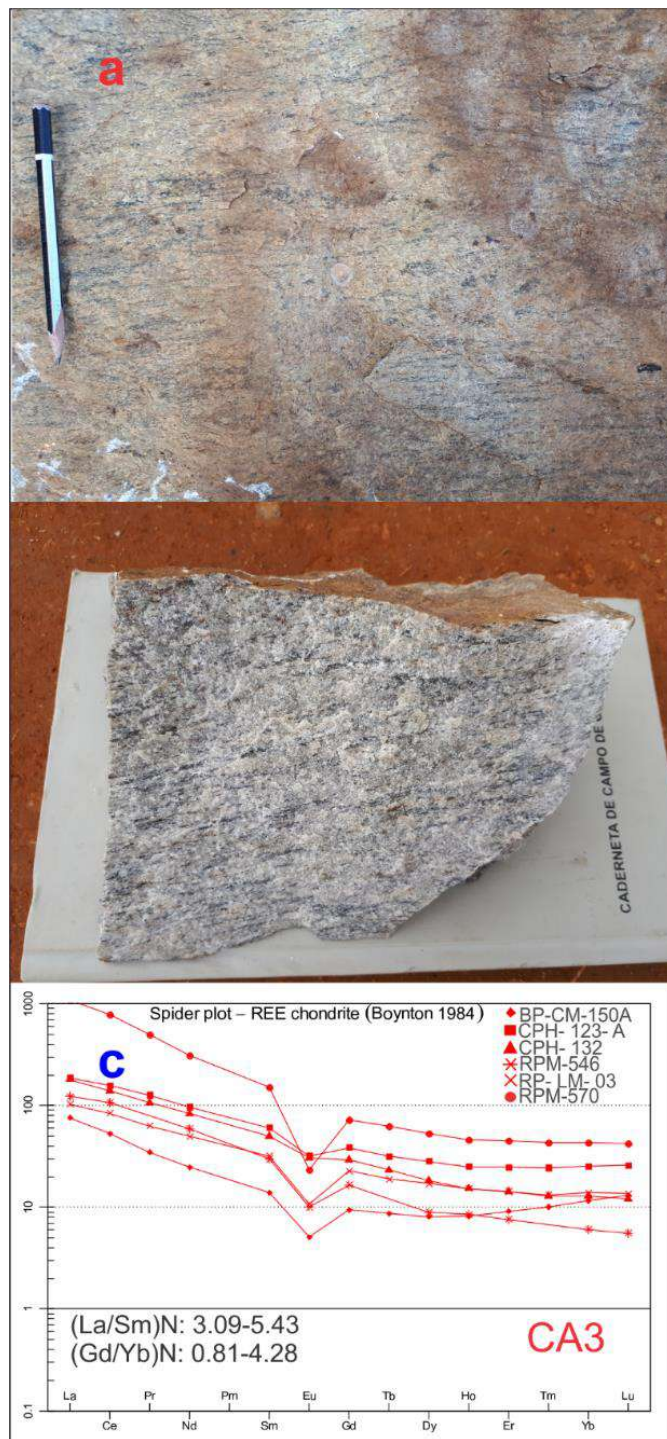
A amostra RPM-570 está representada por um granulito charnockítico leucocrático (Figura 4a,b), foliado com evidências pontuais de migmatização no afloramento coletado. O protólito desse granulito é granítico com assinatura intraplaca, apresentando enriquecimento de ETR leves e marcante anomalia negativa de Eu (Figura 4c). Mais informações geoquímicas podem ser encontradas no artigo apresentado no item 6.2. Os cristais de zircão são translúcidos e são geralmente de cor marrom clara, apresentando algumas inclusões. Eles são subédricos à euédricos, prismáticos com bordas subarredondadas, variando de tamanho de 155 à 300 μm e razão comprimento/largura de 2:1 and 5:1. A grande maioria dos cristais de zircão apresentam um fino zoneamento oscilatório, mas zoneamento em setor e núcleos homogêneos também foram observados. Bordas arredondadas e convolutes também foram notadas e apresentam baixa razão Th/U (<0.11), relacionada provavelmente à recristalização metamórfica. Treze análises dentro dos domínios de zoneamento oscilatório foram feitas e mostram variáveis razões de Th/U (0,49 e 1,43; Tabela A1 – Apêndice C). Três dessas análises estão fora do limite de discordância aceitável (-5% < D < +5%), indicando perda de Pb. Os dados permitiram o cálculo de uma idade concordante de 1781 ± 10 Ma (Figura 5) com moderado MSWD (4.6). Essa idade é interpretada como a idade de cristalização do protólito desse granulito. A média ponderada de idades $^{207}\text{Pb}/^{206}\text{Pb}$ é de 1776 ± 14 Ma (Figura 21) e robustece essa interpretação. Usando todos os cristais de zircão (magmáticos e metamórficos), foi obtida uma linha Discordia com intercepto superior de 1767 ± 12 Ma e intercepto inferior de 604 ± 11 Ma (Figura 5), que refletem respectivamente a cristalização magmática e o sobrecrescimento metamórfico. As idades modelo de Hf ($T_{\text{DM}} \text{Hf}$) (Tabela A2 – Apêndice C) variam de 2.88 a 2.4 Ga com valores de $\epsilon\text{Hf}_{(\text{t})}$ fortemente negativos, entre -5 a -17,8 (Figuras 6 e 7). Seu $T_{\text{DM}} \text{Nd}$ é de 2.39 Ga. A razão inicial $^{87}\text{Sr}/^{86}\text{Sr}$ remete à alguma perturbação no sistema isotópico Rb-Sr. Esses dados

coligidos se referem a uma fonte crustal sideriana com intensa contaminação crustal no momento de seu alojamento (Estateriano).

O episódio estateriano intraplaca reportado nesse trabalho apresenta correlação temporal com o granulito básico alcalino (amostra CJE-44: 1765 ± 34 Ma – Heilbron *et al.* 2010) datado em uma pedreira na própria área de estudo (Conservatória-RJ). Na região de Juiz de Fora, esse episódio magmático também foi encontrado para rochas do CJF em um granulito charnockítico com idade de 1656 Ma (Heilbron *et al.*, 2010). Isso reforça, que esse episódio magmático foi bimodal, característico de riftes intracontinentais.

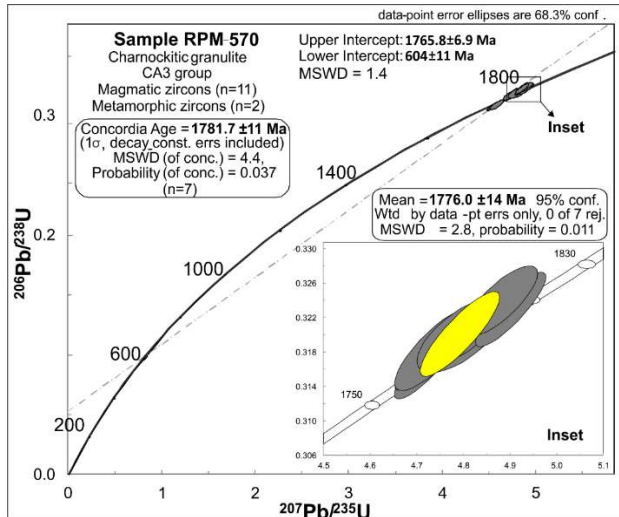
Esse episódio magmático felsico pode ser correlacionado com os metagranitos anorogênicos da suíte Borrachudos, Catolé e Lagoa Real no bloco Guanhães, Domínio Espinhaço Central e Norte (Magalhães *et al.* 2018 e referências dentro). Essas ocorrências têm range de idades entre 1790 e 1700 Ma e estão relacionadas ao processo de rifteamento do Cráton São Francisco. Os dados de Lu-Hf de metavulcânicas estaterianas do bloco Guanhães pode ser correlacionado aos dados da amostra RPM-570 (Figura 7), com $\epsilon\text{Hf}_{(t)}$ em zircão bem negativos, fruto do magmatismo intraplaca com grande contaminação crustal sofrida por esses magmas.

Figura 4 – Fotos em escala de afloramento (a), de amostra de mão (b) e assinatura ETR do granulito charnockítico leucocrático (amostra RPM-570).



Fonte: O autor, 2020.

Figura 5 – Diagrama Wetherill Concordia com cálculo de idade concordante e média ponderada de idades $^{206}\text{Pb}/^{207}\text{Pb}$ para o granulito charnockítico leucocrático (RPM-570) do CJF na área de estudo.



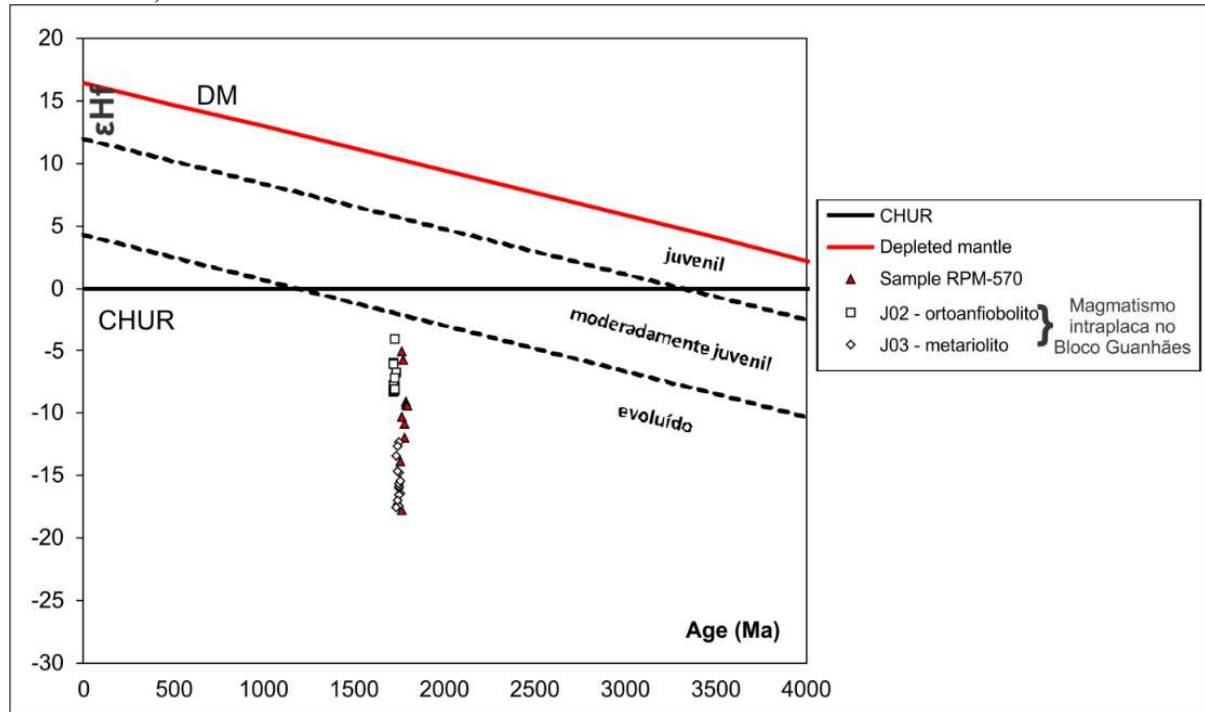
Fonte: O autor, 2020.

Figura 6 – Prancha com todos os grãos de zircão da amostra RPM-570 utilizados para cálculo de idade concordante de cristalização e análises Hf pontuais, além de algumas informações petrogenéticas dos sistemas Sm-Nd e Sr-Sr com a idade de cristalização U-Pb obtida para essa amostra.



Fonte: O autor, 2020.

Figura 7- Correlação dos parâmetros petrogenéticos ϵHf e $T_{\text{DM}} \text{ Hf}$ com a amostra estateriana da área de estudo (RPM-570) com anfibolitos e metariolitos relativos ao magmatismo intraplaca do Bloco Guanhães (1.74 Ga).



Nota: Dados Lu-Hf obtidos em Magalhães *et al.* (2018).

Fonte: O autor, 2020.

CONSIDERAÇÕES FINAIS

O Complexo Juiz de Fora é uma unidade geológica que apresenta uma grande variação composicional, geocronológica e isotópica. Portanto, a pesquisa científica no Complexo Juiz de Fora deve ser a mais multidisciplinar possível, incluindo correlações regionais.

A coleta de amostras foi feita a partir de análises geoquímicas elementares e isotópicas prévias, o que otimizou muito a pesquisa científica. A quantidade de informações geológicas retiradas em seis amostras foi marcante e auxiliou muito na evolução do Complexo Juiz de Fora durante todo o Paleoproterozoico.

Integrando-se as ferramentas geoquímicas isotópicas e elementares com as idades geocronológicas que os dois artigos trazem, é claro que o ciclo orogênico Paleoproterozoico reuniu suítes relacionadas à subducção tanto sideriana (grupo LK), quanto riaciana (grupo Ca3a, sanukitoides e TTG). Há também algumas suítes sem idades estabelecidas na literatura que foram interpretadas pelos parâmetros petrogenéticos e geoquímicos delas. São elas: os adaquitos de alta sílica, que seriam resultado da fusão de crosta inferior sobrepesada; e os outros granitóides de alto Ba-Sr que seriam produto de um magmatismo de médio K tardí a pós-colisional, bem reconhecido em outras unidades de embasamento que participaram do ciclo orogênico Paleoproterozoico.

Uma contribuição importante é o estudo de correlação regional no tocante o sistema orogênico Paleoproterozoico Minas-Bahia. As manifestações magnáticas do Sideriano (de 2450 à 2350 Ma) foram reportadas mais no Sul do Cráton São Francisco, com episódios mais primitivos (*juvenis*) no Cinturão Mineiro e no Complexo Juiz de Fora. Tal episódio magnético não foi reportado nos trabalhos mais recentes no Complexo Mantiqueira e Bloco Piedade. Já o episódio de arco no Riaciano (2200 a 2100 Ma) é bem disseminado em todo o orógeno, juntamente com o evento colisional (metamorfismo granulítico entre 2080 e 2050 Ma). Os granitos sin-colisionais (2060 à 2050 Ma) na parte Norte são mais recorrentes que na região sul assim como o magmatismo tardí a pós-colisional (<2020 Ga).

Quanto às correlações desse ciclo paleoproterozoico na contraparte oeste africana, apesar da falta de dados geocronológicos e geoquímicos, uma diferença marcante é o magmatismo sideriano, apenas encontrado no lado brasileiro. O embasamento Kimeziano na região do Congo parece se correlacionar com o Complexo Juiz de Fora no range de idades riacianas e também pelas presenças de grãos de zircão juvenis, se configurando como uma grande linha de pesquisa futura na correlação riaciana entre Brasil e África.

O estudo geocronológico e geoquímico isotópico dessa dissertação reúne evidências locais sobre o Complexo Juiz de Fora e que podem ser sumarizadas nos tópicos abaixo:

- a) O arco Juiz de Fora foi um arco de grande amplitude temporal, com pelo menos 3 episódios magmáticos gerados ao longo do Sideriano e Riaciano. O Complexo Juiz de Fora na área de estudo possui protólitos dioríticos siderianos de arco, fato inédito na literatura. Esse magmatismo é juvenil à moderadamente juvenil e a contribuição arqueana é pouco frequente;
- b) O episódio magnético de arco datado do Riaciano é moderadamente juvenil à evoluído. A contribuição arqueana é clara nessas amostras e se relaciona ao input de cristais de zircão detriticos arqueanos nas fontes juvenis. Baseado nas assinaturas de Lu-Hf, as amostras riacianas do Complexo Juiz de Fora na área de estudo não são tão juvenis se comparado à outras ocorrências do CJF à norte;
- c) A contribuição crustal arqueana a partir de dados Lu-Hf é nítida em todas as amostras, enquanto no sistema Sm-Nd essa contribuição é tímida. Esse *decoupling* entre os sistemas Sm-Nd e Lu-Hf se configura uma linha de pesquisa futura para o Complexo Juiz de Fora, já que um substrato arqueano para o Juiz de Fora deve ser investigado nessa unidade. Grãos de zircão herdado de até 2.52 Ga reportados nesse trabalho não são conclusivos;
- d) Os granitoides do Complexo Juiz de Fora possuem pelo menos 3 suites magmáticas cálcio-alcalinas, registradas pelos eventos magmáticos de arco riaciano entre 2.2 e 2.1 Ga (1-plútuns TTG; 2- sanukitóides; 3- grupo Ca3a), uma suíte composta por adakitos de alta sílica (pós 2.09 Ga) e outra de granitóides de alto Ba-Sr pós-colisionais (possivelmente posteriores à 2.0 Ga). Além disso, há um episódio granítico intra-placa no Estateriano marcado por granitos anorogênicos;
- e) Há pelo menos três séries magmáticas toleíticas no Complexo Juiz de Fora: uma sideriana juvenil (gabros e dioritos toleíticos de ca. 2.44-2.42 Ga) e outra riaciana também juvenil (ca. 2.13 Ga) e outra de assinatura E-MORB relacionada possivelmente relacionada à extensão Meso-Neoproterozoicas das bacias Carandaí e Andrelândia;
- f) O metamorfismo paleoproterozoico (2.03-2.02 Ga) foi descrito na área de estudo por grãos e bordas de zircão metamórfico e por cristais de zircão cristalizados de um líquido anatético desse evento metamórfico;

- g) Uma perturbação no sistema isotópico Lu-Hf foi identificada no granulito máfico (BP-CM-151). Esse distúrbio pode estar relacionado à fracionamentos no sistema Lu-Hf devido sucessivos metamorfismos de alto grau (Schmitz *et al.* 2004) nessa amostra;
- h) No Complexo Juiz de Fora ocorre uma série alcalina relacionado à magmatismo intra-placa estateriano e ele tem caráter bimodal (rochas básicas e ácidas), comum à riftes intracontinentais. Um episódio magmático intraplaca foi detectado na área de estudo e é correlacionável ao magmatismo anorogênico da suíte Borrachudos (Bloco Guanhães) e a sauíte Lagoa Real (Bloco Gavião);
- i) O metamorfismo brasileiro (600 a 580 Ma) está presente na maioria das amostras da área de estudo.

Com relação a pesquisas futuras, recomenda-se o estudo de elementos traços e o de isótopos de Oxigênio em zircão, para a investigação de fontes crustais ou mantélicas nos diferentes episódios magmáticos do Complexo Juiz de Fora.

REFERÊNCIAS

- Aguilar Gil, C., Alkmim, F.F., Lana, C., Farina, F., 2017. Paleoproterozoic assembly of the São Francisco craton, SE Brazil: new insights from UePb titanite and monazite dating. *Precambrian Research*, **289**: 95–115.
- Allègre C. J., Poirer J.P., Humler E., Hofmann A. W. 1995. The chemical composition of the Earth. *Earth Planetary Science Letters*. 134:515–526.
- Alkmim F.F. & Teixeira W. 2017. The Paleoproterozoic Mineiro Belt and the Quadrilátero Ferrífero In: Heilbron M., Cordani U., Alkmim F.F. (eds.). *São Francisco Craton, Eastern Brazil: Tectonic Genealogy of a Miniature Continent*. Regional Geology Reviews. Springer, p. 71-94.
- Alkmim F.F. & Teixeira W. 2017. The Paleoproterozoic Mineiro Belt and the Quadrilátero Ferrífero In: Heilbron M., Cordani U., Alkmim F.F. (eds.). *São Francisco Craton, Eastern Brazil: Tectonic Genealogy of a Miniature Continent*. Regional Geology Reviews. Springer, p. 71-94.
- Alkmim, F.F., Brito Neves, B.B., Alves, J.A.C., 1993. Arcabouço tectônico do Cráton do São Francisco e uma revisão. In: Dominguez, J.M., Misi, A. (Eds.), O Cráton do São Francisco. Reunião Preparatória do 2º Simposio sobre o Cráton do São Francisco, pp. 45e62. Salvador, SBG/Núcleo BA/SE/SGM/CNPq.
- Almeida J.C.H., Tupinambá M, Heilbron M., Trouw R. 1998. Geometric and kinematic analysis at the Central Tectonic Boundary of the Ribeira belt, Southeastern Brazil, In: SBG, Congresso Brasileiro Geologia. Anais, v.39, p. 32.
- André J.L.F., Valladares C.S., Duarte BP. 2009. O Complexo Juiz de Fora na região de Três Rios (RJ): Litogegeoquímica, geocronologia U-Pb (LA-ICPMS) e geoquímica isotópica de Nd e Sr. *Revista Brasileira de Geociências*, **39**(4):773–793.
- Araujo, L.E.A.B., Heilbron, M., Valeriano, C.M., Teixeira, W., Neto, C.C.A. 2019. Lithogeochemical and Nd-Sr isotope data of the orthogranulites of the Juiz de Fora complex, SE-Brazil: insights from a hidden Rhyacian Orogen within the Ribeira belt. *Brazilian Journal of Geology*, **Vol.49**, n.3, e20190007.
- Armstrong, R.L., 1981. Radiogenic isotopes; the case for crustal recycling on a near-steady-state no-continental-growth Earth. Royal Society of London Philosophical Transactions 301, 443–472.
- Arth, J.G., Hanson, G.N., 1972. Quartz diorites derived by partial melting of eclogite or amphibolite at mantle depths. *Contributions to Mineralogy and Petrology*, 37,: 161–174.
- Ávila, C.A., Teixeira, W., Bongiolo, E.M., Dussin, I.A., 2014. The Tiradentes suite and its role in the Rhyacian evolution of the Mineiro belt, São Francisco Craton: Geochemical and U-Pb geochronological evidences. *Precambrian Research*, **243**: 221–251.

Ávila, C.A., Teixeira, W., Cordani, U.G., Moura, C.A.V., Pereira, R.M. 2010. Rhyacian (2.23–2.20) juvenile accretion in the southern São Francisco craton, Brazil: Geochemical and isotopic evidence from the Serrinha magmatic suite, Mineiro belt. *Journal of South American Earth Sciences*, **29**:143–159.

Babinski M., Brito-Neves B.B., Machado N., Noce C.M., Uhlein A., Van Schmus W.R., 1994. Problema na metodologia U/Pb em zircões de vulcânicas continentais: o caso do Grupo Rio dos Remédios, Supergrupo Espinhaço, no Estado da Bahia. In: 38º Congresso Brasileiro de Geologia. Camboriú, Boletim de Resumos Expandidos, SBG, 2, pp. 409–410.

Bahlburg, H., Vervoort, J.D., DuFrane, S.A., Carlotto, V., Reimann, C., Cárdenas, J., 2011. The U-Pb and Hf isotope evidence of detrital zircons of the Ordovician Ollantaytambo Formation, southern Peru, and the Ordovician provenance and paleogeography of southern Peru and northern Bolivia. *Journal of South America Earth Sciences*, **32**:196–209.

Barbosa, J. S. F. and Sabaté, P. 2002. Geological features and the Paleoproterozoic collision of four Archean crustal segments of the São Francisco Craton, Bahia, Brazil. A synthesis. *Anais da Academia Brasileira de Ciências*, **74**: 343–359.

Barbosa, J. S. F., Peucat, J.-J. et al. 2008. Petrogenesis of the late-orogenic Bravo granite and surrounding high-grade country rocks in the Palaeoproterozoic orogen of Itabuna–Salvador–Curacá block, Bahia, Brazil. *Precambrian Research*, **167**:35–52.

Barbosa N.S., Teixeira W., Ávila C.A., Montecinos P.M., Bongiolo E.M., Vasconcellos F.F. 2018. U-Pb geochronology and coupled Hf-Nd-Sr isotopic-chemical constraints of the Cassiterite Orthogneiss (2.47–2.41-Ga) in the Mineiro belt, São Francisco craton: Geodynamic fingerprints beyond the Archean-Paleoproterozoic Transition. *Precambrian Research*, **326**:399–416.

Barbosa, N.S., Teixeira, W., Ávila, C.A., Montecinos, P.M., Bongiolo, E.M., 2015. 2.17–2.10 Ga plutonic episodes in the Mineiro belt, São Francisco Craton, Brazil: U-Pb ages, geochemical constraints and tectonics. *Precambrian Research*, **270**, 204–225.

Barbosa N.S., Teixeira W., Ávila C.A., Montecinos P.M., Bongiolo E.M., Vasconcellos F.F. 2018. U-Pb geochronology and coupled Hf-Nd-Sr isotopic-chemical constraints of the Cassiterite Orthogneiss (2.47–2.41-Ga) in the Mineiro belt, São Francisco craton: Geodynamic fingerprints beyond the Archean-Paleoproterozoic Transition. *Precambrian Research*, **326**:399–416.

Bellieni G., Comin-Chiaromonti P., Marques L.S., Melfi A.J., Piccirillo E.M., Nardy A.J.R., Roisemberg, A. 1984. High and low TiO₂ flood-basalts from the Paraná Plateau (Brazil): petrology and geochemical aspects bearing on their mantle origin. *Neues Jahrbuch Miner. Abh.*, **150**:273–306.

Bento dos Santos T., Munhá J.M., Tassinari C.G.G., Fonseca P.E., Dias Neto C. 2011. Metamorphic P-T evolution of granulites in the central Ribeira Fold Belt, SE Brazil, *Geosciences Journal*, **15**(1):27–51.

Bersan, S.M., Costa, A.F.O., Danderfer Filho A., Abreu F. R., Lana, C., Queiroga, G., Storey, C., Moreira, H. 2020. Paleoproterozoic juvenile magmatism within the northeastern sector of

the São Francisco paleocontinent: Insights from the shoshonitic high Ba-Sr Montezuma granitoids. *Geoscience Frontiers*, in press.

Bersan, S.M., Danderfer Filho A., Abreu F. R., Lana, C. 2018. Petrography, geochemistry and geochronology of the potassic granitoids of the Rio Itacambiruçu Supersuite: implications for the Meso- to Neoarchean evolution of the Itacambira-Monte Azul block. *Brazilian Journal of Geology*, **48**(1): 1-24.

Black, L.P., Kamo, S.L., Allen, C.M., Aleinikoff, J.N., Davis, D.W., Korsch, R.J. and Foudoulis, C., 2003. TEMORA 1: a new zircon standard for Phanerozoic U-Pb geochronology. *Chemical geology*, **200**(1-2), pp.155-170.

Brito-Neves B.B., Sá J.M., Nilson A.A., Botelho N.F. 1995. A Tafrogênese Estateriana nos blocos paleoproterozóicos da América do Sul e processos subsequentes. *Geonomos*, Vol.3(2):1-21.

Boynton W.V. 1984. Cosmochemistry of the rare earth elements; meteorite studies. In: Henderson, P. (eds.). *Rare earth element geochemistry*. Amsterdam, Elsevier Sci. Publ. Co., p. 63-114.

Bruno, H., Elizeu, V., Heilbron, M., Valeriano, C.M., Strachan, R., Fowler, M., Bersan, S., Moreira, H., Dussin, I., Silva, L.G.E., Tupinambá, M., Almeida, J.C.H., Neto, C., Storey, C. 2020. Neoarchean and Rhyacian TTG-Sanukitoid suites in the southern São Francisco Paleocontinent, Brazil: Evidence for diachronous change towards modern tectonics. *Geoscience Frontiers*, in press.

Cameron W.E., Nisbet E.G., Dietrich V.J. 1979. Boninites, komatiites and ophiolitic basalts. *Nature*, **280**: 550-553.

Campos Neto, M.C. 2000. Orogenic Systems from Southwestern Gondwana: An approach to Brasiliano-PanAfrican Cycle and Orogenic Collage in Southeastern Brazil. In: Cordani, U.G.; Milani, E.J.; Thomaz Filho, A.; Campos, D.A. (Eds.). *Tectonic Evolution of South América*. Rio de Janeiro, 31st International Geological Congress, Rio de Janeiro, p. 335–365.

Cardoso C.D., Ávila C.A., Neumann R., Oliveira E.P., Valeriano C.M., Dussin I. 2019. A Rhyacian continental arc during the Evolution of the Mineiro belt, Brazil: constraints from the Rio Grande and Brumado metadiorites. *Lithos*, **326-327**:246-264.

Carvalho, M. J. and Oliveira, E. P. 2003 Geologia do tonalito Itareru, bloco Serrinha, Bahia: uma intrusão sin-tectônica do início da colisão continental no segmento norte do orógeno Itabuna - Salvador - Curaçá. *Revista Brasileira de Geociências*, **33** (Suplemento), 55–68.

Cawood, P.A., Kröner, A., Collins, W.J., Kusky, T.M., Mooney, W.D., Windley, B.F., 2009. Accretionary Orogens through Earth history. In: Cawood, P.A., Kröner, A. (Eds.), *Earth Accretionary Systems in Space and Time*. Geol. Soc. (Lond.) Spec. Publ. 318, 1–36.

Chemale Jr. F., Dussin I.A., Alkmim F.F., Martins, M.S. Queiroga, G., Armstrong R., Santos M.N. 2012. Unravelling a Proterozoic basin history through detrital zircon geochronology: the case of the Espinhaço Supergroup, Minas Gerais, Brazil. *Gondwana Research*, **22**:200–206.

- Cheng Q.C., Macdougall J.D., Lugmair G.W. 1993. Geochemical studies of Tahiti, Taehitia and Mehetia, Society island chain. *Journal of Volcanology and Geothermal Research*, 55:155-184.
- Clift P. D., Vannucchi P., Morgan J. P. (2009) Crustal redistribution, crust–mantle recycling and Phanerozoic evolution of the continental crust. *Earth-Science Reviews*, 97:80–104.
- Conceição, H., Silva, R. M. L., Macambira, M. J. B., Scheller, T., Marinho, M. M., Correia, R. D. 2003. 2,09 Ga idade mínima da cristalização do batólito sienítico Itiúba: um problema para o posicionamento do clímax do metamorfismo granulítico (2,05–2,08 Ga) no cinturão móvel Salvador-Curaçá, Bahia. *Revista Brasileira de Geociências*, 33, 395–398.
- Cordani, U.G. and K. Sato, 1999. Crustal evolution of the South American Platform, based on Sm-Nd isotopic systematic on granitoid rocks. *Episodes*, 22: 167–173.
- Cordani U.G., Delhal L., Ledent O. 1973. Orogénèses Superposées dans le precambrien du Brésil Sud-Oriental (États de Rio de Janeiro et de Minas Gerais). *Rev. Bras. Geociências*.3(1):1-22.
- Corfu, F., Hanchar, J.M., Hoskin, P.W. and Kinny, P., 2003. Atlas of zircon textures. *Reviews in mineralogy and geochemistry*, 53(1), pp.469-500.
- Costa, A.G. 1998. The granulite-facies rocks of the northern segment of the Ribeira Belt, eastern Minas Gerais, SE Brazil. *Gondwana Research*, n.1:367-372.
- Cox K.G., Bell J.D., Pankhurst R.J. 1979. The interpretation of igneous rocks. London, Allen and Unwin, 450p.
- Crawford A.J., Falloon T.J., Green D.H. 1989. Classification, petrogenesis and tectonic setting of boninites In: Crawford A.J. (eds.). Boninites. London: Unwin-Hyman, p. 1-49.
- Cutts, K., Lana, C., 2019. The complex tale of Mantiqueira and Juiz de Fora: A comment on “Eoarchean to Neoproterozoic crustal evolution of the Mantiqueira and Juiz de Fora Complexes, SE Brazil: Petrology, geochemistry, zircon U-Pb geochronology and Lu-Hf isotopes”. *Precambrian Research*, 332: 105305.
- Cutts, K., Lana, C., Alkmim, F., Peres, G.G., 2018. Metamorphic imprints on units of the southern Araçuaí belt, SE Brazil: The history of superimposed Transamazonian and Brasiliano orogenesis. *Gondwana Research*, 58: 211-234.
- D'Agrella-Filho, M.S., Teixeira, W., da Trindade, R.I., Patroni, O.A. and Prieto, R.F., 2020. Paleomagnetism of 1.79 Ga Pará de Minas mafic dykes: Testing a São Francisco/Congo-North China-Rio de la Plata connection in Columbia. *Precambrian Research*, 338, p.105584.
- D'Agrella-Filho, M.S., Cordani, U.G., 2017. The Paleomagnetic Record of the São Francisco-Congo Craton. In: Heilbron, M., Cordani, U.G., Alkmim, F.F. (Eds.), *São Francisco Craton, Eastern Brazil. Regional Geology Reviews*. Springer, Cham. Degler R., Pedrosa-Soares A.C., Novo T., Tedeschi M., Silva L.C., Dussin I., Lana C. 2018. Rhyacian-Orosirian isotopic records from the basement of the Araçuaí-Ribeira orogenic system (SE Brazil): Links in the Congo-São Francisco paleocontinent. *Precambrian Research*, 317:179-195.

D'el-Rey Silva, L. J. H., Dantas, E. L., Teixeira, J. B. G., Laux, J. H. & Silva, M. G. 2007. U-Pb and Sm-Nd geochronology of amphibolites from the Curaçá Belt, São Francisco Craton, Brazil: tectonic implications. *Gondwana Research*, **12**:454–467.

Delgado I.M., Souza J.D., Silva L.C., Silveira Filho N.C., Santos R.A., Pedreira A.J., Guimarães J.T., Angelim L.A.A., Vasconcelos A.M., Gomes I.P., Lacerda Filho J.V., Valente C.R., Perrotta M.M., Heineck C.A.. 2002. Escudo Atlântico. In: Bizzi L.A., Schobbenhaus C., Vidotti M., Gonçalves J.H. (eds.), Geologia, Tectônica e Recursos Minerais do Brasil. texto, mapas & SIG. CPRM - Serviço Geológico do Brasil, Brasília, 692 p.

Delhal J., Ledent D., Cordani U. G. 1969. Idades Pb/U; Sr/Rb et Ar/K de Formations Metamorphiques et Granitique du Sud-Est du Brasil (Etats de Rio de Janeiro e Minas Gerais). *Annales de la Société Géologique Belge*, v. 92, pp. 271-283.

Delhal, J., Ledent, D., 1978. Donees geochronologiques dans la region de Matadi (Zaire) relatives a lasyenite de laMpozo et auxmetarhyolites. Departement Geologic et Mineralogie, Musee Royal Afrique Centrale, Rapport annuel 1977, Tervuren, Belgique, 99–110.

Delhal, J. and Ledent, D. 1976. Age et evolution comparee des gneiss migmatitiques prézadiniens des regions de Boma et de Mpoko-Tombagadio (Bas-Zaire). *Ann. Soc. Geol. Belg.*, **99**:165-187.

Dessimoz M., Müntener O., Ulmer P. 2012. A case for hornblende dominated fractionation of arc magmas: the Chelan complex (Washington Cascades). Contributions to Mineralogy and Petrology, **163**:567–589.

DePaolo D.J. 1981. A neodymium and strontium isotopic study of the Mesozoic calc-alkaline granitic batholiths of the Sierra Nevada and Peninsular Ranges, California. *Journal of Geophysical Research: Solid Earth*, **86**:10470-10488.

DePaolo D.J. 1988. *Neodymium isotope geochemistry: An introduction*. New York, 187pp.

Djama, L.M., Leterrier, J-L., Michard, A. 1992. Pb, Sr and Nd isotope study of the basement of the Mayumbian belt (Guena gneisses and Mfoubou granite, Congo): implications for crustal evolution in Central Africa. *Journal of African Earth Sciences*, **14**(2):227–237.

Duarte B.P., Figueiredo M.C.H., Campos Neto M., Heilbron M. 1997. Geochemistry of the granulite fácies orthogneisses of Juiz de Fora Complex, Central Segment of the Ribeira Belt, Southeastern Brazil. *Revista Brasileira de Geociências*, **27**(1):67-82.

Duarte B.P. & Heilbron M. 1999. Metamorphic Evolution of the Early to Medium Proterozoic Granulite Fácies Rocks of the Central Segment of the Brasiliano-Panafrican Ribeira Belt, Southeastern Brazil. In: European Union of Geosciences. Strasbourg, France, 1999. Journal of Conference Abstracts. Strasbourg, Cambridge Publications. 4:792.

Duarte B.P., Heilbron M., Campos Neto M.C. 2000. Granulite/charnockite from the Juiz de Fora Domain, central segment of the Brasiliano-Pan-African Ribeira belt. *Revista Brasileira de Geociências*, **30**:358–362.

- Duarte B.P., Valladares, C.S., Valente S.C., Heilbron M. 2001b. Embasamento Arqueano a Eoproterozóico do Setor Central da Faixa Ribeira. In: SBGq, Congr. Bras. Geoq., 8, e Simpósio de Geoquímica dos Países do Mercosul, 1, Curitiba, 2001. CD-ROM de Resumos Expandidos, 1-5.
- Duarte B.P., Valladares, C.S., Valente S.C., Heilbron M. 2002. Petrologia do embasamento Arqueano a Eo-Proterozóico do setor central da Faixa Ribeira. Submetido para publicação na Geochimica Brasiliensis
- Duarte B.P., Valente S., Heilbron M., Campos Neto M.C. 2004. Petrogenesis of orthogneisses of the Mantiqueira Complex, Central Ribeira Belt, SE Brazil: an Archean to Paleoproterozoic basement unit reworked during the Pan-African Orogeny. *Gondwana Research*, **7**:437–450.
- Dussin, I.A. and Dussin, T.M. 1995. Supergrupo Espinhaço: Modelo de Evolução Geodinâmica. *Geonomos*, **1**:19–26.
- Faure G. 1986. Principles of Isotope Geology, 2nd ed. Wiley, New York, 555 pp.
- Figueiredo M.C.H. & Teixeira W. 1996. The Mantiqueira Metamorphic Complex, Eastern Minas Gerais State: preliminary geochronological and geochemical results. *Anais da Acad. Bras. Cienc.*, **68**(2): 223-246.
- Fischel D.P., Pimentel M.M., Fuck R.A., Costa A.G., Rosière C.A. 1998. Geology and Sm-Nd isotopic data for the Mantiqueira and Juiz de Fora Complexes (Ribeira Belt) in the Abre Campo Manhaçu region, Minas Gerais, Brazil. In: International Conference on Basement Tectonics. *Abstracts*, v.14, p. 21-23.
- Fonseca, A. C. 1993. Esboço geocronológico da região de Cabo Frio, Estado do Rio de Janeiro. PhD thesis, University of São Paulo, Brazil.
- Frost B.R., Arculus R.J., Barnes C.G., Collins W.J., Ellis D.J., Frost C.D. 2001. A geochemical classification of granitic rocks. *Journal of Petrology*, **42**:2033-2048.
- Fyfe, W.S., 1978. Evolution of the Earth's crust: modern plate tectonics to ancient hot-spot tectonics? *Chemical Geology* **23**, 89–114.
- Gerdes, A., Zeh, A., 2006. Combined U-Pb and Hf isotope LA-(MC-)ICP-MS analyses of detrital zircons: comparison with SHRIMP and new constraints for the provenance and age of an Armorican metasediment in central Germany. *Earth Planet. Sci. Lett.*, **249**:47–61.
- Gerdes, A., Zeh, A., 2009. Zircon formation versus zircon alteration – new insights from combined U-Pb and Lu-Hf in-situ LA-ICP-MS analyses, and consequences for the interpretation of Archean zircon from the Central Zone of the Limpopo Belt. *Chem. Geol.*, **261**: 230–243.
- Gonçalves L., Farina F., Lana C., Pedrosa-Soares A.C., Alkmim F., Nalini H.A. 2014. New U-Pb Idades and lithochemical attributes of the Ediacaran Rio Doce magmatic arc, Araçuaí confined orogen, Southeastern Brazil. *Journal of South America Earth Science*, **52**:1–20.

- Goscombe B.D., Gray D. 2007. The Coastal Terrane of the Kaoko Belt, Namibia: outboard arc-terrane and tectonic significance. *Precambrian Research*, 155:139–158.
- Goscombe B.D., Gray D. 2008. Structure and strain variation at mid-crustal levels in a transpressional orogen: a review of Kaoko Belt structure and the character of West Gondwana amalgamation. *Gondwana Research Focus Paper*, 13:45–85.
- Goscombe B.D., Foster D.A., Gray D., Wade B., Marsellos A., Titus J. 2017b. Deformation correlations, stress field switches and evolution of an orogenic intersection: the Pan-African Kaoko-Damara orogenic junction, Namibia. *Geoscience Frontiers*, 8:1187–1232.
- Glikson, A.Y., 1971. Primitive Archean element distribution patterns: chemical evidence and geotectonic significance. *Earth and Planetary Science Letters* 12, 309–320.
- Guimarães, J. T. 2005. Projeto Ibitiara-Rio de Contas, Estado da Bahia, Escala 1:200.000. Serviço Geológico do Brasil, CPRM, 217p.
- Greene, A. R., S. M. DeBari, P. B. Kelemen, J. Blusztajn, and P. D. Clift (2006), A detailed geochemical study of island arc crust: The Talkeetna Arc section, south-central Alaska, *J. Petrol.*, 47, 1051– 1093.
- Grochowski, J., Kuchenbecker, M., Barbuena, D., Novo, T.A. 2019. Os plútôns Felício e Mercês: registros da orogênese riaciana-orosiriana no Bloco Guanhães. In: IV Simpósio do Cráton São Francisco (SCSF), Aracaju. *Anais*, p. 42.
- Guimarães, J.T., Teixeira, L.R., Silva, M.G., Martins, A.A.M., Filho, E.L.A., Loureiro, H.S.C., Arcanjo, J.B., Dalton de Souza, J., Neves, J.P., Mascarenhas, J.F., Melo, R.C., Bento, R.V., 2005. Datações U/Pb em rochas magmáticas intrusivas no Complexo Paramirim e no Rifte Espinhaço: Uma contribuição ao estudo da Evolução Geocronológica da Chapada Diamantina. In: SBG/BA-SE, Simpósio do Cráton do São Francisco, Salvador, Anais de Resumos Expandidos, pp.159e161.
- Hacker, B.R., Mehl, L., Kelemen, P.B., Rioux, M., Behn, M.D., Luffi, P., 2008. Reconstruction of the Talkeetna intra-oceanic arc of Alaska through thermobarometry. *J. Geophys. Res.* 113.
- Hanson, G. N. 1980. Rare Earth elements in petrogenetic studies of igneous systems. *Annual Review of Earth and Planetary Science*. 8:371-406.
- Hartmann L.A., Endo I., Suita M.T.F., Santos J.O.S., Frantz J.C., Carneiro M.A., Naughton N.J., Barley M.E. 2006. Provenance and age delimitation of Quadrilátero Ferrífero sandstones based on zircon U–Pb isotopes. *Journal of South American Earth Sciences*, 20: 273–285.
- Hasui Y., Carneiro C.D.R., Coimbra A.M. 1975. The Ribeira Fold Belt. *Revista Brasileira de Geociências*, 5:257–267.
- Heilbron M. 1993. *Evolução tectono-metamórfica da Seção Bom Jardim de Minas (MG) – Barra do Piraí (RJ). Setor Central da Faixa Ribeira*. Tese de Doutorado, Inst. de Geociências, Universidade de São Paulo, São Paulo, 268 p.

Heilbron M., Figueiredo M.C.H. (in memorian), Machado R. 1997. Lithogeochemistry of paleoproterozoic orthogranulites from Rio Preto (MG) - Vassouras (RJ) region, central Ribeira Belt. *Revista Brasileira de Geociências*, **27**(1):83-99.

Heilbron M., Tupinambá M., Almeida J.C.H., Valeriano C.M., Valladares C.S., Duarte B.P. 1998. New constraints on the tectonic organization and structural styles related to the Brasiliano collage of the central segment of the Ribeira belt, SE Brazil. In: Abstracts of the International Conference on Precambrian and Craton Tectonics/ International Conference on Basement Tectonics. Ouro Preto, Brasil, *Extended Abstracts*, v. 14, p.15-17.

Heilbron M., Mohriak W.U., Valeriano C.M., Milani E., Almeida J.C.H., Tupinambá M. 2000. From Collision to Extension: The Roots of the Southeastern Continental Margin of Brazil. In: Mohriak W.U., Talwani M. (eds.). *Atlantic Rifts and Continental Margins*, AGU, vol. 115, pp. 1–32.

Heilbron M., Pedrosa-Soares A.C., Campos Neto M., Silva L.C., Trouw R.A.J., Janasi V.C. 2004a. A Província Mantiqueira In: Mantesso-Neto V., Bartorelli A., Carneiro C.D.R., Brito-Neves B.B. (eds.). *O desvendar de um continente: a moderna geologia da América do Sul e o legado da obra de Fernando Flávio Marques de Almeida*, pp. 203–234.

Heilbron M., Valeriano C.M., Tassinari C.C.G., Almeida J.C.H., Tupinambá M., Siga Jr O., Trouw R.A.J. 2008. Correlation of Neoproterozoic terranes between the Ribeira Belt, SE Brazil and its African counterpart: comparative tectonic evolution and open questions. In: Pankhurst R.J, Trow R.A.J, Brito-Neves B.B, De Witt M.J. (eds.). West Gondwana: *Pre-Cenozoic Correlations across the South Atlantic Region*. London, Geological Society, Special Publication, 294 pp. 211-232.

Heilbron M., Duarte B.P., Valeriano C.M., Simonetti A., Machado N., Nogueira J.R. 2010. Evolution of reworked Paleoproterozoic basement rocks within the Ribeira belt (Neoproterozoic), SE-Brazil, based on U/Pb geochronology: Implications for paleogeographic reconstructions of the São Francisco-Congo paleocontinent. *Precambrian Research*, **178**:136-148.

Heilbron M., Euzébio R., Peixoto C., Tupinambá M., Guia C., Peternel R., Silva L.G., Ragatky C.D. 2013. O Complexo Juiz de Fora na Folha Santo Antônio de Pádua 1:100.000: geologia e geoquímica. *Geociências*, **32**:10-23.

Heilbron M., Cordani U, Alkmim, F., Reis H. 2017. Tectonic Genealogy of a Miniature Continent In: Heilbron M., Cordani U.G., Alkmim F.F. (eds.). São Francisco Craton, Eastern Brazil: Tectonic Genealogy of a Miniature Continent. *Regional Geology Reviews*, Springer, pp. 321–330.

Heilbron M, Oliveira C, Lobato M, Valeriano C.M., Dussin I., Dantas E., Simonetti, A., Bruno H., Corrales F., Socoloff E. 2019. The Barreiro suite in the central Ribeira Belt (SE-Brazil): a late Tonian tholeiitic intraplate magmatic event in the distal passive margin of the São Francisco Paleocontinent. *Brazilian Journal of Geology*, **49**(2):1-19.

Hunter, D.R., 1970. The Ancient gneiss complex in Swaziland. Transactions of the Geological Society of South Africa 73, 107–150.

- Hurley, P.M., Almeida de, F.F.M., Melcher, G.C., Cordani, U.G., Rand, J.R., Kawashita, K., Vandoros, P., Pinson, W.H., Fairbairn Jr., H.W., 1967. Test of continental drift by comparison of radiometric ages. A pre-drift reconstruction shows matching geologic age provinces in West Africa and Northern Brazil. *Science*, **157**:495–500.
- Irvine, T.M. and Baragar, W.R. 1971. A guide to the chemical classification of common volcanic rocks. *Canadian Journal of Earth Sciences*, **8**:523–548.
- Jackson, S.E., Pearson, N.J., Griffin, W.L., Belousova, E.A., 2004. The application of laser ablation-inductively coupled plasma-mass spectrometry to in-situ U-Pb zircon geochronology. *Chem. Geo*, **211**: 47–69.
- Janoušek V., Farrow C.M., Erban V. 2006. Interpretation of whole-rock geochemical data in igneous geochemistry: introducing Geochemical Data Toolkit (GCDkit). *Journal of Petrology*, **47**(6):1255–1259.
- Kuribara Y., Tsunogae T, Takamura Y, Santosh M, Costa A, Rosiére C. 2019. Eoarchean to Neoproterozoic crustal evolution of the Mantiqueira and the Juiz de Fora Complexes, SE Brazil: Petrology, geochemistry, zircon U-Pb geochronology and Lu-Hf isotopes. *Precambrian Research*, **323**:82–101.
- Lana, C., Farina, F., Gerdes, A., Alkmim, A., Gonçalves, G.O., Jardim, A., 2017. Characterization of zircon reference materials via high precision U-Pb LA-MC-ICPMS. *J. Anal. At. Spectrom.* **32**: 2011–2023.
- Lana, C., Alkmim, F.F., Armstrong, R., Scholz, R., Romano, R., Nalini, H.A. 2013. The ancestry and magmatic evolution of Archaean TTG rocks of the Quadrilátero Ferrífero province, southeast Brazil. *Precambrian Research*, **230**:1–30.
- Laurent, O., Martin H., Moyen J.F., Doucelance R. 2014 The diversity and evolution of late Archean granitoids: evidence for the onset of ‘modern-style’ plate tectonics between 3.0 and 2.5 Ga. *Lithos*, **205**: 208–235.
- Ledru, P., Johan, V., Milési, J.P., Tegyey, M., 1994. Makers of the last stage of the Paleoproterozoic collision: evidence for 2 Ga continent involving circum-South Atlantic provinces. *Precambrian Research*, **69**:169–191.
- Lerouge, C., Cocherie A., Toteu, S.F., Penaye, J., Milesi, J-P., Tchameni, R., Nsifa, E.N., Fanning, C.M., Deloule, E. 2006. Shrimp U–Pb zircon age evidence for Paleoproterozoic sedimentation and 2.05 Ga syntectonic plutonism in the Nyong Group, South-Western Cameroon: consequences for the Eburnean-Transamazonian belt of NE Brazil and Central Africa. *Journal of African Earth Sciences*, **44**:413–427.
- Ludwig, K.R., 2011. Isoplot/Ex Version 4: A Geochronological Toolkit for Microsoft Excel: Geochronology Center. Berkeley, California, USA. Machado N., Valladares C., Heilbron M., Valeriano C.M. 1996. U-Pb geochronology of the central Ribeira Belt (Brazil) and implications for the evolution of the Brazilian Orogeny. *Precambrian Research*, **79**:347–361.
- Marshak, S., Tinkham, D., Alkmim, F.F., Brueckner, H.K., Bornhorst, T., 1997. Dome and keel provinces formed during Paleoproterozoic orogenic collapse-Diapir clusters or core

complexes? Examples from the Quadrilátero Ferrífero (Brazil) and the Penokean Orogen (USA). *Geology*, **25**: 415–418.

Martin, H. 1986. Effect of steeper Archean geothermal gradient on geochemistry of subduction-zone magmas. *Geology*, **14**: 753– 756.

Maurin, J. C., Mpemba-Boni, J., Pin, C. and Vicat, J. P. 1990. La granodiorite de Les Saras un témoin de magmatisme eburnéen (2 Ga) au sein de la chaîne ouest-congolaise: conséquences géodynamiques. *C. R. Acad. ScL Paris* **310**, 571-575.

McGregor, V.R., 1973. The early Precambrian gneisses of the Godthab district, West Greenland. *Philosophical Transactions of Royal Society of London A273*, 343–358.

McMillan, N.J., Harmon, R.S., Moorbathe, S., Lopez-Escobar, L., Strong, D.F., 1989. Crustal sources involved in continental arc magmatism: a case study of volcano MochoChoshuenco, southern Chile. *Geology*, **17**: 1152–1156.

Medeiros, E.L., 2013. Geologia e geocronologia do complexo Santa Izabel na região de Urandi, Bahia. Universidade Federal da Bahia, p. 203. Dissertação de Mestrado.

Mello, E. F., Xavier, R. P., McNaughton, N. J., Hagemann, S. G., Fletcher, I. & Snee, L. 2006. Age constraints on felsic intrusions, metamorphism and gold mineralization in the Paleoproterozoic Rio Itapicuru greenstone belt, NE Bahia State, Brazil. *Mineralium Deposita*, **40**: 849–866.

Meschede, M. 1986. A method of discriminating between different types of mid-ocean ridge basalts and continental tholeiites with the Nb-Zr-Y diagram. *Chemical Geology*, **56**:207-218.

Miller R. McG. 1983. The Pan-African Damara Orogen of Southwest Africa/Namibia In: Miller R. McG. (eds.). Evolution of the Damara Orogen. Special Publication of the Geological Society of South Africa, vol. 11, pp. 431–515.

Moyen, J.F., Martin, H., 2012. Forty years of TTG research. *Lithos*, **148**: 312–336.

Noce C., Pedrosa-Soares A.C., Silva L.C., Armstrong R., Piuzana D. 2007. Evolution of polycyclic basement complexes in the Araçuaí Orogen, based on U-Pb SHRIMP data: Implications for Brazil Africa links in Paleoproterozoic time. *Precambrian Research*, **159**: 60–78.

Noce, C.M., Machado, N., Teixeira, W. 1998. U–Pb geochronology of gneisses and granitoids in the Quadrilátero Ferrífero (Southern São Francisco Craton): age constraints for Archean and Paleoproterozoic magmatism and metamorphism. *Revista Brasileira de Geociências*, **28(1)**: 95–102.

Novo, T.; Pedrosa-Soares, A.C. ; Noce, C.M. ; Alkmim, F.F. ; Dussin, I. 2010. Rochas charnockíticas do sudeste de Minas Gerais: a raiz granulítica do arco magmático do Orógeno Araçuaí. *Revista Brasileira de Geociências*, v. 40, p. 573-592.

- Oliveira, E. P., Carvalho M. J., McNaughton N. J.. 2004a. Evolução do segmento norte do orógeno Itabuna-Salvador-Curaçá: cronologia da acresção de arcos, colisão continental e escape de terrenos. *Geologia USP, Série científica*, **4** (1):24–39.
- Oliveira E.P., McNaughton N., Armstrong R. 2010. Mesoarchaean to Palaeoproterozoic growth of the northern segment of the Itabuna–Salvador–Curaçá Orogen, São Francisco Craton, Brazil. In: Kusky T, Mingguo Z, Xiao W (eds.) *The Evolving Continents: Understanding Processes of Continental Growth*. Geol Soc London Spec Publ 338: 263–286.
- Oliveira, E. P., Mello, E. F., McNaughton, N. T. 2002. Reconnaissance U-Pb geochronology of early Precambrian quartzites from the Caldeirão belt and their basement, NE São Francisco Craton, Bahia, Brazil: implications for the early evolution of the Palaeoproterozoic Salvador-Curaçá Orogen. *Journal of South American Earth Sciences*, **15**: 349–362.
- Othman, D.B., Polvé, M. and Allègre, C.J., 1984. Nd—Sr isotopic composition of granulites and constraints on the evolution of the lower continental crust. *Nature*, **307**(5951), pp.510–515.
- Pearce, J. A. 1983 Role of the sub-continental lithosphere in magma genesis at active continental margins. In *Continental basalts and mantle xenoliths* (ed. C. J. Hawkesworth & M. J. Norry), pp. 230-249. Nantwich, Cheshire: Shiva.
- Pearce, J.A. and Gale, G.H. 1977. Identification of ore-deposition environment from trace-element geochemistry of associated igneous host rocks: Geological Society, London, Special Publication, 7:14-24.
- Pearce, J.A. and Norry, M.J., 1979. Petrogenetic implications of Ti, Zr, Y, and Nb variations in volcanic rocks. *Contrib. Mineral. Petrol.*, **69**: 33–47.
- Pearce J.A., Harris N.W., Tindle A.G. 1984. Trace element discrimination diagrams for the tectonic interpretation of granitic rocks. *Journal of Petrology*, **25**:956-983.
- Peate D.W., Hawkesworth C.J., Mantovani M.S.M. 1992. Chemical stratigraphy of the Paraná lavas (South America): classification of magma-types and their spatial distribution. *Bulletin of Volcanology*, **55**:119–139.
- Peccerillo, A. and Taylor, S.R. 1976. Geochemistry of Eocene calc-alkaline volcanic rocks from the Kastamonu area, Northern Turkey. *Contribution to Mineralogy and Petrology*, **58**: 63-81.
- Pedrosa-Soares A.C. & Noce C.M. 1998. Where is the suturezone of the Neoproterozoic Aracuaí-West-Congo orogen? In: 14th Int. Conf. Basement Tectonics Abs. Universidade Federal de Ouro Preto, Ouro Preto, Expanded abstracts, 35–37.
- Pedrosa-Soares, A.C., Dussin, I., Nseka, P., Baudet, D., Fernandez-Alonso, M., Tack, L. 2016. Tonian rifting events on the Congo-São Francisco paleocontinent: New evidence from U-Pb and Lu-Hf data from the Shinkakasa plutonic complex (Boma region, West Congo Belt, Democratic Republic of Congo). In: International Geologica Belgica Meeting. Mons, 5., Belgium. Abstract Book..., p. 44.

- Pedrosa-Soares A.C., Wiedmann-Leonardos C.M. 2000. Evolution of the Araçuaí Belt and its connections to the Ribeira Belt In: Cordani U.G., Milani E.J., Thomaz Filho A., Campos, D.A. (eds.). Tectonic Evolution of South America, p. 265–288.
- Pedrosa-Soares A.C., Alkmim F.F. 2011. How many rifting events preceded the development of the Araçuaí-West Congo orogen? *Geonomos*, 19(2):244-251.
- Pedrosa-Soares A.C., Noce C.M., Wiedemann C.M., Pinto C.P. 2001. The Araçuaí–West Congo orogen in Brazil: An overview of a confined orogen formed during Gondwanaland assembly. *Precambrian Research*, 110:307-323.
- Pedrosa-Soares A.C., Alkmim F.F., Tack L., Noce C.M., Babinski M., Silva L.C., Martins-Neto M.A. 2008. Similarities and differences between the Brazilian and African counterparts of Neoproterozoic Araçuaí-West Congo orogen In: Pankhurst R., Trouw R., Brito-Neves B B., De Witt, M.J. (eds.). The Gondwana Peleocontinent in the South Atlantic Region. Geological Society of London, Special Publications, 294, p. 153-172.
- Peucat, J. J., Barbosa, J. S. F., Araújo Pinho I. C., Paquette J. L., Martin H., Fanning, C. M., Menezes Leal A. B., Cruz C. P.S., 2011. Geochronology of granulites from the south Itabuna-Salvador-Curaçá Block, São Francisco Craton (Brazil): Nd isotopes and U-Pb zircon ages. *Journal of South American Earth Sciences*, 31:397–413.
- Pinho, I.C.A.P., Martins, A.A.M., Cruz Filho, B.E., Wosniak, R., A.A.M.M., Oliveira, R.L.M., 2013. Mapa Geológico Folha Brumado (1:100.000). Serviço Geológico do Brasil.
- Porada, H., 1989. Pan-African rifting and orogenesis in southern to equatorial Africa and eastern Brazil. *Precambrian Research*, 44:103–136.
- Ragatky D., Tupinamba M., Heilbron M., Duarte B.P., Valladares C. 1999. New Sm/Nd isotopic data from pre-1.8 Ga basement rocks of central Ribeira Belt, SE Brazil. In: South American Symposium on Isotope Geology, 2. Córdoba, Argentina, Expanded abstracts, p. 433-436.
- Reymer, A., Schubert, G., 1984. Phanerozoic addition rates to the continental crust and crustal growth. *Tectonics* 3 (1), 63–77.
- Rios, C. D.; Davis D. W.; Conceição, H.; Macambira, M. J. B.; Peixoto, A. A.; Cruz Filho, B. E. da, Oliveira L. L. 2000. Ages of granites of the Serrinha nucleus, Bahia (Brazil): an overview. *Revista Brasileira de Geociências*, 30: 74–77.
- Rogers, J.J.W., Santosh, M., 2004. Continents and Supercontinents. Oxford University Press, Oxford, pp. 289.
- Rogers, J.J.W., Santosh, M., 2009. Tectonics and surface effects of the supercontinent Columbia. *Gondwana Research*, 15: 373–380.
- Rosa, M. L. S. 1999. Geologia, geocronologia, mineralogia, litoquímica e petrologia do batólito monzo - sienítico Guanambi – Urandi (SW - Bahia). Unpl. Dr. Thesis. Instituto de Geociências, Universidade Federal da Bahia, Salvador, 186p.

Rudowski, L. Petrologie et geo chimie des granites transamazoniens de Campo Formoso et Carnaíba (Bahia, Brésil), et des phlogopites a emeraudes associées. 1989. 290 f. These (Doctorat en Pétrologie, Géochimie et Métallogénie)-Laboratoire de Géologie Appliquée, Université Paris, Paris, 1989.

Santos C. O. 2017. Caracterização Geoquímica, Isotópica E Idade U-Pb Da Suíte Barreiro, Domínio Juiz De Fora, Faixa Ribeira, MG. Tese de Mestrado, Universidade do Estado do Rio de Janeiro, Rio de Janeiro, 120 p.

Santos, M.M., Lana, C., Scholz, R., Buick, I., Schmitz, M.D., Kamo, S.L., Gerdes, A., Corfu, F., Tapster, S., Lancaster, P. and Storey, C.D., 2017. A new appraisal of Sri Lankan BB zircon as a reference material for LA-ICP-MS U-Pb geochronology and Lu-Hf isotope tracing. *Geostandards and Geoanalytical Research*, **41**(3): pp.335-358.

Santos M.N., Chemale Jr F., Dussin I.A., Martins M.S., Queiroca G., Pinto R.T.R., Santos A.N., Armstrong R. 2015. Provenance and paleogeographic reconstruction of a mesoproterozoic intracratonic sag basin (Upper Espinhaço Basin, Brazil). *Sedimentary Geology*, **318**(1):40-57.

Santosh, M., Maruyama, S., Sato, K., 2009a. Anatomy of a Cambrian suture in Gondwana: pacific-type orogeny in southern India? *Gondwana Research*, **16**: 321–341.

Santos Pinto, M. A., Peucat, J.J., Matin, H., Sabaté, P. 1998. Recycling of the Archaean continental crust: the case study of the Gavião Block, Bahia, Brazil. *Journal of South American Earth Science*, **11**, 487–498.

Shand, S. J., 1943. Eruptive Rocks. Their Genesis, Composition, Classification, and Their Relation to Ore-Deposits with a Chapter on Meteorite. John Wiley & Sons, New York.

Silva, L.C., Pedrosa-Soares, A. C., Armstrong, R., Pinto, C.P., Magalhães, J.T. R., Silva, Pinheiro, M.A.P., Santos, G.G. 2016. Disclosing the Paleoarchean to Ediacaran history of the São Francisco craton basement: The Porteirinha domain (northern Araçuaí orogen, Brazil). *Journal of South American Earth Sciences*, **68**:50-67.

Silva, L.C., 2006. Geocronologia aplicada ao mapeamento regional, com ênfase na técnica U-Pb SHRIMP. Serviço Geológico do Brasil, Publicações Especiais 1, 132.

Schmitt RS, Trouw RAJ, Van Schmus WR, Passchier CW. 2008b. Cambrian orogeny in the Ribeira Belt (SE Brazil) and correlations within West Gondwana: ties that bind underwater. In: Pankhurst RJ, Trouw RAJ, Brito Neves BB, de Wit MJ (eds). West Gondwana: Pre-Cenozoic Correlations Across the South Atlantic Region. Spec Publ Geol Soc London, vol 294, pp 279–296.

Schmitt R.S., Trouw R.A.J., Van Schmus W.R., Pimentel M.M. 2004. Late amalgamation in the central part of Western Gondwana: new geochronological data and the characterization of a Cambrian collision orogeny in the Ribeira belt (SE Brazil). *Precambrian Research*, **133**: 29–61.

Schmitt, R.S., 2001. Orogenia Búzios—Um evento tectonometamórfico cambro-ordoviciano caracterizado no Domínio Tectônico de Cabo Frio, Faixa Ribeira—sudeste do Brasil. *Unpublished PhD Thesis*.

Seixas, L. A. R., Bardintzeff, J. M., Stevenson, R., Bonin, B., 2013. Petrology of the high-Mg tonalites and dioritic enclaves of the ca. 2130 Ma Alto Maranhão suite: Evidence for a major juvenile crustal addition event during the Rhyacian orogenesis, Mineiro Belt, southeast Brazil. *Precambrian Research*, **238**:18–41.

Seixas, L.A.R., David, J., Stevenson, R., 2012. Geochemistry, Nd isotopes and U–Pb geochronology of a 2350 Ma TTG suite, Minas Gerais, Brazil: implications for the crustal evolution of the southern São Francisco craton. *Precambrian Research*, **196**:61–80.

Seth B., Kroner A., Mezger K., Nemchin A.A, Pidgeon R.T, Okrusch M. 1998. Archaean to Neoproterozoic magmatic events in the Kaoko belt of NW Namibia and their geodynamic significance. *Precambrian Research*, **92**:341–363.

Shand S.J. 1943. Eruptive Rocks. 2nd edn. New York, John Wiley, 444 p.

Silva L..C., Armstrong R., Delgado I.M., Pimentel M.M., Arcanjo J.B., Melo R.C. de, Teixeira L.R., Jost H., Cardoso Filho J.M., Pereira L.H.M. 2002. Reavaliação da evolução geológica em terrenos Pré-Cambrianos Brasileiros com base em novos dados U-Pb SHRIMP, Parte I: Limite centro-oriental do Craton do São Francisco na Bahia. *Revista Brasileira de Geociências*, **32**:161–172.

Silva, L. C.; Armstrong, R.; Noce, C. M.; Carneiro, M. A.; Pimentel, M.; Pedrosa Soares, A. C.; Leite, C. A.; Vieira, V. S.; Silva, M. A. da; Paes, J. de. C.; Cardoso Filho, J. M. 2002. Reavaliação da evolução geológica em terrenos pré-cambrianos brasileiros com base em novos dados U-Pb SHRIMP, Parte II: orógeno Araçuaí, cinturão mineiro e Cráton do São Francisco meridional. *Revista Brasileira de Geociências*, **32**, 513–528.

Sláma, J., Košler, J., Condon, D.J., Crowley, J.L., Gerdes, A., Hanchar, J.M., Horstwood, M.S., Morris, G.A., Nasdala, L., Norberg, N., Schaltegger, U., 2008. Plešovice zircon- a new natural reference material for U-Pb and Hf isotopic microanalysis. *Chem. Geol.*, **249**: 1–35.

Smithies R.H., Champion D.C., Sun S.-S. 2004. Early evidence for LILE-enriched mantle source regions: diverse magmas from the c. 3.0 Ga Mallina Basin, Pilbara Craton, NW Australia. *Journal of Petrology*, **45**:1515–1537.

Souza-Oliveira, J.S., Peucat, J.J., Barbosa, J.S.F., Correia-Gomes, L.C., Cruz, S.C.P., Leal, A.B.M., Paquette, J.L., 2014. Lithogeochemistry and geochronology of the subalkaline felsic plutonism that marks the end of the Paleoproterozoic orogeny in the Salvador-Esplanada belt, São Francisco craton (Salvador, state of Bahia, Brazil). *Braz. J. Geol.* **44**:221–234.

Stern R. J., Scholl D. W. (2010) Yin and yang of continental crust creation and destruction by plate tectonic processes. *International Geology Review*, **52**:1–31.

Stowe, C.W., 1973. The older tonalite gneiss complex in the Selukwe area, Rhodesia. In: Lister, L. (Ed.), *Symposium on Granites, Gneisses and Related Rocks*, 3. Geological Society of South Africa Special Publication, pp. 85–95.

- Streckeisen, A. 1974. Classification and nomenclature of plutonic rocks: Recommendations of the IUGS subcommission on the systematics of igneous rocks. *Geologische Rundschau*, 63: 773-786.
- Sun, S.-S., 1980, Lead isotope study of young volcanic rocks from mid-ocean ridges, ocean islands and island arcs: Royal Society of London Philosophical Transactions, ser. A, v. 297, p. 409-445.
- Sun S.-S. and McDonough W. F. 1989. Chemical and isotopic systematics of oceanic basalts: Implications for mantle composition and processes. In *Magmatism in the Ocean Basins*(ed. A. D. Saunders and M. J. Norry), pp. 313–345. Geol. Soc. Spec. Publ. 42.
- Sun, S.-S. and Nesbitt, R.W. 1978. Geochemical regularities and genetic significance of ophiolitic basalts. *Geology*, 6:689-693.
- Tack, L., Wingate, M.T.D., Lie'geois, J.-P., Fernandez-Alonso, M., Deblond, A., 2001. Early Neoproterozoic magmatism (1000–910 Ma) of the Zadinian and Mayumbian groups (Bas-Congo): onset of Rodinia rifting at the western edge of the Congo craton. *Precambrian Research*, 110:227–306.
- Tanaka T., Togashi S., Kamioka H., Amakawa H., Kagami H., Hamamoto T., Yuhara M., Orihashi Y., Yoneda S., Shimizu H., Kunimaru T., Takahashi K., Yanagi T., Nakano T., Fujimaki H., Shinjo R., Asahara Y., Tanimizu M., Dragusaru C. 2000. JNdI-1: a neodymium isotopic reference in consistency with LaJolla neodymium. *Chemical Geology*, 168: 279–281.
- Tarney J. & Jones C.E. C.E. 1994. Trace element geochemistry of orogenic igneous rocks and crustal growth models. *Geological Society of London Journal*, 151, 855-868.
- Taylor, S.R., McLennan, S.M., 1985. *The Continental Crust: Its Composition and Evolution*. Blackwell, Oxford.
- Teixeira, L. R. 2005 (Org.). Projeto Projeto Ibitiara-Rio de Contas: relatório temático de litogegeoquímica. Salvador: Serviço Geológico do Brasil, CPRM, 43p.
- Teixeira, W., Ávila, C.A., Dussin, I.A., Vasques, F.S.G., Hollanda, M.H.M., 2012. Geocronologia U-Pb (LA-ICPMS) em zircão detritico de rochas metassedimentares paleoproterozoicas da parte sul do Craton do São Francisco: proveniência, delimitação temporal e implicações tectônicas. 12º Simpósio de Geologia do Sudeste/16º Simpósio de Geologia de MG. Nova Friburgo, Sociedade Brasileira de Geologia, Anais, CDROM, p. 12.
- Teixeira, W., Ávila, C.A., Nunes, L.C., 2008. Nd–Sr isotopic geochemistry and U–Pb geochronology of Fé granitic gneiss and Lajedo granodiorite: implications for Paleoproterozoic evolution of the Mineiro belt, southern São Francisco Craton. *Geologia USP Série Científica*, 8:53–73.
- Teixeira W., Ávila C.A., Bongiolo E.M., Hollanda M.H.B.M., Barbosa N.S., 2014. Idade and tectonic significance of the Ritápolis batholith, Mineiro belt (Southern São Francisco Craton): U–Pb LA-ICPMS, Nd isotopes and geochemical evidence. In: 9th South American Symposium on Isotope Geology – SSAGI, São Paulo, Brazil. *Program and Abstracts*, p. 225.
- Teixeira W., Ávila C.A., Dussin I.A., Corrêa Neto A.V., Bongiolo E.M., Santos J.O., Barbosa N.S. 2015. Juvenile accretion episode (2.35–2.32 Ga) in the Mineiro belt and its role to the

Minas accretionary orogeny: Zircon U–Pb–Hf and geochemical evidences. *Precambrian Research*, **256**:148–169.

Teixeira W., Ávila C.A., Bongiolo E.M., Hollanda M.H.B.M., Barbosa N.S., 2014. Age and tectonic significance of the Ritápolis batholith, Mineiro belt (Southern São Francisco Craton): U–Pb LA-ICPMS, Nd isotopes and geochemical evidence. In: 9th South American Symposium on Isotope Geology – SSAGI, São Paulo, Brazil. Program and Abstracts, p. 225.

Thiéblemont, D., Callec, Y., Fernandez-Alonso, M., & Chène, F. 2018. A geological and isotopic framework of Precambrian terrains in western Central Africa: An introduction. In S. Siegesmund, M. A. S. Basei, P. Oyhantçabal, & S. Oriolo (Eds.), *Geology of Southwest Gondwana, Regional Geology Reviews* (pp. 107– 132). Berlin, Heidelberg: Springer-Verlag.
 Thiéblemont, D., Castaing, C., Billa, M., Bouton, P., Préat, A. 2009. Notice explicative de la Carte géologique et des Ressources minérales de la République gabonaise à 1/1,000,000. DGMG Editions, Ministère des Mines, du Pétrole, des Hydrocarbures, Libreville, p 384.

Toteu, S.F., Van Schmus, W.R., Penaye, J., Nyobé, J.B. 1994. U–Pb and Sm–Nd evidence for Eburnian and Pan-African high-grade metamorphism in cratonic rocks of southern Cameroon. *Precambrian Research*, **67**:321–347.

Thorpe, R. S., Francis, P. W., & Harmon, R. S. 1981. Andean andesites and crustal growth. Philosophical Transactions of the Royal Society of London A 301: 305–320.

Trouw R.A.J, Heilbron M., Ribeiro A., Paciullo F.V.P, Valeriano C.M., Almeida J.C.H., Tupinambá M., Andreis R.R. 2000. The Central Segment of the Ribeira Belt In: Cordani U.G, Milani E.J., Thomaz-Filho A., Campos D.A. (eds.). Tectonic Evolution of South America, Rio de Janeiro, 31st International Geological Congress, p. 287-310.

Tupinambá M., Teixeira W., Heilbron M. 2000. Neoproterozoic Western Gondwana assembly and subduction-related plutonism: the role of the Rio Negro Complex in the Ribeira Belt, South-eastern Brazil. Revista Brasileira Geociências, 30:7-11.

Tupinambá M., Heilbron M., Duarte B.P., Nogueira J.R., Valladares C., Almeida J.C.H., Silva L.G.E., Medeiros S.R., Guia C., Miranda A.W.A., Ragatky C.D., Mendes J., Ludka I. 2007. Geologia da Faixa Ribeira Setentrional: Estado da Arte e Conexões com a Faixa Aracuaí. Geonomos, 15:67–79.

Tupinambá M., Heilbron M., Teixeira W. 2012. Evolução Tectônica e Magmática da Faixa Ribeira entre o Neoproterozoico e o Paleozoico Inferior na Regiao Serrana do Estado do Rio de Janeiro, Brasil. Anuário do Instituto de Geociências da UFRJ, 35:140-151.

Trompette, R., 1994. Geology of Western Gondwana (2000–500 Ma). Pan-AfricanBrasiliano aggregation of South America and Africa. A.A. Balkema, pp. 350.

Valeriano C.M., Vaz G.S., Medeiros S.R., Neto C.C.A., Ragatky C.D. 2008. The Neodymium isotope composition of the JNdi-1 oxide reference material: results from the LAGIR Laboratory, Rio de Janeiro. In: Proceedings of the VI South American Symposium on Isotope Geology. San Carlos de Bariloche, Argentina, (CD-ROM), pp. 1-2.

- Valladares, C.S., Duarte, B.P., Machado, H.T., Viana, S.M., Figueiredo, P.L.C., 2017. Genesis and evolution of a Paleoproterozoic basement inlier within west Gondwana addressed by Sm/Nd isotopic geochemistry and Zr saturation thermometry. *J. S. Am. Earth Sci.* **80**: 95–106.
- Valladares C.S., Duarte B.P., Heilbron M., Ragatky C.D. 2000. Tectono-magmatic evolution of the western terrane and the Paraíba do Sul klippe of the Neoproterozoic Ribeira orogenic belt, southeastern Brazil. *Revista Brasileira de Geociências, Brasil*, **30**(1):1–6.
- Valladares C.S., Souza S.F., Ragatky C.D. 2002. The Quirino Complex: a Transamazonian Magmatic Arc of the Central Segment of the Brasiliano/Pan-African Ribeira Belt, SE Brazil. *Revista Universidade Rural: Série Ciências Exatas e da Terra, Rio de Janeiro*, **21**(1):49–61.
- Valladares, C.S.; Figueiredo, M.C.; Heilbron, M.; Teixeira, W. 1997. Geochemistry and Geochronology of Paleoproterozoic gneissic rocks of the Paraíba do Sul Complex, Barra Mansa Region, Rio de Janeiro, Brazil. Número Temático: Geoquímica do Pré-cambriano. *Revista Brasileira de Geociências*, **27** (1): 111-120.
- Van Achterbergh, E., Ryan, C.G., Jackson, S.E. and Griffin, W.L., 2001, Data reduction software for LA-ICP-MS: appendix; In Sylvester, P.J. (ed.), Laser Ablation –ICP-Mass Spectrometry in the Earth Sciences: Principles and Applications, Mineralogical Association of Canada Short Course Series, Ottawa, Ontario, Canada. 29, 239-243.
- Veizer, J., Jansen, S.L., 1979. Basement and sedimentary recycling and continental evolution. *Journal of Geology*, **87**: 341–370.
- Verma S.P., Guevara M., Agrawal S. 2006. Discriminating four tectonic settings: Five new geochemical diagrams for basic and ultrabasic volcanic rocks based on log-ratio transformation of major-element data. *Journal of Earth System Science*, **115**:485–528.
- Wang, Q., Xu, J.F., Jian, P., Bao, Z.W., Zhao, Z.H., Li, C.F., Xiong, X.L., Ma, J.L., 2006. Petrogenesis of adakitic porphyries in an extensional tectonic setting, Dexing, South China: implications for the genesis of porphyry copper mineralization. *Journal of Petrology*, **47**:119–144.
- Weber, F., Gauthier-Lafaye, F., Whitechurch, H., Ulrich, M. and El Albani, A., 2016. The 2-Ga Eburnean Orogeny in Gabon and the opening of the Francevillian intracratonic basins: A review. *Comptes Rendus Geoscience*, **348**(8), pp.572-586.
- White, A.J.R., Jakes, P., Christie, D., 1971. Composition of greenstones and the hypothesis of seafloor spreading in the Archaean. Geological Society of Australia Special Publication, 3: 47–56.
- Wise, S.A. and Waters, R.L. 2007. Certificate of Analysis Standard Reference Material® 987 Strontium Carbonate (Isotopic Standard), NIST National Institute of Standards & Technology, 2 pp.
- Williams, I.S., 1998. U–Th–Pb geochronology by ion microprobe. In: McKibben, M.A., Shanks, W.C., Ridley, W.I. (Eds.), *Applications of Microanalytical Techniques to*

- Understanding Mineralizing Processes. *Reviews in Economic Geology*, **7**, pp. 1–35. Wilson, M. 1989. *Igneous Petrogenesis*. Unwin Hyman, London.
- Wilson, J.F., 1973. Granites and gneisses of the area around Mashaba, Rhodesia. Geological Society of South Africa (Special Publication) **3**, 79–84.
- Windley, B.F., Bridgwater, D., 1971. The evolution of Archaean low- and high-grade terrains. Geological Society of Australia Special Publication **3**: 33–46.
- Wu, Y. and Zheng, Y., 2004. Genesis of zircon and its constraints on interpretation of U-Pb age. *Chinese Science Bulletin*, **49**(15), pp.1554-1569.
- Zhao, G., Cawood, P.A., Wilde, S.A., Sun, M., 2002. Review of global 2.1–1.8 Ga orogens: implications for a pre-Rodinia supercontinent. *Earth Science Reviews*, **59**(1): 125–162.
- Zhao, G., Sun, M., Wilde, S.A., Li, S., 2004. A Paleo-Mesoproterozoic supercontinent: assembly, growth and breakup. *Earth Science Reviews*, **67** (1): 91–123.

APÊNDICE A – Lithogeochemical and Nd-Sr isotope data of the orthogranulites of the Juiz de Fora complex, SE-Brazil: insights from a hidden Rhyacian Orogen within the Ribeira belt (Artigo Científico)

ARTICLE

DOI: 10.1590/2317-4889201920190007

BJGEO
Brazilian Journal of Geology



Lithogeochemical and Nd-Sr isotope data of the orthogranulites of the Juiz de Fora complex, SE-Brazil: insights from a hidden Rhyacian Orogen within the Ribeira belt

Lucas Eduardo de Abreu Barbosa Araujo^{1*}, Monica Heilbron^{1,2}, Claudio de Morisson Valeriano^{1,2}, Wilson Teixeira³, Carla Cristine Aguiar Neto¹

Abstract

New petrography, geochemistry and Sm-Nd and Sr data from the orthogranulites of the Juiz de Fora complex in southern Rio de Janeiro State and compiled information provide insights on the petrogenetic and tectonic evolution. The complex comprises several geochemical groups including mafic orthogranulites (three tholeiitic and one alkaline) and felsic orthogranulites (three calc-alkaline and one tholeiitic/low K calc-alkaline). New geochemical and isotope data, combined with available U-Pb data suggest a long evolutionary history from the Paleoproterozoic to the Neoproterozoic. The oldest magmatic episode produced juvenile to slightly contaminated arc-type Rhyacian rocks, as well as granitic rocks related to collision or post-collision episodes. Altogether these rocks integrate part of a dismembered Rhyacian orogen within the Ribeira belt. Few T_{DM} Nd model ages yielded 2.75 to 2.58 Ga, suggesting minor Archean contribution for magma genesis. Some of the basic granulites' bodies yield Meso- to Neoproterozoic T_{DM} Nd model ages, which may refer to an extensional magmatism. Orthogranulites present granulite facies paragenesis, related to the youngest tectonic episode in the Juiz de Fora Complex (Brasiliano Orogeny). The new data are potentially important for Paleoproterozoic reconstruction models, due to the predominantly juvenile character of the Juiz de Fora complex, as similarly worldwide.

KEYWORDS: Paleoproterozoic juvenile arcs; Statherian Taphrogenesis; Juiz de Fora Complex.

INTRODUCTION

The São Francisco Paleocontinent (Heilbron *et al.* 2000, 2004, 2008, Trouw *et al.* 2000), is a landmass that encompasses the Archean nuclei within São Francisco-Congo and adjoining Paleoproterozoic belts. In SE Brazil, the Paleoproterozoic Mineiro, Mantiqueira and Juiz de Fora belts accreted onto the southern São Francisco Archean nuclei in the Siderian to Orosirian (Alkmim & Teixeira 2017, Barbosa *et al.* 2018, Heilbron *et al.* 2010). This important episode of continental crust growth is ascribed to the Minas accretionary orogeny (Teixeira *et al.* 2014, 2015). The São Francisco-Congo Paleocontinent behaved as a stable mass until the Statherian, when an important period of bimodal intraplate magmatism and extensional tectonics resulted in the Espinhaço rift system

(Babinski *et al.* 1994, Dussin & Dussin 1995, Brito-Neves *et al.* 1995, Chemale Jr. *et al.* 2012).

The borders of the São Francisco Paleocontinent were deeply reworked during formation of Western Gondwana in the Neoproterozoic, highlighted by the surrounding marginal belts (Heilbron *et al.* 2010). In this context, the Juiz de Fora complex (JFC) represents one of these reworked basement units that crop out in the Ribeira belt. The JFC has large spatial distribution extending from the limit between the states of Rio de Janeiro and São Paulo to eastern Minas Gerais.

The JFC comprises orthogranulites and orthogneisses of wide compositional variability, and occurs as NE-trending thrust-sheets, with NW vergence and dextral lateral component, tectonically interleaved with Neoproterozoic metasedimentary rocks of the Andrelândia Group. The latter represents one of the supracrustal passive margin units of the Neoproterozoic orogenic system (Heilbron *et al.* 1998, 2004, Trouw *et al.* 2000).

The investigation of the basement inliers in the central segment of the Ribeira belt is one of the key points for understanding the nature of the Neoproterozoic orogen in SE-Brazil (Heilbron *et al.* 1998, 2000, 2010, Noce *et al.* 2007, Degler *et al.* 2018). In a broader view, this system includes the Araçuaí orogen to the north (Pedrosa-Soares & Noce 1998, Pedrosa-Soares & Wiedmann-Leonardos 2000, Pedrosa-Soares *et al.* 2001, 2008), and the Dom Feliciano belt to the south, as well as the West-Congo and Kaoko belts

Supplementary data

Supplementary data associated with this article can be found in the online version: [Supplementary Table A1](#) and [Supplementary Table A2](#).

¹Universidade do Estado do Rio de Janeiro – Rio de Janeiro (RJ), Brazil.
E-mails: lucaseduardo9393@gmail.com, monica.heilbron@gmail.com, wteixeir@usp.br

²Universidade de Salzburg – Salzburg, Austria.

³Universidade de São Paulo – São Paulo (SP), Brazil. E-mail: wteixeir@usp.br

*Corresponding author.



© 2019 The authors. This is an open access article distributed under the terms of the Creative Commons license.

in Africa (Miller 1983, Seth *et al.* 1998, Goscombe & Gray 2007, 2008, Goscombe *et al.* 2017).

In order to contribute to the understanding of the tectonic evolution of the JFC, this work brings new petrographic, geochemical and Nd-Sr isotope data, as well as systematic geologic mapping of the JFC orthogranulites in southern Rio de Janeiro. The new data is compared with previously published U-Pb geochronology and geochemistry works on the study area (Machado *et al.* 1996, Heilbron *et al.* 2010), as well as with regional data from the JFC (Silva *et al.* 2002, Noce *et al.* 2007, Degler *et al.* 2018, Kuribara *et al.* 2019).

TECTONIC SETTING

Ribeira Belt (Hasui *et al.* 1975, Trouw *et al.* 2000, Heilbron *et al.* 2000, 2004, 2008) resulted from multiple diachronic collisions during the Neoproterozoic (ca. 605–520 Ma). From NW to SE, it is divided into four tectono-stratigraphic terranes (Heilbron *et al.* 1998):

- Occidental Terrane, where the study area is located, considered as part of the reworked margin of São Francisco Paleocontinent;
- Paraíba do Sul-Embú Terrane, thrusted over the Occidental Terrane;
- Oriental Terrane, consisted of magmatic arc rocks and associated metasedimentary units;
- Cabo Frio Terrane, which was accreted against the Ribeira belt at ca. 520 Ma (Schmitt *et al.* 2004).

Except for the Oriental Terrane, they comprise Paleoproterozoic basement associations and Meso- to Neoproterozoic metasedimentary units (Valladares *et al.* 2000, 2002, Heilbron *et al.* 2010, Schmitt *et al.* 2004). The collision between the Occidental and Oriental Terranes produced a conspicuous suture zone, the Central Tectonic Boundary (CTB) (Almeida *et al.* 1998). This sector of the Ribeira belt also contains several granitoid rocks of pre-, syn- and post collisional character (Tupinambá *et al.* 2012).

The Occidental Terrane (Heilbron *et al.* 1998) essentially comprises two basement units (Mantiqueira and Juiz de Fora complexes) and the Neoproterozoic Andrelândia Group. The Mantiqueira Complex (Heilbron *et al.* 1998, 2010, Noce *et al.* 2007, Duarte *et al.* 2000, 2004) covers amphibolite facies orthogneisses containing layers of amphibolites and meta-ultramafic lenses (Heilbron *et al.* 2017, Noce *et al.* 2007). During the convergence that produced the Ribeira Belt, two thrust systems were formed in the Occidental Terrane (Fig. 1A), playing important role in the architecture of the Mantiqueira and Juiz de Fora complexes (Heilbron *et al.* 2010). In the lower thrust system (Andrelândia Tectonic Domain), Mantiqueira Complex represents the basement unit, overlain by the Andrelândia Group. In the upper thrust system (Juiz de Fora Domain), supracrustal rocks represent the distal facies of the same metasedimentary unit, but tectonically interleaved with the JFC rocks.

The Juiz de Fora and Mantiqueira basement complexes show deep reworking and crustal shortening during the Neoproterozoic Brasiliano orogeny, given by structural,

metamorphic and geochronological evidence (Heilbron *et al.* 2010, Degler *et al.* 2018). In particular, the JFC and interlayered supracrustal rocks underwent granulite facies metamorphism, as indicated by mineral paragenesis with peak temperatures between 800 and 895°C (Duarte *et al.* 2000, Bento dos Santos *et al.* 2011, Degler *et al.* 2018). Additionally, the JFC rocks exhibit retrograde mineral paragenesis and a pervasive mylonitic foliation, acquired during the final stages of thrusting during the Brasiliano orogeny.

Previous authors reported that the JFC orthogranulites display geochemical compositions varying from basic to acid (Heilbron *et al.* 1997, 1998, 2000, Duarte *et al.* 1997, Noce *et al.* 2007, Kuribara *et al.* 2019), with predominance of enderbitic to charnockitic granulites and subordinated basic granulites. The latter shows tholeiitic character, while felsic granulites display calc-alkaline affinity (Heilbron *et al.* 1998, Duarte *et al.* 1997). The protoliths of the basic granulites are enriched Mid Ocean Ridge Basalts (E-MORB) and Island Arc Tholeiites (IAT) gabbroic rocks formed in extensional or island arc settings. Felsic granulites are interpreted as formed in volcanic arc to syn-collisional tectonic settings (Heilbron *et al.* 1998, Duarte *et al.* 1997, Kuribara *et al.* 2019).

The available zircon U-Pb crystallization ages mainly span between 2.20 to 2.07 Ga (Machado *et al.* 1996, Silva *et al.* 2002, Noce *et al.* 2007, André *et al.* 2009, Heilbron *et al.* 2010, Degler *et al.* 2018, Kuribara *et al.* 2019). In contrast, some mafic granulites with documented zircon U-Pb ages of ca. 2.4 and 1.8 Ga show E-MORB tholeiitic and intraplate alkaline signatures, respectively (Heilbron *et al.* 2010). Locally, ca. 2.98 Ga-old granulite was reported nearby Juiz de Fora (Silva *et al.* 2002) with metamorphic age in zircon rims of $2,856 \pm 44$ Ma. In addition, (E-MORB tholeiitic) mafic granulites have been dated at 766 Ma, in the Miracema region (Heilbron *et al.* 2019, Santos 2017).

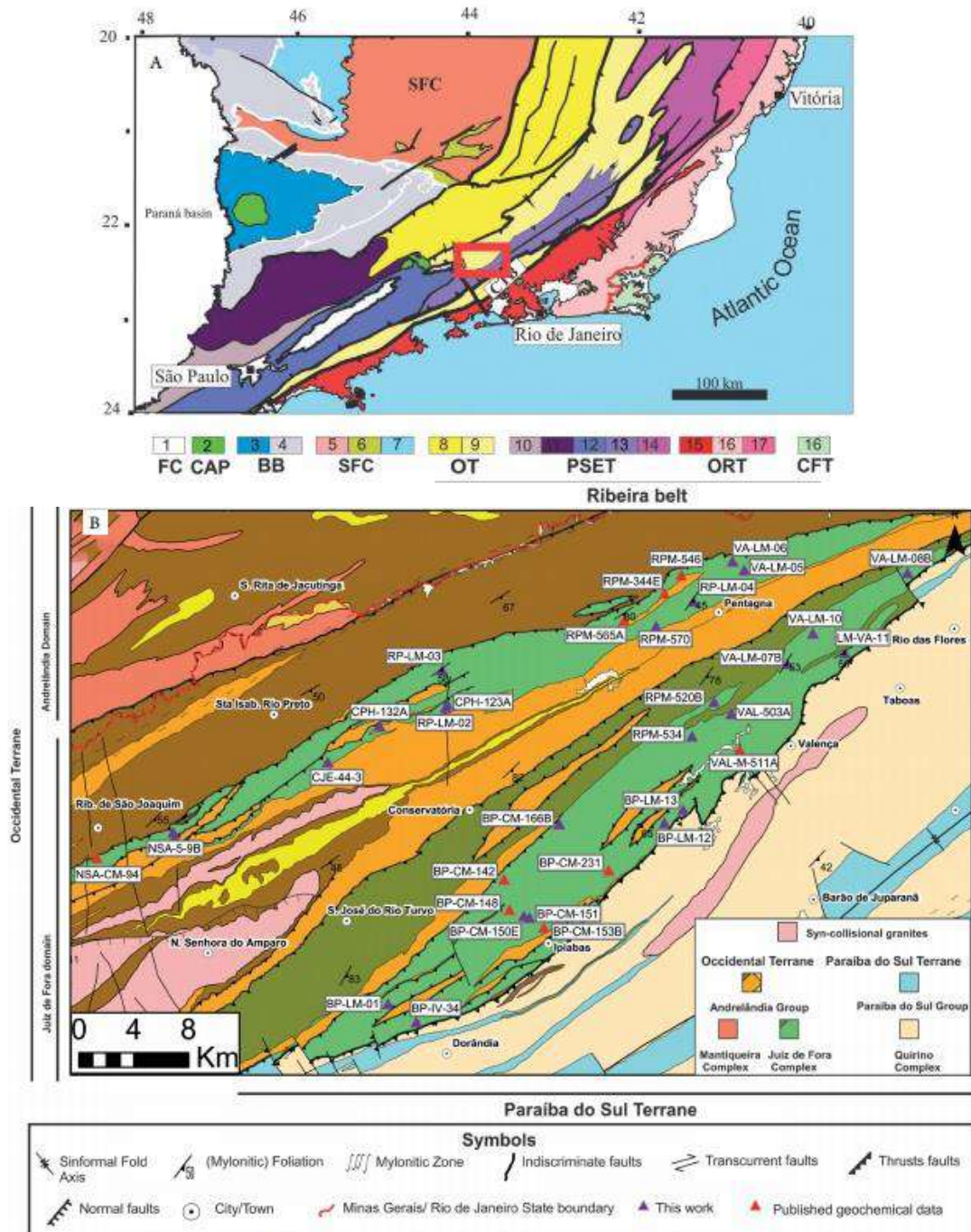
Old fashion whole rock Rb-Sr reference isochrones, integrating several JFC outcrops, yielded ages ranging from 2.65 to 2.25 Ga in a first attempt to unravel the tectonic history of the granulitic rocks (Delhal *et al.* 1969, Cordani *et al.* 1973). However, these ages will be not considered here, given the accuracy of the U-Pb data. In a similar manner, K-Ar ages of 1,570 to 1,220 Ma on pyroxene and plagioclase of the JFC rocks (Delhal *et al.* 1969, Cordani *et al.* 1973) have dubious or no geologic significance. In contrast, a large set of 0.62–0.52 Ga U-Pb ages reported for the JFC rocks better defines the age of regional metamorphic overprint (Machado *et al.* 1996, Noce *et al.* 2007, Bento dos Santos *et al.* 2011, André *et al.* 2009, Heilbron *et al.* 2010, Degler *et al.* 2018, Kuribara *et al.* 2019). This age interval is consistent with previously published amphibole and biotite K-Ar ages (615 to 497 Ma) for granulite rocks from Juiz de Fora and Carangola regions (Delhal *et al.* 1969, Cordani *et al.* 1973). Furthermore, in the same locations, Rb-Sr mineral isochrons yielded ages from 600 to 496 Ma, confirming the relevance of the Neoproterozoic metamorphic overprint (e.g., Cordani *et al.* 1973).

Previously published Sm-Nd T_{DM} model ages for the JFC felsic granulites in the regions of Abre Campo-Manhuaçu (Minas Gerais) and Três Rios (Rio de Janeiro) vary between

2.20 and 2.13 Ga (Fischel *et al.* 1998), and 2.37 Ga (André *et al.* 2009), suggesting juvenile character for the Paleoproterozoic protoliths. Additional Sm-Nd model ages of 2.18 and 2.03 Ga obtained by Degler *et al.* (2018) also support this hypothesis. On the other hand, significantly older Sm-Nd T_{DM} model ages of 3.2 and 2.9 Ga were reported for granulitic rocks ascribed to

the JFC within the Araçuaí belt (Fischel *et al.* 1998). Available Lu-Hf T_{DM} model ages yield results between 3.45 and 2.26 Ga, with most results related with Siderian to Rhyacian periods (Degler *et al.* 2018, Kuribara *et al.* 2019).

From a tectonic point of view, the JFC was interpreted as derived from a Paleoproterozoic intra-oceanic arc (Machado *et al.* 1996,



FC: Fanerozoic cover; CAP: Cenozoic Alkaline plutons; BB: Brasília belt; SFC: São Francisco Craton; OT: Occidental Terrane; PSET: Paraíba do Sul and Espírito Santo Terranes; OBT: Oriental Terrane; GCF: Cabeceira do Galho Terrane.

Figure 1. (A) Tectonic subdivision of the Ribeira belt as proposed by Heilbron *et al.* (2017) with study area in the red rectangle. (B) Geological map showing the NE–SW green stripe of the Laje da Fazenda complex and the location of studied samples.

Heilbron *et al.* 1997, 2010, Silva *et al.* 2002). Alternatively, Kuribara *et al.* (2019) argued that JFC is a volcanic arc magmatic system with two episodes of juvenile magma generation, in the Siderian and the Orosirian. These magmas were sourced by melting of a Paleoarchean microcontinent. Another crust recycling period was proposed by Kuribara *et al.* (2019), in continental arc magmatism on Late Neoproterozoic. Cutts *et al.* (2019) argued that it seems unnecessary to make up an Archean microcontinent as a part of JFC. The Archean T_{DM} Hf model ages obtained by Kuribara *et al.* (2019) could be related to Archean sediments supplied from the São Francisco Craton as detrital zircons that were later subducted below the Siderian juvenile arc of JFC.

The available Rb-Sr, K-Ar, U-Pb, Sm-Nd and Lu-Hf isotope data for the JFC is summarized in the supplementary material (Suppl. Tab. A1).

MATERIALS AND METHODS

Geochemistry

Forty JFC granulite samples were selected for geochemical study. Preparation included their crushing and milling at the *Laboratório de Preparação de Amostras* (LGPA) of Universidade do Estado do Rio de Janeiro. Major and trace element analyses were performed by Activation Laboratories (Ontario, Canada). The analytical techniques included Lithium Metaborate/Tetraborate Fusion and ICP (MS) methodologies. Details on the analytical techniques used are presented in the laboratory website (<http://www.actlabs.com/page.aspx?menu=74&app=244&cat1=595&tp=2&lk=no>).

New and previously published geochemical data (Heilbron 1993, Heilbron *et al.* 1998) were used in order to cover a larger spatial distribution of the JFC within the study area (Fig. 1B). Treatment of the data of different laboratories was carried out using the Geochemical Data ToolKIT (GCDkit) of Janoušek *et al.* (2006) and MS Excel software. For the rare earth element (REE) diagrams, the chondritic contents for normalization were compiled from Boynton (1984).

Sm-Nd and Sr isotopes

For Sm-Nd and Sr analyses, ten basic granulites, twelve enderbites to charno-enderbites and six charnockitic granulites were selected from the same pulp of twenty-eight JFC samples used for the geochemistry study.

Sm-Nd and Sr isotopic analyses were conducted in the Laboratory of Geochronology and Radiogenic Isotopes (LAGIR) of Universidade do Estado do Rio de Janeiro. Chemical procedures were carried out in clean rooms with use of sub-boiling distillation of Milli-Q® water and PA Merck® acids (Cardoso *et al.* 2019). Between 25 and 50 mg of the pulverized samples were subjected to digestion in Savillex® vessels on hot plates, after the addition of proportional amounts of a double ^{149}Sm - ^{150}Nd tracer solution. A mixture of concentrated HF and HNO_3 was applied for 3 days, followed by further digestion with HCl 6N for 2 days. Separation of Sr and REE used cation exchange following conventional techniques

with Teflon columns filled with Biorad® AG50W-X8 resin (100–200 mesh) in HCl medium. For the separation of Sm and Nd, a secondary column was used with the Eichrom LN-B-25S (50–100 µm) resin. After evaporation, Sm, Nd and Sr were separately loaded onto previously degassed Re filaments assembled in double mounts, using H_3PO_4 as ionization activator. Isotope ratios were measured using a ThermoScientific TRITON thermal ionization mass spectrometer (TIMS) in static mode with up to 8 Faraday collectors. Measured isotope ratios are reported with absolute standard errors (2σ) below 10^{-5} . Measured ratios were normalized respectively to the natural constant ratios of $^{146}\text{Nd}/^{144}\text{Nd} = 0.7219$, $^{147}\text{Sm}/^{152}\text{Sm} = 0.5608$ and $^{88}\text{Sr}/^{86}\text{Sr} = 8.3762$. Average $^{143}\text{Nd}/^{144}\text{Nd}$ ratio of repeated measurements of the JNDI-1 standard (Tanaka *et al.* 2000) was 0.512098 ± 0.000006 ($n = 322$). Average $^{87}\text{Sr}/^{86}\text{Sr}$ ratio of the NBS-987 standard (Wise & Waters 2007) was 0.710239 ± 0.000008 ($n = 158$). Repeated analyses of the BCR and AVG rock reference materials from the United States Geologic Survey yielded $^{147}\text{Sm}/^{144}\text{Nd}$ ratios with reproducibility within 1% (Valeriano *et al.* 2008). Neodymium (T_{DM}) model ages were calculated using the depleted mantle model of DePaolo (1981).

RESULTS

Field and petrographic observations

The internal structure of the Juiz de Fora structural domain in the study area (Fig. 1B) is represented by a tectonic interleaving between the orthogranulites of JFC with the metasedimentary rocks of the Andrelândia Group within two NW vergent thrust sheets. A lateral dextral component attesting the oblique collision was reported by Heilbron *et al.* (2000). To the south, the JFC rocks are in tectonic contact with the overlying orthogneiss of the Quirino Complex and the metasedimentary rocks of the Paraíba do Sul group that make up Paraíba do Sul Terrane (Heilbron *et al.* 2000, Tupinambá *et al.* 2007).

The JFC granulites crop out in both the lower and upper thrust sheets, respectively extending along strike for 75 km, between the cities of Manoel Duarte (Minas Gerais) and Ribeirão de São João (Rio de Janeiro), and for 61 km between the cities of Rio das Flores (Rio de Janeiro) and Dorândia (Rio de Janeiro) (Fig. 1B). The outcrops are typically small quarries and road cuts. The rocks display deep green to pale brown colors depending on their primary composition and internal structure. The composition of orthogranulites varies from mafic to felsic (charno-enderbites, enderbites and charnockites) rocks, with predominance of charno-enderbites (Fig. 2A). The samples' geographic coordinates, as well as its petrographic classification, can be found in a supplementary table (Suppl. Tab. A2).

Charno-enderbites occur as the main rock type (Fig. 2B), showing coarse to medium grain size. Normally, enderbites (Fig. 2C), as a variation of charno-enderbites, present a medium to fine grain size and green darker colors. The textures of charno-enderbites and enderbites vary from granoblastic to mylonitic, depending on the location within the thrust sheet pile. Charnockites (Fig. 2D) are commonly coarse-grained pale

light green injections or leucosomes within all rock types cited above. Typical textures are granoblastic (Fig. 3A), with massive aspect. Folded felsic granulites (Fig. 2D) occur in more deformed zones. Charnockites may also occur as the main lithotype in some outcrops, normally with pervasive foliation.

The essential mineralogy of felsic granulites (Fig. 3A) consists of plagioclase, quartz, K-feldspar, orthopyroxene (hypersthene), hornblende, biotite and (diopside) clinopyroxene. Zircon, apatite, ilmenite and magnetite are the accessory minerals. K-feldspar contents are remarkably different among felsic granulites. Charnockites are K-feldspar rich, while K-feldspar in enderbitic terms is rare. Diopside occurs only in enderbites and in some groups of charno-enderbites. Hornblende and biotite are commonly retrograde minerals in all granulitic rocks.

Mafic bands/enclaves and centimeter-thick lenses occur within felsic types (Figs. 2B, 2C and 2D), but can be distinguished as isolated mafic bodies. They show massive structure, medium to fine grain size and deep green original colors. Mafic granulites consist of plagioclase, diopside, hypersthene, hornblende and traces of quartz, with local coronitic garnet around pyroxene (Fig. 3B). Retrograde biotite, sericite and carbonates are also present. Apatite, zircon, magnetite, ilmenite and pyrite are the accessory minerals.

Textures and external colors vary as a function of deformation, with deep green colors and granoblastic textures in the center of the large thrust sheets, and pale green to whitish

colors in the mylonitic varieties along the tectonic contacts with Andrelândia Group rocks. In more deformed granulites, foliation is defined by mafic minerals, with porphyroclasts of orthopyroxene surrounded by hornblende and biotite fringes (Fig. 3C). Ultramylonitic types, very common nearby the city of Conservatoria (Fig. 1B), are represented by highly stretched black and white banded gneisses with minor orthopyroxene relicts. Within felsic mylonitic types, feldspar porphyroclasts with anti-perthitic structures and quartz ribbons (Fig. 3D) are common features.

Geochemistry

Forty samples were divided into mafic and felsic granulites, according to field observation. The former with twelve samples of basic composition, and the latter with 28 samples of intermediate to acid composition. They were classified in magmatic series and then subdivided into subgroups based on REE patterns and field relationships, with four subgroups for each group.

Mafic Granulites

Mafic granulites (Tab. 1) display gabbroic composition (Cox *et al.* 1979) and are subdivided into the alkaline (four samples) and tholeiitic sub-alkaline (eight samples) series (Figs. 4A and B). The tholeiitic trend is marked by iron enrichment in the AFM diagram of Figure 4B (Irvine & Baragar 1971).

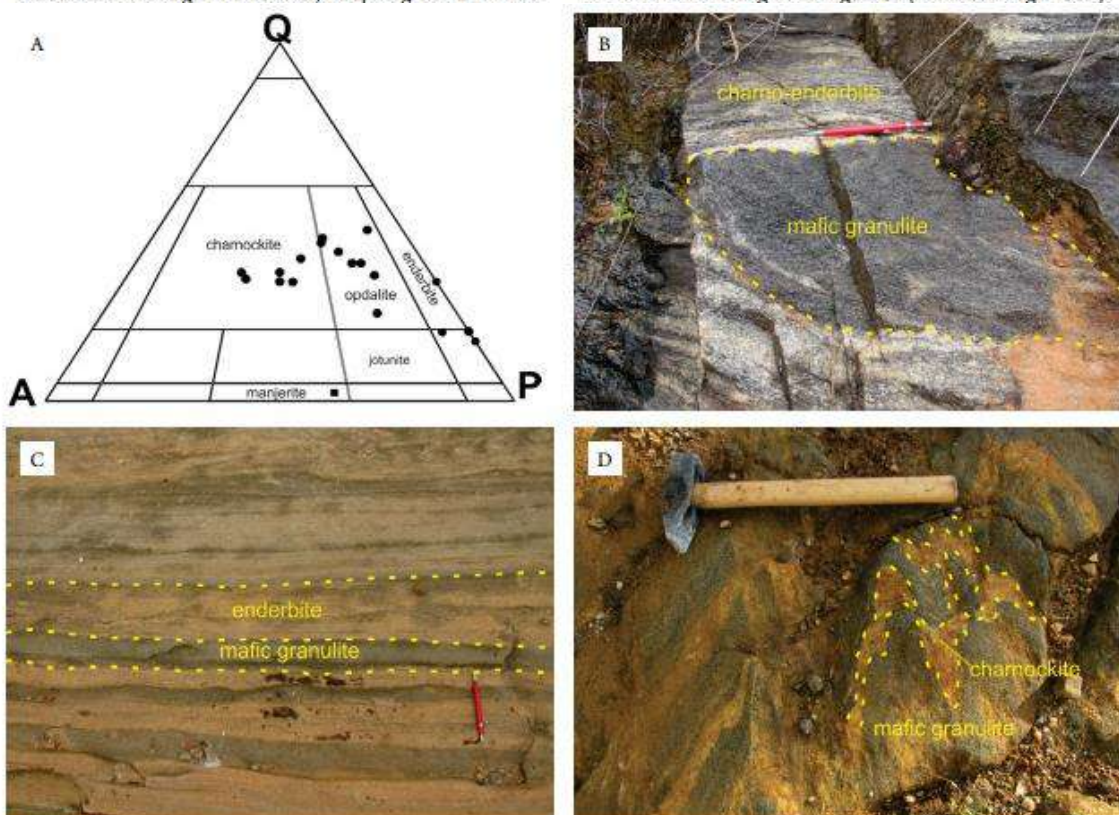


Figure 2. Field aspects of the orthogranulites of the JFC: (A) QAP petrographic diagram (Streckeisen 1974) for the felsic granulites of the studied area; (B) Charnoenderbites with band/enclave of the mafic granulites; (C) Deformed strips of mafic granulites within enderbites; (D) Mafic granulite with folded charnockite leucosomes.



OPX: hypersthene; CPX: diopside; QTZ: quartz; PLG: plagioclase; KF: k-feldspar; HBL: hornblende; BT: biotite; OP: opaque minerals.

Figure 3. Petrographic features of the JFC orthogranulites. (A) mineralogy and granoblastic texture in the charnoenderbite; (B) mineralogy and granoblastic texture in the mafic granulite; (C) grano-porphyroblastic texture in the charno-enderbite, with opx partially substituted by biotite and hornblende; (D) mylonitic texture in a charnockite type with quartz ribbons and feldspar porphyroclasts.

Few samples display CIPW normative nepheline and absence of normative orthopyroxene (Tab. 2), suggesting their affinity with alkaline basalts. The other samples plot in the sub-alkaline field and contain hypersthene and olivine (Tab. 2), therefore classified as olivine tholeiites.

- Alkaline samples occur as mafic bodies in the outcrop, with sharp boundaries with the sic rocks. These rocks are nominated here as BA group, showing high ($> 2.2\%$) TiO_2 (Peate *et al.* 1992, Bellieni *et al.* 1984), enrichment in light rare earth elements (LREE) and conspicuously negative Eu anomaly (Fig. 5A). The tholeiitic rocks display low TiO_2 ($< 2.2\%$) and are heterogeneous in chemical composition. Based on their REE signatures, they were subdivided into three groups, as follows:
- 1) The first tholeiitic group (TH1), with three samples (blue symbols), shows minor LREE enrichment, less prominent negative Eu anomalies and flat heavy rare earth elements (HREE) distribution when compared with the alkaline group (Fig. 5B). Rocks of this group occur as mafic bands/enclaves associated to felsic rocks;
 - 2) The second tholeiitic group (TH2), also represented by three samples (green symbols), displays flatter REE distribution patterns, with subtle LREE enrichment and absence of Eu anomalies (Fig. 5C);
 - 3) The third tholeiitic group (TH3) has the lowest total REE content and displays LREE depletion and a completely flat

REE pattern. Two samples only present these characteristics (Fig. 5D).

Both TH2 and TH3 groups occur as mafic bodies in the outcrop, not always associated with felsic rocks. They also contrast with the TH1 group by their less evolved characteristics and REE distribution patterns, which are compatible respectively with E- and N-MORB basalts, highlighted by La/Sm normalized ratios higher and lower than 1 (Fig. 5D).

Tectonic discrimination diagrams (Fig. 6) corroborate the proposed subdivision, with the BA group plotting in the intraplate fields (Figs. 6A and 6B) or continental rift field (Fig. 6C). The tholeiitic groups plot on plate margin field (Fig. 6A), with the TH1 group related to convergent plate margin (Island Arc Tholeiite) and TH2 and TH3 groups, suggestive of extensional tectonic settings (MORB — Figs. 6B and 6C).

Felsic granulites

The felsic rocks of the JFC show predominantly granodioritic compositions, with minor diorites and granites (Fig. 7A — Cox *et al.* 1979). They display calc-alkaline subalkaline signatures (Figs. 7B and 7C — Irvine & Baragar 1971, Peccerillo & Taylor 1976) with metaluminous character according to their Shand index (Fig. 7D — Shand 1943). Only two

Table 1. Major (%) and trace elements (ppm) data from orthogranulites of the JFC in the studied area.

Samples	RP-LM-2B	VA-LM-7A	BP-CM-151	BP-LM-01	VA-LM-7B	VA-LM-10	BIP-IV-34	VA-LM-8B	VA-LM-11B	RP-LM-04	BP-LM-13	VA-LM-05	VA-LM-06	BP-LM-12	CPH-132	CPH-123A	RP-LM-03	RPM-570
Group	BA	TH1	TH3	TH3	BK	BK	CA1	CA1	CA1	CA1	CA1	CA1	CA1	CA2	CA3	CA3	CA3	
SiO ₂	48.1	50.1	50.2	47.8	56.6	58.8	55.3	59.2	57.1	62.4	64.1	67.00	69.3	63.5	57.6	62.7	63.9	73.3
TiO ₂	2.76	1.35	0.53	12.2	0.6	1.02	0.9	0.64	0.83	0.64	0.57	0.43	0.51	0.58	1.82	0.89	0.57	0.42
Al ₂ O ₃	13.51	16.41	13.5	12.88	19.71	16.52	15.8	16.84	16.83	15.26	14.55	15.47	14.02	16.61	15.41	13.37	15.4	11.9
Fe ₂ O ₃	15.01	11.94	10.43	15.92	6.62	8.16	10.51	7.26	8.00	5.9	7.18	3.59	4.59	5.66	8.14	7.45	5.96	3.11
MnO	0.21	0.17	0.19	0.25	0.1	0.13	0.19	0.09	0.1	0.08	0.15	0.04	0.06	0.09	0.13	0.1	0.11	0.04
MgO	6.18	47	7.96	6.8	2.81	2.99	5.47	3.05	3.53	2.32	3.16	1.52	1.84	2.32	3.65	2.91	2.34	0.38
CaO	9.02	8.52	15.24	13.5	6.62	6.52	6.71	4.58	5.8	4.6	4.49	3.85	3.61	4.7	5.63	4.03	4.03	1.3
Na ₂ O	3.00	3.28	2.01	2.01	5.16	4.53	3.45	3.81	3.66	3.69	3.08	3.61	3.73	3.84	3.06	3.3	4.35	2.09
K ₂ O	1.71	0.56	0.29	0.09	0.58	0.48	0.99	2.72	1.83	2.84	2.72	3.29	1.76	1.54	3.02	3.5	1.23	5.9
P ₂ O ₅	1.21	0.22	0.04	0.11	0.31	0.18	0.26	0.25	0.27	0.23	0.2	0.16	0.1	0.12	0.77	0.32	0.17	0.05
LOI	0.05	21	0.25	-0.28	0.84	0.57	-0.04	0.66	0.65	0.53	0.25	0.9	0.96	0.81	0.62	0.65	1.45	0.32
Total	100.7	99.4	100.7	100.4	99.9	99.9	99.6	99.2	98.6	98.5	100.6	99.9	100.6	99.8	99.2	99.5	98.9	
V	240	236	226	334	98	109	166	89	126	86	75	48	84	80	120	94	56	11
Ba	1021	188	63	13	390	188	656	1072	1163	991	824	913	422	683	1332	1104	265	770
Sr	457	338	142	105	687	523	601	519	679	479	527	416	307	612	555	198	459	207
Y	42	42	12	21	14	15	16	16	14	19	14	14	9	5	27	51	27	84
Zr	241	125	30	42	120	120	121	182	158	213	141	205	148	153	233	292	144	446
Cr	290	70	470	120	50	60	140	<20	80	30	70	30	60	60	110	60	<20	
Co	48	39	49	62	24	28	35	22	27	24	25	23	25	23	26	23	22	19
Ni	130	50	140	120	50	40	60	<20	30	<20	<20	30	30	30	40	40	30	<20
Rb	71	<2	<2	<2	<2	<2	33	100	65	84	72	106	74	53	76	144	31	175
Nb	16	10	1	3	3	7	6	8	8	11	6	10	5	5	24	19	11	21
Hf	5.7	33	0.7	1.3	3	2.8	3	44	3.6	5.4	3.5	5.1	3.4	3.6	54	7	3.8	12.1
Ta	0.9	0.8	0.2	-0.1	0.1	0.6	0.2	0.3	0.2	0.5	0.3	0.4	0.2	0.1	1.3	1.3	0.7	1.9
W	34	35	56	71	74	94	37	77	59	135	126	160	145	102	38	70	87	202
Th	0.9	0.2	0.1	<0.1	0.1	0.4	0.5	2.3	0.2	5.9	0.8	3	1.7	0.4	37	5.8	6.5	132

Table 1. (Cont.). Rare earth elements (ppm) data from orthogranulites of the JFC in the studied area.

Samples	RP-LM-2B	VA-LM-7A	BP-CM-151	BP-LM-01	VA-LM-7B	VA-LM-10	BIP-IV-34	VA-LM-8B	VA-LM-11B	RP-LM-04	BP-LM-13	VA-LM-05	VA-LM-06	BP-LM-12	CPH-132	CPH-123A	RP-LM-3	RPM-570
Group	BA	TH1	TH3	TH3	BK	BK	CA1	CA1	CA1	CA1	CA1	CA1	CA1	CA2	CA3	CA3	CA3	
La	60.80	15.7	2	2.1	18.5	9.5	16.6	34.5	18.9	56.9	25.6	45.4	30.3	19.5	55.9	58	32.1	335
Ce	134	36.7	5.1	7.2	37.4	22.1	40.5	65.7	41.5	111	45.5	80	57.5	36.2	113	127	67.9	636
Pr	16.3	5.6	0.74	1.2	4.4	2.9	5.5	7.3	5.3	11.9	4.9	8	6.1	3.9	13	15.4	7.71	60.6
Nd	68.7	25.4	4.2	6.7	18.7	12.6	24.5	27.6	22.9	42.4	18	27.5	21.3	14.7	49.8	58	29.8	188
Sm	13.3	6.7	1.1	2.5	3.8	3.1	5.6	5.3	5.2	7.4	3.5	4.6	3.3	2.3	9.8	11.8	6.2	29.3
Eu	3.2	1.8	0.4	0.9	1.2	1.3	1.3	1.5	1.5	1.5	1.1	1.3	0.8	1.4	2.23	2.3	0.7	1.7
Gd	11.1	7.2	1.8	3.3	3.5	3.4	4.6	4.4	4.4	5.6	3.1	3.3	2.4	1.7	7.6	10	5.9	18
Tb	1.6	1.3	0.3	0.6	0.5	0.5	0.6	0.6	0.6	0.7	0.5	0.5	0.3	0.2	1.1	1.5	0.9	3
Dy	8.6	7.7	2.2	4.2	2.9	3.2	3.5	3.5	3.2	4.00	2.7	2.6	1.7	1.1	5.9	9.1	5.5	17.1
Ho	1.6	1.6	0.5	0.9	0.5	0.6	0.6	0.6	0.6	0.7	0.5	0.5	0.3	0.2	1.1	1.8	1.1	3.3
Er	4.5	4.7	1.5	2.6	1.5	1.9	1.8	1.6	1.5	2	1.5	1.4	0.8	0.5	3	5.2	3	9.5
Tm	0.6	0.7	0.2	0.3	0.2	0.2	0.2	0.2	0.2	0.2	0.2	0.1	0.1	0	0.4	0.7	0.4	1.4
Yb	3.8	4.7	1.4	2.5	1.3	1.8	1.6	1.4	1.2	1.7	1.4	1.2	0.8	0.5	2.7	5.3	2.9	9.1
Lu	0.6	0.7	0.2	0.4	0.2	0.2	0.2	0.2	0.1	0.2	0.2	0.1	0.1	<1	0.3	0.8	0.4	1.37

samples (RPM-344 and BP-CM 148) show alkaline character, given by their high alkalis (Fig. 7A) and other LILE contents.

Using the same approach based on REE chondrite-normalized signatures, the sub-alkaline samples were tentatively subdivided into four groups (Fig. 8):

- Low-K calc-alkaline rocks (LK group — black symbols) are represented by three dioritic enderbites. They show less fractionated REE pattern, with $(\text{La}/\text{Yb})_{\text{N}}$ ranging between 1.8 and 9.5 and varied Eu anomalies (Fig. 8A);
- CA1 calc-alkaline group (blue symbols) presents dioritic to granodioritic compositions, and enrichment in LREE and flat HREE patterns (Fig. 8B). This group shows $(\text{La}/\text{Yb})_{\text{N}}$ in a range between 6.9 and 25.5;
- CA2 calc-alkaline group (green symbols) is predominantly consisted of granitic rocks. They have characteristically

positive Eu anomalies and more depleted HREE patterns (Fig. 8C). This group presents a more fractionated REE pattern marked by $(\text{La}/\text{Yb})_{\text{N}}$ in a range between 20.6 and 49.6;

- CA3 calc-alkaline group (red symbols) has a more expanded composition, with dioritic to granitic rocks, more enriched in total REE (99.7 to 1,314) with less fractionated REE patterns ($\text{La}/\text{Yb})_{\text{N}} = 6.5$ to 26.6) and prominent negative Eu anomalies (Fig. 8D).

Most samples present magnesian characteristics, except the more evolved rocks of CA2 and CA3 groups, which are ferroan (Fig. 9A — Frost *et al.* 2001). CA1 and LK groups are calcic to calcic-alkalic, while CA2 and CA3 groups are calc-alkalic to alkali-calcic (Fig. 9B — Frost *et al.* 2001). Joining these characteristics, the CA1 and LK groups plot in the magmatic arc field, while the CA2 and CA3 show

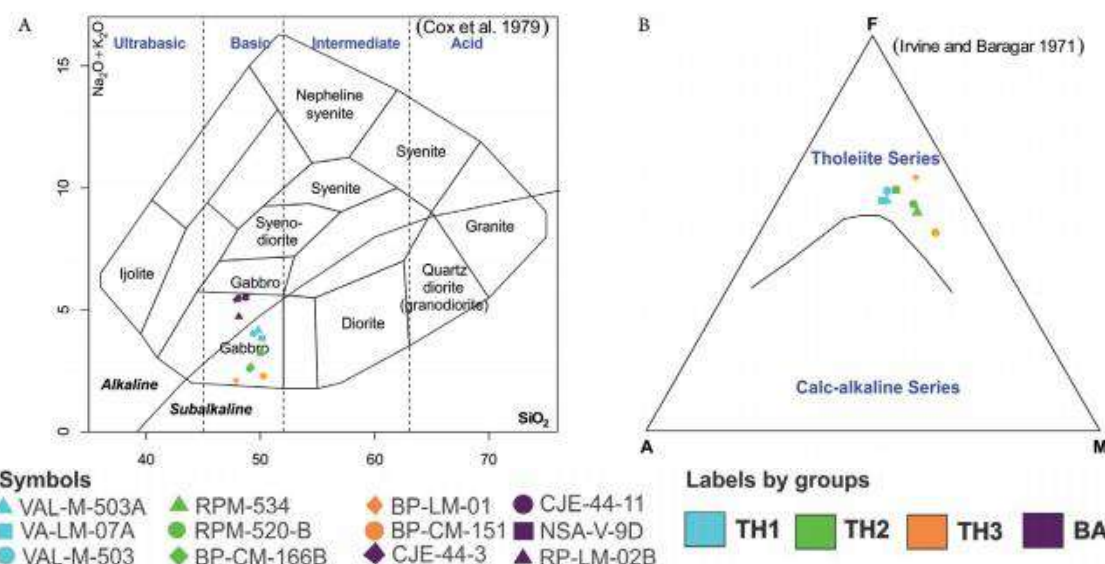


Figure 4. Geochemical diagrams of mafic granulites. (A) TAS diagram (Cox *et al.* 1979) classifying the samples according to its protholiths and magmatic series; (B) Classification of sub-alkaline samples into tholeiitic or calc-alkaline sub-series through AFM diagram (Irvine & Baragar 1971).

Table 2. Normative minerals for the analyzed basic orthogranulites of the JFC.

Samples	Or	Ab	An	Ne	Di	Hy	OI	II	Ap	Sum	Classification	Group
CJE-44-11	8.27	30.0	11.3	2.54	20.60	0.00	17.18	6.65	1.73	98.27	alkalii basalt	BA
RP-LM-02B	10.11	25.4	18.3	0.00	15.52	1.02	22.29	5.26	2.87	100.80	olivine tholeiite	BA
CJE-44-3	8.27	28.8	12.6	2.71	20.88	0.00	16.43	6.65	1.66	98.01	alkalii basalt	BA
NSA-5-9D	8.27	34.5	12.7	0.08	15.12	0.00	19.30	6.27	1.37	97.62	alkalii basalt	BA
VAL-M-503	4.91	27.1	19.7	0.00	20.16	6.19	16.29	3.42	0.55	98.33	olivine tholeiite	TH1
VAL-M-503A	5.08	27.9	20.3	0.00	20.41	5.45	15.45	3.42	0.57	98.59	olivine tholeiite	TH1
VA-LM-07A	3.31	27.8	28.4	0.00	10.47	17.98	6.30	2.58	0.52	97.32	olivine tholeiite	TH1
RPM-520B	1.12	20.3	29.6	0.00	22.72	13.38	8.10	2.85	0.26	98.34	olivine tholeiite	TH2
RPM-534	0.95	21.2	28.1	0.00	24.62	10.66	10.03	2.66	0.28	98.50	olivine tholeiite	TH2
BP-CM-166B	1.95	24.5	24.8	0.00	20.07	16.50	7.25	3.42	0.55	99.02	olivine tholeiite	TH2
BP-CM-151	1.71	16.9	27.0	0.06	39.89	0.00	13.79	1.01	0.10	100.49	alkalii basalt	TH3
BP-LM-01	0.53	17.0	25.9	0.00	34.07	0.70	19.94	2.32	0.26	100.69	olivine tholeiite	TH3

signatures of more evolved arc rocks to syn-collisional granitoids (Fig. 9C — Pearce *et al.* 1984).

Sm-Nd and Sr-Sr-isotopes

The measured and calculated isotope ratios, along with parameters such as $f_{\text{Sm}/\text{Nd}}^{\text{SM}}$, $\varepsilon_{\text{Nd}_{(e)}}$, and T_{DM} and T_{CHUR} model

ages are shown in Table 3. Fractionation factors ($f_{\text{Sm}/\text{Nd}}$) of the samples vary between -0.03 and -0.67. Few samples yielded $^{147}\text{Sm}/^{143}\text{Nd}$ values above 0.17 and very low $f_{\text{Sm}/\text{Nd}}$ ratios between -0.03 and -0.12, suggesting isotopic evolutions very similar to that of the Chondritic Uniform Reservoir (CHUR) (DePaolo 1988). In these cases, their T_{CHUR} model ages were calculated.

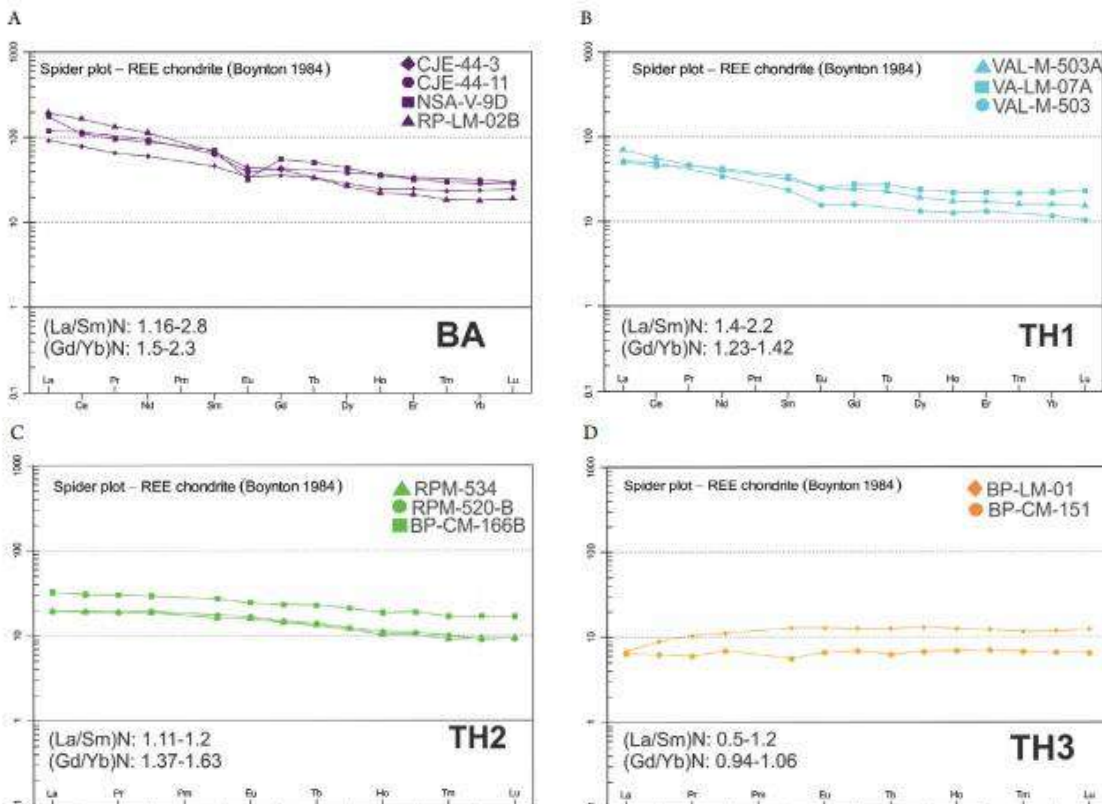


Figure 5. REE's chondrite normalized spidergram (Boynton 1984) of mafic granulites from study area. (A) BA group; (B) TH1 group; (C) TH2 group; (D) TH3 group.

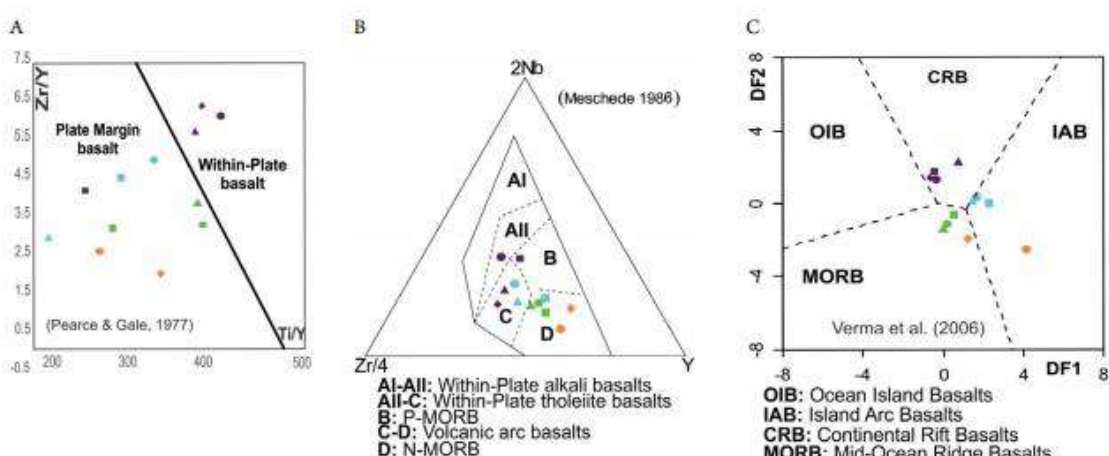


Figure 6. Geotectonic settings of studied mafic granulites. (A) Classification of basalts accordingly its position on the tectonic plate (Pearce & Gale 1977); (B) tectonic classification focusing on different tectonic setting for tholeiitic basalts (Meschede *et al.* 1986); (C) Tectonic classification for samples with basic or ultrabasic compositions (Verma *et al.* 2006). Symbols as in the Figure 4.

Felsic rocks predominantly yielded Sm-Nd T_{DM} ages between 2.48 and 2.03 Ga (Fig. 10) with weakly positive or slightly negative $\epsilon_{\text{Nd}_{(t)}}$ values (-3.94 to +0.08). Few felsic samples yielded T_{DM} ages from 2.75 to 2.58 Ga. These rocks yield significantly negative $\epsilon_{\text{Nd}_{(t)}}$ values (-6.91 to -5.5). We note that two felsic granulite samples (VA-LM-06 and CPH-132) yielded younger Orosirian Sm-Nd T_{DM} model ages (1.93 and 1.90 Ga), as shown in Figure 10.

The basic rocks have varied Sm-Nd T_{DM} ages (Fig. 10), according to their geochemical signatures: The TH1 group, with IAT signatures and the BA group with intraplate signatures exhibit normal $^{147}\text{Sm}/^{143}\text{Nd}$ and fSm/Nd values. The TH1

group yielded roughly similar T_{DM} ages of 2.35–2.27 Ga with weakly negative to positive $\epsilon_{Nd}_{(t)}$ values (-0.88 to +0.08). In contrast, the BA group yielded T_{DM} model ages between 2.52–2.21 Ga, with higher negative $\epsilon_{Nd}_{(t)}$ values (-7.32 and -1.92). The TH2 and TH3 groups, with respectively E- and N-MORB signatures, show no Sm/Nd fractionation relative to the CHUR, presenting positive $\epsilon_{Nd}_{(t)}$ values (+0.33 to +3.83).

For the calculation of initial isotopic parameters, such as $\epsilon_{\text{Nd}}^{(i)}$ and $^{87}\text{Sr}/^{86}\text{Sr}_{(i)}$ values, the available U-Pb ages reported in the literature for the same geochemical groups (see Suppl. Tab. A1) were used, including ages previously obtained within the study area (Machado *et al.* 1996, Heilbron *et al.* 2010).

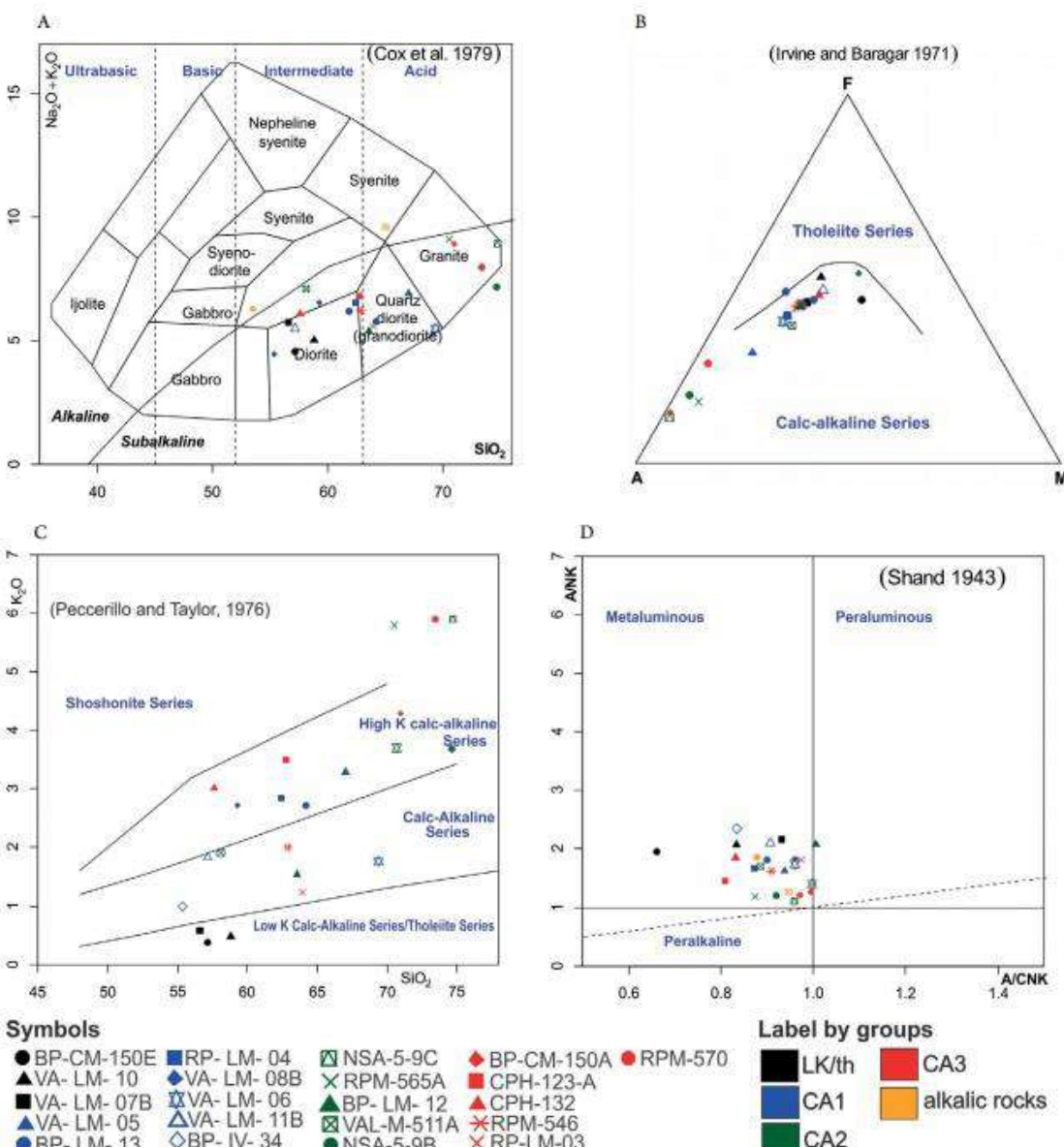


Figure 7. Geochemical classification plots of studied felsic granulites. (A) Protholiths classification and magmatic series classification (Cox et al. 1979); (B) classification of sub-alkaline samples into tholeiitic or calc-alkaline sub-series through AFM diagram (Irvine & Baragar 1971); (C) Classification of calc-alkaline rocks (Peccerillo & Taylor 1976); (D) Alumina Saturation Index classification (Shand 1943).

The T_{DM} and geochemical signature obtained were used to decide which U-Pb crystallization age should be applied for the calculation of the Sr initial ratios and $\epsilon\text{Nd}(t)$. Selected ages were:

- 2.1 Ga for calc-alkaline silicic arc rocks;
- 1.76 Ga for alkaline intra-plate mafic rocks;
- 766 Ma for MORB tholeiitic mafic rocks (see Suppl. Tab. A1).

The basic, intermediate and acid granulites yielded initial $^{87}\text{Sr}/^{86}\text{Sr}_{(i)}$ ratios, respectively of 0.700–0.702, 0.703–0.704 and 0.710–0.715. Two samples (CPH-123A and RPM-570) yielded anomalous initial ratios of 0.693 and 0.751. The anomalously low value may indicate disequilibrium in the Rb-Sr systematic, as expected for granulite facies rocks in the presence

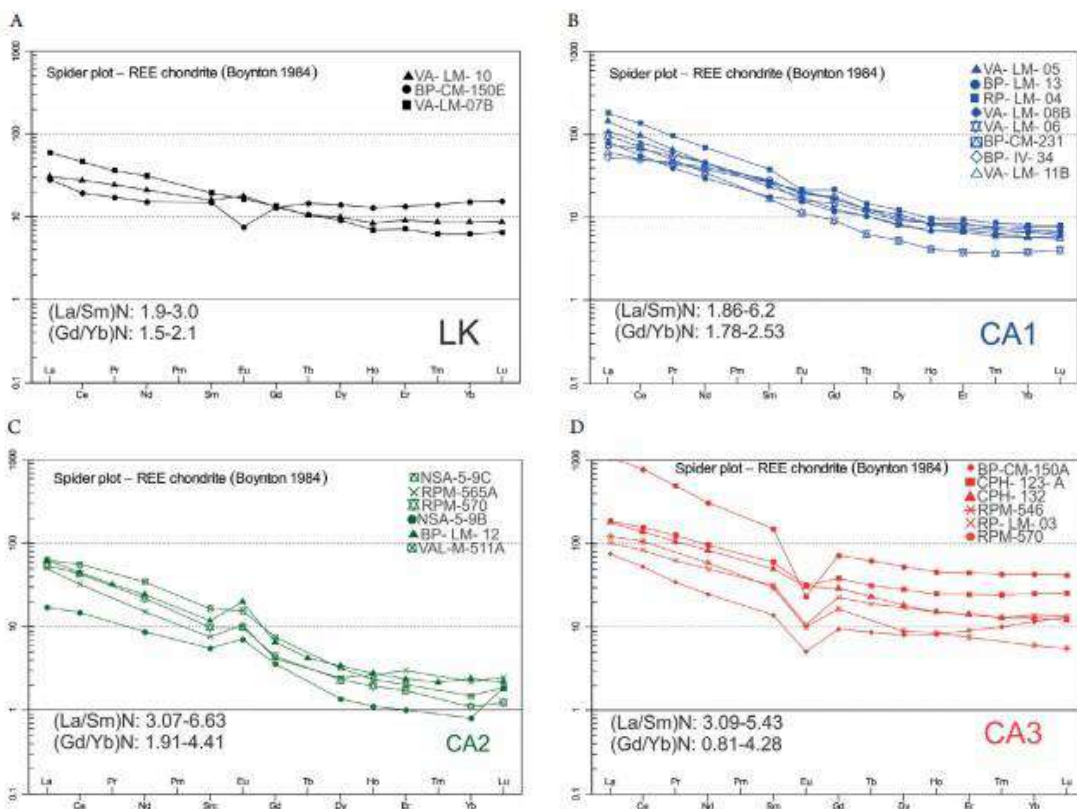


Figure 8. REE's chondrite normalized spidergram (Boynton 1984) of felsic granulites within study area. (A) LK group; (B) CA1 group; (C) CA2 group; (D) CA3 group.

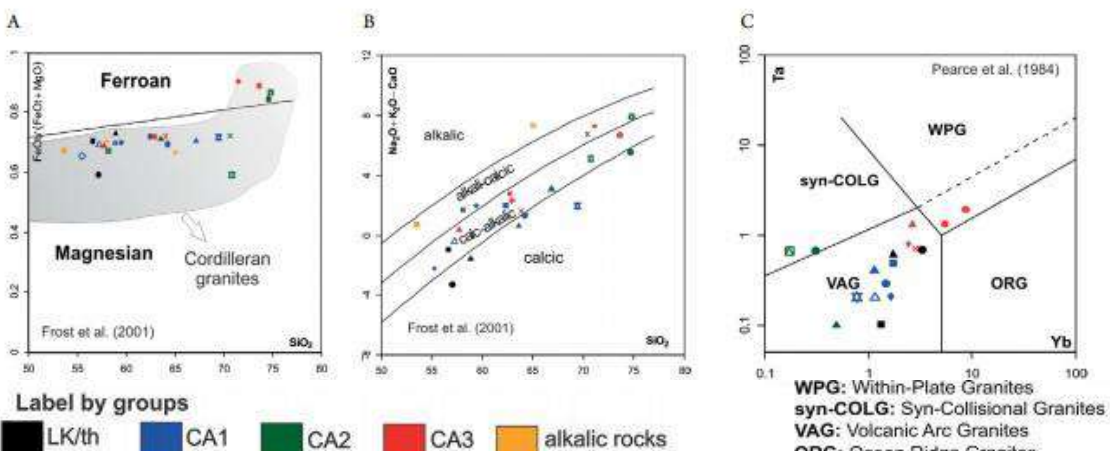


Figure 9. Geotectonic plots of studied felsic granulites. (A) Classification accordingly Fe Number and SiO_2 (Frost et al. 2001); (B) classification accordingly Modified Alkali-Lime Index (MALI) and Aluminium Saturation Index (ASI) (Frost et al. 2001); (C) tectonic classification for granitoids (Pearce et al. 1984).

of melting. The very high $^{87}\text{Sr}/^{86}\text{Sr}_{\text{(i)}}$ value is consistent with crustal contamination in the upper crust. Therefore, they will not be considered hereafter.

Figure 11 shows the correlation of the Nd and Sr signatures for the felsic granulites studied, displaying arc-related affinity, modelled for 2.1 Ga. Most samples plot in the lower crust field (Faure 1986). Basic rocks samples and diorites of the TH1 and LK groups, respectively, are possibly derived from a predominant juvenile component due to its greater similarity to the Bulk Earth composition (Allégre *et al.* 1995).

DISCUSSION

Petrogenetic parameters, sources and metamorphism

Felsic granulite samples show similar mineralogy, with progressive increase in quartz, K-feldspar in the granitic samples (Fig. 12). In particular the CA1 and CA3 groups display more expanded compositions, from diorites to granites, while the LK and CA2 groups show more restrict compositions, respectively with diorites and granites. The LK group may be considered as evolved members of the TH1 group (Fig. 13), since both share a more primitive IAT signature with similar REE patterns. The felsic CA2 group displays characteristically positive Eu anomalies, explained by plagioclase accumulation. Furthermore, this group has slightly depleted HREE patterns, possibly indicating either the presence of residual garnet in the source rocks, as suggested by Heilbron *et al.* (1998) or early amphibole fractionation in the source rock (Dessimoz *et al.* 2012). The CA1, LK and TH1 groups have slightly negative to absent Eu anomalies that are suggestive of either an oxidizing signature of magma and/or plagioclase-rich mantle sources (Wilson 1989). The LREE enrichment of the CA1 group may be attributed to the enrichment of mantle sources, a common feature in modern oceanic arcs (Smithies *et al.* 2004, Sun & Nesbitt 1978, Cameron *et al.* 1979, Crawford *et al.* 1989). The same effect of LREE enrichment in rocks of the BA group may be explained by small degrees of partial melting of their sources, as expected for alkali basalts (Cheng *et al.* 1993). The CA3 and BA groups have a strong negative Eu anomaly, possibly due to low oxygen fugacity and temperature of its magma formation (Hanson 1980). The very high LREE enrichment noticed in the REE spidergram (Fig. 8) of sample RPM-570, when compared to the other samples, may be attributed to the presence of allanite. Depleted LREE signature of the TH3 group suggests a derivation from a LREE depleted garnet-free source and/or a high degree of partial melting in the source.

Considering the petrogenetic parameters, we postulate that felsic granulites from the LK group, mafic granulites of the TH1 group and most samples of the CA1 group represent juvenile Paleoproterozoic protoliths, due to their weakly negative to slightly positive $\epsilon\text{Nd(t)}$ values (-3.94 to +0.08) and low $^{87}\text{Sr}/^{86}\text{Sr}_{\text{(i)}}$ values (0.701 to 0.702 — mean variation). Negative $\epsilon\text{Nd(t)}$ values (-7.32 e -1.92) of the intraplate basic rocks of the BA group constitute isotopic evidence of crustal

contamination. Positive $\epsilon\text{Nd(t)}$ values of the TH2 and TH3 groups (+0.33 to +3.83) suggest juvenile mantle sources. $^{87}\text{Sr}/^{86}\text{Sr}_{\text{(i)}}$ values of the less evolved TH2 and TH3 groups are close to those of the chondrite reservoir ($^{87}\text{Sr}/^{86}\text{Sr}_{\text{(i)CHUR}} = 0.699$), suggesting isotopic affinity with a depleted source. The CA2 group has higher $^{87}\text{Sr}/^{86}\text{Sr}_{\text{(i)}}$ values (0.705–0.722), T_{DM} model ages (2.31 to 2.03 Ga) and weakly negative to positive $\epsilon\text{Nd}_{\text{(i)}}$ values (-2.91 to +1.65), that could have been derived from an enriched continental source.

All geochemical groups, with different tectonic signatures and varied T_{DM} model ages, show similar granulite facies paragenesis. For instance, the granulite rocks of the JFC display $\text{opx} + \text{plg} + \text{qtz} \pm \text{cpx} \pm \text{hbl} \pm \text{kf} + \text{zr} + \text{il} + \text{ap} \pm \text{aln}$, or $\text{grt} + \text{cpx} + \text{qtz} + \text{plg} \pm \text{opx} \pm \text{hbl} + \text{il} + \text{mgt} \pm \text{zr}$ assemblages, suggestive for progressive metamorphism with intermediate to high pressures. Mylonitic rocks show retrogressive paragenesis ($\text{hbl} + \text{bt}$) pointing to the upper amphibolite facies conditions. These observations are consistent with published works of JFC rocks (Duarte *et al.* 1997, Heilbron *et al.* 1998). Together, these petrographic evidences and the geochronological background, reinforce that the study area was overprinted by the Brasiliense regional granulite facies overprint, in the context of the Ribeira belt (see Suppl. Tab. A1).

Regional correlations and proposed geochronologic evolution

New geochemical and isotopic data allow correlation with other published data for the JFC. Figure 14 shows the regional distribution of new and compiled data for the JFC (Tab. 4).

The geochemical characteristics of the CA1 group are similar to the most widespread rocks of the JFC, highlighted by the medium-K calc-alkaline granulites (tonalites and diorites, characterized by LREE enrichment) described by most authors in the Central Segment of the Ribeira belt, as reported by Heilbron *et al.* (1998, 2010), Duarte *et al.* (1997) and Heilbron *et al.* (2013). Ages between ca. 2.2 and 2.07 Ga have been reported in the literature for similar rocks. On the other hand, the CA2 group, corresponds to the enderbitic granulite gneisses from Manhuaçu of Costa (1998), and to the high-K calc-alkaline suite of André *et al.* (2009) in the Três Rios region, with U-Pb ages of ca. 2.1 Ga (Fig. 14). Both associations are also characterized by lower HREE contents, positive Eu anomalies and $(\text{La/Yb})_{\text{N}}$ ratios between 25 and 36.

Most of the obtained Sm-Nd T_{DM} model ages for the felsic granulites yielded values of ca. 2.3 to 2.5 Ga with $\epsilon\text{Nd}_{\text{(i)}}$ values between -0.4 to -3.5. These values are very similar to the data reported for the High-K calc-alkaline granulites of the Três Rios region (André *et al.* 2009) equivalent to the CA2 group, and for the enderbitic granulites of the Abre Campo-Manhuaçu region in Minas Gerais State (Fischel *et al.* 1998), equivalent to our CA1 group. Altogether, these T_{DM} model ages between ca. 2.2 and 2.3 Ga with slightly positive $\epsilon\text{Nd(t)}$ values reinforce our interpretation that the JFC is mostly represented by juvenile Paleoproterozoic arc related rocks. However, few felsic granulites yielded older T_{DM} model ages of ca. 2.75 to 2.58 Ga, suggesting that some older material could have contributed to the formation of these rocks. Similar older Archean

Table 3. Isotopic data (Sr-Sm-Nd) of the JFC orthogranulites in the studied area.

Sample	Group	Tectonic	Sm ppm	Nd ppm	Rb ppm	Sr ppm	$^{143}\text{Nd}/^{144}\text{Nd}$ (m)	abs st error	$^{147}\text{Sm}/^{144}\text{Nd}$ (m)	$^{87}\text{Sr}/^{86}\text{Sr}$ (m)	abs st error	t (Ma)	$\epsilon\text{Nd}(0)$	f 0 Ma	T_{CHUR} (Ga)	ϵNd (t)	T_{int} (Ga)	$^{87}\text{Sr}/^{86}\text{Sr}$ (i)
CJE-44-3	BA	WPB	8.8	36.3	22	154	0.511983	0.000007	0.1469	0.743873	0.000010	1700	-12.8	-0.25	2	-1.92	2.21	0.729750
NSA-V-9D	BA	WPB	14.2	55.7	20	121	0.511948	0.000005	0.1541	0.746576	0.000004	1700	-13.5	-0.22	2.46	-4.19	2.51	0.732017
RP-LM-02B	BA	WPB	13.3	68.7	71	457	0.511331	0.000005	0.1132	0.713961	0.000009	1700	-25.5	-0.42	2.38	-7.32	2.42	0.681405
VAL-503A	TH1	IAT	5.8	24.6	19	246	0.511842	0.000005	0.1424	0.709357	0.000009	2100	-15.5	-0.28	2.22	-0.88	2.35	0.701442
VA-LM-7A	TH1	IAT	6.7	25.4	2	338	0.511842	0.000002	0.1486	0.702990	0.000008	2100	-12.9	-0.24	2.09	0.08	2.26	0.702524
RPM-520B	TH2	E-MORB	3.4	11.8	4	186	0.512549	0.00001	0.1756	0.703277	0.000008	766	-1.7	-0.11	0.64	0.33	1.74	0.701697
RPM-534	TH2	E-MORB	3.3	11.4	2	182	0.512529	0.000006	0.1734	0.703177	0.000005	766	-2.1	-0.12	0.71	0.16	1.73	0.701371
BP-CM-166B	TH2	WPB	5.3	18.3	1	143	0.512544	0.000008	0.1755	0.704639	0.00001	766	-1.8	-0.11	0.68	0.24	1.75	0.701721
BP-LM-01	TH3	N-MORB	2.5	6.7	1.4	105	0.512881	0.000005	0.2060	0.702775	0.000009	766	4.7	0.05	3.93	3.83	1.87	0.702414
BP-CM-151	TH3	N-MORB	1.1	3.6	1	156	0.512557	0.000006	0.1911	0.703523	0.00001	2100	-1.6	-0.03	2.2	-0.08	2.53	0.694775
BP-CM-150E	LK	VAG	2.7	9.2	3	266	0.512347	0.000005	0.1772	0.705195	0.000007	2100	-5.7	-0.1	2.26	-0.42	2.46	0.701307
VA-LM-07B	LK	VAG	3.8	18.7	1.8	687	0.511358	0.000006	0.1174	0.702051	0.000005	2100	-25	-0.4	2.45	-3.6	2.48	0.701822
VA-LM-10	LK	VAG	3.1	12.6	1.7	523	0.51185	0.000003	0.1435	0.701996	0.000003	2100	-15.4	-0.27	2.25	-1.03	2.35	0.701712
RP-LM-04	CA1	VAG	7.4	42.4	84	479	0.511126	0.000002	0.1019	0.727850	0.000007	2100	-29.5	-0.48	2.42	-3.94	2.46	0.712509
VA-LM-08B	CA1	VAG	5.3	27.6	100	519	0.511158	0.000007	0.1100	0.721125	0.000009	2100	-28.9	-0.44	2.59	-5.5	2.58	0.704270
VA-LM-05	CA1	VAG	4.6	27.5	106	416	0.511055	0.000003	0.0953	0.735108	0.000007	2100	-30.9	-0.52	2.37	-3.54	2.41	0.712818
VA-LM-06	CA1	VAG	3.3	21.3	74	307	0.511146	0.000013	0.0946	0.722811	0.000009	1900	-23	-0.52	1.75	1.93	1.93	0.703761
VA-LM-11B	CA1	VAG	5.2	22.9	65	679	0.511347	0.000007	0.1277	0.710433	0.000008	2100	-25.2	-0.35	2.83	-6.61	2.75	0.702059
BP-LM-13	CA1	VAG	3.5	18	72	527	0.511178	0.000005	0.1129	0.717722	0.000010	2100	-28.5	-0.43	2.64	-5.91	2.62	0.705771
BP-IV-34	CA1	VAG	5.6	24.5	33	601	0.511621	0.000008	0.1317	0.707303	0.000006	2100	-19.8	-0.33	2.37	-2.32	2.43	0.702500
NSA-V-9C	CA2	VAG-SYN	0.7	3.8	120	145	0.511619	0.000009	0.1129	0.781207	0.000009	2000	-19.9	-0.43	1.85	1.65	2.03	0.722440
BP-LM-12	CA2	VAG-SYN	2.3	14.7	53	612	0.511209	0.000006	0.0994	0.713146	0.000007	2000	-27.9	-0.49	2.23	-2.91	2.31	0.705570
NSA-V-9B	CA2	VAG-SYN	1.1	5.5	127	135	0.511633	0.000009	0.1215	0.770051	0.000006	2000	-19.6	-0.38	2.03	-0.29	2.18	0.716769
BP-CM-150A	CA3	VAG	2.7	15.8	160	247	0.511257	0.000005	0.1044	0.751285	0.000007	2100	-26.9	-0.47	2.27	-2.06	2.34	0.703021
RP-LM-03	CA3	VAG-WPG	6.2	29.8	31	459	0.511729	0.000007	0.1243	0.711980	0.000003	2100	-17.7	-0.37	1.91	1.81	2.09	0.706075
CPH-132	CA3	VAG-WPG	9.8	49.8	76	555	0.511703	0.000004	0.1119	0.713070	0.000008	1900	-18.2	-0.43	1.68	2.46	1.9	0.702250
CPH-123A	CA3	VAG-WPG	11.8	58	144	198	0.511247	0.000002	0.1177	0.756710	0.000004	2100	-27.1	-0.4	2.67	-5.85	2.64	0.693092
RPM-570	CA3	VAG-WPG	29.3	188	175	207	0.510999	0.000006	0.0909	0.825790	0.000008	2100	-32	-0.54	2.35	-3.45	2.39	0.751838

Braz. J. Geol. (2019), 49(3): e20190007

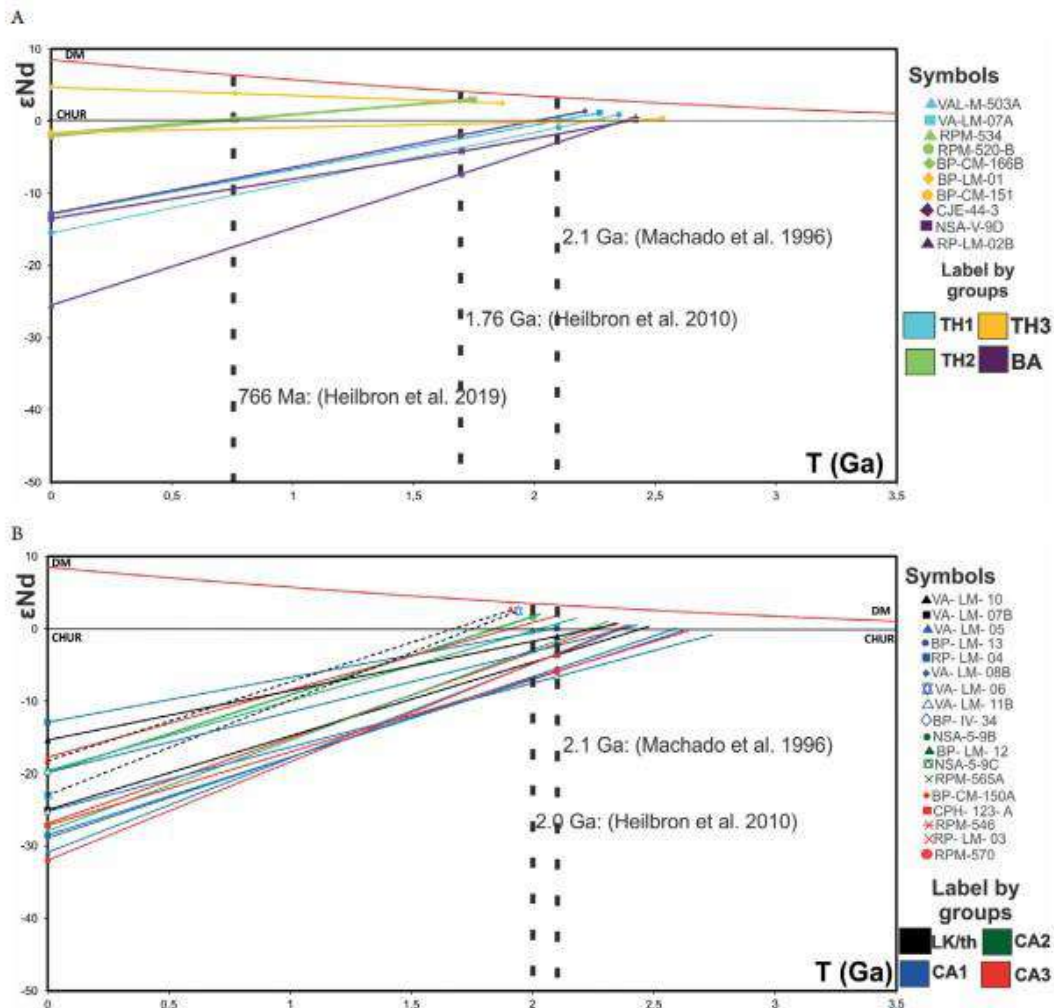


Figure 10. Nd evolution diagram ($\epsilon_{\text{Nd}} \times \text{Time}$) for the (A) basic and (B) felsic rocks of the JFC. Depleted Mantle data extracted from DePaolo (1981).

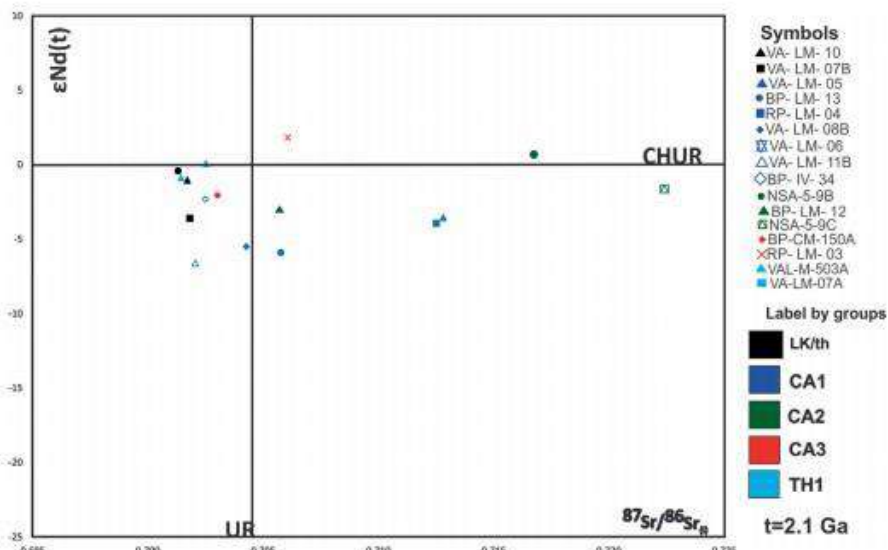


Figure 11. Nd-Sr correlation diagram of JFC arc rocks at 2.1 Ga. Uniform Reservoir data extracted from DePaolo (1988).

model ages were described for the northern segment of the Ribeira (Silva *et al.* 2002, Kuribara *et al.* 2019, Fischel *et al.* 1998). On the other hand, few Orosirian T_{DM} model ages of samples VA-LM-06 (CA1 group) and CPH-132 (CA3 group) do not show correlation with any previously published data for the JFC rocks. These samples present the youngest T_{DM} model ages of JFC, never reported before in the literature, and could represent a younger episode of felsic rocks generation within the complex.

The alkaline basic granulites of the study area, the BA group, with intraplate signatures, were previously detected in the study area with U-Pb ages of ca. 1.7 to 1.6 Ga, Sm-Nd T_{DM} model ages of 2.14 Ga and ϵ_{Nd} values of -7.32 to -1.92 (Ragatky *et al.* 1999, Heilbron *et al.* 2010). These characteristics are suggestive for intraplate magmatism probably related to the development of Mesoproterozoic basins, such as the Espinhaço rift.

Basic granulitic rocks of the TH3 group show similarities with the High-Mg group of Duarte *et al.* (1997) for the Juiz de Fora region (Fig. 14). Both present N-MORB signatures and a wide span of T_{DM} model ages (ca. 2.4 Ga to 1.87 Ma).

These model ages results should be regarded with care, because of the very little evolved isotopic characteristics of these rocks.

On the other hand, tholeiitic rocks of the TH2 group in the study area are very similar to those described both in the Santo Antonio de Pádua region (Heilbron *et al.* 2013), and to the medium-Mg tholeiitic group in the Juiz de Fora region (Duarte *et al.* 1997). All these basic granulites display E-MORB like REE distribution patterns and present younger Mesoproterozoic T_{DM} model ages (from 1.87 to 1.74), that speculatively could be related to development of the younger Meso- to Neoproterozoic basins, i.e., Carandaí (as proposed by Ribeiro *et al.* 2013) and/or Andrelândia.

Previously available U-Pb data together with the Nd-Sr isotopic constraints for the JFC suggests the recognition of four tectono-magmatic events, unraveling the complexity of this basement association in the central portion of the Ribeira belt (Tab. 4, Fig. 15):

- The most common U-Pb crystallization ages of the felsic granulites span between ca. 2.2 to 2.07 Ga with juvenile signatures are regarded as subduction related magmatism, probably evolving from an immature intra-oceanic magmatic arc to a more evolved setting. They are represented by the IAT and the alc-alkaline CA1 and CA2 groups. Part of the samples of the CA1 group yielded older T_{DM} model ages between 2.7 and 2.6 Ga, suggesting that some Archean material could have been involved in the generation of these rocks. Until now, only one occurrence of Archean granitoid rocks within the JFC was reported by Silva *et al.* (2002) in the vicinity of the city of Juiz de Fora (Fig. 15A). Rocks of the CA3 group, showing more evolved signatures, suggest that the older and more primitive arc-related rocks could have contributed to the generation of this geochemical group;
- Charnockitic rocks of the CA2 group belong to the High-K calcalkaline group and could have resulted from the melting of the previously formed arc-related rocks. The CA2 granitic group was probably generated during the collision of the Juiz de Fora arc with the São Francisco Paleocontinent between ca. 2.07 and 2.04 Ga, or either following the main collision episode, during later stages of the Rhyacian Orogeny (Fig. 15B, Tab. 4);
- One single c. 1.7 Ga alkaline basic rock (high TiO_2 and LREE content and negative Eu anomaly) with ca. 2.14 T_{DM} model age is correlated with the Statherian extensional episode (Fig. 15C) that resulted in the development of the Espinhaço intraplate basin (Santos *et al.* 2015);
- The basic granulite rocks of the TH2 and TH3 groups, with younger T_{DM} model ages could be related with the development of younger Meso-Neoproterozoic basins (Fig. 15C). More recently, one single intraplate basic body of ca. 766 Ma (Heilbron *et al.* 2019) was interpreted as coeval with the development of the Andrelândia basin (Trouw *et al.* 2000). Similar Cryogenian ages have been reported for metabasic rocks intercalated with the Macaúbas metasedimentary rocks in northern Araçuaí belt (Pedrosa-Soares & Alkmim 2011);
- The tectonic evolution of JFC ends with the superposition of the deformation and high-grade metamorphism related to the

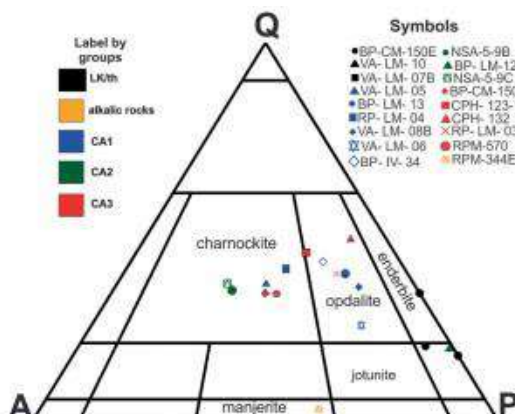


Figure 12. QAP diagram (Streckeisen 1974) for the felsic granulites with the adopted geochemical subdivision. See text for the discussions.

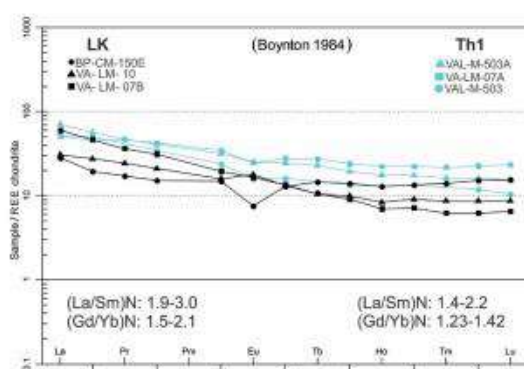


Figure 13. REE Comparison (Boynton 1984) between intermediate felsic rocks of the BK group with the basic rocks of the TH1 group.

Brasiliense Orogeny between ca. 620 to 524 Ma (see Suppl. Tab. A1) that resulted from docking of outboard terranes (Paraíba do Sul-Socorro and Oriental) onto the reworked passive margin of the SF paleocontinent, during the development of the Ribeira belt, as proposed by Tupinambá *et al.* (2000) and Heilbron *et al.* (2000, 2017). This superposition resulted in intense tectonic interdigititation and granulite

facies metamorphism observed in all rocks of the studied area. Final exhumation of the orthogranulites was associated to intense mylonite fabric generation under retrogressive amphibolite facies conditions (Heilbron *et al.* 1998).

The envisaged tectonic evolution of the JFC in the study area is similar to previously proposed models (Heilbron *et al.*

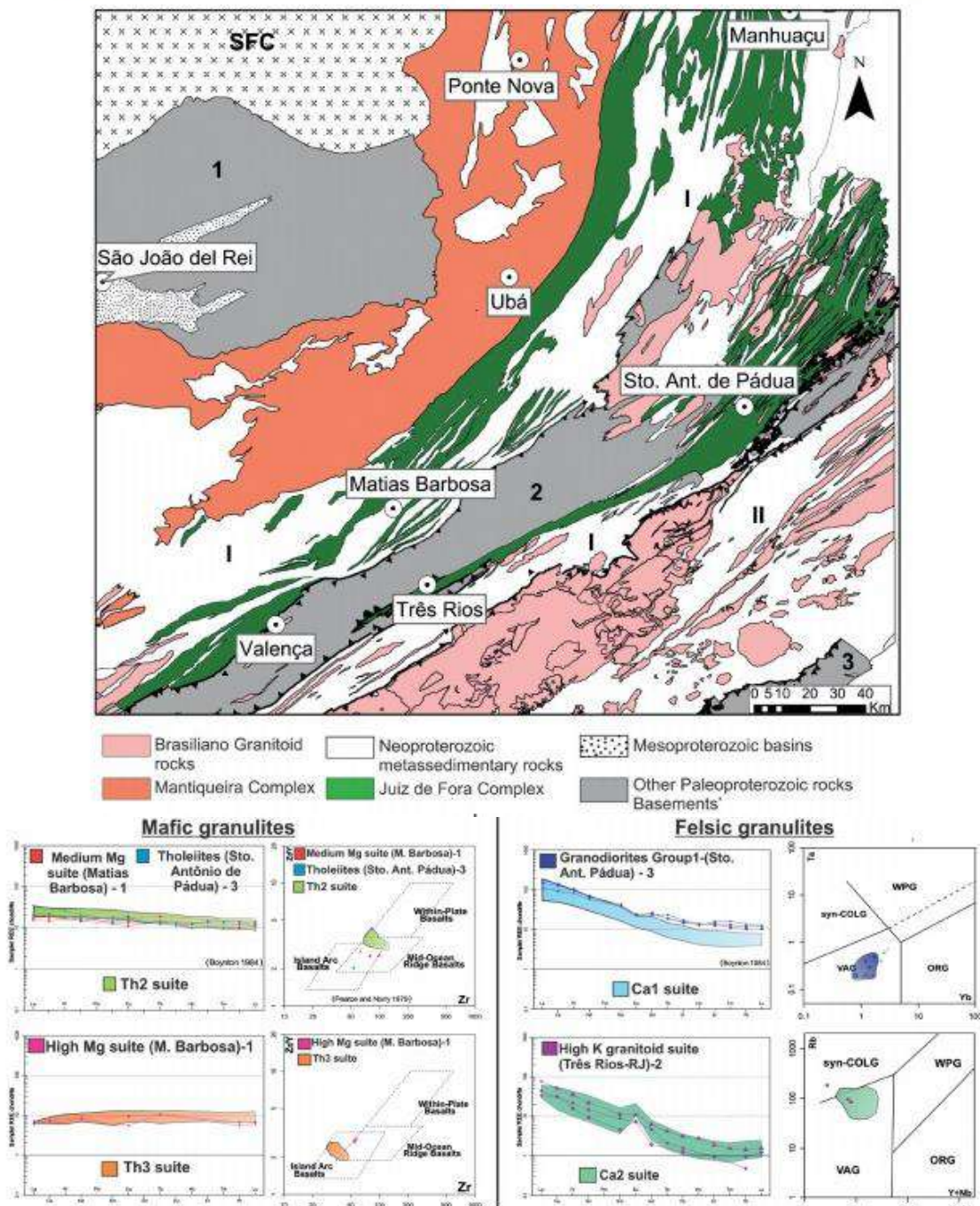


Figure 14. Tectonic Regional map with geochemical correlations of JFC between different regions of Minas Gerais and Rio de Janeiro. Paleoproterozoic basement (gray): (1) Mineiro Belt; (2) Parába do Sul Terrane of Ribeira Belt (Quirino Complex); (3) Cabo Frio Terrane (Região dos Lagos Complex). Neoproterozoic metasediments (white): (I) Andrelândia Megassequence; (II) Costeiro Domain of Ribeira Belt; Data from: (1) Duarte *et al.* (1997); (2) André *et al.* (2009); (3) Heilbron *et al.* (2013).

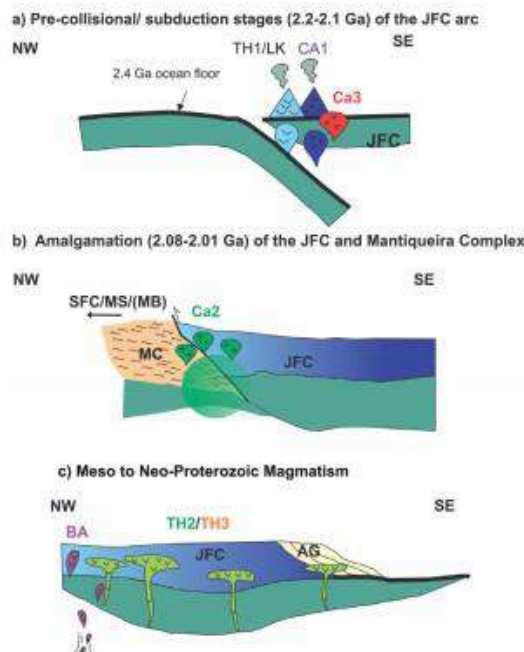
2010, Alkmim & Teixeira 2017) and compatible with the available U-Pb data for this unit (Heilbron *et al.* 2010, Machado *et al.* 1996, Silva *et al.* 2002, Noce *et al.* 2007, Degler *et al.* 2018, Kuribara *et al.* 2019).

CONCLUSIONS

The obtained geochemical and isotopic data reinforce the idea that the orthogranulites of the JFC had a very complex and protracted tectonic evolution, recording several tectonic events throughout the Proterozoic. The oldest event of Rhyacian age points out to an arc setting that produced juvenile to slightly contaminated tholeiitic to calc-alkaline rocks. This was followed by collision or either post-collision episodes, given by more evolved (granitic) rocks. Altogether, these rocks integrate part of a dismembered Rhyacian orogenic belt hidden within the Neoproterozoic Ribeira belt (Heilbron *et al.* 2008, 2010, Silva *et al.* 2002, Degler *et al.* 2018, Kuribara *et al.* 2019). Minor contribution from Archean material participated in the evolution of the magmatic arc, as indicated by a few T_{DM} model ages of ca 2.75 to 2.58 Ga and $\delta^{18}\text{O}$ values of -6.61 to -5.91.

The new data are potentially important for Paleoproterozoic reconstruction models, due to the predominantly juvenile character of the Rhyacian JFC, as similarly observed in other belts of Brazil and worldwide.

On the other hand, some of the large deformed layers of the basic granulites point out to extensional settings that could be related to the opening of rift to passive margin sequences, possibly correlated with the Statherian Espinhaço Supergroup or either to the Meso-Neoproterozoic rift to passive margin basins development (Carandai rift and/or Andrelândia basin).



SFC: São Francisco paleoplate; MC: Mantiqueira Complex; JFC: Juiz de Fora Complex; AG: Andrelândia Group.

Figure 15. Envisaged tectonic evolution of the JFC in the focused area: (A) subduction stages of Juiz de Fora arc, focusing on the groups proposed on this work: LK/TH1- shallower melting and CA1- deeper melting; (B) docking of the JFC terrane to the border of the older Archean active margin represented by Mantiqueira Complex, with the formation of CA2 group: syn-collisional granitoids; (C) Basic alkaline magmatism (BA group) on JFC related to the Statherian Taphrogenesis and Basic magmatism possibly related to the opening of Carandai and/or Andrelândia basins (TH2 and TH3 groups).

Table 4. Petrographic, geochemical and isotopic data obtained for the studied orthogranulites from Juiz de Fora Complex.

Geochemical groupings	Essential Mineralogy	Protholith	Tectonic Settings	U-Pb age	T_{DM}	Tectonic Event
TH1+BK	plg, opx, cpx, hbl, bt ± kf	Gabbros to diorites	IAT	2.2 Ga?	2.48–2.27 Ga	Rhyacian Subduction
CA1	plg, opx, qtz, cpx, Hbl, bt ± kf	Diorites to tonalites	VAG	2.1 Ga	2.75–2.6 Ga 2.5–2.2 Ga 1.93 Ga	Rhyacian Subduction Archean inheritance
CA3	qtz, plg, opx, kf, bt ± hbl	Tonalites to granites	VAG-intraplate	?	2.64 Ga–2.39–1.9 Ga	Late Rhyacian Subduction Archean inheritance
CA2	plg, qtz, kf ± opx, bt, hbl	Granites	VAG-Syn-collisional	2.08 Ga	2.31–2.03 Ga	Rhyacian Subduction-Collision
BA	opx+cpx+plg+bt+hbl+qtz	Gabbros	Intra-plate	1.76 Ga	2.51–2.21 Ga	Statherian Extension
TH2	opx+cpx+plg+hbl+grd	Gabbros	E-MORB	?	1.74–1.73 Ga	Meso-Neoproterozoic Extension ?
TH3			N-MORB	?	1.87 Ga	Meso-Neoproterozoic Extension ?

ACKNOWLEDGEMENTS

The first author thanks the Coordenação de Aperfeiçoamento de Pessoal de Nível Superior for the Geosciences Graduate Program scholarship. The authors acknowledge the support of the Laboratório de Processamento

de Amostras (LGPA) and Laboratório de Geocronologia e Isótopos Radiogênicos (LAGIR) of Universidade do Estado do Rio de Janeiro (UERJ), the CNPq grants of Monica Heilbron, Claudio Valeriano and Wilson Teixeira, and FAPERJ-CNE for funding the research.

ARTICLE INFORMATION

Manuscript ID: 20190007. Received on: 02/07/2019. Approved on: 07/16/2019.

LEA collected geological data on field work, obtained, processed and interpreted analytical data, wrote the manuscript, prepared all figures, maps and diagrams, and discussed all data. MH wrote the manuscript, reviewed all manuscript and contributed with Discussions. WT reviewed all manuscript and contributed with Discussion. CV reviewed all manuscript and contributed with Discussions. CN processed Nd and Sr data analysis.

Competing interests: The authors declare no competing interests.

REFERENCES

- Alkmim F.F. & Teixeira W. 2017. The Paleoproterozoic Mineiro Belt and the Quadrilátero Ferrífero. In: Heilbron M., Cordani U., Alkmim F.F. (eds.), São Francisco Craton, Eastern Brazil: Tectonic Genealogy of a Miniature Continent. Regional Geology Reviews. New York, Springer, p. 71-94.
- Allégre C.J., Poirier J.P., Humler E., Hofmann A.W. 1995. The chemical composition of the Earth. *Earth Planetary Science Letters*, 134(3-4):515-526. [https://doi.org/10.1016/0012-821X\(95\)00123-T](https://doi.org/10.1016/0012-821X(95)00123-T)
- Almeida J.C.H., Tupinambá M., Heilbron M., Trouw R. 1998. Geometric and kinematic analysis at the Central Tectonic Boundary of the Ribeira belt, Southeastern Brazil. In: Congresso Brasileiro de Geologia. Anais... Sociedade Brasileira de Geologia, v. 39, p. 32.
- André J.L.E., Valladares C.S., Duarte B.P. 2009. O Complexo Juiz de Fora na região de Três Rios (RJ): Litogeocímica, geocronologia U-Pb (LA-ICPMS) e geoquímica isotópica de Nd e Sr. *Revista Brasileira de Geociências*, 39(4):773-793.
- Babinski M., Brito-Neves B.B., Machado N., Noce C.M., Uhlein A., Van Schmus W.R., 1994. Problema na metodologia U/Pb em zircões de vulcânicas continentais: o caso do Grupo Rio dos Remédios, Supergrobo Espinhaço, no Estado da Bahia. In: 38º Congresso Brasileiro de Geologia. Boletim de Resumos Expandidos... SBG, Camboriú, 2, p. 409-410.
- Barbosa N.S., Teixeira W., Ávila C.A., Montecinos P.M., Bongiolo E.M., Vasconcellos F.F. 2018. U-Pb geochronology and coupled Hf-Nd-Sr isotopic-chemical constraints of the Cassiterite Orthogneiss (2.47–2.41-Ga) in the Mineiro belt, São Francisco craton: Geodynamic fingerprints beyond the Archean–Paleoproterozoic Transition. *Precambrian Research*, 326:399-416. <https://doi.org/10.1016/j.precamres.2018.01.017>
- Bellieni G., Corini-Chiaromonti P., Marques L.S., Melfi A.J., Piccirillo E.M., Nardi A.J.R., Roisemberg A. 1984. High and low TiO_2 flood-basalts from the Paraná Plateau (Brazil): petrology and geochemical aspects bearing on their mantle origin. *Neues Jahrbuch für Mineralogie Abhandlungen*, 150:273-306.
- Bento dos Santos T., Munhá J.M., Tassanini C.G.G., Fonseca P.E., Dias Neto C. 2011. Metamorphic P-T evolution of granulites in the central Ribeira Fold Belt, SE Brazil. *Geosciences Journal*, 15(1):27-51. <https://doi.org/10.1007/s12303-011-0004-1>
- Boynton W.V. 1984. Cosmochemistry of the rare earth elements; meteorite studies. In: Henderson P. (ed.). *Rare earth element geochemistry*. Amsterdam, Elsevier, p. 63-114.
- Brito-Neves B.B., Sá J.M., Nilson A.A., Botelho N.F. 1995. A Tafrogênese Estateriana nos blocos paleoproterozóicos da América do Sul e processos subsequentes. *Geomas*, 3(2):1-21. <http://dx.doi.org/10.18285/geomas.v3i2.205>
- Cameron W.E., Nisbet E.G., Dietrich V.J. 1979. Boninites, komatiites and ophiolitic basalts. *Nature*, 280:550-553. <https://doi.org/10.1038/280550a0>
- Cardoso C.D., Ávila C.A., Neumann R., Oliveira E.P., Valeriano C.M., Dussin I. 2019. A Rhyacian continental arc during the Evolution of the Mineiro belt, Brazil: constraints from the Rio Grande and Brumado metadiorites. *Lithos*, 326-327:246-264. <https://doi.org/10.1016/j.lithos.2018.12.025>
- Chemale Jr. F., Dussin I.A., Alkmim F.F., Martins M.S., Queiroga G., Armstrong R., Santos M.N. 2012. Unravelling a Proterozoic basin history through detrital zircon geochronology: the case of the Espinhaço Supergroup, Minas Gerais, Brazil. *Gondwana Research*, 22(1):200-206. <https://doi.org/10.1016/j.gr.2011.08.016>
- Cheng Q.C., Macdougall J.D., Lugmair G.W. 1993. Geochemical studies of Tahiti, Tahitia and Mehetia, Society island chain. *Journal of Volcanology and Geothermal Research*, 55(1-2):155-184. [https://doi.org/10.1016/0377-0273\(93\)90096-A](https://doi.org/10.1016/0377-0273(93)90096-A)
- Cordani U.G., Delhal J., Ledent D. 1973. Orogenéses superposées dans le précambrien du Brésil SudOriental (Etats de Rio de Janeiro et Minas Gerais). *Revista Brasileira de Geociências*, 3(1):1-22.
- Costa A.G. 1998. The granulite-facies rocks of the northern segment of the Ribeira Belt, eastern Minas Gerais, SE Brazil. *Gondwana Research*, 1(3-4):367-372. [https://doi.org/10.1016/S1342-937X\(05\)70852-2](https://doi.org/10.1016/S1342-937X(05)70852-2)
- Cox K.G., Bell J.D., Pankhurst R.J. 1979. *The interpretation of igneous rocks*. London, Allen and Unwin, 450 p.
- Crawford A.J., Falloon T.J., Green D.H. 1989. Classification, petrogenesis and tectonic setting of boninites. In: Crawford A.J. (ed.). *Boninites*. London: Unwin-Hyman, p. 1-49.
- Cutts K., Lanza C. 2019. The complex tale of Mantiqueira and Juiz de Fora: A comment on "Eoarchean to Neoproterozoic crustal evolution of the Mantiqueira and the Juiz de Fora Complexes, SE Brazil: Petrology, geochemistry, zircon U-Pb geochronology and Lu-Hf isotopes". *Precambrian Research*, 332(105305):1-3.
- Degler R., Pedrosa-Soares A.C., Novo T., Tedeschi M., Silva L.C., Dussin I., Lanza C. 2018. Rhyacian-Orosirian isotopic records from the basement of the Araçuaí-Ribeira orogenic system (SE Brazil): Links in the Congo-São Francisco paleocontinent. *Precambrian Research*, 317:179-195. <https://doi.org/10.1016/j.precamres.2018.08.018>
- Delhal J., Ledent D., Cordani U.G. 1969. Ages Pb/U; Sr/Rb et Ar/K de Formations Métamorphiques et Granitique du Sud-Est du Brésil (Etats de Rio de Janeiro et Minas Gerais). *Annales de la Société Géologique Belge*, 92:271-283.
- DePaolo D.J. 1981. A neodymium and strontium isotopic study of the Mesozoic calc-alkaline granitic batholiths of the Sierra Nevada and Peninsular Ranges, California. *Journal of Geophysical Research: Solid Earth*, 86:10470-10488.
- DePaolo D.J. 1988. *Neodymium isotope geochemistry: an introduction*. Berlin, Springer-Verlag, 187 p.
- Dessimoz M., Müntener O., Ulmer P. 2012. A case for hornblende dominated fractionation of arc magmas: the Chelan complex (Washington Cascades). *Contributions to Mineralogy and Petrology*, 163(4):567-589. <https://doi.org/10.1007/s00410-011-0685-5>
- Duarte B.P., Figueiredo M.C.H., Campos Neto M., Heilbron M. 1997. Geochemistry of the granulite facies orthogneisses of Juiz de Fora Complex, Central Segment of the Ribeira Belt, Southeastern Brazil. *Revista Brasileira de Geociências*, 27(1):67-82. <http://doi.org/10.25249/0375-7536.19976782>

- Duarte B.P., Heilbron M., Campos Neto M.C. 2000. Granulite/charnockite from the Juiz de Fora Domain, central segment of the Brasiliano-Pan-African Ribeira belt. *Revista Brasileira de Geociências*, 30(3):358-362. <http://doi.org/10.25249/0375-7536.200030358362>
- Duarte B.P., Valente S., Heilbron M., Campos Neto M.C. 2004. Petrogenesis of orthogneisses of the Mantiqueira Complex, Central Ribeira Belt, SE Brazil: an Archean to Paleoproterozoic basement unit reworked during the Pan-African Orogeny. *Gondwana Research*, 7(2):437-450. [https://doi.org/10.1016/S1342-937X\(05\)70795-4](https://doi.org/10.1016/S1342-937X(05)70795-4)
- Dussin I.A. & Dussin T.M. 1995. Supérgrupo Espinhaço: Modelo de Evolução Geodinâmica. *Geonomas*, 3:19-26.
- Faure G. 1986. *Principles of Isotope Geology*. 2nd ed. New York, Wiley, 555 p.
- Fischel D.P., Pimentel M.M., Fuch R.A., Costa A.G., Rosière C.A. 1998. Geology and Sm-Nd isotopic data for the Mantiqueira and Juiz de Fora Complexes (Ribeira Belt) in the Abre Campo Manhaçu region, Minas Gerais, Brazil. In: International Conference on Basement Tectonics. *Abstracts...* v.14, p. 21-23.
- Frost B.R., Barnes C.G., Collins W.J., Arculus R.J., Ellis D.J., Frost C.D. 2001. A geochemical classification of granitic rocks. *Journal of Petrology*, 42(11):2033-2048. <http://doi.org/10.1093/petrology/42.11.2033>
- Gonçalves L., Farina F., Lana C., Pedrosa-Soares A.C., Alkmim F., Nalini Jr. H.A. 2014. New U-Pb ages and lithochemical attributes of the Ediacaran Rio Doce magmatic arc, Araçai confine orogen, Southeastern Brazil. *Journal of South America Earth Science*, 52:1-20. <http://dx.doi.org/10.1016/j.jsames.2014.02.008>
- Goscombe B.D., Foster D.A., Gray D., Wade B., Marsellos A., Titus J. 2017. Deformation correlations, stress field switches and evolution of an orogenic intersection: the Pan-African Kaoko-Damara orogenic junction, Namibia. *Geoscience Frontiers*, 8(6):1187-1232. <https://doi.org/10.1016/j.gsf.2017.05.001>
- Goscombe B.D., Gray D. 2007. The Coastal Terrane of the Kaoko Belt, Namibia: outboard arc-terrane and tectonic significance. *Precambrian Research*, 155(1-2):139-158. <https://doi.org/10.1016/j.precamres.2007.01.008>
- Goscombe B.D., Gray D. 2008. Structure and strain variation at mid-crustal levels in a transpressional orogen: a review of Kaoko Belt structure and the character of West Gondwana amalgamation. *Gondwana Research Focus Paper*, 13(1):45-85. <http://dx.doi.org/10.1016/j.gr.2007.07.002>
- Hanson G.N. 1980. Rare Earth elements in petrogenetic studies of igneous systems. *Annual Review of Earth and Planetary Science*, 8(1):371-406. <http://dx.doi.org/10.1146/annurev.ea.08.050180.002103>
- Hasui Y., Carneiro C.D.R., Coimbra A.M. 1975. The Ribeira Fold Belt. *Revista Brasileira de Geociências*, 5(4):257-267.
- Heilbron M. 1993. *Evolução tectono-metamórfica da Seção Bom Jardim de Minas (MG) - Barra do Piraí (RJ). Setor Central da Faixa Ribeira*. Tese de Doutorado, Instituto de Geociências, Universidade de São Paulo, São Paulo, 268 p.
- Heilbron M., Cordani U., Alkmim F., Reis H. 2017. Tectonic Genealogy of a Miniature Continent. In: Heilbron M., Cordani U.G., Alkmim F.F. (eds.). *São Francisco Craton, Eastern Brazil: Tectonic Genealogy of a Miniature Continent*. Regional Geology Reviews. New York, Springer, p. 321-330.
- Heilbron M., Duarte B.P., Valeriano C.M., Simonetti A., Machado N., Nogueira J.R. 2010. Evolution of reworked Paleoproterozoic basement rocks within the Ribeira belt (Neoproterozoic), SE-Brazil, based on U/Pb geochronology: Implications for paleogeographic reconstructions of the São Francisco-Congo paleocontinent. *Precambrian Research*, 178(1):136-148. <http://dx.doi.org/10.1016/j.precamres.2010.02.002>
- Heilbron M., Euzébio R., Peixoto C., Tupinambá M., Guia C., Peternel R., Silva L.G., Ragatky C.D. 2013. O Complexo Juiz de Fora na Folha Santo Antônio de Pádua 1:100.000: geologia e geoquímica. *Geociências*, 32(1):10-23.
- Heilbron M., Machado R., Figueiredo M.C.H. 1997. Lithogeochemistry of paleoproterozoic orthogranulites from Rio Preto (MG) - Vassouras (RJ) region, central Ribeira Belt. *Revista Brasileira de Geociências*, 27(1):83-99. <http://doi.org/10.25249/0375-7536.19978398>
- Heilbron M., Mohriak W.U., Valeriano C.M., Milani E., Almeida J.C.H., Tupinambá M. 2000. From Collision to Extension: The Roots of the Southeastern Continental Margin of Brazil. In: Mohriak W.U., Talwani M. (eds.). *Atlantic Rifts and Continental Margins*. AGU, v. 115, p. 1-32.
- Heilbron M., Oliveira C., Lobato M., Valeriano C.M., Dussin I., Dantas E., Simonetti A., Bruno H., Corrales F., Socoloff E. 2019. The Barreiro suite in the central Ribeira Belt (SE-Brazil): a late Tonian tholeiitic intraplate magmatic event in the distal passive margin of the São Francisco Paleocontinent. *Brazilian Journal of Geology*, 49(2):1-19. <http://dx.doi.org/10.1590/2317-4889201920180129>
- Heilbron M., Pedrosa-Soares A.C., Campos Neto M., Silva L.C., Trouw R.A.J., Janasi V.C. 2004. A Província Mantiqueira. In: Mantesso-Neto V., Bartorelli A., Carneiro C.D.R., Brito-Neves B.B. (eds.). *O desvendar de um continente: a moderna geologia da América do Sul e o legado da obra de Fernando Flávio Marques de Almeida*. São Paulo, Editora Beira, p. 203-234.
- Heilbron M., Tupinambá M., Almeida J.C.H., Valeriano C.M., Valladares C.S., Duarte B.P. 1998. New constraints on the tectonic organization and structural styles related to the Brasiliano collage of the central segment of the Ribeira belt, SE Brazil. In: International Conference on Precambrian and Craton Tectonics/International Conference on Basement Tectonics. *Extended Abstracts...* Ouro Preto, v. 14, p. 15-17.
- Heilbron M., Valeriano C.M., Tassinari C.C.G., Almeida J.C.H., Tupinambá M., Siga Jr. O., Trouw R.A.J. 2008. Correlation of Neoproterozoic terranes between the Ribeira Belt, SE Brazil and its African counterpart: comparative tectonic evolution and open questions. In: Pankhurst R.J., Trouw R.A.J., Brito-Neves B.B., De Witt M.J. (eds.). *West Gondwana: Pre-Cenozoic Correlations across the South Atlantic Region*. London, Geological Society, Special Publication, 294, p. 211-232.
- Irvine T.M. & Baragar W.R. 1971. A guide to the chemical classification of common volcanic rocks. *Canadian Journal of Earth Sciences*, 8(5):523-548. <https://doi.org/10.1139/e71-055>
- Janoušek V., Farrow C.M., Erban V. 2006. Interpretation of whole-rock geochemical data in igneous geochemistry: introducing Geochemical Data Toolkit (GCDkit). *Journal of Petrology*, 47(6):1255-1259. <https://doi.org/10.1093/petrology/egl013>
- Kuribara Y., Tsunogae T., Takamura Y., Santosh M., Takamura Y., Costa A., Rosière C. 2019. Eoarchean to Neoproterozoic crustal evolution of the Mantiqueira and the Juiz de Fora Complexes, SE Brazil: Petrology, geochemistry, zircon U-Pb geochronology and Lu-Hf isotopes. *Precambrian Research*, 323:82-101. <http://dx.doi.org/10.1016/j.precamres.2019.01.008>
- Machado N., Valladares C., Heilbron M., Valeriano C.M. 1996. U-Pb geochronology of the central Ribeira Belt (Brazil) and implications for the evolution of the Brazilian Orogeny. *Precambrian Research*, 79(3-4):347-361. [https://doi.org/10.1016/0301-9268\(95\)00103-4](https://doi.org/10.1016/0301-9268(95)00103-4)
- Meschede M. 1986. A method of discriminating between different types of mid-ocean ridge basalts and continental tholeites with the Nb-Zr-Y diagram. *Chemical Geology*, 56(3-4):207-218. [https://doi.org/10.1016/0009-2541\(86\)90004-5](https://doi.org/10.1016/0009-2541(86)90004-5)
- Miller R. McG. 1983. The Pan-African Damara Orogen of Southwest Africa/Namibia. In: Miller R. McG. (ed.). *Evolution of the Damara Orogen*. Special Publication of the Geological Society of South Africa, v. 11, p. 431-515.
- Noce C., Pedrosa-Soares A.C., Silva L.C., Armstrong R., Piazana D. 2007. Evolution of polycyclic basement complexes in the Araçai Orogen, based on U-Pb SHRIMP data: Implications for Brazil Africa links in Paleoproterozoic time. *Precambrian Research*, 159(1):60-78. <http://dx.doi.org/10.1016/j.precamres.2007.06.001>
- Pearce J.A. & Gale G.H. 1977. Identification of ore-deposition environment from trace-element geochemistry of associated igneous host rocks. *Geological Society, London, Special Publication*, 7:14-24. <https://doi.org/10.1144/GSL.SP.1977.007.01.03>
- Pearce J.A., Harris N.W., Tindle A.G. 1984. Trace element discrimination diagrams for the tectonic interpretation of granitic rocks. *Journal of Petrology*, 25(4):956-983.
- Peate D.W., Hawkesworth C.J., Mantovani M.S.M. 1992. Chemical stratigraphy of the Paraná lavas (South America): classification of magma-types and their spatial distribution. *Bulletin of Volcanology*, 55(1-2):119-139. <https://doi.org/10.1007/BF00301125>

- Peccerillo A. & Taylor S.R. 1976. Geochemistry of Eocene calc-alkaline volcanic rocks from the Kastamonu area, Northern Turkey. *Contribution to Mineralogy and Petrology*, 58(1):63-81. <https://doi.org/10.1007/BF00384745>
- Pedrosa-Soares A.C. & Alkmim F.F. 2011. How many rifting events preceded the development of the Araçai-West Congo orogen? *Geonomos*, 19(2):244-251. <http://doi.org/10.18285/geonomos.v19i2.56>
- Pedrosa-Soares A.C. & Noce C.M. 1998. Where is the suture zone of the Neoproterozoic Araçai-West-Congo orogen? In: 14th International Conference of Basement Tectonics. *Expanded abstracts...* Ouro Preto, Universidade Federal de Ouro Preto, p. 35-37.
- Pedrosa-Soares A.C., Alkmim F.F., Tack L., Noce C.M., Babinski M., Silva L.C., Martins-Neto M.A. 2008. Similarities and differences between the Brazilian and African counterparts of Neoproterozoic Araçai-West Congo orogen. In: Pankhurst R., Trouw R., Brito-Neves B.B., De Witt, M.J. (eds.). *The Gondwana Paleoland in the South Atlantic Region*. Geological Society of London, Special Publications, v. 294, p. 153-172.
- Pedrosa-Soares A.C., Noce C.M., Wiedemann C.M., Pinto C.P. 2001. The Araçai-West Congo orogen in Brazil: An overview of a confined orogen formed during Gondwanaland assembly. *Precambrian Research*, 110(1):307-323. [http://doi.org/10.1016/S0301-9268\(01\)00174-7](http://doi.org/10.1016/S0301-9268(01)00174-7)
- Pedrosa-Soares A.C., Wiedemann-Leonardos C.M. 2000. Evolution of the Araçai Belt and its connections to the Ribeira Belt. In: Cordani U.G., Milani E.J., Thomaz Filho A., Campos, D.A. (eds.). *Tectonic Evolution of South America*. Rio de Janeiro, IGC Brasil, p. 265-288.
- Ragatky D., Tupinambá M., Heilbron M., Duarte B.P., Valladares C. 1999. New Sm/Nd isotopic data from pre-1.8 Ga basement rocks of central Ribeira Belt, SE Brazil. In: 2º South American Symposium on Isotope Geology. *Expanded abstracts...* Córdoba, Argentina, p. 433-436.
- Ribeiro A., Teixeira W., Dussin I.A., Avila C.A., Nascimento D. 2013. U-Pb LA-ICP-MS detrital zircon ages of the São João do Rei and Carandai basins: new evidence of intermittent Proterozoic rifting in the São Francisco paleocontinent. *Gondwana Research*, 24:713-726.
- Santos C.O. 2017. *Caracterização Geoquímica, Isotópica E Idade U-Pb Da Suite Barreiro, Domínio Juiz De Fora, Faixa Ribeira, MG*. Tese, Universidade do Estado do Rio de Janeiro, Rio de Janeiro, 120 p.
- Santos M.N., Chemale Jr. F., Dussin I.A., Martins M.S., Queiroga G., Pinto R.T.R., Santos A.N., Armstrong R. 2015. Provenance and paleogeographic reconstruction of a mesoproterozoic intracratonic sag basin (Upper Espinhaço Basin, Brazil). *Sedimentary Geology*, 318:40-57. <http://dx.doi.org/10.1016/j.sedgeo.2014.12.006>
- Schmitt R.S., Trouw R.A.J., Van Schmus W.R., Pimentel M.M. 2004. Late amalgamation in the central part of Western Gondwana: new geochronological data and the characterization of a Cambrian collision orogeny in the Ribeira belt (SE Brazil). *Precambrian Research*, 133(1):29-61. <http://dx.doi.org/10.1016/j.precamres.2004.03.010>
- Seth B., Kröner A., Mezger K., Nemchin A.A., Pidgeon R.T., Okrusch M. 1998. Archaean to Neoproterozoic magmatic events in the Kaoko belt of NW Namibia and their geodynamic significance. *Precambrian Research*, 92(4):341-363. [https://doi.org/10.1016/S0301-9268\(98\)00086-2](https://doi.org/10.1016/S0301-9268(98)00086-2)
- Shand S.J. 1943. *Eruptive Rocks*. 2º ed. New York, John Wiley, 444 p.
- Silva L.C., Noce C.M., Carneiro M.A., Pimentel M., Pedrosa-Soares A.C., Leite C.A., Vieiro V.S., Paes V.J.C., Cardoso Filho J.M., Silva M.A. 2002. Reavaliação da evolução geológica em terrenos Pré-Cambrianos Brasileiros com base em novos dados U-Pb SHRIMP, Parte II: Orógeno Araçai, Cinturão Mineiro e Cratôn São Francisco Meridional em Minas Gerais. *Revista Brasileira de Geociências*, 32(4):513-528.
- Smithies R.H., Champion D.C., Sun S.-S. 2004. Early evidence for LILE-enriched mantle source regions: diverse magmas from the c. 3.0 Ga Mallina Basin, Pilbara Craton, NW Australia. *Journal of Petrology*, 45(8):1515-1537. <http://doi.org/10.1093/petrology/egh014>
- Streckeisen A. 1974. Classification and nomenclature of plutonic rocks: Recommendations of the IUGS subcommission on the systematics of igneous rocks. *Geologische Rundschau*, 63(2):773-786. <https://doi.org/10.1007/BF01820841>
- Sun S.-S. & Nesbitt R.W. 1978. Geochemical regularities and genetic significance of ophiolitic basalts. *Geology*, 6(11):689-693. [https://doi.org/10.1130/0091-7613\(1978\)6%3C689:GRAGSO%3E2.0.CO;2](https://doi.org/10.1130/0091-7613(1978)6%3C689:GRAGSO%3E2.0.CO;2)
- Tanaka T., Togashi S., Kamioka H., Amakawa H., Kagami H., Hamamoto T., Yuhara M., Orihashi Y., Yoneda S., Shimizu H., Kunimura T., Takahashi K., Yanagi T., Nakano T., Fujimaki H., Shinjo R., Asahara Y., Tanimizu M., Dragunow C. 2000. JNd-1: a neodymium isotopic reference in consistency with La Jolla neodymium. *Chemical Geology*, 168(3-4):279-281. [https://doi.org/10.1016/S0009-2541\(00\)00198-4](https://doi.org/10.1016/S0009-2541(00)00198-4)
- Teixeira W., Ávila C.A., Bongiolo E.M., Hollanda M.H.B.M., Barbosa N.S. 2014. Age and tectonic significance of the Ritápolis batholith, Mineiro belt (Southern São Francisco Craton): U-Pb LA-ICPMS, Nd isotopes and geochemical evidence. In: 9º South American Symposium on Isotope Geology - SSAGI, São Paulo, Brazil. *Program and Abstracts...* p. 225.
- Teixeira W., Ávila C.A., Dussin I.A., Corrêa Neto A.V., Bongiolo E.M., Santos J.O., Barbosa N.S. 2015. Juvenile accretion episode (2.35-2.32 Ga) in the Mineiro belt and its role to the Minas accretionary orogeny: Zircon U-Pb-Hf and geochemical evidences. *Precambrian Research*, 256:148-169. <http://dx.doi.org/10.1016/j.precamres.2014.11.009>
- Trouw R.A.J., Heilbron M., Ribeiro A., Paciulli E.P., Valeriano C.M., Almeida J.C.H., Tupinambá M., Andreis R.R. 2000. The Central Segment of the Ribeira Belt. In: Cordani U.G., Milani E.J., Thomaz-Filho A., Campos D.A. (eds.). *Tectonic Evolution of South America*, Rio de Janeiro. 31st International Geological Congress, p. 287-310.
- Tupinambá M., Heilbron M., Duarte B.P., Nogueira J.R., Valladares C., Almeida J.C.H., Silva L.G.E., Medeiros S.R., Almeida C.G., Miranda A.W.A., Ragatky C.D., Mendes J., Ludka I. 2007. Geologia da Faixa Ribeira Setentrional: Estado da Arte e Conexões com a Faixa Araçai. *Geonomos*, 15(1):67-79. <https://doi.org/10.18285/geonomos.v15i1.108>
- Tupinambá M., Teixeira W., Heilbron M. 2000. Neoproterozoic Western Gondwana assembly and subduction-related plutonism: the role of the Rio Negro Complex in the Ribeira Belt, South-eastern Brazil. *Revista Brasileira de Geociências*, 30(1):7-11.
- Tupinambá M., Teixeira W., Heilbron M. 2012. Evolução Tectônica e Magnética da Faixa Ribeira entre o Neoproterozoico e o Paleozoico Inferior na Região Serrana do Estado do Rio de Janeiro, Brasil. *Anuário do Instituto de Geociências da UFRRJ*, 35(2):140-151. https://doi.org/10.11137/2012_2_140_151
- Valeriano C.M., Vaz G.S., Medeiros S.R., Neto C.C.A., Ragatky C.D. 2008. The Neodymium isotope composition of the JNd-1 oxide reference material: results from the LAGIR Laboratory, Rio de Janeiro. In: VI South American Symposium on Isotope Geology. *Proceedings...* San Carlos de Bariloche, Argentina, p. 1-2. (CD-ROM)
- Valladares C.S., Duarte B.P., Heilbron M., Ragatky C.D. 2000. The tectono-magnetic evolution of the western terrane and the Paraíba do Sul klippe of the Neoproterozoic Ribeira orogenic belt, southeastern Brazil. *Revista Brasileira de Geociências*, 30(1):1-6.
- Valladares C.S., Souza S.F., Ragatky C.D. 2002. The Quirino Complex: a Transamazonian Magmatic Arc of the Central Segment of the Brasiliano/Pan-African Ribeira Belt, SE Brazil. *Revista Universidade Rural: Série Ciências Exatas e da Terra*, Rio de Janeiro, 21(1):49-61.
- Verma S.P., Guevara M., Agrawal S. 2006. Discriminating four tectonic settings: Five new geochemical diagrams for basic and ultrabasic volcanic rocks based on log-ratio transformation of major-element data. *Journal of Earth System Science*, 115(5):485-528. <http://doi.org/10.1007/BF02702907>
- Wilson M. 1989. *Igneous Petrogenesis*. London, Unwin Hyman.
- Wise S.A. & Waters R.L. 2007. *Certificate of Analysis Standard Reference Material® 987 Strontium Carbonate (Isotopic Standard)*. NIST National Institute of Standards & Technology 2 p.

APÊNDICE B – Crustal evolution of the Juiz de Fora Complex: A Siderian to Rhyacian juvenile arc and its tectonic implications for Minas-Bahia orogeny and correlations with the Western Central Africa belt (Artigo Científico)

Summary:

INTRODUCTION

MATERIALS AND METHODS

U-Pb geochronology

Lu-Hf isotopic analysis

GEOLOGIC FRAMEWORK

São Francisco Craton

Juiz de Fora Complex

RESULTS

In situ U-Pb zircon ages and Hf, Nd and Sr isotopes

Elementary Geochemistry

DISCUSSIONS

Tectonic evolution of Juiz de Fora Complex

Correlations and Tectonic implications for Minas-Bahia orogen

São Francisco-Congo Correlations along Paleoproterozoic

CONCLUSIONS

ACKNOWLEDGEMENTS

REFERENCES

Crustal evolution of the Juiz de Fora Complex: A Siderian to Rhyacian juvenile arc and its tectonic implications for Minas-Bahia orogeny and correlations with the Western Central Africa belt

Lucas Eduardo de Abreu Barbosa Araujo¹; Monica Heilbron¹; Wilson Teixeira²; Ivo Antônio Dussin¹; Claudio de Morisson Valeriano¹; Henrique Bruno¹; Gabriel Paravidini¹; Matheus Castro¹

¹ Universidade do Estado do Rio de Janeiro, Faculdade de Geologia, Programa de Pós-graduação em Geociências, TEKTOS Grupo de Pesquisa em Geotectônica, Rua São Francisco Xavier, 524, Maracanã. 20550-900, Rio de Janeiro, RJ, Brazil.

² Instituto de Geociências - Universidade de São Paulo. Rua do Lago, 562. 05508-080. São Paulo, SP, Brazil. e-mails: lucaseduardo9393@gmail.com; monica.heilbron@gmail.com; valeriano.claudio@gmail.com; wteixeir@usp.br

ABSTRACT

The Juiz de Fora Complex (JFC) is one of the basement units of the Occidental Terrane in the Central Ribeira belt, regarded as part of the reworked border of the São Francisco paleoplate. The JFC comprises orthogranulites with varied geochemical compositions, deformational fabrics, and ages, in Brasiliano granulite facies. This work presents new zircon U-Pb (SHRIMP) ages and Lu-Hf (LA-ICPMS) data, besides whole-rock Sr and Sm-Nd isotopic data from JFC orthogranulites from southwest Rio de Janeiro state in order to better constrain the Paleoproterozoic tectonic evolution of this unit. Six samples, chosen by their element compositions, were selected for U-Pb and Lu-Hf analysis. A low-K tholeiitic diorite presents age of ca. 2.44 Ga. Two calc-alkaline granodiorites have distinct geochemical signatures (eg. TTG and sanukitoid) yielded crystallization ages of ca. 2.2 Ga. A high-K granodiorite presenting sanukitoid signature shows crystallization age of ca. 2.18 Ga. A tholeiitic mafic granulite presents age of ca. 2.13 Ga. Metamorphic rims around the magmatic cores present ages from 600 to 580 Ma confirming the Neoproterozoic overprint, but the mafic granulite also has Paleoproterozoic granulite-facies metamorphic rims and grains. Few inherited zircon crystals between ca. 2.53, 2.38, and 2.2 Ga were identified among the samples. The whole-rock Nd and Sr isotopic data of dated samples show that Siderian, Rhyacian (2.2 Ga) and Rhyacian (2.13 Ga) magmatism episodes are moderately juvenile, moderately juvenile to evolved, and moderately juvenile, respectively with Siderian to Rhyacian Nd TDM model ages. Minor Archean contribution is also observed by the Nd TDM model ages. On the other hand, the obtained Hf TDM model ages among the samples vary from Archean to Siderian (3.2-2.4 Ga), with negative to slightly positive $\epsilon\text{Hf(t)}$ values (-13 to +2), contrasting with the whole-rock Nd signatures, suggesting recycling of Archean material from reworked detrital zircon. The envisaged geological evolution starts during the Siderian (ca. 2.44 Ga) with crystallization of the more primitive arc rock (tholeiitic diorite) marking the initial stage of arc development. Arc-related rocks with TTG and sanukitoid signatures are representative from a heterogeneous, with a mixture of juvenile (oceanic slab) and archean (metasedimentary sequence) sources varying the proportion of each source, according the pluton signature. A collisional episode, correlated to Minas-Bahia orogeny, at around ca. 2035Ma is marked by Paleoproterozoic zircon rims and grains. A Paleoproterozoic (ca. 2026 Ma) anatetic melt is proposed in a high-K granodiorite with in-situ and in-source leucosomes. During the Brasiliano orogeny, 600-580 Ma granulite facies metamorphism, coupled with deformation, is recorded in the studied samples. The magmatic episodes from Juiz de Fora Complex and Mineiro Belt are quite similar, with the occurrence of TTG and sanukitoid plutons on both units, but JFC seems to have a longer duration of Rhyacian arc magmatism and a distinguishing diachronic metamorphic event among other basement units involved on Minas-Bahia orogeny. This study also comprises important considerations about geochronological and isotopic correlations for Minas-Bahia basement units and its African basement counterparts (Western Central African Belt).

Keywords: Siderian arc rocks, Rhyacian juvenile subduction, Minas-Bahia orogen;

INTRODUCTION

The magmatism of the active continental margin and the accretion of exotic terranes (eg., Island arcs, oceanic plateaus) are some of the continental growth mechanisms (Stern and Scholl, 2010; Clift *et al.*, 2009a; Cawood *et al.*, 2009). There are several examples of these

processes throughout the geological record, such as Andean active continental margin (Thorpe *et al.* 1981) and the accreted Talkeetna island arc at Alaska (Greene *et al.* 2006; Hacker *et al.* 2008). Most of the crustal growth models indicate that ~75% of the crust was formed between 2000 and 3000 Ma, suggesting a significant continental growth during that period (e.g., Hunter, 1970; Glikson, 1971; White *et al.*, 1971; Windley and Bridgwater, 1971; Arth and Hanson, 1972; McGregor, 1973; Stowe, 1973; Wilson, 1973; Fyfe, 1978; Veizer and Jansen, 1979; Armstrong, 1981; Reymer and Schubert, 1984; Taylor and McLennan, 1985, 1995; Santosh *et al.*, 2009a). The end of this interval is correlative with the agglutination of the Columbia Supercontinent (Zhao *et al.*, 2002, 2004; Rogers and Santosh, 2004, 2009), that have had its major episodes of amalgamation between the Rhyacian to Orosirian period (ca. 2100 to 1900 Ma). Following recent paleomagnetic reconstructions on Paleoproterozoic (D’Agrella Filho *et al.* 2019), this supercontinent integrated Laurentia, Baltica, Siberia, East Antarctica, India, Rio de La Plata, North China, Congo, and São Francisco continental landmasses.

The São Francisco and Congo landmasses are important pieces of global correlations because they shared a similar geological history from the Paleoproterozoic until the Cretaceous (Gondwana break-up). The first orogenic cycle in common have occurred on Paleoproterozoic and is known as the Minas-Bahia orogeny at São Francisco paleoplate (Alkmim and Teixeira, 2017) and as the Eburnean Orogeny at Western Central Africa (Toteu *et al.* 1994; Feybesse *et al.* 1998). This orogenic cycle in the São Francisco-Congo paleoplate have started with the development of both continental magmatic arcs (Cruz *et al.* 2016; Peucat *et al.* 2011) emplaced on Archean nucleus and intra-oceanic arcs (Ávila *et al.* 2014; Barbosa *et al.* 2015; Noce *et al.* 2007; Heilbron *et al.* 2010) followed by an amalgamation of these terranes onto the present Archean nucleus of the São Francisco and Congo.

The southern part of this orogen, named Minas Accretionary orogen (Teixeira *et al.* 2015) corresponds to the amalgamation of magmatic arcs (eg. Mineiro Belt, Mantiqueira Complex, Juiz de Fora) of distinct signatures onto Archean nucleus of São Francisco paleoplate. The Juiz de Fora Complex (JFC) is interpreted as a Rhyacian (ca. 2.2 to 2.05 Ga) intra-oceanic arc developed between the continental blocks São Francisco and Congo. There is a Siderian (ca. 2.42 Ga) E-MORB tholeiitic mafic granulite, located on the northern portion of JFC, assumed as a relict of former oceanic crust (Heilbron *et al.* 2010) between these continental landmasses. A recent tectonic study reinterprets siderian magmatic pulses of Juiz de Fora Complex as arc-related magmatism due to inherited zircon crystals with similar ages (2372 ± 48 Ma: Kuribara *et al.* 2019), increasing, therefore, the period of subduction on this unit. Despite the available isotopic dataset indicating juvenile magmas on Rhyacian (Degler *et al.*

2018; Kuribara *et al.* 2019; Noce *et al.* 2007), isotopic signatures for the siderian magmatism and its tendency are missing on JFC records. On proposed tectonic models (Noce *et al.* 2007; Heilbron *et al.* 2010; Aguilar *et al.* 2017), the Juiz de Fora arc has been docked onto Mantiqueira Complex at Late Rhyacian, but there is no geochronological evidence supported this assumption on JFC, such as paleoproterozoic metamorphic zircon rims/overgrowths observed on Mantiqueira Complex. The intense granulite-facies Neoproterozoic metamorphic overprint on Juiz de Fora Complex (Duarte and Heilbron, 1999) could have reset the paleoproterozoic metamorphic evidence.

In this study, we provide new U-Pb zircon ages (SHRIMP) and Lu-Hf isotopic analysis in zircons, as well as, the treatment of whole-rock isotopic data of orthogranulites that present distinct geochemical signatures (Araujo *et al.* 2019) in order to constrain the crustal evolution from Juiz de Fora Complex during Paleoproterozoic. In addition, the petrogenetic evolution of the magmatic episodes will be investigated through the isotopic signature (Sr, Nd, and Hf) of rocks. Finally, the tectonic implications of Juiz de Fora Complex on the São Francisco-Congo paleocontinent and regional correlations with other Paleoproterozoic terranes of this continental landmass will be discussed in this paper.

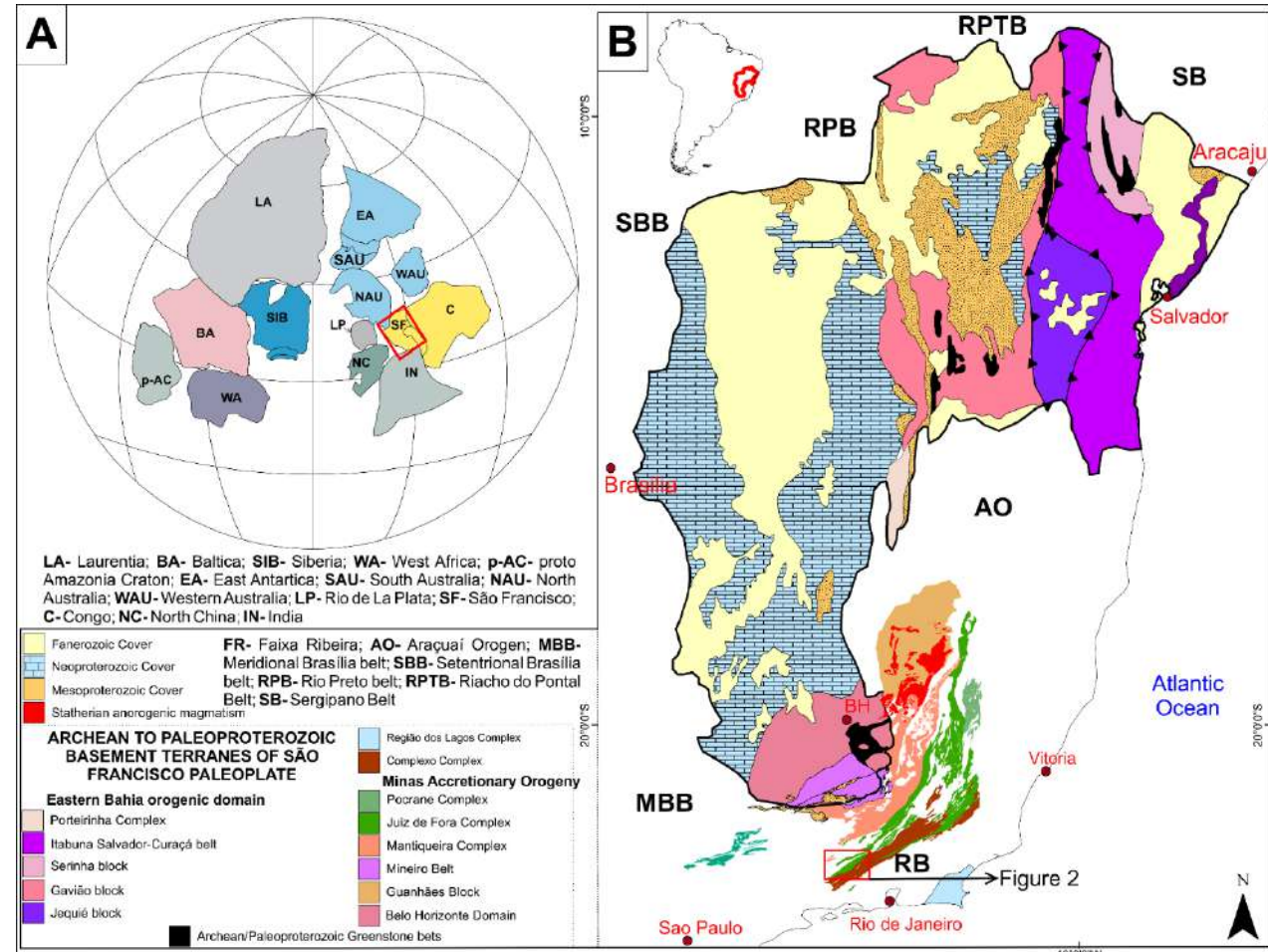


Figure 1. a) Reconstruction map of Columbia supercontinent at 1790 Ma. São Francisco paleoplate on red rectangle. Modified from D'Agrella *et al.* 2019. B) Simplified map of the São Francisco Craton emphasizing the archean to Paleoproterozoic basement terranes from São Francisco Paleoplate. Modified from Alkmim *et al.* (1993).

4.3.2. ANALYTICAL METHODS

4.3.2.1. U-Pb Geochronology

Five samples presenting distinct geochemical signatures (Araujo et al. 2019) were collected for the U-Pb and Lu-Hf studies. The sample preparation techniques were carried out at Rio de Janeiro State University and include grain size reduction using a hammer, followed by washing, crushing, and grinding using both a jaw crusher and a disk-mill. The zircon grains were separated and concentrated by densimetric (Wifley Table and Metilen Iodite, Bromoforme liquids) and electrodynamic (Frantz and magnet) procedures. The zircon grains were hand-picked and mounted in an epoxy resin (together with TEMORA standard) and imaged using cathodoluminescence (CL) imaging on a VPSEM FEI Quanta 250 scanning electron microscope housed at the São Paulo University. The CL images were used to examine the interior textures of zircon grains and to assess the analysis spots. The textures were interpreted according to the criteria of Wu and Zheng (2004) and Corfu et al. (2003).

The U-Pb zircon isotopic measurements were carried out at the São Paulo University using the Sensitive High-Resolution Ion Microprobe machine (SHRIMP-IIe), following the analytical procedures described in Williams (1998). Seventeen spots (average number) were analyzed from each sample. The results were corrected for common Pb using the measured ^{204}Pb . The Uranium and thorium abundances and U/Pb isotopic ratios were calibrated against the TEMORA1 (Black et al. 2003) standard. The errors are reported at 1σ level. Error in Standard calibration was 0.12% (not included in the above errors but required when comparing data from different mounts).

Due to the complexity of the mafic granulite (sample BP-CM-151), this rock has been analyzed again by the LA-ICPMS method as well. The U-Pb zircon isotopic measurements of this sample were carried out at Universidade Federal de Ouro Preto using a Thermo-Finnegan Neptune multi-collector ICP-MS coupled with a Photon-Machines 193 nm excimer laser system (LA-MC-ICP-MS). Data acquisition followed the method described by Lana et al. (2017). A spot size of 20 μm was used with a 6 Hz repetition rate and laser fluence of 1–2 J.cm $^{-2}$. Raw data were corrected offline using the GLITTER® software package (Van Achterbergh et al., 2001). The errors are 2σ level.

All zircon data is represented in Supplementary Table 1. The analyzes were treated on Excel software and the age calculations were performed on Isoplot© 4.15 (Ludwig, 2011). We

adopt discordance values lower than and high values of Pbc (>0.5%) or f206c (>0.005) as criteria of the analytical data exclusion in order to calculate Concordia ages.

4.3.2.2. Lu-Hf isotopic analyzes

The crystallization zircon spots that display better concordance values (-5% < Disc. < +5%) were chosen in order to obtain the Lu-Hf zircon isotopic analyzes. The analyzes were carried out at the Federal University of Ouro Preto using Thermo-Finnigan Neptune multi-collector ICP-MS coupled to a Photon-Machines 193 nm excimer laser system (LA-MCICP-MS). The acquisition of the data followed the methods described on Gerdes and Zeh (2006, 2009). The laser spot size used was 50 μ m and the data (75 analyzes; Supplementary Table 2) were collected in static mode during 60 s of ablation. The spots were drilled with a repetition rate of 6 Hz and the normal signal intensity was ca. 10 V for 177Hf. Mass bias corrections of Lu-Hf isotopic ratios were done applying the variations of standards: BB (age: 560 Ma; 176Hf/177Hf=0.2816713 -Santos et al. 2017), Mudtank (age:732 Ma; 176Hf/177Hf=0.282504), GJ-1 (age:602 Ma; 176Hf/177Hf=0.2820000 - Jackson et al., 2004) and Plešovice (age: 337 Ma; 176Hf/177Hf=0.2820000 - Sláma et al., 2008).

4.3.2.3. Sr-Nd treatment

The analyzes reported on Araujo et al. (2019) coupled with the calculated U-Pb zircon crystallization ages were used in order to obtain the petrogenetic parameter, such as ε Nd(t) and $^{87}\text{Sr}/^{86}\text{Sr}$ (i). Further details on isotopic measurements and data acquisition at the LAGIR Lab of the Rio de Janeiro State University could be found on Araujo et al. (2019).

4.3.3. GEOLOGIC FRAMEWORK

4.3.3.1. São Francisco Craton and Congo paleoplates

The Archean and Paleoproterozoic blocks of the present São Francisco and Congo Cratons had been amalgamated during diachronic orogenic episodes along Rhyacian-Orosirian (ca. 2100 to 2000 Ma) to form segments of the Columbia supercontinent (Figure 1a). This orogenic cycle is referred to as Eburnean orogeny on West Africa (Weber et al. 2016) and Minas-Bahia orogeny (Alkmim and Teixeira, 2017) on Eastern São Francisco side. During the

Brasiliano-Panafrican Orogeny (ca. 620-490 Ma), the border of the São Francisco-Congo paleocontinent has been reworked with deformation and metamorphic overprint to form an important part of West Gondwana (Cordani and Sato, 1999; Campos Neto, 2000; Alkmim et al. 2001).

The Eburnean orogenic belt (Western Central Africa belt - ca. 2100-2000 Ma) consists on the collision of the Archean nuclei with strong reworking on high-grade metamorphism on the Nterm-Chailu block and Angola Shield as well as the Paleoproterozoic supracrustal sequences, such as Francevillian basins (Feybesse et al. 1998). Syn to late (ca. 2060 to 1930 Ma) intense plutonism occurs on this belt (Lerouge et al. 2006; Djalma et al. 1992; Thieblemont et al. 2009a) with few reports of plutonic rocks from continental margin arcs (Delhal & Ledent, 1976). These plutonic rocks units extend from SW Cameroon to NW Angola and have different names accordingly the country: The Nyoung Group (SW Cameroon- Toteu et al. 1994; Lerouge et al. 2006), the Ogooué orogenic domain on Gabon (Weber et al. 2016), the Mayombe basement from Gabon to Congo (Djalma et al. 1992) and the Kimezian Supergroup from DRC to NW Angola (Pedrosa-Soares et al. 2016; Delhal and Ledent, 1976). These two latter units outcrop as basement units of West Congo Belt (Thieblémont et al. 2018).

On the Brazilian side, the Minas-Bahia orogenic event (2.5-2.0 Ga) have consisted on the amalgamation of Archean nuclei and/or Paleoproterozoic arcs/belts (Alkmin and Teixeira, 2017). Focusing on the northern segment of this Paleoproterozoic orogenic system, this cycle started with the development of continental margin arcs during Rhyacian at Itabuna-Salvador-Curaçá belt and Gavião Block (Peucat et al. 2011; Cruz et al. 2016). The development of greenstone belts terranes (Rio Itapicuru and Rio Capim: Oliveira et al. 2010) is coeval to this period on Serrinha block (Figure 1b). These magmatic arcs and greenstone belt terranes have been accreted onto Archean blocks and its subsequent collision has led to intense granulite-facies metamorphism (ca. 2100 to 2050 Ma) on these blocks (Barbosa and Sabaté, 2004). Ending this tectonic cycle, there were intense syn- to post-collisional plutonism in all terranes (Oliveira et al. 2010; Barbosa and Sabaté, 2004), including on the Porteirinha Complex (Silva et al. 2016; Bersan et al. 2020).

At the southern segment of the Paleoproterozoic orogen (location of the study area), Paleoproterozoic arcs have developed since the Siderian (eg. Mineiro Belt: Barbosa et al. 2018) to Rhyacian (eg. Mantiqueira Complex and Juiz de Fora Complex: Noce et al. 2007; Heilbron et al. 2010). These arcs were accreted onto archean blocks (Piedade Block- Bruno et al. 2020; Belo Horizonte Domain- Lana et al. 2013). The Mineiro Belt have been accreted onto Belo Horizonte Archean Domain (Ávila et al. 2010) and Mantiqueira Complex onto Piedade Block

(Bruno et al. 2020) in a local event called Minas Accretionary orogen (Teixeira et al. 2015), provoking intense Rhyacian-Orosirian (ca. 2100 to 2050 Ma) granulite-facies metamorphism reported on these belts and adjacent archean blocks (Aguilar et al. 2017; Moreira et al. 2018; Ávila et al. 2010; Cutts et al. 2018; Silva et al. 2002; Heilbron et al. 2010; Bruno et al. 2020). The collision between the Mineiro Belt and Mantiqueira Complex is still unknown. The authors have considered that Juiz de Fora Complex is part of Minas Accretionary orogen (Teixeira et al. 2015) because, in all previously proposed tectonic models (Noce et al. 2007; Heilbron et al. 2010), this unit was supposedly docked onto Mantiqueira Complex. However, there is no evidence of this Paleoproterozoic metamorphism in Juiz de Fora Complex due to strongly Neoproterozoic granulite-facies overprint (Heilbron et al. 2010; Duarte and Heilbron, 1999).

There are other two Paleoproterozoic basement units reworked within the Ribeira Belt, the Quirino and Região dos Lagos Complex. The Quirino Complex comprises Rhyacian orthogneisses with mafic and ultramafic enclaves (Machado et al. 1996), presenting juvenile sources and archean reworking as the petrogenetic mechanism (Valladares et al. 2002). The Região dos Lagos Complex is constituted by Orosirian orthogneisses with mafic enclaves, amphibolite layers, and dykes (Fonseca, 1993; Schmitt et al. 2004). Degler et al. (2018) constrained that these basement terranes being part of the Eastern Rhyacian-Orosirian Orogenic system (E-ROOS) associated with Eastern Bahia Orogenic Domain, only by its crustal isotopic signature, even without any evidence of accretion of these blocks on São Francisco Paleoplate by present-day. The amphibolite-facies metamorphism is present in these complexes (Schmitt et al. 2004; Valladares et al. 2002).

4.3.3.2. Juiz de Fora Complex

The Juiz de Fora Complex, the focus of the study, is interpreted as a Paleoproterozoic intra-oceanic arc (Noce et al. 2007; Heilbron et al. 2010) which comprises granitoids and mafic rocks metamorphosed on granulite-facies in Brasiliano orogenic event (Duarte and Heilbron, 1999) that culminates on the Gondwana configuration (Figure 2a). It is tectonically interlayered (as thrust sheets – Figure 2b) with supracrustal metasedimentary rocks from Andrelândia Group (Pacciulo et al. 2004a), composing the most deformed tectonic domain from Occidental Terrane of Ribeira Belt (Heilbron et al. 2004a). The Juiz de Fora Complex is one of the basement units of Ribeira Belt and Araçuaí Belt (Noce et al. 2007).

The Juiz de Fora Complex extends along the Brazilian southeastern states (Minas Gerais, Rio de Janeiro, and Espírito Santo). The granitoid rocks comprise heterogeneous

magmatic suites (Araujo et al. 2019, Duarte et al. 1997) with a predominance of calc-alkaline diorites and granodiorites represented by enderbitic to charnoenderbitic granulites. The mafic granulites also have distinct magmatic series, varying from tectonic settings (E-MORB, IAT, and WPT gabbroic rocks – Araujo et al. 2019; Heilbron, 1993). The previous geochronological dataset from Juiz de Fora Complex points out to ages between ca. 2.2 and 2.05 Ga (Noce et al. 2007; Degler et al. 2018; Kuribara et al. 2019; Heilbron et al. 2010; Machado et al. 1996). One Archean felsic orthogranulite was described at the Juiz de Fora city (Silva et al. 2002). Mafic granulites, with E-MORB tholeiitic and WPT alkaline signatures, have provided ages of ca. 2.42 Ga and ca. 1.77 Ga (Heilbron et al. 2010). The juvenile character of Juiz de Fora Paleoproterozoic magmatism is supported by the predominance of subchondritic (around zero) to positive $\epsilon_{\text{Nd}}(t)$ and $\epsilon_{\text{Hf}}(t)$ values of these rocks with Siderian to Rhyacian TDM Nd and TDM Hf model ages (Degler et al. 2018; Kuribara et al. 2019; Araujo et al. 2019; Fischel et al. 1998; André et al. 2009) pointing out to mantle sources. On the other hand, a minor Archean component can be attributed to Juiz de Fora protoliths because of the reported Hf TDM (by 3.45 Ga – Kuribara et al. 2019) and TDM Nd (by 2.75 Ga – Araujo et al. 2019). A compilation of geochronological and isotopic data can be obtained on Araujo et al. 2019.

In the focused area, the Juiz de Fora Complex consists of enderbitic granulites with mafic enclaves (Figure 2a), charnoenderbitic granulites with mafic bands (Figure 2b) and granoblastic textures (Figure 2c). Massive mafic granulites also occur (Figure 2d) and evidence of partial melting, such as in-situ and in-source leucosomes (Figure 2e) can be observed in some outcrops. There is a lack of information on the field relationships between these lithologies because of the paucity of outcrops in the study area. The deformation grade increases accordingly the proximity of the Neoproterozoic thrust boundaries (Figure 1b), developing a strong mylonitic foliation close to the contacts with the Neoproterozoic metasedimentary units. Foliation normally dips towards SE following the major trend of the Ribeira Belt (Heilbron et al. 1998).

The observed textures the orhogranulites vary accordingly the deformation of these rocks can be granoblastic (Figure 2f), mylonitic, or granolepidoblastic. The granulation of JFC rocks is commonly medium to coarse. The felsic granulites normally have paragenesis consisting of plagioclase + hypersthene + quartz \pm k-feldspar \pm diopside with retrograde hornblende and biotite (Figure 2g), whereas the mafic granulites (Figure 2h) present plagioclase + diopside + hypersthene \pm quartz \pm garnet. Some of the mafic granulites have coronytic garnet around pyroxene crystals (Araujo et al. 2019). Further details of the JFC local geology on the studied area can be gathered from Araujo et al. (2019).

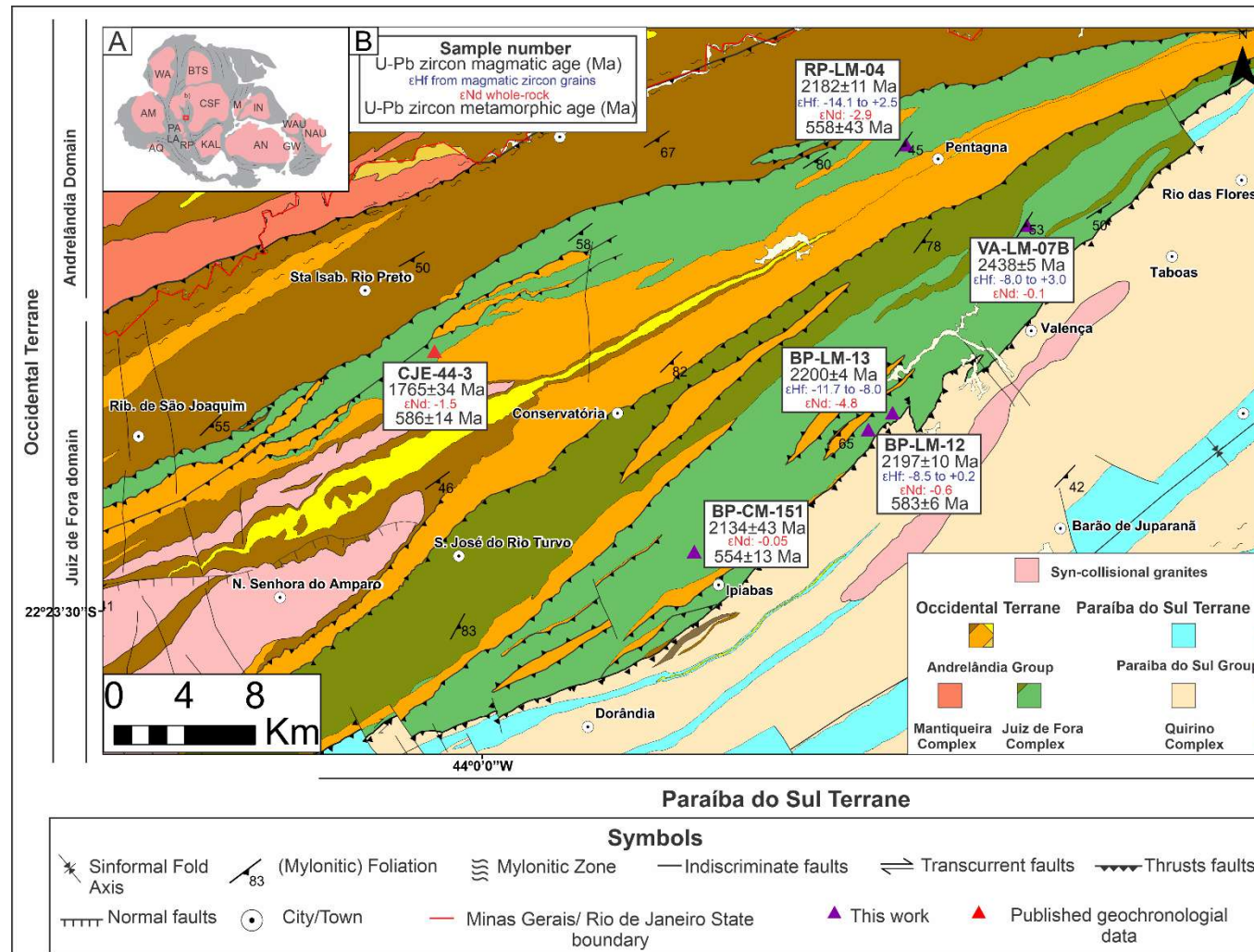


Figure 2. A) Gondwana reconstruction map with the inset of studied area in the red square. Cratons: AM- Amazonia; AN- Antarctica; AQ – Arequipa; BTS - Borborema-Trans Sahara; CSF - Congo São Francisco; GW – Gawler; IN – India; LA - Luís Alves; KAL- Kalahari; M – Madagascar; NAU - North Australia; PA – Paranapanema; RP - Rio de La Plata; WA - West Africa; WAU - Western Australia. B) Geological map of studied area (Modified from Araujo *et al.* 2019).

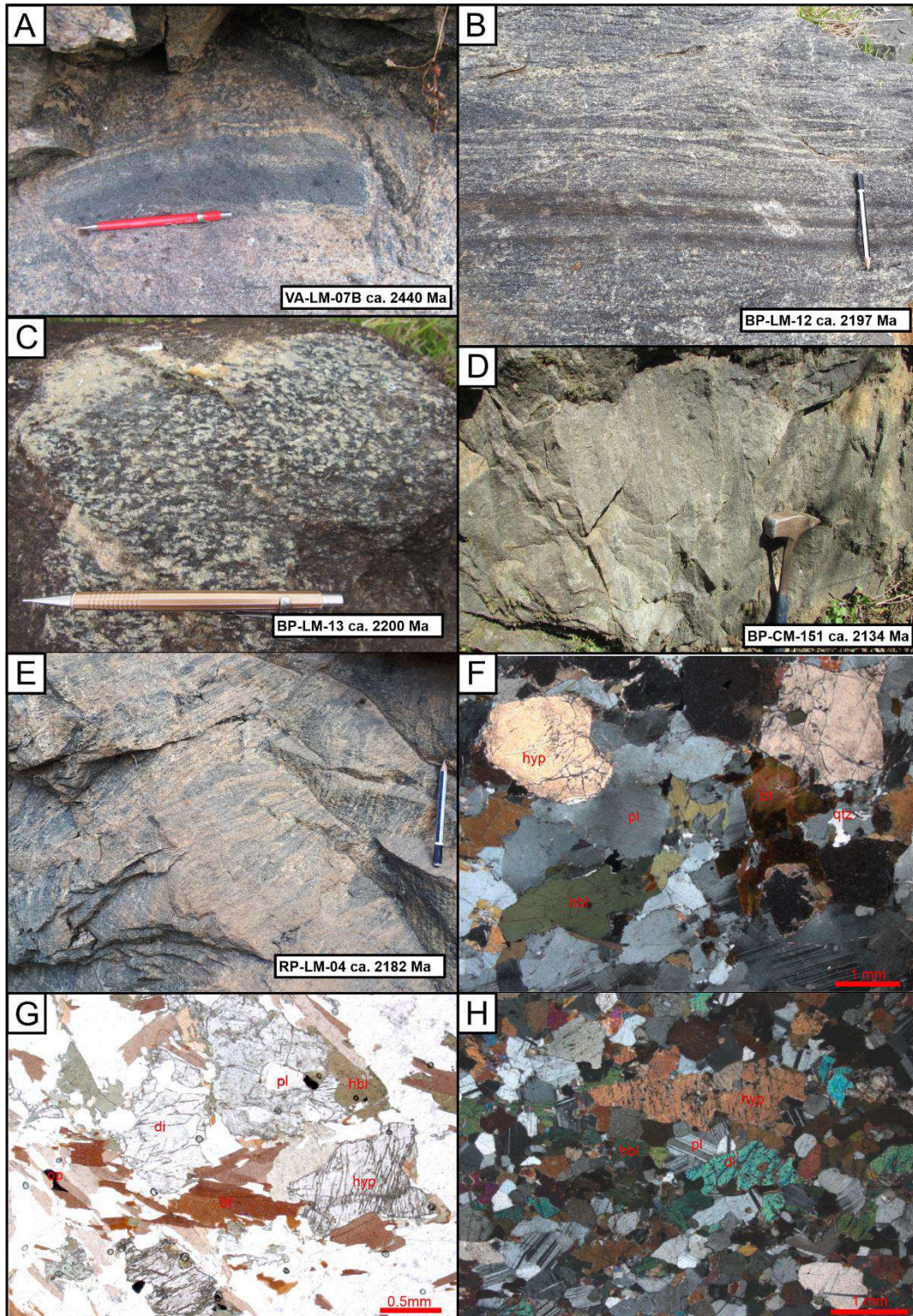


Figure 3. Field relations and petrography of orthogranulites from studied area. A) Enderbitic granulite with mafic enclave (Sample VA-LM-07B); B) Charnoenderbitic granulite interlayered with mafic bands (Sample BP-LM-12); C) Porphyroblastic charnoenderbitic granulite (Sample BP-LM-13); D) Massive mafic granulite (Sample BP-CM-151); E) Charnoenderbitic granulite with in-situ and in-source leucosomes (Sample RP-LM-04); F) Granoblastic texture and typical granulite-facies paragenesis for felsic granulites (Sample VA-LM-07B); G) Pyroxene substitution to hornblende and biotite related to retrograde metamorphism (Sample BP-LM-12); H) Granoblastic texture and typical granulite-facies paragenesis for mafic granulites (Sample BP-CM-151).

4.3.4. RESULTS

4.3.4.1. Zircon U-Pb ages, zircon Hf and whole-rock Nd-Sr isotopes

In this section, we describe the results obtained from the isotopic analyses (Supplementary Table 1). The major exclusion criteria for the obtained data were calculated errors, the percentage of discordance (Disc. \pm 5%) and common Pb values (<0.5%). Concordia or Intercept ages determinations of each sample (Figure 5) will be discussed here.

4.3.4.1.1. Sample VA-LM-07B:

This sample is an enderbitic granulite with associated mafic bands (Figure 3a,f). The rock was collected from an outcrop with evidence of partial melting, such as tinny leucosomatic veins. The zircon crystals of this sample are translucent to dark opaque with colors that vary from light to dark brown. They are subhedral, short to long prismatic with sub-rounded borders, ranging in size from 174 to 288 μm , and the length/width ratios mostly between 2:1 and 5:1. The CL images show a homogeneous group of long prismatic zircons presenting a well-developed magmatic oscillatory zoning (Figure 4). Most of the grains display a thin overgrowth, with homogeneous white/gray colors (not wide enough for spot analyses), which could indicate metamorphic origin. Eleven analyses of zircon crystals with oscillatory zoning show variable Th/U (0.38 and 0.74; Supplementary Table 1). Most all of these analyses are within the adopted discordance limits ($-5\% < D < +5\%$), except by spots 4.1 and 9.1. These analyses rendered a concordant age of 2440.2 ± 4.8 Ma interpreted crystallization age (Figure 5a). This assumption is corroborated by $^{207}\text{Pb}/^{206}\text{Pb}$ weighted average mean age of 2451 ± 21 Ma (Figure 5).

The initial $^{176}\text{Hf}/^{177}\text{Hf}$ ratios of the magmatic zircons from this sample varied from 0.281161 to 0.281374. The Hf TDM model ages yield values between ca. 2.90 and 2.48 Ga with positive to negatives $\epsilon_{\text{Hf}}(t)$ values between -8 and +3 (most frequent value: +1, Figure 7 and Supplementary Table 2). Whole-rock Sr-Nd isotopes (Figure 7) supports a juvenile to moderately juvenile mantle source from the dioritic protolith, with low $^{87}\text{Sr}/^{86}\text{Sr(i)}$ (0.7017) and chondritic $\epsilon_{\text{Nd}}(t)$ value (-0.1).

4.3.4.1.2. Sample BP-LM-13:

Sample BP-LM-13 is referred to as a charnoenderbitic granulite with coarse granulation and hypersthene and plagioclase porphyroblasts. The zircon crystals are translucent to dark and vary from light to dark brown. They are subhedral, prismatic with sub-rounded borders, ranging

in size from 155 to 290 μm , and the length/width ratios are mostly between 2:1 and 5:1. Most cores in CL images present a fine magmatic oscillatory zoning. Homogeneous white/gray rims are also observed (Figure 4). Thirteen analyses in zircons with oscillatory zoning presented variable Th/U ratios (0.48 and 0.73; Supplementary Table 1). All these analyses are within the discordance limits (-5% < D < +5%), but two spots (eg. Spots 4.1 and 9.1) present low concordance errors (ρ), and they are not used in age calculation. The data regression yields a Concordia age of 2200 ± 3.5 Ma with a low MSWD (0.064) interpreted as the rock crystallization age (Figure 5d). The $^{207}\text{Pb}/^{206}\text{Pb}$ weighted average mean age of 2201 ± 6.7 Ma reinforces this assumption (Figure 5b). One rim (5.2) is concordant at $^{207}\text{Pb}/^{206}\text{Pb} = 2288 \pm 27$ Ma (Th/U = 1.33) but without geological meaning. Metamorphic age could not be calculated.

The $^{176}\text{Lu}/^{177}\text{Hf}$ ratios of the igneous zircon crystal present a narrow variation of the ratios from 0.281046 to 0.281150. The Hf TDM model ages yield between 3.11 and 2.91 Ga (with a major frequency of about 2.92 Ga) and negative $\epsilon\text{Hf(t)}$ values varying between -8 and -11.7 (Figure 7 and Supplementary Table 2). This sample has $^{87}\text{Sr}/^{86}\text{Sr(i)}$ and $\epsilon\text{Nd(t)}$ values of 0.705193 and -4.8 (Figure 7), respectively, which are compatible with the participation of an Archean crustal component on the granodiorite's magma genesis.

4.3.4.1.3. Sample BP-LM-12:

Sample BP-LM-12 is a foliated charnoenderbitic granulite with associated mafic bands. The zircon crystals are translucent to opaque and vary from light to dark brown. They are subhedral, prismatic with sub-rounded borders, ranging in size from 235 to 465 μm , and their length/width ratios presented values mostly between 2:1 and 5:1. The crystals present a noTable quantity of fractures (Figure 4). The cores in CL images present a thick magmatic oscillatory zoning. Homogeneous thick gray rims are observed with a higher common Pb percentage than the normal range (<0.5%) and Th/U ratios higher than expected for metamorphic overgrowths. Twelve analyses in zircon oscillatory zoning show variable Th/U (0.26 and 0.72; Supplementary Table 1). The majority of the crystals have discordance percentage out of the adopted concordance range due to Pb loss. Therefore, it was only possible to calculate a Concordia line with upper and lower intercept ages (Figure 5d), interpreted as representing respectively the magmatic crystallization at 2197 ± 10 Ma and metamorphic overgrowths at 588 ± 18 Ma (MSWD = 1.5). This latter metamorphic age is corroborated by a calculated Concordia age (Figure 5c) for these rims at 583 ± 6 Ma with low MSWD (0.069). One inherited zircon was found (eg. spots 12.1 and 12.2) and has $^{207}\text{Pb}/^{206}\text{Pb}$ age of 2388 ± 41 Ma (Th/U = 0.38).

The zircon crystals $^{176}\text{Lu}/^{177}\text{Hf}(t)$ values varying from 0.281161 to 0.281374. The Hf TDM model ages range displayed values between 2.56 to 2.48 Ga and with slightly negative (-1.7 to -0.9; Figure 7 and Supplementary Table 2). The initial $^{87}\text{Sr}/^{86}\text{Sr}$ ratio of 0.705215 and chondritic $\epsilon\text{Nd}(t)$ of -0.6 (Figure 7) coupled with zircon Hf data suggest a mantle source with some degree of crustal contamination on its magma genesis.

4.3.4.1.4. Sample RP-LM-04:

Sample RP-LM-04 is a charnockitic granulite with protomylonitic texture and partial melting evidence. The zircon crystals are translucent to very dark and vary from light to dark brown. The crystals are subhedral to anhedral, prismatic with rounded borders, ranging in size from 155 to 220 μm , and the length/width ratios mostly between 2:1 and 5:1. Cathodoluminescence images (Figure 4) reveal two populations, one with short prismatic crystals with oscillatory zoning (Th/U ratios between 0.41 and 0.67) and the other with long-rounded typology showing planar zoning and anomalous Th/U ratios (1.38 to 2.02, Figure 6). Detailed information can be found on Supplementary Table 1. Most of analyses have high values of D ($+6\% < D < +18\%$). Because of intense Pb loss, it was only possible to calculate Discordia lines (Figure 5f). The adopted interpretation is that the older upper intercept represents the magmatic crystallization (prismatic typology) at 2182 ± 11 Ma (Figure 5d) and the lower intercept interpreted marks the Neoproterozoic metamorphic overprint obtained by the gray rims at 561 ± 41 Ma. The long-rounded grains showing planar zoning also define a Discordia line (2nd Discordia) with upper intercept (2026 ± 30 Ma) possibly related to Paleoproterozoic melt crystallization from anatetic melting on granulite-facies (Figure 5f). This typology seems to lose Pb for the Neoproterozoic event, which is showed by the lower intercept of this Discordia.

Despite the high discordance percentage of zircon crystal of this sample, we have analyzed the two typologies in Lu-Hf systematics. The magmatic zircon crystals show a large variation on $^{176}\text{Lu}/^{177}\text{Hf}$ ratios between 0.281017 and 0.2814 with TDM Hf model ages varying between ca. 2.93 and 2.30 Ga (concentration: 2.9 Ga) and the $\epsilon\text{Hf}(t)$ values range from -14.1 to +2.5 (Figure 7 and Supplementary Table 2). Only one grain is on the accepted range limit of discordance and presents this positive $\epsilon\text{Hf}(t)$ value (+2.5). These data coupled with whole-rock negative ϵNd values (-2.9) and high initial $^{87}\text{Sr}/^{86}\text{Sr}$ ratio of 0.7119 (Figure 7) reveal a juvenile component with the participation of older crustal material and/or crustal contamination in the genesis of the precursor magma.

4.3.4.1.5. Sample BP-CM-151:

Sample BP-CM-151 is a massive mafic granulite presenting medium granulation and some felsic bands interlayered. The zircon crystals are translucent to opaque and vary from light to dark brown. They are subhedral to euhedral, prismatic with sub-rounded borders, ranging in size from 95 to 255 µm, and the length/width ratios mostly between 2:1 and 4:1. Most cores in CL images present a striking magmatic oscillatory zoning, as well as, some homogeneous thin white rims are noticed. This sample had 21 zircon crystals analyzed first by SHRIMP methodology. These analyses were important to know about the zircon populations along the Concordia curve, but the number of analyses was insufficient to reach a robust interpretation of the crystallization age of the sample. Therefore, we analyzed 50 spots on zircon crystals by the LA-ICPMS technique in order to get a better interpretation of the crystallization age and the metamorphic and inheritance events of this sample.

Thirteen SHRIMP analyses in zircon crystals show variable Th/U (0.45 and 1.68; Supplementary Table 1). Most of the analyses yield on the Concordia curve, presenting four populations with distinct characteristics. The first population, yielding values around 2450 Ma (Figure 5c), is the long prismatic crystal (4:1) of zircon showing oscillatory zoning parallel to its elongation. It was interpreted as the typology representative of magmatic crystallization. The second population, concentrated around 2200 Ma (Figure 5c), is constituted by prismatic crystals with fine concentric oscillatory zoning and some Pb loss. The third population, around 1950 Ma, is presented by two homogeneous gray rims (7.2 and 9.1 – Figure 4). There is a metamorphic grain dated at 591 ± 7 Ma. Because of this variability within the Concordia curve and their CL features, we interpret that this sample underwent two metamorphic events, in a double-stage model, with three intercepts (Figure 6a). The first intercept is magmatic crystallization (2453 ± 70 Ma – MSWD: 2.2) and the other intercepts are metamorphic events (1st: 1969 ± 16 Ma – MSWD: 2.2 / 2nd: 602 ± 100 Ma – MSWD: 1.2). One inherited zircon was found (spot 6.1) and is concordant at $207\text{Pb}/206\text{Pb}$ age of 2525 ± 41 Ma (Th/U = 0.59).

In the LA-ICPMS analysis, the zircon spots present the same distribution of the obtained ages obtained by the SHRIMP, repeating the populations cited above. Therefore, the interpretation is quite similar. In addition, we have noticed that there are 16 inherited zircon crystals showing oscillatory and planar zonings between 2400 Ma and 2200 Ma, with markable zircon inheritance peaks at ca. 2395 ± 19 Ma, 2301 ± 20 Ma and 2211 ± 14 Ma (Figure 5d). The two younger zircon crystals with igneous characteristics (eg. Spots 15 and 47- Figure 4) were interpreted as the correct crystallization age (Figure 5d) as depicted by an upper intercept at 2134 ± 43 Ma (MSWD: 0.016). The hypothesis of two metamorphic events was confirmed

because of some of the concordant spots at around 2030 and 1970 Ma presents fir-tree textures spots 59 and 9.1 – figure 6b). in CL images, suggestive of granulite facies metamorphism (Wu and Zheng (2004): In addition, we have found one Orosirian metamorphic rim (spot 36- age: 2008 ± 42 Ma) around a Rhyacian core (Figure 4). The Neoproterozoic metamorphism was also identified by metamorphic rims and neoformed metamorphic grains around 615 and 560 Ma. The crystal that presented the first Orosirian metamorphic event seems to lose Pb to the second Neoproterozoic metamorphism. The calculation of the Concordia lines had always the lower intercept in the Neoproterozoic (554 ± 13 Ma; MSWD: 0.016 – Figure 6b), with the older upper intercept representing the Rhyacian crystallization age and the younger probably meaning the Orosirian metamorphic event (2033 ± 35 Ma; MSWD: 0.0114 – Figure 6b).

The $^{176}\text{Lu}/^{177}\text{Hf}$ ratios of the inherited zircon crystals present a large variation between 0.280145 and 0.281308 values. The TDM Hf model ages of these crystals vary between 3.25 Ga and 2.57 Ga, with some spots presenting older model ages (larger than 3.45 Ga). Its $\epsilon\text{Hf}(t)$ values reflect this variation, with negative to weakly positive values (-14.5 to +1.6) and also anomalous strongly negatives (lesser than -20.6). The analytical Lu-Hf data (Figure 7 and Supplementary Table 2) for this mafic granulite may indicate some disturbance in the Lu-Hf system because of the superimposed metamorphic events that this sample could have undergone. It was considered only the normal Hf parameters, discarding, therefore the anomalous parameters (Supplementary Table 2). The $\epsilon\text{Nd}(t)$ value of this sample is -0.05 (Figure 7), which is consistent with the participation of a chondritic source on the magma genesis of this gabbro. This mafic granulite yields misleading $^{87}\text{Sr}/^{86}\text{Sr(i)}$ value (<0.700) against its age and then it will be not considered hereafter.

The Table 1 synthetizes the main isotopic signatures of JFC orthogranulites

Table 1. Summary table for the main isotopic characteristics of the studied sample from Juiz de Fora Complex.

Sample	Lithology	Age (Ma)	$\epsilon\text{Hf(t)}$ magmatic zircon	TDM Hf (Ga)	Inheritanc e (Ma)	$\epsilon\text{Hf(t)}$ inherited zircon	$\epsilon\text{Nd(t)}$	TDM Nd (Ga)	$^{87}\text{Sr}/^{86}\text{Sr(i)}$	Source
VA-LM-07B	Enderbitic Granulite	2440 ± 4.8	(-8.0 to +1.7)	3.10 to 2.54	n.a.	n.a.	-0.1	2.48	0.7017	Mantle
BP-LM-12	Charnoenderbiti c granulite	2197 ± 10	(-8.5 to +0.2)	2.90 to 2.49	2388	n.a.	-0.6	2.31	0.7052	Mantle/crust
BP-LM-13	Charnoenderbiti c granulite	2200 ± 3.5	(-11.7 to -8)	3.11 to 2.91	n.a.	n.a.	-4.8	2.62	0.705193	Crustal
BP-CM-151	Mafic Granulite	2134 ± 43	n.a.	3.08 to 2.68	2525-2210	(-4.3 to +1.1)	-0.05	2.52	0.6944	Mantle
RP-LM-04	Charnockitic granulite	2182 ± 11	(-14.1 to +2.5)	3.1 to 2.78	n.a.	n.a.	-2.9	2.46	0.7119	Mantle/Crus t

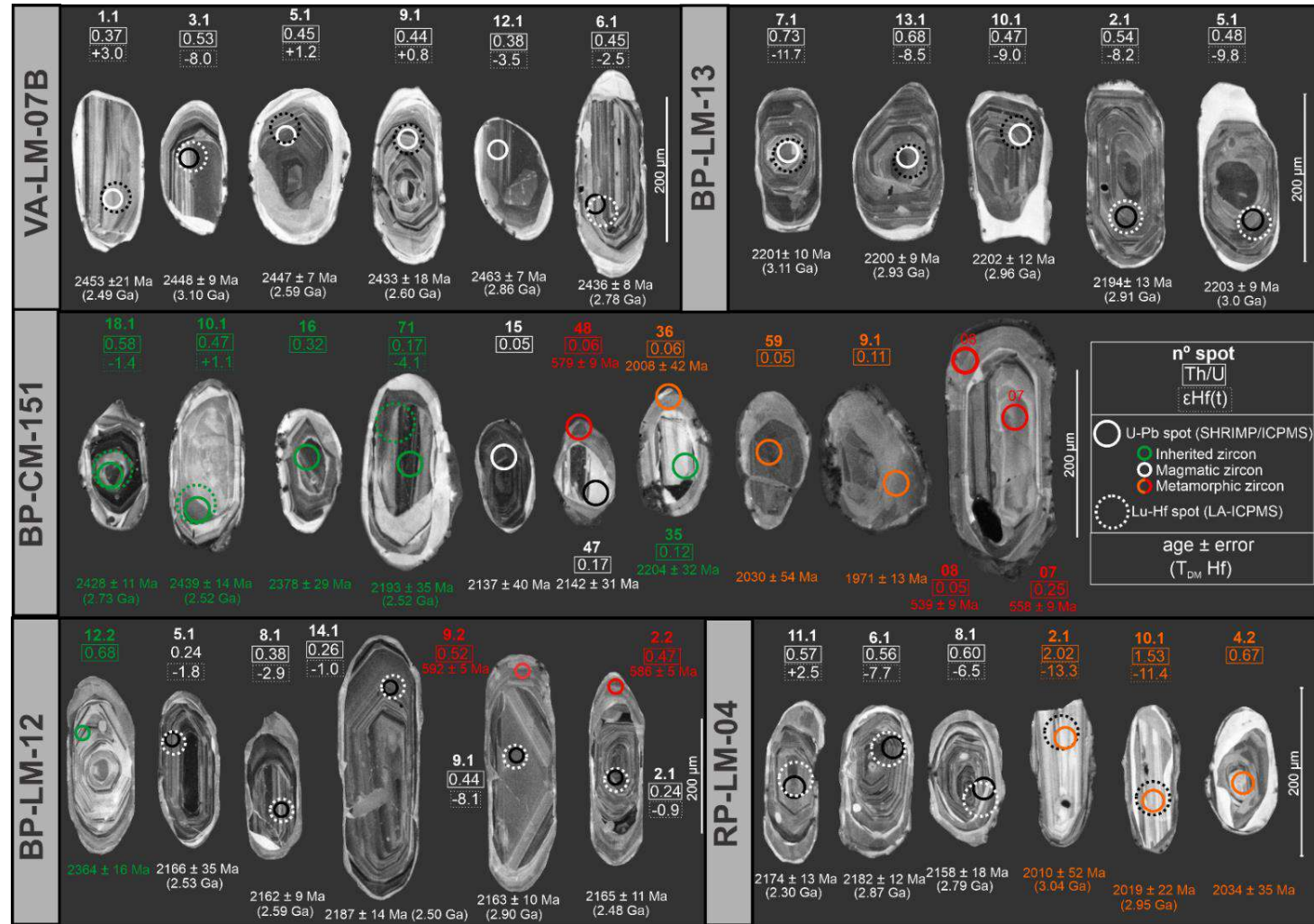


Figure 4. Cathodoluminescence (CL) images of analyzed zircon crystals of the orthogranulitic samples from Juiz de Fora Complex. Anatetic melt zircon grains on sample RP-LM-04 have been considered metamorphic grains.

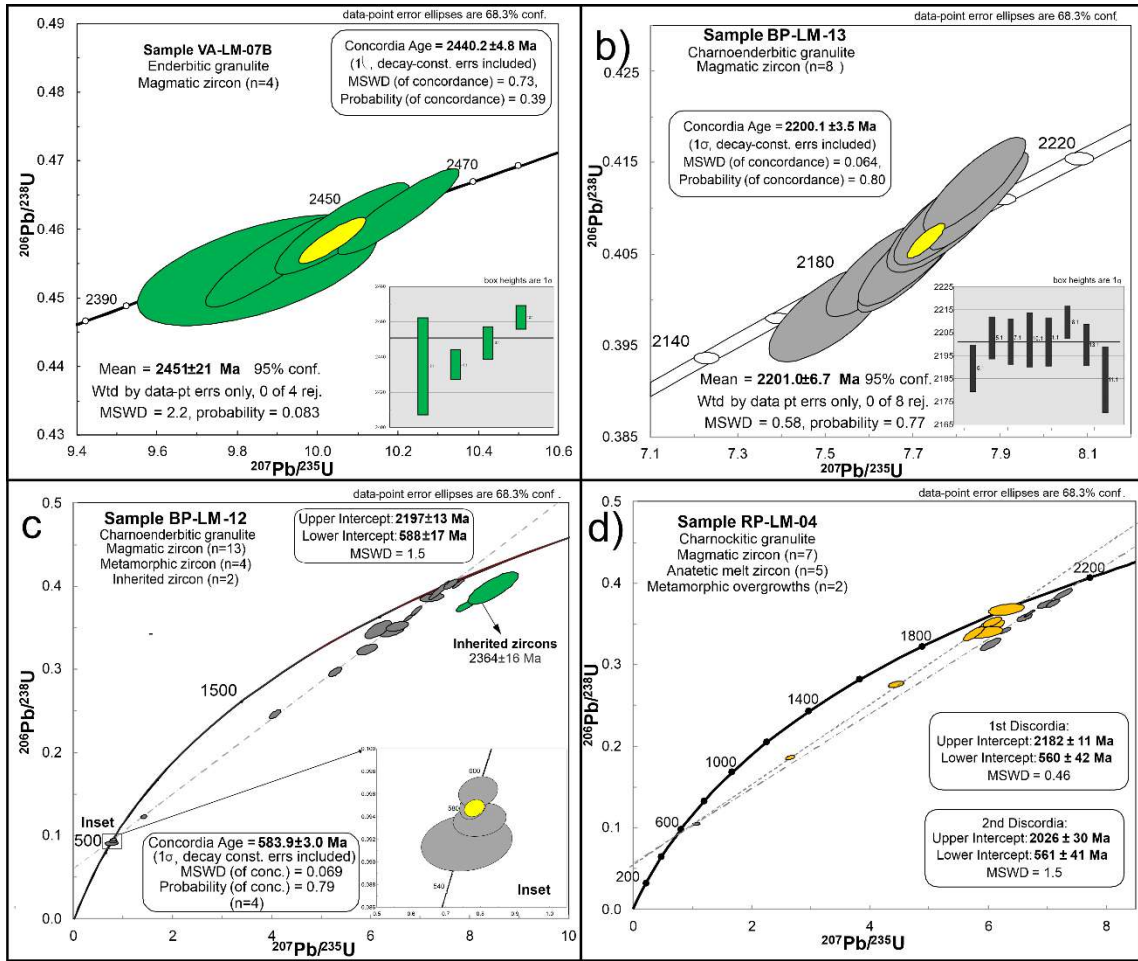


Figure 5. Concordia or Discordia diagrams presenting orthogranulites' ages from Juiz de Fora Complex at the studied area. A) Concordia and $207\text{Pb}/206\text{Pb}$ weighted average mean ages for enderbitic granulite (VA-LM-07B); B) Concordia and $207\text{Pb}/206\text{Pb}$ weighted average mean ages for coarse charnockitic granulite (BP-LM-13); C) Discordia line for charnoenderbitic granulite (BP-LM-12). The inherited zircon crystals are represented by green ellipses; D) Discordia lines for charnoenderbitic granulite (RP-LM-04) with younger and older upper intercepts representing magmatic crystallization (orange ellipses) and inheritance (gray ellipses) respectively. The lower intercept is referred to as metamorphism.

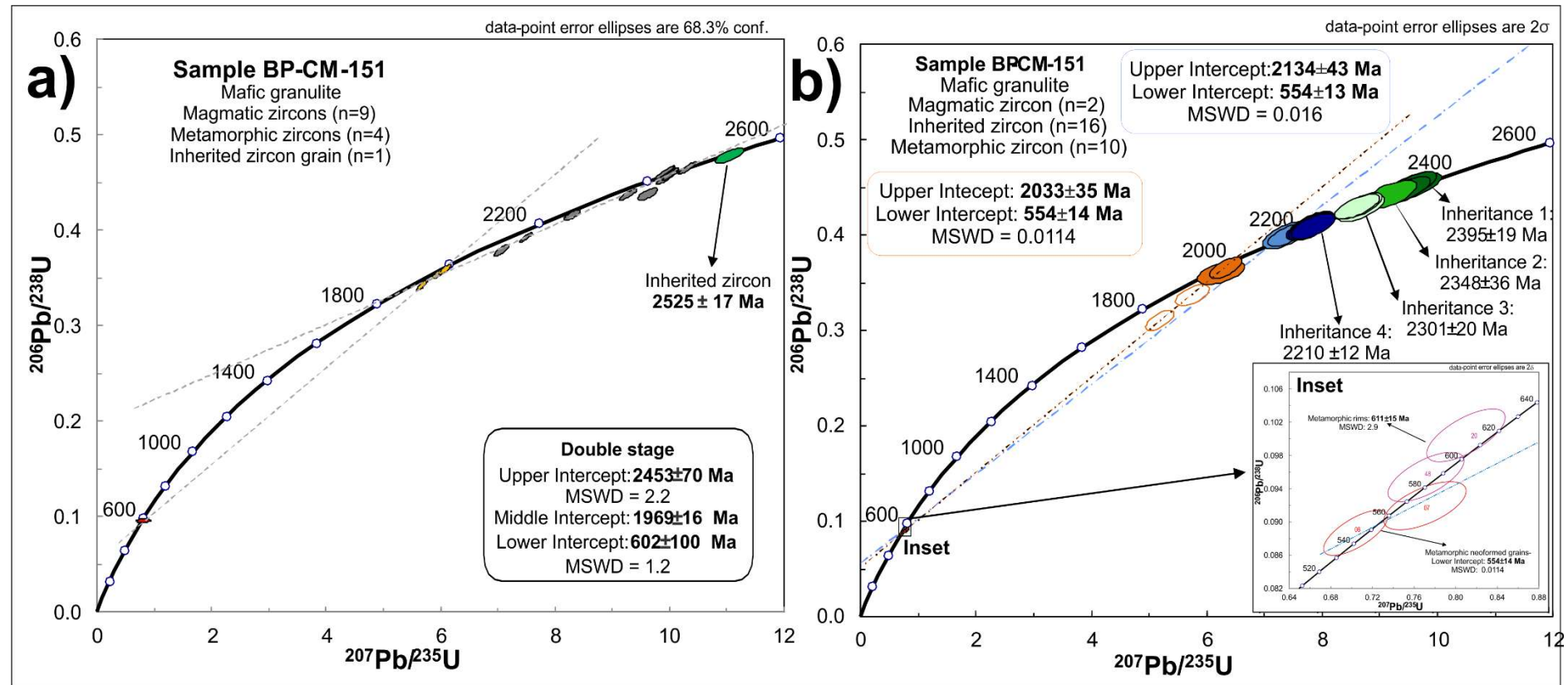


Figure 6. Wetherill Concordia diagram for massive mafic granulite (BP-CM-151). a) SHRIMP analysis. Metamorphic rims, metamorphic grain, magmatic crystals, and inherited zircon crystals are represented by yellow, red, gray, and green ellipses, respectively; b) LA-ICPMS analysis. Siderian inherited crystals, Rhyacian inherited crystals, Rhyacian magmatic crystals, Orosirian metamorphic rims/grains, and Neoproterozoic rims/grains are represented by green, dark blue, blue, orange, and red ellipses, respectively.

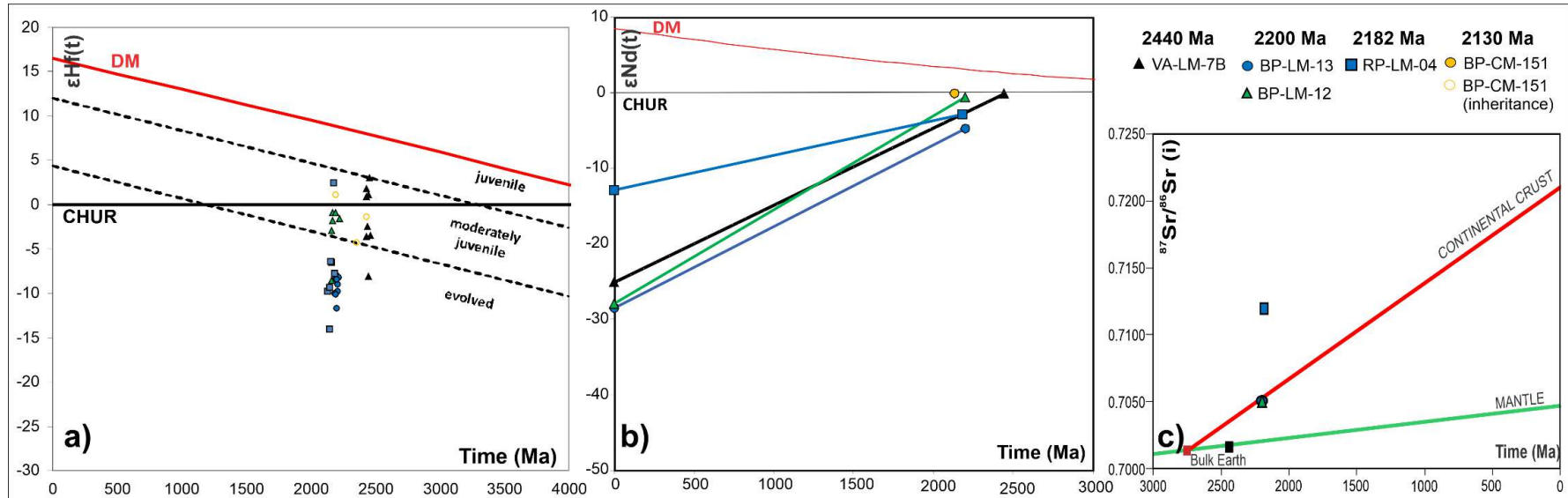


Figure 7. Hf, Nd, and Sr Isotopes evolution of the studied samples from Juiz de Fora Complex. A) zircon $\epsilon\text{Hf}(t)$ values trough time. grey dashed lines classify fields of juvenile (0–5 ϵ -units below DM), moderately juvenile (5–12 ϵ -units below DM), and evolved (> 12 ϵ -units below DM), according to Bahlburg et al., (2011). We assume the average crust using $^{176}\text{Lu}/^{177}\text{Hf} = 0.015$ (Griffin et al., 2002); B) Whole-Rock $\epsilon\text{Nd}(t)$ evolution. Uniform Reservoir data extracted from DePaolo (1988); C) Sr evolution diagram (initial $^{87}\text{Sr}/^{86}\text{Sr}$ vs. Time (Ma)) of Othman et al., (1984).

4.3.4.2. Revisiting the Lithogeochemistry

After the geochronology study carried out, we decided to revisit the geochemical data set from Araujo et al. (2019) in order to distinguish the geochemical groups with Nd TDM Model and U-Pb ages, observe the geochemical features of the dated samples (filled symbols) as well as apply the new petrogenetic classification of granitoids based on systematic presented by Laurent et al. (2014). Non-dated rocks are represented by empty symbols.

The intermediate and acid rocks are classified as diorites and granodiorites (Fig. 8a – Cox et al. 1979) with the most rocks plotting on the calc-alkaline field, with exception of the tholeiitic diorites already classified as Low K calc-alkaline series group (Araujo et al. 2019) in the SiO₂ vs. K₂O diagram (Fig. 8b - Peccerillo and Taylor, 1976). This group conveys on metaluminous rocks (Figure 8c) which present moderate LREE enrichment (Figure 9a), low fractionating (La/YbN – 1 to 9), negative anomalies of Nb-Ta and Ti (arc-like rocks signature) and positive Pb anomalies (Figure 9b). The dated sample VA-LM-07B (ca. 2440 Ma) belongs to this group.

The most of other granitoids display high Ba-Sr signatures (Tarney and Jones, 1994), and using a petrogenetic classification by a ternary plotting suggested by Laurent et al. (2014) coupled with Nd TDM model ages, the high Ba-Sr granitoids have been subdivided into two groups: TTG suite, sanukitoid suite and the CA3pc granitoids (Fig. 8d). The TTG suite, represented by the sample BP-LM-12 (ca. 2197 Ma), yields on the TTG-like field of the La/YbN vs. YbN diagram (Martin, 1986). This sample presents positive Eu and Sr anomaly and negative P anomaly besides HREE depletion (Figure 9c,d) and similar pattern and contents of REE and trace elements (Figure 9c,d) of the average TTG (Laurent et al. 2014), such as Mg# (0.4), La (19.5-30 ppm) and Yb (0.5-0.8 ppm). The sanukitoid suite shows slightly negative Eu anomaly (Figure 9e), variable LREE enrichment, and negative anomalies of Nb-Ta, Ti and, P (suggestive of subduction-related magmas) and strongly positive Pb anomaly higher than the other groups (Figure 9f). There are two dated samples in this group: BP-LM-13 (ca. 2200 Ma) and RP-LM-04 (ca. 2182 Ma). The latter sample shows much higher contents of incompatible elements than the first one. The CA3pc granitoids present similar geochemical characteristics to sanukitoid group and higher negative Eu anomaly, but this group has been separated from other ones (TTG and snkt. Groups) because of its younger Nd TDM ages (ca. 2.09 to 1.9 Ga) than U-Pb ages. Therefore, this group has been related to a late to post-collisional magmatism.

There are also two geochemical groups that resemble the REE and trace element patterns from mentioned above groups and have been separated from others by their younger TDM

model ages than ca. 2.1 Ga. The CA2ad group has similar REE and trace elements signatures from TTG suite such as positive Sr anomaly, high (La/Yb)N (Figure 8e), and HREE depletion (Figure 9c,d), although with much higher SiO₂ (70-74.6 wt%) and thus being classified as high silica adakites derived from thickened lower crust (Figure 8f - Wang et al. 2006). The last group of granitoids, the CA3a group, shows resembling REE and trace elements patterns (Figure 9g,h) from CA3pc, although presents older Nd TDM model ages, being interpreted to Rhyacian arc magmatism (ca. 2.2 Ga). The new geochemical groups and assumptions are synthetised in Table 2.

The basic rocks are classified as tholeiitic gabbros (Figure 8a,b), showing a flat REE pattern (Boynton, 1984) and LREE depletion similar to MORB pattern (Figure 9g). On the other hand, LREE depletion is typical of island-arc tholeiitic basalts (Wilson, 1989). Furthermore, the trace elements from sample BP-CM-151 are quite similar from Island-arc tholeiitic pattern (Sun, 1980; normalization: Pearce, 1983), having spikes on Sr, Ba, and K (Figure 9h). This group also yields in island arc field on Zr vs. Zr/Y diagram (Pearce & Norry, 1979 – Figure 8f). The sample BP-CM-151 (ca. 2130 Ma) is a representative sample of this group.

Table 2. Synthesis of the geochemical groups and its tectonic significances, coupled with U-Pb and Nd T_{DM} model ages.

Sample	TDM Nd	idade U-Pb	Araujo <i>et al.</i> 2019	Geochemical Grouping	Protoliths	Tectonic classification
VA- LM- 07B	2.48 Ga	2.44 Ga	LK	LK	Low K tholeitic diorites	Pre-collisional stage
BP-CM-150E	2.46 Ga	-	LK	LK		
VA- LM- 10	2.35 Ga	-	LK	LK		
VA- LM- 11B	2.75 Ga	-	CA1	CA1		
BP- LM- 13	2.62 Ga	2.20 Ga	CA1	CA1		
VA- LM- 08B	2.58 Ga	-	CA1	CA1	High Ba-Sr granitoids	Sanukitoid suite
RP- LM- 04	2.46 Ga	2.18 Ga	CA1	CA1		
BP- IV- 34	2.43 Ga	-	CA1	CA1		
VA- LM- 05	2.41 Ga	-	CA1	CA1		
BP-CM-142A	2.41 Ga		-	-		
CPH- 123- A	2.64 Ga	ca. 2.20 Ga*	CA3	CA3a	Medium to high K granitoids	Arc-related magmatism
RPM-546	-		CA3	CA3a		
BP- LM- 12	2.31 Ga	2.197 Ga	CA2	CA2ttg	High Ba-Sr granitoids	TTG suite
NSA-5-9B	2.18 Ga	-	CA2	CA2PC	High SiO ₂ adakites	High-P thickened Lower crust partial melting
NSA-5-9C	2.03 Ga	-	CA2	CA2PC		
RPM-565A	-	-	CA2	CA2PC		
RP- LM- 03	2.09 Ga	ca. 1.96 Ga*	CA3	CA3PC	High Ba-Sr granitoids	Late-collisional
CPH- 132	1.9 Ga		CA3	CA3PC		Medium K magmatism

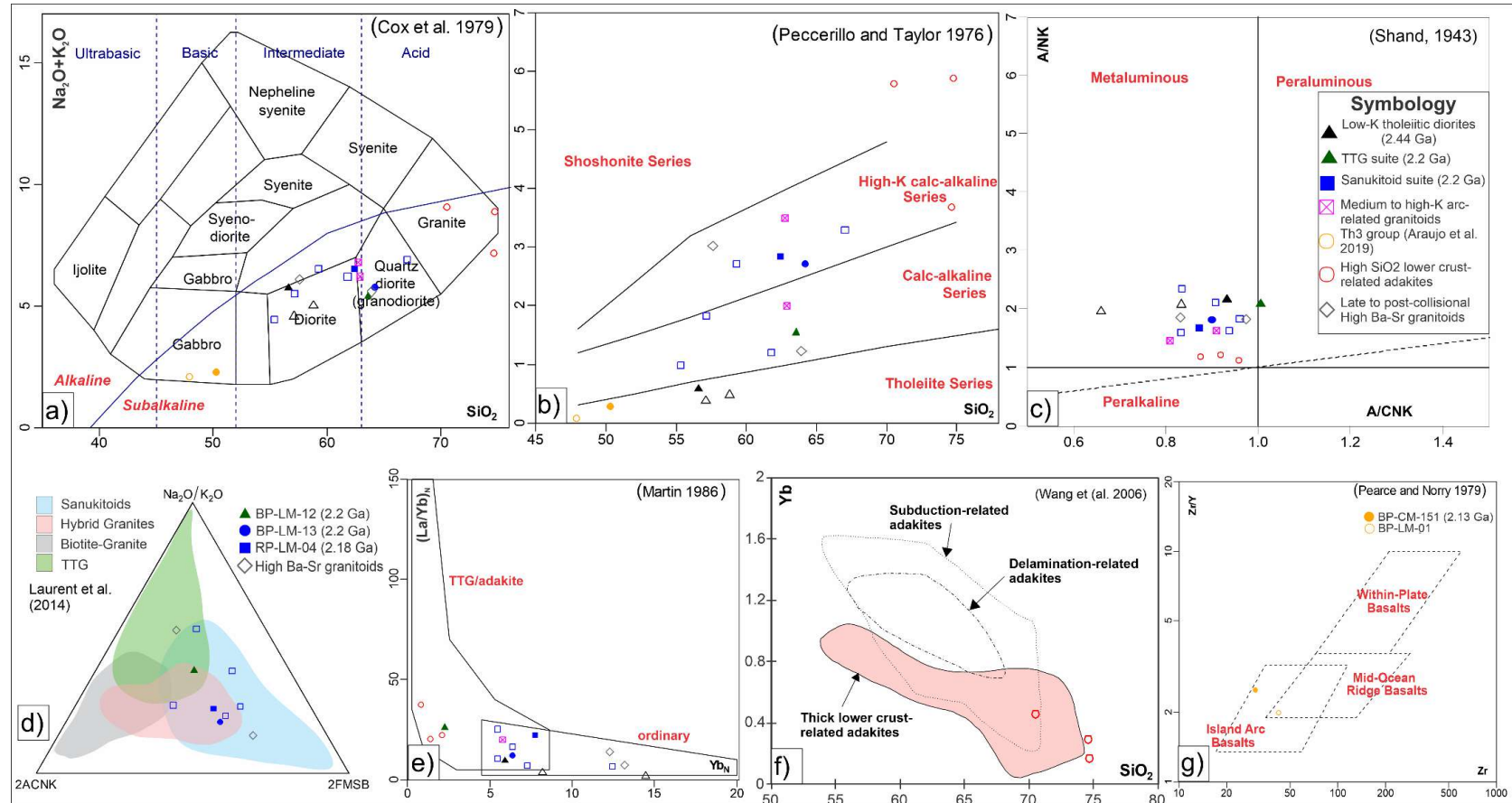


Figure 8. Classification, petrogenetic and tectonic diagrams of the orthogranulites from Juiz de Fora Complex. A) $\text{SiO}_2 \times \text{alkalis}$ (Cox *et al.* 1979) for protoliths and magmatic series classifications; B) $\text{SiO}_2 \times \text{K}_2\text{O}$ (Peccerillo and Taylor, 1976) for sub-alkaline series classification; C) Classification of granitoids based on Alumina Silica Index (Shand, 1973); D) Ternary classification diagram for high Ba-Sr granitoids from Laurent *et al.* (2014). Vertices are: $2 \times \text{A/CNK}$ (molar $\text{Al}_2\text{O}_3/(\text{CaO} + \text{K}_2\text{O} + \text{Na}_2\text{O})$ ratio); $\text{Na}_2\text{O}/\text{K}_2\text{O}$ and $2 \times (\text{FeOt} + \text{MgO}) \times (\text{Sr} + \text{Ba})$ wt.% (=FMSB); E) Diagram for adakite/TTG discrimination (Martin, 1986) for high Ba-Sr granitoids; F) Geochemical classification of adakite petrogenesis (Wang *et al.* 2006); G) Geotectonic discrimination for mafic rocks from distinct geotectonic positions (Pearce and Norry, 1979)

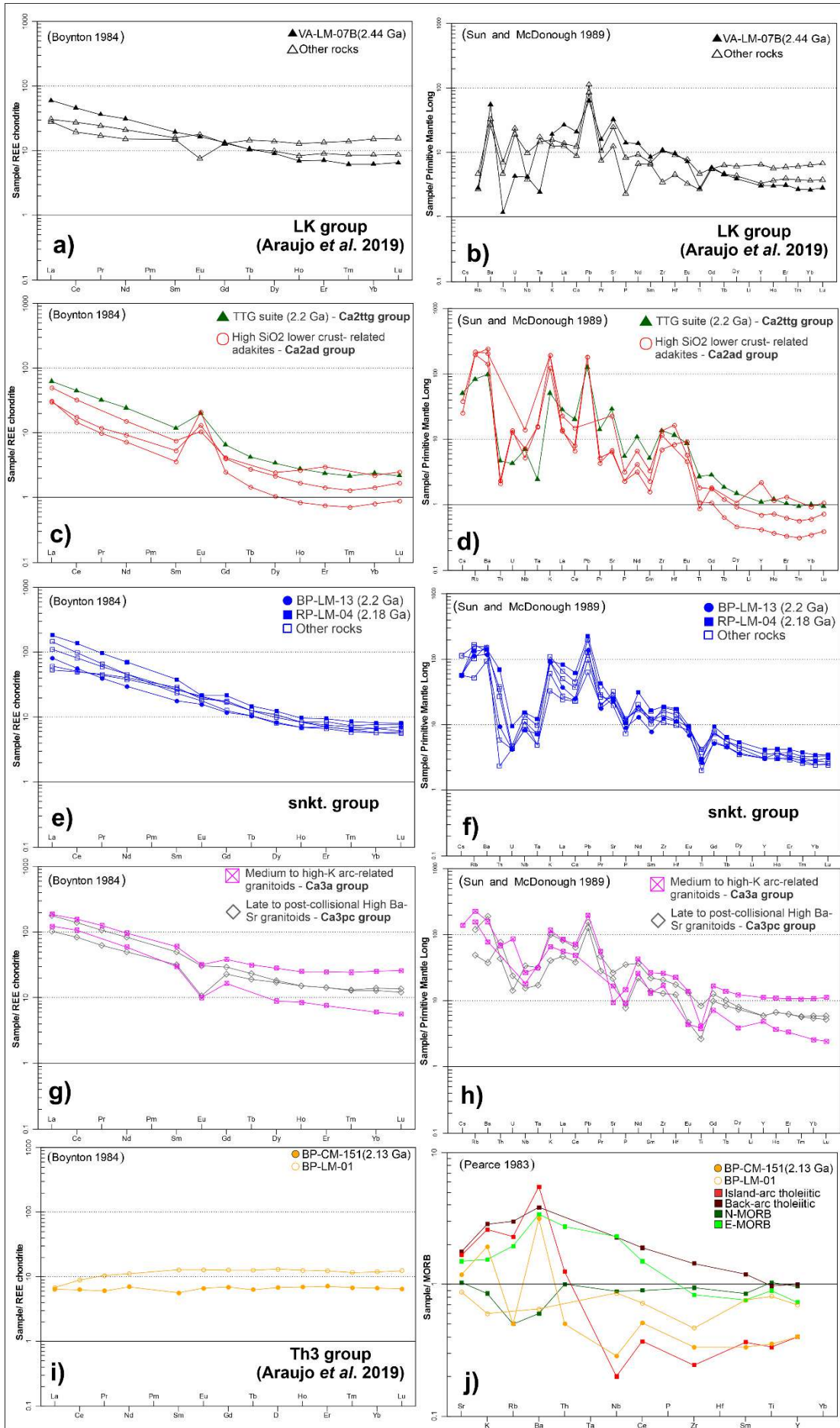


Figure 9. REE and trace elements patterns for studied samples from Juiz de Fora Complex. The normalization for REE spidergrams was made by chondrite (Boynton, 1984). The normalization for trace elements was made by Primitive Mantle (Sun and McDonough, 1989) for granitoids and by MORB (Pearce, 1983) for basic rocks. A and B) LK group (Araujo et al. 2019); C and D) TTG and CA2ad groups; E and F) Sanukitoid group; G and H) CA3a and CA3pc groups; I) REE pattern of TH3 group (Araujo et al. 2019); J) Trace element spidergram of TH3 group and comparison with well-known basalts tectonic patterns (IAT, BAT, N-MORB, and E-MORB: Wilson, 1989 and references therein).

4.3.5. DISCUSSION

4.3.5.1 Tectonic Evolution of Juiz de Fora Complex in the studied area

The U-Pb zircon ages and in situ Lu-Hf zircon isotopic signature, besides the lithogeochemical and whole-rock Sr and Nd isotopic data have provided crucial constraints on the tectono-termal events of the Juiz de Fora Complex at the studied area. All dated samples present the LILE (Sr, K, Ba, Pb) enrichment relative to HFS elements, similar to arc-related signatures (McMillan et al. 1989). The magmatic events can be divided into three episodes: a) an early period, comprehending juvenile magmatism at ca. 2440 Ma; b) a moderately juvenile to evolved magmatism at ca. 2200-2180 Ma; c) the latter period, comprising juvenile magmatism at ca. 2130 Ma. The isotopic studies (Sr, Nd, and Hf) allowed important insights on the petrogenesis of precursor magmas of each magmatic episode. The temporal evolution of the studied magmatic rocks is described below.

In addition, we have identified two metamorphic events within the Juiz de Fora Complex' orthogranulites, including a suggestion of Orosirian metamorphism, never described before and the well-known Neoproterozoic metamorphism. These metamorphic episodes are also presented in this item.

4.3.5.1.1. Early primitive arc stage at ca. 2440 Ma

This magmatic episode is represented by the enderbitic granulite (sample VA-LM-07B) presents tholeiitic tendency and arc-related signature (Araujo et al. 2019). This Siderian arc magmatic episode was never described before within the Juiz de Fora Complex, and similar ages were only described as inherited zircon crystals (Kuribara et al. 2019). Anyway, tholeiitic rocks of ca. 2.4 Ga were described in the northern part of the State by Heilbron et al., (2010). Although interpreted as E-Morb ocean floor rocks, it is possible that this dated rock belonged to the same family, as it is not easy to distinguish between very primate arc-related rocks and enriched ocean floor basalts.

This magmatic episode is juvenile to moderately juvenile on Lu-Hf zircon systematics ($\epsilon\text{Hf(t)}$) values from -8 to +3 with a most frequent value of +1). The whole-rock Nd and Sr isotopes also point out to Nd and Sr depleted mantle juvenile source (Figure 10c). The crustal residence age (TDM Nd) of 2.48 Ga indicates that there is a crustal residence of 40 Ma for this magmatic episode. The TDM Hf model ages pointed out to a prior archean crustal component on the genesis of this magmatic episode and it is attributed to archean sediments from Mantiqueira Microcontinent that were subducted below the JFC arc. It is the first magmatic episode of intra-oceanic arc magmatism on Juiz de Fora Complex (Figure 11a).

The samples BP-LM-12 and BP-CM-151 have Siderian (2400 to 2300 Ma) inherited zircon crystals as well. This could indicate the JFC could have had another magmatic episode on Later Siderian. This hypothesis becomes stronger with other Siderian inherited zircon grains from Juiz de Fora Complex reported on Manhuaçu surroundings (Kuribara et al. 2019). On the other hand, the arc-related Siderian magmatism could have been continuous as depicted by on the inheritance distribution of mafic granulite (Figure 6b).

4.3.5.1.2. The Moderately juvenile to evolved stage – 2200 to 2182 Ma

This magmatic episode comprises the charnoenderbitic granulites (samples BP-LM-12 and BP-LM-13). Their protoliths are high Ba-Sr calc-alkaline arc-related granodiorites with distinct element and isotopic signature. The sample BP-LM-12 have TTG tendency (HREE depletion and positive Eu anomaly) with isotopic parameters indicating a juvenile to moderately juvenile Siderian source (most frequent $\epsilon\text{Hf(t)}$ values of -0.9; $\epsilon\text{Nd(t)}$: -0.6; TDM Nd: 2.30 Ga and most frequent TDM Hf model ages at 2.50 Ga, despite some older ages). The sample BP-LM-13 is a sanukitoid (LREE enrichment and negative Eu anomaly) with isotopic geochemistry revealing an evolved Archean source ($\epsilon\text{Hf(t)}$ values between -11.7 and -8; $\epsilon\text{Nd(t)}$: -4.8; TDM Nd: 2.62 Ga and TDM Hf ages between 3.1 and 2.9 Ga), as shown in Figure 10. Probably, this magmatic episode has mixed sources (mantellic Juvenile and crustal) and differences on the isotopic signatures could be related to the proportion of participation of each source. In this view, we interpret that the subducted oceanic lithosphere brought both Archean metasedimentary rocks (from West Mantiqueira Microcontinent) and underlying oceanic crust and these two end-members were the predominance sources of the mentioned rocks. On the other hand, the similar values of $^{87}\text{Sr}/^{86}\text{Sr(i)}$ (0.705) points out some crustal participation on their precursor magmas, maybe by the older part of the arc. The inherited zircon found (age: ca. 2380 Ma) on sample BP-LM-12 can confirm older arc rocks contamination. This moment

in the arc evolution, coeval mantle-derived magmas and crustal derived magmas coupled with crustal contamination are suggestive of a mature arc stage (Figure 11b).

The protolith of the sample RP-LM-04 is a granodiorite with sanukitoid signature that presents the higher contents of REE and trace elements among this geochemical group (figure 8e,f). This rock shows two distinct zircon typologies with different crystallization ages. The older one, ca. 2182 Ma, is regarded as crystallization age of the rock with ca. 2182 Ma and the younger cluster, ca. 2026 Ma, is interpreted as an anatetic melt typology. Its isotopic signature ($^{87}\text{Sr}/^{86}\text{Sr}(i)$: 0.7119; $\epsilon\text{Nd}(t)$ of -2.9; $\epsilon\text{Hf}(t) = -14.1$ to +2.5 – Figure 10) pointed out to mixture of mantle and crustal sources with predominance of latter. Based on its age error range, this sample is interpreted as the continuation of Rhyacian arc magmatic episode.

This age range has correlated to other occurrences from Juiz de Fora Complex at Ipanema, Bananal de Baixo, and Juiz de Fora cities (Degler et al. 2018; Novo et al. 2010; Heilbron et al. 2010). The Pocrane Complex also has chronocorrelated rocks on this time range (Degler et al. 2018). On the other hand, there were not described any evolved rock (as sample BP-LM-13) on Juiz de Fora Complex until the present moment.

4.3.5.1.3. The renew moderately Juvenile arc stage 2130 Ma

This episode is constrained by the mafic granulite (sample BP-CM-151) with gabbroic protolith and island-arc tholeiitic tendency. Its isotopic signature demonstrates a juvenile to moderately juvenile mantellic source on this magma genesis (subchondritic $\epsilon\text{Nd}(t)$ value: -0.05; TDM Nd: 2.52 Ga and $^{87}\text{Sr}/^{86}\text{Sr}(i)$: 0.701 – Figure 10a). This sample has recorded all previous magmatic stages by inherited zircon crystals, including the older (ca. 2525 Ma) archean inherited zircon crystal among the samples. Commonly, mafic rocks have more juvenile tendencies than other rocks. So, it is impossible to predict that all rocks from this proposed magmatic episode would be entirely juvenile. Coincidence or not, this magmatic episode on the study area (Figure 11c) is correlated to most of the juvenile rocks reported on Juiz de Fora Complex and Pocrane Complex (Degler et al. 2018; Noce et al. 2007).

4.3.5.1.4. Rhyacian to Orosirian Collision (at ca. 2035 to 2026 Ma)

This Orosirian tectono-thermal event is evidenced by metamorphic rims of ca. 2010 to 2030 Ma overgrown around older cores as well by younger new zircon crystals of ca. 1970 to

1940 Ma), that presents fir-tree textures on CL images (sample BP-CM-151), suggestive of granulite facies metamorphism (Wu and Zheng, 2004). This metamorphic episode is here interpreted as the result of the collision between the Juiz de Fora and Mantiqueira Complexes (Figure 11d) completing the history of the Minas Accretionary-Collision Orogeny (Teixeira et al. 2015). The detection of this metamorphic episode on Juiz de Fora Complex rocks was expected but had not been reported yet. On the other hand, the Rhyacian to Orosirian metamorphism is well-described on Mantiqueira Complex (Cutts et al. 2018; Heilbron et al. 2010) and Mineiro Belt (Moreira et al. 2018).

Furthermore, the sample RP-LM-04 (age: 2182 Ma) presents a younger rounded and planar zoning zircon crystals (2026 ± 30 Ma) which should have been related to the melt crystallization during partial melting (Wu and Zheng, 2004) on granulite facies. This assumption may be supported by the partial melting evidence identified on outcrop (Figure 3e) and reinforced by age similarity with the detected metamorphic event (2035 ± 36 Ma) on mafic granulite (Sample BP-CM-151). Contamination by this young typology in the sample preparation' procedures might be a cause for the presence of the contrasting typologies for the sample BP-LM-04.

Similar magmatic age interval (on Rhyacian-Orosirian transition) has been reported on the Juiz de Fora Complex at São João do Manhuaçu region (Kuribara et al. 2019), with only two spots pointing out to juvenile magmatism at 2051 ± 30 Ma.

4.3.5.1.5. Other non-dated magmatic episodes

As the continuous episodes of mantle extraction, it is normal to expect that the refractory residue had been thickened. The melting of this crustal level at high-P could be the mechanism to generate the high silica adakites of the studied area. The younger Nd T_{DM} ages than 2.18 Ga suggest that this magmatic episode (not shown on the proposed tectonic model) is younger than other ones. In addition, non-dated high Ba-Sr granitoids with Nd T_{DM} model ages younger than 2.09 Ga could be related to the late to post-collisional magmatic episode (Figure 11e) on Juiz de Fora Complex. We correlate these rocks with other younger Juiz de Fora Complex outcrops, such as a ca. 1966 Ma high-K calc-alkaline pluton (Heilbron *et al.* 2010).

4.3.5.1.6. Neoproterozoic Metamorphism

The Neoproterozoic metamorphism is recorded on the samples BP-LM-12, BP-CM-151, and RP-LM-04 as gray color homogeneous overgrowths around older cores and/or by neoformed zircon crystals (BP-CM-151 – Figure 6). This granulite metamorphic overprint is so strong that the Orosirian overgrowths (sample BP-CM-151) seem to lose Pb for this younger metamorphic event. The sample RP-LM-04 was the most affected rock for the Neoproterozoic granulite metamorphism on the studied area because almost all zircon crystals are discordant ($D > 6\%$). In addition, the association of this metamorphic event and that of the Paleoproterozoic can be related to the isotopic disturbance (Lu-Hf) on zircon crystals from mafic granulite (BP-CM-151 – Supplementary material 2).

This metamorphic event is related to the collision of Occidental Terrane onto Oriental Terrane on the orogeny that forms the Ribeira Belt (Heilbron *et al.* 2004a). This tectono-thermal event had been widely described on Juiz de Fora Complex (Degler *et al.* 2018; Kuribara *et al.* 2019; Noce *et al.* 2007; Machado *et al.* 1996; Heilbron *et al.* 2010) and is responsible for current granulite facies mineral assembly of each studied samples (Figures 3e,f,g).

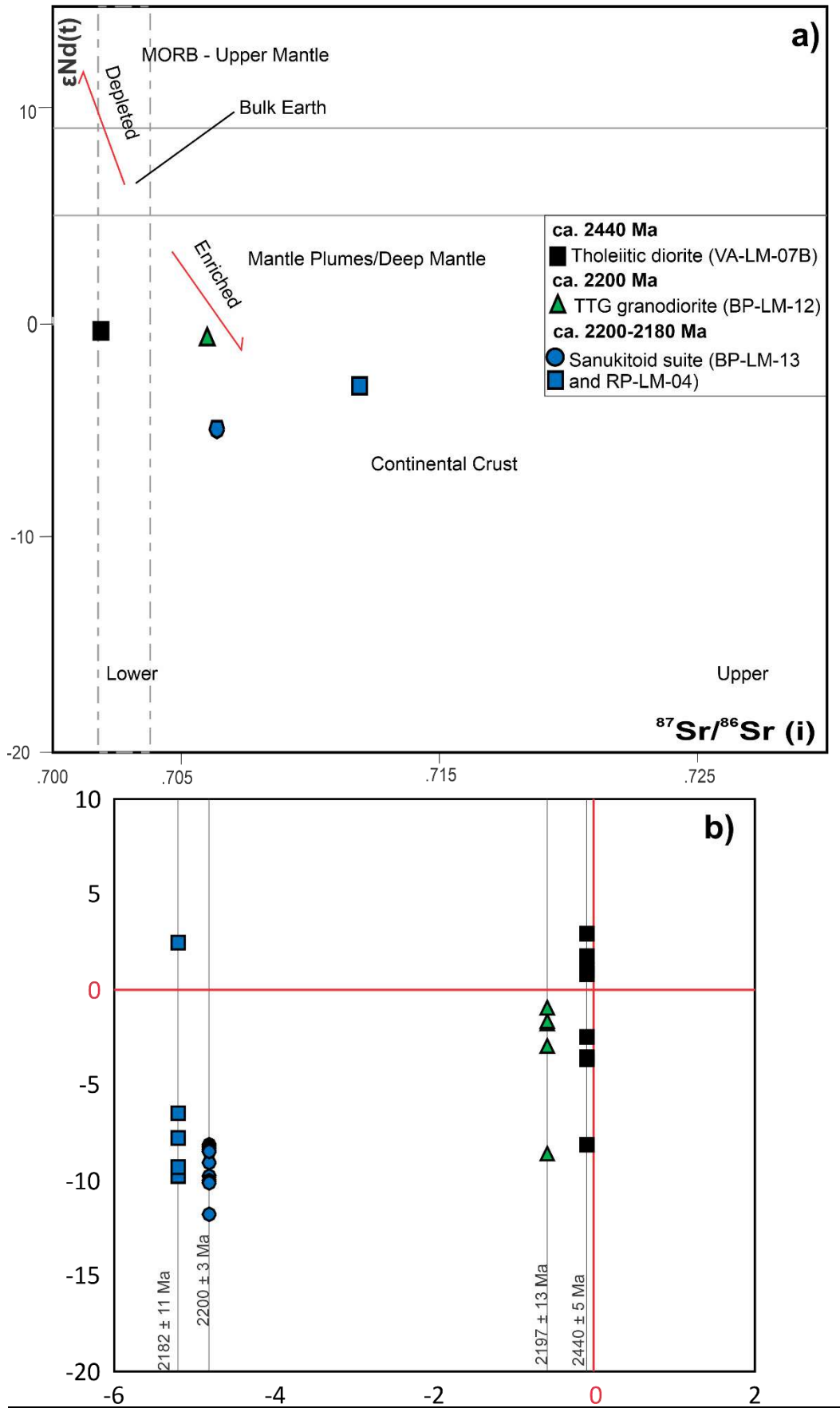


Figure 10. Isotopes (Nd, Sr, Hf) Correlation diagrams of the studied samples from Juiz de Fora Complex. A) $\epsilon\text{Nd(t)}$ vs. $^{87}\text{Sr}/^{86}\text{Sr(i)}$ at crystallization age of each sample; B) zircon $\epsilon\text{Hf(t)}$ vs. Whole-Rock $\epsilon\text{Nd(t)}$.

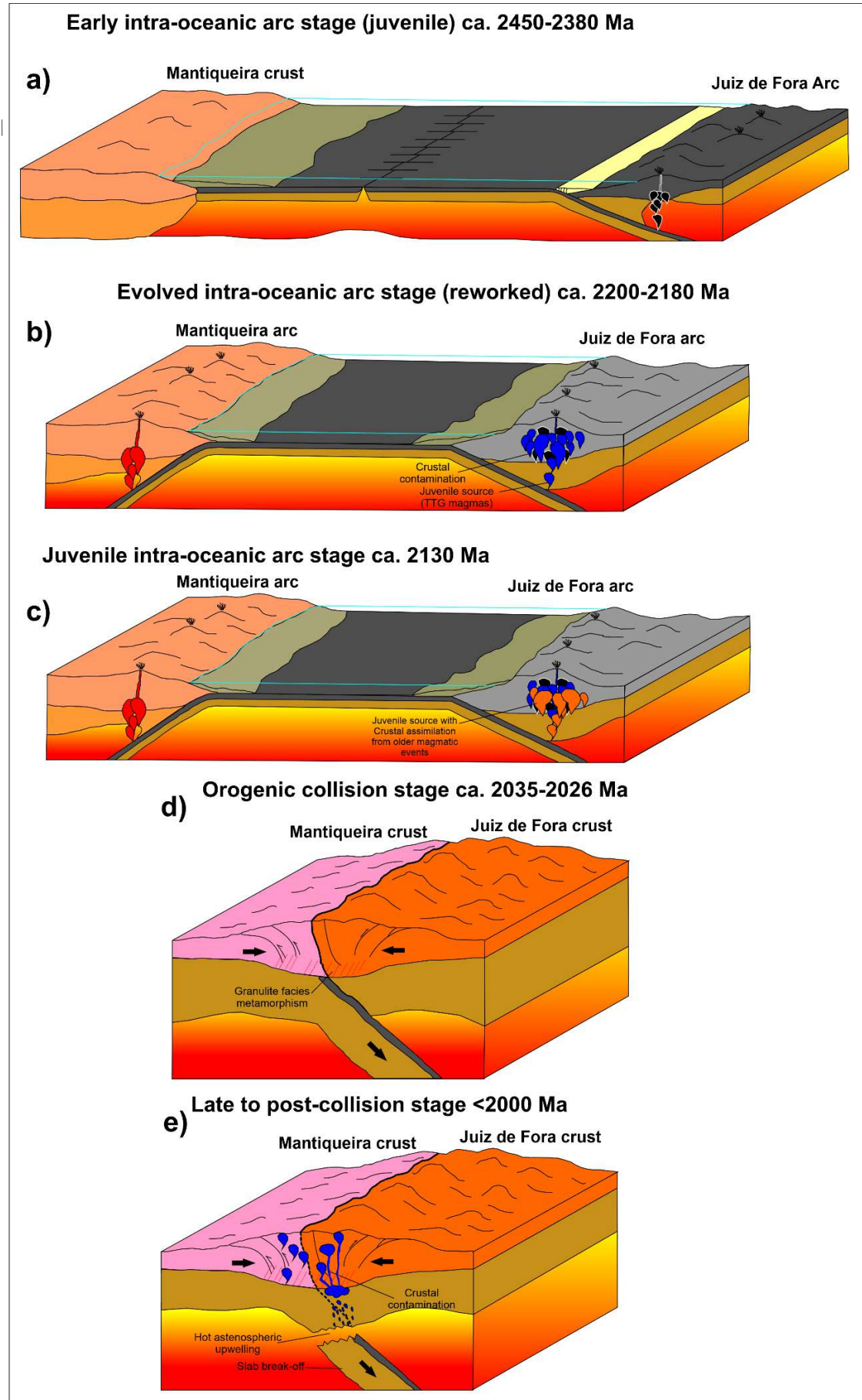


Figure 11. Envisaged tectono-thermal Evolution from Juiz de Fora Complex at studied area. a) Early intra-oceanic juvenile stage at ca. 2400 Ma; b) Moderately Juvenile to Evolved arc stage at 2200-2180 Ma; c) Juvenile arc stage at ca. 2130 Ma; d) Orogenic collision at ca. 2035 Ma; e) Late collisional magmatism younger than ca. 2000 Ma.

4.3.5.2. Correlations within the Minas-Bahia orogenic system

On this item, geochronological and isotopic correlations between the Paleoproterozoic tectono-thermal events on the studied area and other events reported on basement terranes of São Francisco paleoplate will be presented. Other exotic paleoproterozoic terranes of the Ribeira Belt will be also discussed (Figure 12).

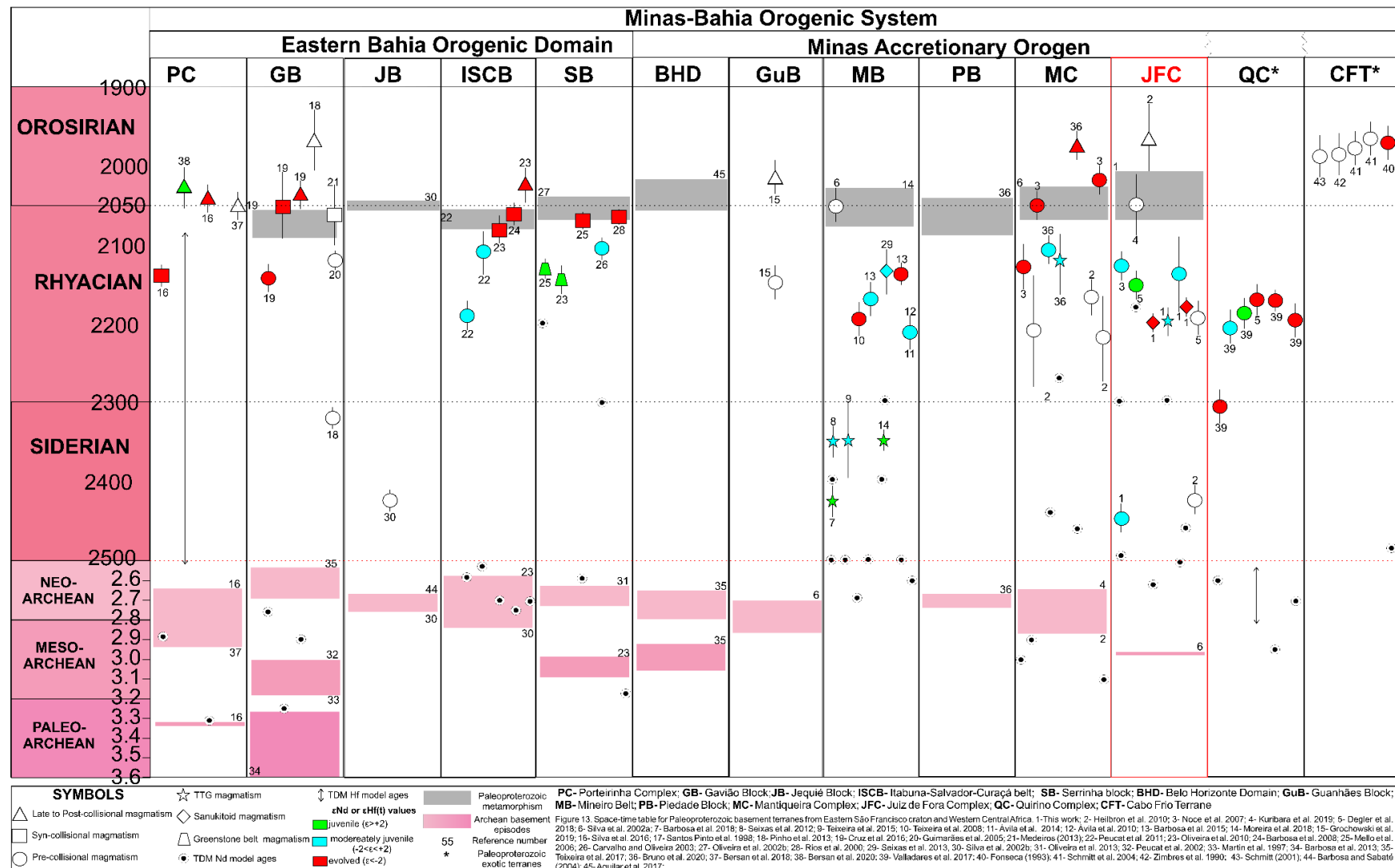


Figure 12. Space-time Table for Paleoproterozoic basement terranes from Eastern São Francisco craton and Western Central Africa. 1-This work; 2- Heilbron et al. 2010; 3- Noce et al. 2007; 4- Kuribara et al. 2019; 5- Degler et al. 2018; 6- Silva et al. 2002a; 7- Barbosa et al. 2018; 8- Seixas et al. 2012; 9- Teixeira et al. 2015; 10- Teixeira et al. 2008; 11- Ávila et al. 2014; 12- Ávila et al. 2010; 13- Barbosa et al. 2015; 14- Moreira et al. 2018; 15- Grochowski et al. 2019; 16- Silva et al. 2016; 17- Santos Pinto et al. 1998; 18- Pinho et al. 2013; 19- Cruz et al. 2016; 20- Guimarães et al. 2005; 21- Medeiros (2013); 22- Peucat et al. 2011; 23- Oliveira et al. 2010; 24- Barbosa et al. 2008; 25- Mello et al. 2006; 26- Carvalho and Oliveira 2003; 27- Oliveira et al. 2002b; 28- Rios et al. 2000; 29- Seixas et al. 2013, 30- Silva et al. 2002b; 31- Oliveira et al. 2013; 32- Peucat et al. 2002; 33- Martin et al. 1997; 34- Barbosa et al. 2013; 35- Teixeira et al. 2017; 36- Bruno et al. 2020; 37- Bersan et al. 2018; 38- Bersan et al. 2020; 39- Valladares et al. 2017; 40- Fonseca (1993); 41- Schmitt et al. 2004; 42- Zimbres et al. 1990; 43- Schmitt (2001); 44- Barbosa and Sabaté (2004); 45- Aguilar et al. 2017.

4.3.5.2.1. The Siderian magmatic arcs

The Siderian arc-related magmatism on Juiz de Fora Complex (sample VA-LM-07B) could be correlated with rocks reported on Mineiro Belt by the Cassiterita (ca. 2470-2410 Ma: Barbosa et al. 2018), Resende Costa (ca. 2.35 Ga: Teixeira et al. 2015) and Lagoa Dourada (ca. 2.35 Ga: Seixas et al. 2012) arc plutons. Differently from the studied area that presents a low K calc-alkaline/tholeiitic dioritic magmatism at this time, all the above-mentioned plutons have TTG signature (Figures 12, 13). Similarly, these rocks are juvenile or moderately juvenile (Figure 12) and have a low crustal residence (Nd TDM around 2.5 Ga). The Cassiterita pluton seems to have similar age (Early Siderian) and isotopic signature (chondritic to positive $\epsilon_{\text{Nd}}(t)$) and low (~0.701) values of $^{87}\text{Sr}/^{86}\text{Sr}(i)$ in comparison with Juiz de Fora, pointing out to primitive magmatic episode on this time (Figure 13).

The Archean to Siderian transition is very important for both the Mineiro Belt and Juiz de Fora Arc as with a remarkable mantle extraction and juvenile crustal addition (model ages of Nd and Hf around 2.5 Ga- Figure 12: Teixeira et al. 2015; Seixas et al. 2013; Degler et al. 2018). The juvenile episode on Itabuna-Salvador Curaçá Rhyacian belt has this same feature (Peucat et al. 2011).

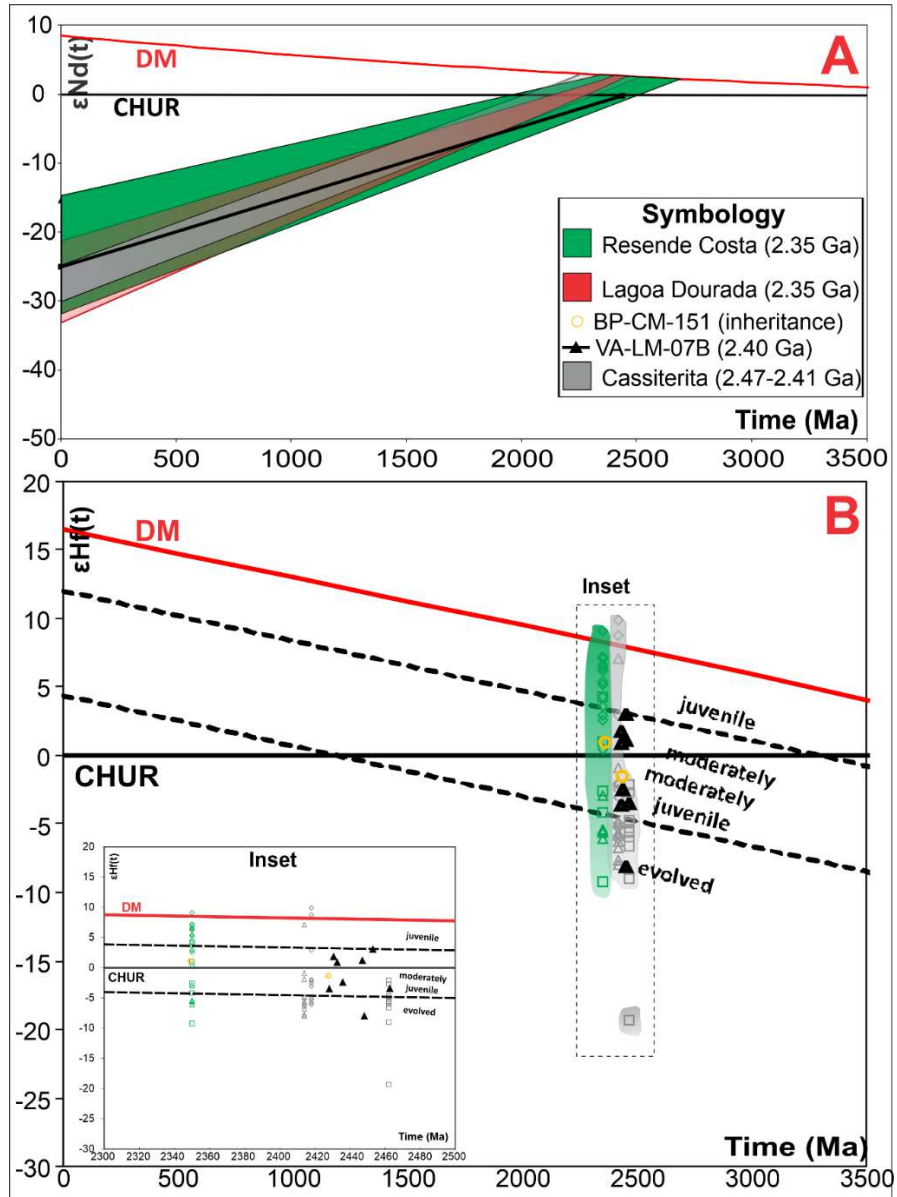


Figure 13. Isotopic correlation of Siderian rocks from JFC (studied área) and Mineiro belt. A) Whole-rock Nd isotopic Evolution diagram, comparing JFC (this work) and Cassiterita (ca. 2.47-2.42 Ga), Resende Costa (ca. 2.35 Ga) e Lagoa Dourada (ca. 2.35 Ga) Plutons. Sm-Nd data obtained by Barbosa et al. 2018, Teixeira et al. 2015 e Seixas et al. 2013. B) Lu-Hf zircon isotopic Evolution diagram of JFC rocks (this work) and Cassiterita and Resende Costa plutons. Lu-Hf data obtained by Barbosa et al. 2018 e Teixeira et al. 2015.

In addition, in the northern cratonic area there were described two calc-alkaline siderian plutons at Jequié (ca. 2.47 Ga: Silva et al. 2002b) and Gavião (ca. 2.32 Ga: Pinho et al. 2013) Blocks, but unfortunately both without geochemical and isotopic constraints.

4.3.5.2.2. The Rhyacian magmatic arc stage

The Rhyacian rocks reported on this study have chronocorrelates on entire the São Francisco Craton basement units as pointed out by the widespread occurrence of ca. 2200 to

2120 Ma arc-related rocks (Figure 12). The isotopic characteristic of these magmatic episodes seems to vary accordingly the presence of Archean nucleus host rock and their petrogenetic classification. Within the Juiz de Fora Complex and Mineiro Belt plutons, there is a lot of moderately juvenile to juvenile TTG and sanukitoids plutons (This study; Moreira et al. 2018; Seixas et al. 2013, Seixas et al. 2012) with markable (enriched) mantle components on the petrogenesis of these magmas. The ca. 2.1 Ga TTG suite on Mantiqueira Complex (Bruno et al. 2020) and the most ca. 2.17-2.10 Ga calc-alkaline plutons from Mineiro Belt are so juvenile (Figure 14) than the TTG suite reported on JFC (This work). On the other hand, evolved rocks, such as sanukitoid suite (this work), are not so common on these basement units, but some ca. 2.19 to 2.13 Ga plutons from Mineiro Belt (Fé, Itumirim and Represa dos Camargos -Teixeira et al. 2008; Barbosa et al. 2015) also has an Archean contribution (whole-rock Nd and zircon Hf TDM model ages) on its petrogenesis. In addition, an evolved rhyacian sanukitoid (ca. 2165 Ma) has been recently reported on Mantiqueira Complex (Bruno et al. 2020) due to a strong paleoarchean contribution.

A possible correlation from juvenile basement units on southern SFC consists of the moderately juvenile to juvenile Rio Itapicuru arc metavolcanics (Oliveira et al. 2010; Mello et al. 2006) at the northern São Francisco Craton. These arc rocks are related to a greenstone belt terrane which has been accreted to a Serrinha Block later (Oliveira et al. 2010). The juvenile signatures were linked with short-lived Paleoproterozoic source rocks (Siderian Nd TDM model ages), except for Itabuna-Salvador Curaçá arc-related rocks (Peucat et al. 2011) where the presence of an Archean nucleus has been described. Thus, its moderately juvenile tendency can be explained by its trondjhemitic magma (Figure 14a) that requires a partial melting of depleted oceanic crust as a source (Moyen and Martin, 2012). Recently, there were occurrences of TTG magmas on Mantiqueira Complex (Bruno et al. 2020), pointing out to similarities between this unit and Itabuna-Salvador-Curaçá belt, whereas the two basement units have reported Juvenile Rhyacian rocks on Archean substratus.

The other basement terranes that present Archean nucleus within Araçuaí and Ribeira Belts have developed within continental margins, generating isotopically evolved rocks (Figure 12), with evidence for crustal reworking as highly negative $\epsilon_{\text{Nd}}(t)$ values, Neoarchean to Paleoarchean TDM Nd model ages and frequently inherited zircon crystals suggestive of crustal assimilation. These evolved signatures (Figure 12) have been reported in the Mantiqueira (Noce et al. 2007; Heilbron et al. 2010; Bruno et al. 2020) and Porteirinha Complexes (Figure 14a-Silva et al. 2016), as well on the Guanhães (Grochowski et al. 2019) and Gavião (Figure 14a-Cruz et al. 2016) Blocks.

The Quirino Complex, at the central Ribeira belt, is another example where occurs arc-related Rhyacian magmatic episodes. It has several magmatic episodes (ca. 2300-2100 Ma-Valladares et al. 2002; Degler et al. 2018) with varied isotopic signature (evolved to juvenile-Valladares et al. 2017) presenting also archean inheritance by zircon grains and Nd TDM model ages (Valladares et al. 2002).

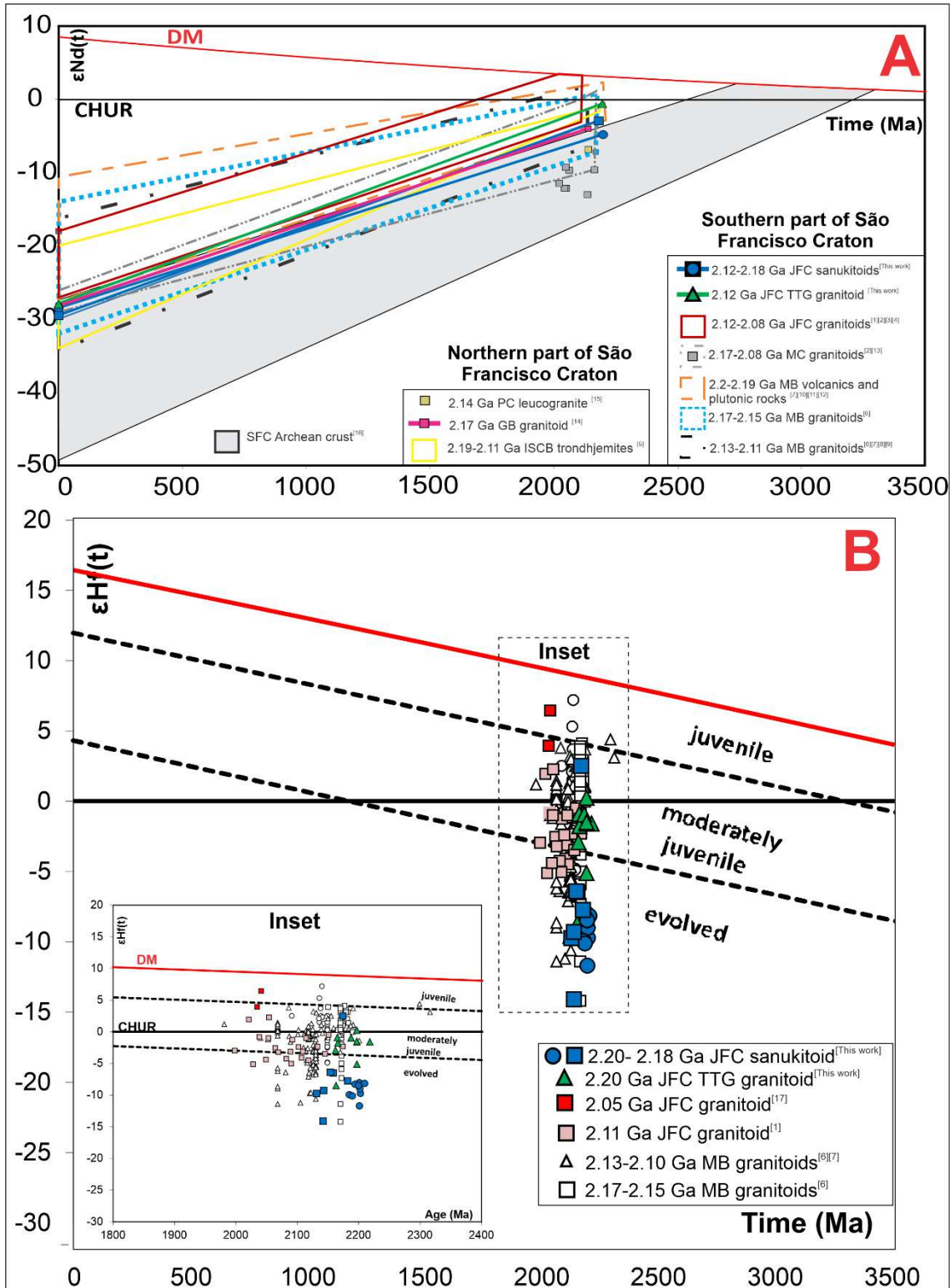


Figure 14. Nd and Hf Isotopic characteristics from basement units from Eastern Bahia Orogenic Domain (EBOD) and the southern São Francisco Craton. A) Nd evolution diagram; B) Hf evolution diagram. References: 1- Degler *et al.* 2018; 2- Noce *et al.* 2007; 3- André *et al.* 2009; 4- Fischel *et al.* 1998; 5- Peucat *et al.* 2011; 6- Barbosa *et al.* 2015; 7- Moreira *et al.* 2018; 8- Seixas *et al.* 2013; 9- Cardoso *et al.* 2018; 10- Teixeira *et al.* 2008; 11- Ávila *et al.* 2010; 12- Ávila *et al.* 2014; 13- Bruno *et al.* 2020; 14- Cruz *et al.* 2016; 15- Silva *et al.* 2016; 16- Teixeira *et al.* 1996; 17- Kuribara *et al.* 2019; The isotopic dataset from Southern Juiz de Fora Complex is represented by symbols (this study). DM- Depleted mantle.

The whole available isotopic dataset for the Minas-Bahia orogenic system is plotted on eNd vs. eSr ($t=2.0$ Ga) diagram (Figure 15) and reinforces the isotope correlations of the Siderian and Rhyacian tholeiitic juvenile episodes from JFC and Mineiro Belt. On the other hand, the sanukitoid magmatism of JFC yields on Mantiqueira Complex and Itauna-Salvador Curaçá belt fields, an expected isotopic signature whereas this magmatism has an important crustal component. This diagram also shows that the southern SFC is more juvenile than the northern part, maybe because in this region there is a predominance of continental active margins where Paleoproterozoic rocks intruded long-lived Archean blocks. The Paleoproterozoic Mantiqueira Complex and Piedade Blocks on southern SFC tip also display this pattern (Figure 15) as shown in Bruno et al. (2020).

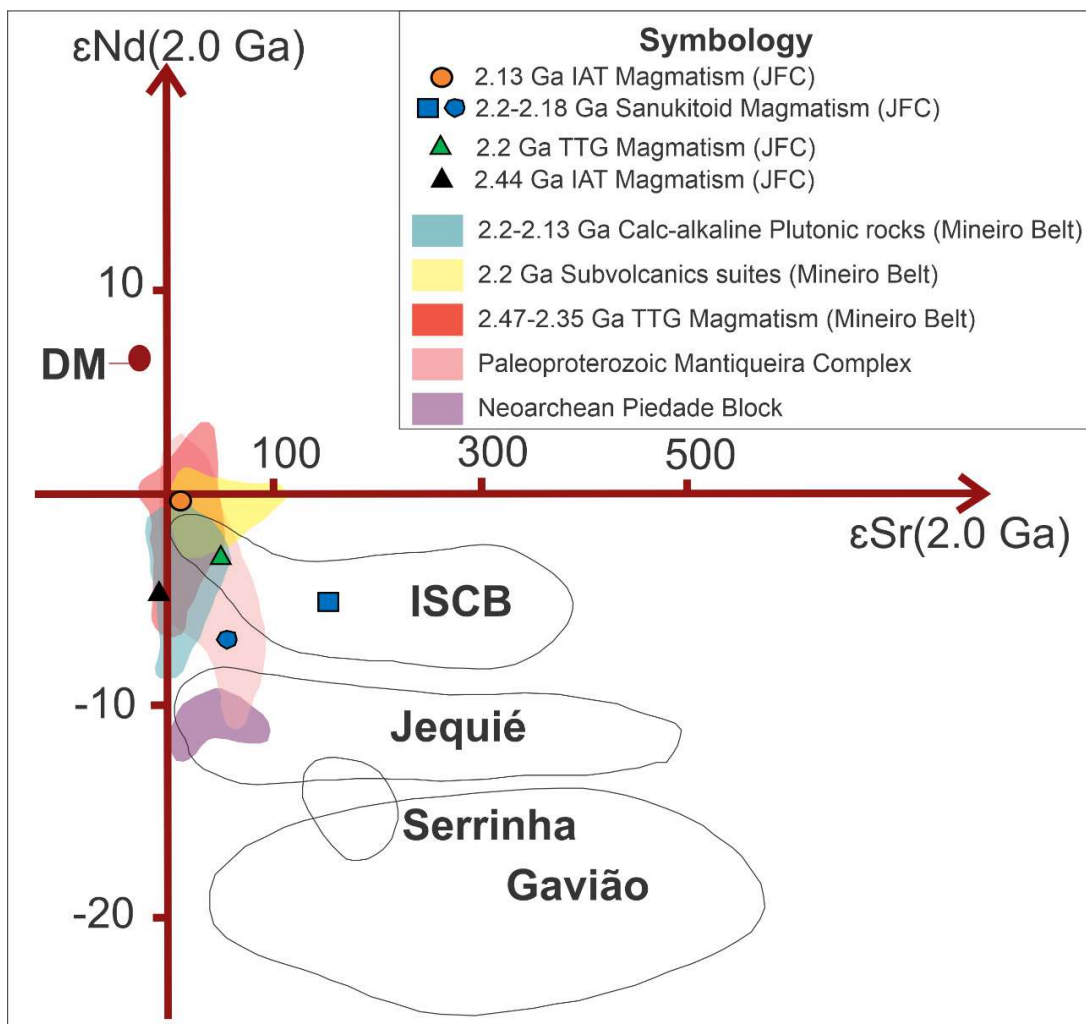


Figure 15. eNd vs. eSr diagram with distinct fields characterized by data from Eastern Bahia Orogenic Domain (Itabuna Salvador-Curaçá Belt, Gavião, Serrinha and Jequié blocks (Modified after Barbosa & Barbosa, 2017). The clouds represent isotopic data from Archean/Paleoproterozoic basement terranes of Southern São Francisco Craton (Piedade Block and Mantiqueira Complex- Bruno *et al.* 2020; Mineiro Belt- Barbosa *et al.* 2015,2018; Ávila *et al.* 2010, 2014; Teixeira *et al.* 2008, 2015). The isotopic dataset from Southern Juiz de Fora Complex is represented by symbols (this study). DM- Depleted mantle.

4.3.5.2.3. The Late Rhyacian-Orosirian Collision (Minas-Bahia Orogeny)

4.3.5.2.3.a. *The record of Metamorphic event*

The Paleoproterozoic metamorphic event recorded on the studied mafic granulite (BP-CM-151) has already been reported on almost all basement terranes of São Francisco paleoplute (Cruz et al. 2016; Silva et al. 2002b; Peucat et al. 2011; Oliveira et al. 2002b, Moreira et al. 2018; Bruno et al. 2020) except within Porteirinha and Guanhães blocks (Figure 12). This granulite-facies metamorphic event in all described basement terranes supports the assumption that a widespread collision paleoproterozoic metamorphic overprinted also the entire Juiz de Fora Complex. As Juiz de Fora Complex is a highly deformed unit by Neoproterozoic deformational phases, it is important to find out this Paleoproterozoic metamorphic episode on massive rocks far away from tectonic boundaries and thrust faults. In addition, not all opx-bearing leucosomes must be Neoproterozoic, such as the charnockitic granulite with widespread leucosomes (RP-LM-04).

Within the Minas Accretionary orogen (Teixeira et al. 2015), it seems there is a difference between the tectono-thermal events within the basement terranes. For instance, at around 2080 Ma, the Juiz de Fora Complex presents a magmatic episode (Noce et al. 2007), coeval with the accretion of Mineiro Belt onto Belo Horizonte domain – Aguilar et al. 2017). The accretion between Mineiro Belt and Piedade Complex is still unknown, but Piedade Block metamorphic ages ranging between 2085 and 2043 Ma reported on Bruno et al. (2020) could be related to this accretion and Piedade-Mantiqueira accretionary history. The metamorphic event, reported on this work, presents a younger metamorphic episode (ca. 2035 to 2026 Ma) than other basement units from Minas-Bahia orogenic system. Therefore, the collision between Mantiqueira and Juiz de Fora Complexes is younger accretion/collision on the Minas Accretionary Orogen.

The long-term duration (2035 to 1950 Ma) of this metamorphic event on Juiz de Fora Complex had already been reported on the Iron Quadrangle Archean pluton and the supracrustal sequences of the Mantiqueira Complex (Acaiaca and Pedra Dourada granulites – Cutts et al. 2018), but in the latter just by metamorphic mineral with low closure temperature for U-Pb systematics (eg. Titanite and Monazite – Aguilar et al. 2017). Titanite ages near ca. 2000 Ma there are related to the collapse of the Minas Orogen with dome-and-keel architecture in the QF (Marshak et al. 1997; Cutts et al. 2019). The fact of the Juiz de Fora Complex being located on the internal zone of this orogenic system could have some relationship with this long-term

duration of metamorphism. On the other hand, the younger granulite-facies metamorphic grains (ca. 1970 to 1950 Ma) could be related to the collision of Juiz de Fora Complex with another basement terrane to the East (eg. Quirino Complex). The lack of Paleoproterozoic metamorphic evidences on Quirino Complex until the present-day preclude this assumption. Degler et al. (2018) groups the Quirino Complex as a part of Rhyacian-Orosirian system only because its evolved results, but there haven't been described any metamorphic event on this unit and it presents a great variation of isotopic signatures and Rhyacian ages from its magmatic episodes. Therefore, we assume that this unit was a microcontinent with unknown location until present moment.

The amphibolite-facies metamorphism of Neoproterozoic age has been also reported for the Mantiqueira Complex (Noce et al. 2007; Heilbron et al. 2010). This study carried out with the southern tip of Juiz de Fora Complex have demonstrated that it is possible to record two granulite facies metamorphism.

4.3.5.3.3.b. The record of Syn- collisional Orosirian magmatism

This period (ca. 2.1 to 2.05 Ga) is coeval to the syn- stage of Minas-Bahia Orogenic system and is marked by evolved granites reported on almost all basement terranes (Figure 12). Some examples are the Itiúba syenite (Itabuna-Salavador Curaçá belt, Oliveira et al. 2010), the Jussiape II syenogranite (Gavião Block, Cruz et al. 2016), the Ambrósio granodiorite (Serinha block, Mello et al. 2006), Gentio pluton (Mineiro Belt: Silva et al. 2002).

4.3.5.3.4. Late to Post-collisional stage

The late collisional magmatic episodes on Minas-Bahia orogen occur at less than ca. 2060 Ma. Recently, high-K late collisional granitoids and whithin-plate tholeiites have been described on Mantiqueira Complex (Bruno et al. 2020), supporting this wide-spread magmatism within all the blocks of the Minas-Bahia orogeny.

The post-collisional plutons, normally with alkaline signature and age less than ca. 2020 Ma, is not recorded on the studied area. However, an occurrence of JFC rock at Itaperuna (ca. 1965 Ma: Heilbron et al. 2010) could be related to the orogenic collapse of Minas-Bahia Orogenic system. There is not any occurrence (by present-day) of dated alkaline plutons on Juiz de Fora Complex. This event is also recorded on Itabuna-Salvador Curaçá, Gavião and Guanhães Blocks and Porteirinha and Mantiqueira Complex (Oliveira et al. 2010; Cruz et al.

2016; Grochowski et al. 2019; Bersan et al. 2020; Bruno et al. 2020). These plutons normally have evolved isotopic signature because the established previous crust can contaminate these magmas (Figure 12), but there is an exception: a juvenile occurrence on Porteirinha Complex points out to successful parcial melting of sub-continenal lithospheric mantle metasomatized by juvenile roots (Bersan et al. 2020).

4.3.5.3. São Francisco-Congo correlations along Paleoproterozoic

Degler et al. (2018) have tried to establish correlations between Brazilian Archean/Paleoproterozoic basement units and African counterparts based on isotopic records. They separated three Rhyacian-Orosirian orogenic systems: W-ROOS, with evolved signature, assembled a major part of São Francisco block (Mantiqueira Complex, some parts of Mineiro Belt and Gavião Block), JU-ROOS, with juvenile signature, assembled the rocks from Juiz de Fora and Pocrane complex and trondhjemites of Itabuna-Salvador Curaçá belt (formerly called Buerarema Complex – Silva et al. 2002), and E-ROOS, with evolved signature, comprising continental margin arcs (Quirino Complex, Região dos Lagos Complex and all basement units from Western Central Africa Belt (WCAB)). On the last item of this paper, we have observed that the southern part of Minas-Bahia orogeny is more complex than Degler et al. (2018) assumed. Most of Mineiro Belt is presented by juvenile plutons, the evolved ones have this characteristic due to subduction of Archean reworked zircon grains from Belo Horizonte Domain (Barbosa et al. 2015). The crustal reworking is almost absent. Moreover, it has been reported several juvenile Rhyacian episodes on Mantiqueira Complex (Bruno et al. 2020), which invalidates the hypothesis from Degler et al. (2018).

The continental Bahia-Gabon cratonic bridge has provided important correlations between the São Francisco and Congo paleoplates (Hurley et al., 1967; Porada 1989; Ledru et al., 1994; Trompette, 1994; D'AgrellaFilho and Cordani, 2017). In this way, southwards on WCAB, the basement units of Kimezian Supergroup (Tack et al. 2001) and Mayombe basement (Djalma et al. 1992, Thiéblemont et al. 2009a) could be a correlation to SE Brazil paleoproterozoic basement units, such as Juiz de Fora Complex. Focusing on the Paleoproterozoic orogenic cycle, we investigate the whole geological history of basement units from São Francisco and Congo paleoplates along this cycle (i.e., magmatic, tectonic, sedimentary, and metamorphic events). On the Brazilian side, the Siderian period (Figure 16, Table 3) had arc plutons on northern and southern SFC with latter more juvenile than other one and coeval development of passive margin sedimentary basin (Minas Basin: Alkmim &

Teixeira, 2017), whereas just on Northern part of WCAB there is a record of rifting from the Archean nuclei to develop Francevillian basins (Weber et al. 2016 and references therein).

The Eastern Bahia Orogenic Domain (EBOD) and Minas Accretionary Orogen (MAO) have had ca. 2.2-2.1 Ga Rhyacian magmatic arcs (Figure 16, Table 3) in which the southern part presenting predominance of juvenile magmatic arcs (i.e. TTG and sanukitoid suites). At ca. 2150 Ma, a greenstone belt sequence has started to develop on Serrinha Block, being a distinguish feature at the northern part. The Juiz de Fora Complex seems to have a longer magmatic episode duration, at least until 2.08 Ga (Noce et al. 2007) or ca. 2.05 Ga (Kuribara et al. 2019). On the African side, the subduction-related magmas are so speculative due to geochronological records. A Tectonic model from Ogooué Orogenic Domain (OOD - Weber et al. 2016), at Gabon, has proposed a subduction start at ca. 2.22 Ga due to high-pressure metamorphism on garnet amphibolites and migmatites. Ca. 2.08 calc-alkaline pluton ended this Rhyacian arc magmatism (Weber et al. 2016 and references therein). In the Mayombé basement and Kimezian Supergroup, at Congo to NW Angola, 2.15 to 2.12 Ga plutons (i.e. Boma and Mpozo-Tombagadio: Delhal and Ledent, 1976) are considered as plutonic manifestations of subduction-related magmas. Pedrosa-Soares et al. (2016) reported quite juvenile zircon grains and archean inheritance for a granodioritic orthogneiss (ca. 2076 Ma) on the Kimezian basement, opening a possibility to extend this arc episode to this period, as well as, on the Juiz de Fora Complex.

The collisional event (Figure 16, Table 3) reported on EBOD and MAO have lasted from ca. 2.09 to 2.05 Ga (Barbosa & Barbosa, 2017; Alkmim and Teixeira, 2017) evidencing a diachronic event between Juiz de Fora Complex and other basement units (see item 5.2.3.a) because it has a younger Orosirian metamorphic episode (ca. 2035 to 2026 Ma: This work). On the northern African counterpart, the collisional event (Eburnean) is only recorded by granulite-facies metamorphism of sedimentary sequences, in which the Nyoung Group being metamorphosed during ca. 2050 to 1985 Ma (Toteu et al. 1994; Lerouge et al. 2006), and the granulite-facies metamorphism on the OOD occurred from 2090 to 2064 Ma (Thieblemont et al. 2009a), similar duration of the EBOD. Djalma et al. (1992) have reported an orosirian recrystallization at ca. 2014 Ma on Guená gneiss, attributing this process to an episodic Pb loss period due to Eburnean orogenesis. Despite the Orosirian metamorphic event is also reported on Juiz de Fora Complex, the lack of robust geochronological data prevents any correlation between these two basement units.

The syn-collisional magmatism (ca. 2.06 to 2.05 Ma- Figure 16, Table 3) is widespread on EBOD (Gavião et al. 2016; Oliveira et al. 2010). At the southern SFC part, the ca. 2.05 Ga

Gentio pluton (Silva et al. 2002) on Mineiro Belt is correlative to this magmatism. Noce et al. (2007) reported other coeval granitoids (without geochemical constraints) on Mantiqueira Complex, configuring a good correlative candidate. The Juiz de Fora Complex has a leucosome crystallization of zircon grains dated at ca. 2025 Ma. There are records of syntectonic eburnean granitoids on Nyoung Group (2.06 to 2.05 Ga: Lerouge et al. 2006) and on Ogooué Orogenic Domain (2.04 Ga: Weber et al. 2016 and references therein). On southern WCAB, at Mayombé basement, this magmatic episode is represented by ca. 2.0 Ga Les Saras syntectonic granodiorite (Maurin et al. 1990) which intrudes on the Paleoproterozoic metasedimentary sequence. There is not any correlative rock on Kimezian Supergroup for this collisional magmatism.

Late to post-collisional magmatism (ca. <2020 Ma) on Minas-Bahia orogeny is represented by high-K to alkaline magmatism, a widespread episode on EBOD (Grochowski et al. 2019; Cruz et al. 2016; Bersan et al. 2020) and with some recent occurrences on Mantiqueira Complex (Bruno et al. 2020). On the African counterpart, at ca. 2000 Ma have occurred the slab break-off process (Weber et al. 2016), provoking the rapid uplift and transfer of asthenospheric material toward the paleoproterozoic sutures as well as following melting and intrusion of Lécoué granite on the suture of Ogooué orogenic Domain (Gabon). Meanwhile, on Kimezian basement, a ca. 1.96 Ma syenite (without geochemical constraints- Delhal & Ledent, 1978) is a possible representative of the late to post-collisional episode on Southern WCAB.

Table 3. Synthesis of Paleoproterozoic geological events of basement units from São Francisco and Congo blocks. EBOD: Eastern Bahia Orogenic Domain; NS-Nyong Series; OOD- Ogooué Orogenic Domain; MaB: Mayombé basement; KS: Kimezian Supergroup. Basement units of Brazilian parts as Figure 12.

Time/Basement unit	EBOD (Bahia)	NS + OOD (SW Cameroon-Gabon)	Minas Orogen (SE Brazil)	Accretionary MaB + KS (Congo-N Angola)
Late to post-collisional magmatism	Intense High-K to Alkaline plutonism	OOD: Lécoué granite (2.0 Ga)	MC: 1.98 Ga; JFC: 1.97 Ga	ca. 1.96 Ga Syenites (KS)
Syn-collisional magmatism	2.06-2.05 rewroking granites	NS: 2.06-2.05 Ga; OOD: 2.04 Ga	2.05-2.04 Ga: MB and MC.	Syntectonic ca. 2.0 Ga Les Saras granodiorite (MaB)
Collisional event	2.09-2.05 Ga granulite-facies metamorphism (metasedimentary and metaigneous rocks)	Only recorded on metasedimentary units. NS: 2.05-1.98 Ga; OOD: 2.09-2.06 Ga	Diacrhetic event. Major: 2.08-2.04 Ga (MB, MC); 2.03-2.02 Ga: JFC	2.01 recrystallization event on Guéra Gneiss (MaB)
Rhyacian Magmatism	Arc Continental margin arcs	Final stage: 2.08 Ga calc-alkaline pluton	Predominance of juvenile magmatic episodes (MB, MC, JFC)	2.15-2.07 Ga Boma and Mpozo plutons (KS)
Paleoproterozoic sedimentary sequence	Deposition of Greensone Belt volcanosedimentary sequence (ca. 2150 Ma)	Deposition of Francevillian basins (ca. 2435 Ma)	Deposition of Passive margin Minas basin	Micaschists (Ncesse Formation)
Siderian magmatism	arc Continental margin arcs?	-	Juvenile TTG/IAT plutons	-

Lerouge *et al.* (2006) have assumed that Nyong Series is related to Itabuna-Salvador Curaçá belt, being an important correlation northward to Juiz de Fora Complex. The lack of geochronological evidence on the southern part of Eburnean basement (Mayombe basement: Congo, Gabon; Kimezian Supergroup- Angola and DRC) does not allow to correlate any of these units to the Juiz de Fora Complex. Juvenile zircon grains from Kimezian basement at ca. 2.07 Ga (Pedrosa-Soares *et al.* 2016) could be an important first step on this correlation. The answer could be in the Mesoproterozoic supracrustal sequences on Africa (eg. Kibara supergroup: Villeneuve and Chorowicz 2004) if they present quite juvenile zircons of ca. 2.44 Ga will attest the collision of these counterparts blocks.

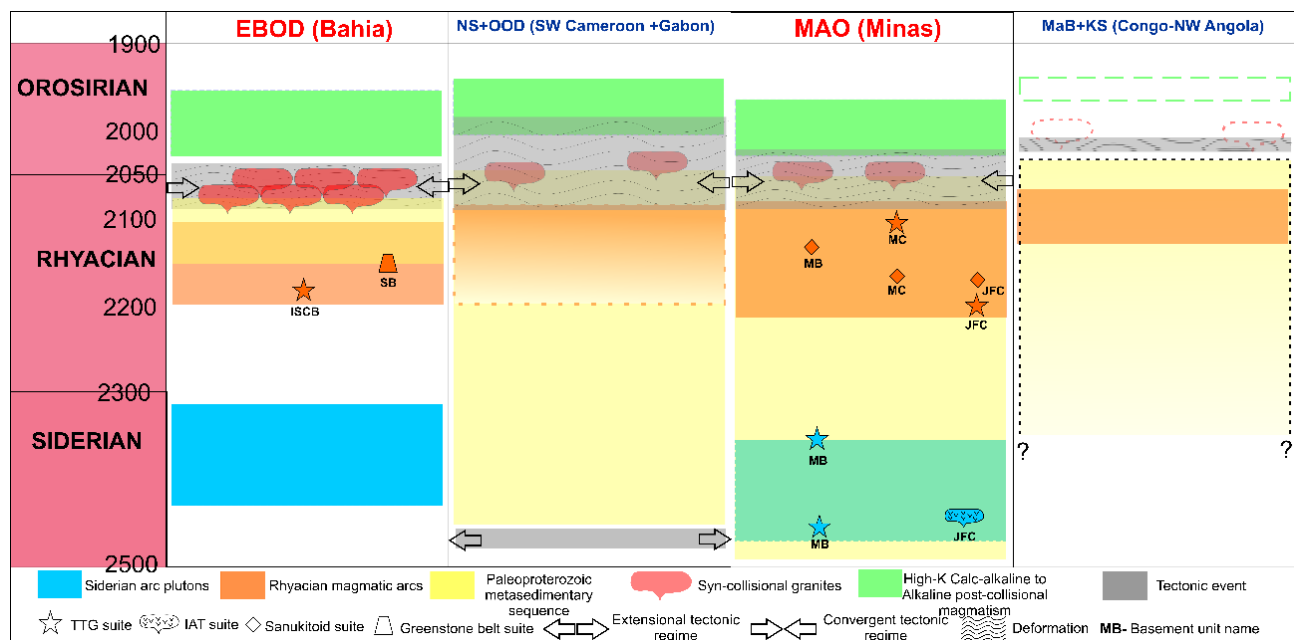


Figure 16. Correlation of magmatic, metamorphic, and sedimentary episodes between Minas-Bahia orogenic system and the Western Central Africa belt. EBOD: Eastern Bahia Orogen Domain; MAO: Minas Accretionary Orogen; NS: Nyoung Series; OOD: Ogooué Orogenic Domain; NG: Nyoung Group; MaB- Mayombé basement; KS- Kimezian Supergroup.

3.6. CONCLUSIONS

The new geological data for the Juiz de Fora Complex in southern Rio de Janeiro State resulted on the following insights and regional tectonic correlations within the broad Minas-Bahia Orogenic System and Western Central Africa belt:

- The rocks of Juiz de Fora Complex show a polycyclic evolution, regarding the magmatic crystallization episodes and metamorphic overprint.

- The Juiz de Fora complex rocks represent a long-lived magmatic arc evolution with at least three episodes of magma generation. This assumption is supported by crystallization ages and inherited zircon crystals.
- The oldest one, represented by Siderian dioritic arc protoliths were described for the first time in the Juiz de Fora complex, coeval with ca. 2.4 Ga ocean floor rocks previously describe, marking the onset of subduction.
- Regarding the more evolved stage of the arc, ca. 2.2 Ga high Ba-Sr granitoids with both TTG and sanukitoid affinities were described by the first time within this block.
- The protoliths of Juiz de Fora Complex shows progressive maturation of the arc, with juvenile input as described elsewhere, but our work also detected an important Archean contribution., explained by subducted archean detrital zircons.
- The orthogranulites of Juiz de Fora Complex have recorded a diachronic Orosirian metamorphic event (ca. 2.03 Ga) of Minas-Bahia orogeny. This overprint suggests the docking westwards onto the Mantiqueira Complex.
- The tectonic evolution of Juiz de Fora Complex in the studied area seems to be very similar with that reported for the Mineiro Belt, with an evolution from intra-oceanic to evolved settings from the Siderian to Rhyacian, suggesting the beginning of the operation of modern plate tectonics, with the participation of both of subducted ocean crust and enriched supra-subduction asthenospheric zones in magma generation.
- Juvenile zircon grains from Komezian granodioritic orthogneiss could be a good correlative of Juiz de Fora Complex on the Western Central African Belt.

ACKNOWLEDGEMENTS

The first author thanks to the *Coordenação de Aperfeiçoamento de Pessoal de Nível Superior* (CAPES) for the scholarship of the Geosciences Graduate Program. The authors acknowledge the support of the *Laboratório de Processamento de Amostras* (LGPA), *Laboratório de Geoquímica Isotópica* (UFOP) and *Laboratório de Geocronologia e Isótopos Radiogênicos* (LAGIR), the Rio de Janeiro de State University (UERJ), the CNPq grants of Monica Heilbron, Claudio Valeriano and Wilson Teixeira, and the FAPERJ-CNE for funding the research.

REFERENCES

- Aguilar Gil, C., Alkmim, F.F., Lana, C., Farina, F., 2017. Paleoproterozoic assembly of the São Francisco craton, SE Brazil: new insights from U-Pb titanite and monazite dating. *Precambrian Research*, **289**: 95–115.
- Alkmim F.F. & Teixeira W. 2017. The Paleoproterozoic Mineiro Belt and the Quadrilátero Ferrífero In: Heilbron M., Cordani U., Alkmim F.F. (eds.). *São Francisco Craton, Eastern Brazil: Tectonic Genealogy of a Miniature Continent*. Regional Geology Reviews. Springer, p. 71-94.
- Alkmim, F.F., Marshak, S. Fonseca, M.A., 2001. Assembling West Gondwana in the Neoproterozoic: Clues from the São Francisco craton region, Brazil. *Geology*, **29**: 319–322.
- Alkmim, F.F., Brito Neves, B.B., Alves, J.A.C., 1993. Arcabouço tectônico do Cráton do São Francisco e uma revisão. In: Dominguez, J.M., Misi, A. (Eds.), O Cráton do São Francisco. Reunião Preparatória do 2º Simposio sobre o Cráton do São Francisco, pp. 45e62. Salvador, SBG/Núcleo BA/SE/SGM/CNPq.
- André J.L.F., Valladares C.S., Duarte BP. 2009. O Complexo Juiz de Fora na região de Três Rios (RJ): Litogeochímica, geocronologia U-Pb (LA-ICPMS) e geoquímica isotópica de Nd e Sr. *Revista Brasileira de Geociências*, **39**(4):773-793.
- Araujo, L.E.A.B., Heilbron, M., Valeriano, C.M., Teixeira, W., Neto, C.C.A. 2019. Lithogeochemical and Nd-Sr isotope data of the orthogranulites of the Juiz de Fora complex, SE-Brazil: insights from a hidden Rhyacian Orogen within the Ribeira belt. *Brazilian Journal of Geology*, **Vol.49**, n.3, e20190007.
- Armstrong, R.L., 1981. Radiogenic isotopes; the case for crustal recycling on a near-steady-state no-continental-growth Earth. Royal Society of London Philosophical Transactions 301, 443–472.
- Arth, J.G., Hanson, G.N., 1972. Quartz diorites derived by partial melting of eclogite or amphibolite at mantle depths. *Contributions to Mineralogy and Petrology*, **37**,: 161–174.
- Ávila, C.A., Teixeira, W., Bongiolo, E.M., Dussin, I.A., 2014. The Tiradentes suite and its role in the Rhyacian evolution of the Mineiro belt, São Francisco Craton: Geochemical and U-Pb geochronological evidences. *Precambrian Research*, **243**: 221–251.
- Ávila, C.A., Teixeira, W., Cordani, U.G., Moura, C.A.V., Pereira, R.M. 2010. Rhyacian (2.23–2.20) juvenile accretion in the southern São Francisco craton, Brazil: Geochemical and isotopic evidence from the Serrinha magmatic suite, Mineiro belt. *Journal of South American Earth Sciences*, **29**:143–159.
- Bahlburg, H., Vervoort, J.D., DuFrane, S.A., Carlotto, V., Reimann, C., Cárdenas, J., 2011. The U-Pb and Hf isotope evidence of detrital zircons of the Ordovician Ollantaytambo Formation, southern Peru, and the Ordovician provenance and paleogeography of southern Peru and northern Bolivia. *Journal of South America Earth Sciences*, **32**:196–209.

- Barbosa, J. S. F. and Sabaté, P. 2002. Geological features and the Paleoproterozoic collision of four Archean crustal segments of the São Francisco Craton, Bahia, Brazil. A synthesis. *Anais da Academia Brasileira de Ciências*, **74**: 343–359.
- Barbosa, J. S. F., Peucat, J.-J. et al. 2008. Petrogenesis of the late-orogenic Bravo granite and surrounding high-grade country rocks in the Palaeoproterozoic orogen of Itabuna–Salvador–Curacá block, Bahia, Brazil. *Precambrian Research*, **167**:35–52.
- Barbosa, N.S., Teixeira, W., Ávila, C.A., Montecinos, P.M., Bongiolo, E.M., 2015. 2.17–2.10 Ga plutonic episodes in the Mineiro belt, São Francisco Craton, Brazil: U-Pb ages, geochemical constraints and tectonics. *Precambrian Research*, **270**, 204–225.
- Barbosa N.S., Teixeira W., Ávila C.A., Montecinos P.M., Bongiolo E.M., Vasconcellos F.F. 2018. U-Pb geochronology and coupled Hf-Nd-Sr isotopic-chemical constraints of the Cassiterita Orthogneiss (2.47–2.41-Ga) in the Mineiro belt, São Francisco craton: Geodynamic fingerprints beyond the Archean-Paleoproterozoic Transition. *Precambrian Research*, **326**:399-416.
- Bersan, S.M., Costa, A.F.O., Danderfer Filho A., Abreu F. R., Lana, C., Queiroga, G., Storey, C., Moreira, H. 2020. Paleoproterozoic juvenile magmatism within the northeastern sector of the São Francisco paleocontinent: Insights from the shoshonitic high Ba-Sr Montezuma granitoids. *Geoscience Frontiers*, in press.
- Bersan, S.M., Danderfer Filho A., Abreu F. R., Lana, C. 2018. Petrography, geochemistry and geochronology of the potassic granitoids of the Rio Itacambiruçu Supersuite: implications for the Meso- to Neoarchean evolution of the Itacambira-Monte Azul block. *Brazilian Journal of Geology*, **48**(1): 1-24.
- Black, L.P., Kamo, S.L., Allen, C.M., Aleinikoff, J.N., Davis, D.W., Korsch, R.J. and Foudoulis, C., 2003. TEMORA 1: a new zircon standard for Phanerozoic U–Pb geochronology. *Chemical geology*, **200**(1-2), pp.155-170.
- Boynton W.V. 1984. Cosmochemistry of the rare earth elements; meteorite studies. In: Henderson, P. (eds.). *Rare earth element geochemistry*. Amsterdam, Elsevier Sci. Publ. Co., p. 63-114.
- Bruno, H., Elizeu, V., Heilbron, M., Valeriano, C.M., Strachan, R., Fowler, M., Bersan, S., Moreira, H., Dussin, I., Silva, L.G.E., Tupinambá, M., Almeida, J.C.H., Neto, C., Storey, C. 2020. Neoarchean and Rhyacian TTG-Sanukitoid suites in the southern São Francisco Paleocontinent, Brazil: Evidence for diachronous change towards modern tectonics. *Geoscience Frontiers*, in press.
- Campos Neto, M.C. 2000. Orogenic Systems from Southwestern Gondwana: An approach to Brasiliano-PanAfrican Cycle and Orogenic Collage in Southeastern Brazil. In: Cordani, U.G.; Milani, E.J.; Thomaz Filho, A.; Campos, D.A. (Eds.). Tectonic Evolution of South América. Rio de Janeiro, 31st International Geological Congress, Rio de Janeiro, p. 335–365.
- Cardoso C.D., Ávila C.A., Neumann R., Oliveira E.P., Valeriano C.M., Dussin I. 2019. A Rhyacian continental arc during the Evolution of the Mineiro belt, Brazil: constraints from the Rio Grande and Brumado metadiorites. *Lithos*, **326-327**:246-264.

- Carvalho, M. J. and Oliveira, E. P. 2003 Geologia do tonalito Itareru, bloco Serrinha, Bahia: uma intrusão sin-tectônica do início da colisão continental no segmento norte do orógeno Itabuna - Salvador - Curaçá. *Revista Brasileira de Geociências*, **33** (Suplemento), 55–68.
- Clift P. D., Vannucchi P., Morgan J. P. (2009) Crustal redistribution, crust–mantle recycling and Phanerozoic evolution of the continental crust. *Earth-Science Reviews*, **97**:80–104.
- Cawood, P.A., Kröner, A., Collins, W.J., Kusky, T.M., Mooney, W.D., Windley, B.F., 2009. Accretionary Orogens through Earth history. In: Cawood, P.A., Kröner, A. (Eds.), Earth Accretionary Systems in Space and Time. Geol. Soc. (Lond.) Spec. Publ. 318, 1–36.
- Conceição, H., Silva, R. M. L., Macambira, M. J. B., Scheller, T., Marinho, M. M., Correia, R. D. 2003. 2,09 Ga idade mímina da cristalização do batólito sienítico Itiúba: um problema para o posicionamento do clímax do metamorfismo granulítico (2,05–2,08 Ga) no cinturão móvel Salvador-Curaçá, Bahia. *Revista Brasileira de Geociências*, **33**, 395–398.
- Cordani, U.G. and K. Sato, 1999. Crustal evolution of the South American Platform, based on Sm-Nd isotopic systematic on granitoid rocks. *Episodes*, **22**: 167–173.
- Corfu, F., Hanchar, J.M., Hoskin, P.W. and Kinny, P., 2003. Atlas of zircon textures. Reviews in mineralogy and geochemistry, **53(1)**, pp.469-500.
- Cutts, K., Lana, C., 2019. The complex tale of Mantiqueira and Juiz de Fora: A comment on “Eoarchean to Neoproterozoic crustal evolution of the Mantiqueira and Juiz de Fora Complexes, SE Brazil: Petrology, geochemistry, zircon U-Pb geochronology and Lu-Hf isotopes”. *Precambrian Research*, **332**: 105305.
- Cutts, K., Lana, C., Alkmim, F., Peres, G.G., 2018. Metamorphic imprints on units of the southern Araçuaí belt, SE Brazil: The history of superimposed Transamazonian and Brasiliano orogenesis. *Gondwana Research*, **58**: 211-234.
- D'Agrella-Filho, M.S., Teixeira, W., da Trindade, R.I., Patroni, O.A. and Prieto, R.F., 2020. Paleomagnetism of 1.79 Ga Pará de Minas mafic dykes: Testing a São Francisco/Congo-North China-Rio de la Plata connection in Columbia. *Precambrian Research*, **338**, p.105584.
- D'Agrella-Filho, M.S., Cordani, U.G., 2017. The Paleomagnetic Record of the São Francisco-Congo Craton. In: Heilbron, M., Cordani, U.G., Alkmim, F.F. (Eds.), *São Francisco Craton, Eastern Brazil. Regional Geology Reviews*. Springer, Cham.
- Delhal, J., Ledent, D., 1978. Donees géochronologiques dans la région de Matadi (Zaire) relatives à la syénite de la Mpozo et aux métarhyolites. Département Géologie et Mineralogie, Musée Royal Afrique Centrale, Rapport annuel 1977, Tervuren, Belgique, 99–110.
- Delhal, J. and Ledent, D. 1976. Age et évolution comparée des gneiss migmatitiques prézadieniens des régions de Boma et de Mpozo-Tombagadio (Bas-Zaire). *Ann. Soc. Geol. Belg.*, **99**:165-187.
- Degler R., Pedrosa-Soares A.C., Novo T., Tedeschi M., Silva L.C., Dussin I., Lana C. 2018. Rhyacian-Orosirian isotopic records from the basement of the Araçuaí-Ribeira orogenic

system (SE Brazil): Links in the Congo-São Francisco paleocontinent. *Precambrian Research*, **317**:179-195.

DePaolo D.J. 1988. *Neodymium isotope geochemistry: An introduction*. New York, 187pp.

Djama, L.M., Leterrier, J-L., Michard, A. 1992. Pb, Sr and Nd isotope study of the basement of the Mayumbian belt (Guena gneisses and Mfoubou granite, Congo): implications for crustal evolution in Central Africa. *Journal of African Earth Sciences*, **14**(2):227–237.

Duarte B.P., Figueiredo M.C.H., Campos Neto M., Heilbron M. 1997. Geochemistry of the granulite fácies orthogneisses of Juiz de Fora Complex, Central Segment of the Ribeira Belt, Southeastern Brazil. *Revista Brasileira de Geociências*, **27**(1):67-82.

Duarte B.P. & Heilbron M. 1999. Metamorphic Evolution of the Early to Medium Proterozoic Granulite Fácies Rocks of the Central Segment of the Brasiliano-Panafrican Ribeira Belt, Southeastern Brazil. In: European Union of Geosciences. Strasbourg, France, 1999. Journal of Conference Abstracts. Strasbourg, Cambridge Publications. 4:792.

Duarte B.P., Valente S., Heilbron M., Campos Neto M.C. 2004. Petrogenesis of orthogneisses of the Mantiqueira Complex, Central Ribeira Belt, SE Brazil: an Archean to Paleoproterozoic basement unit reworked during the Pan-African Orogeny. *Gondwana Research*, **7**:437–450.

Feybesse, J-L., Johan, V., Triboulet, C., Guerrot, C., Mayaga-Mikolo, F., Bouchot, V., Eko N'dong, J. 1998. The West Central African belt: a model of 2.5–2.0 Ga accretion and two-phase orogenic evolution. *Precambrian Research*, **87**:161–216.

Fischel D.P., Pimentel M.M., Fuck R.A., Costa A.G., Rosière C.A. 1998. Geology and Sm-Nd isotopic data for the Mantiqueira and Juiz de Fora Complexes (Ribeira Belt) in the Abre Campo Manhaçu region, Minas Gerais, Brazil. In: International Conference on Basement Tectonics. *Abstracts*, v.14, p. 21-23.

Fonseca, A. C. 1993. Esboço geocronológico da região de Cabo Frio, Estado do Rio de Janeiro. PhD thesis, University of São Paulo, Brazil.

Fyfe, W.S., 1978. Evolution of the Earth's crust: modern plate tectonics to ancient hot-spot tectonics? *Chemical Geology* **23**, 89–114.

Gerdes, A., Zeh, A., 2006. Combined U-Pb and Hf isotope LA-(MC-)ICP-MS analyses of detrital zircons: comparison with SHRIMP and new constraints for the provenance and age of an Armorican metasediment in central Germany. *Earth Planet. Sci. Lett.*, **249**:47–61.

Gerdes, A., Zeh, A., 2009. Zircon formation versus zircon alteration – new insights from combined U-Pb and Lu-Hf in-situ LA-ICP-MS analyses, and consequences for the interpretation of Archean zircon from the Central Zone of the Limpopo Belt. *Chem. Geol.*, **261**: 230–243.

Gonçalves L., Farina F., Lana C., Pedrosa-Soares A.C., Alkmim F., Nalini H.A. 2014.

New U-Pb Idades and lithochemical attributes of the Ediacaran Rio Doce magmatic arc, Araçuaí confined orogen, Southeastern Brazil. *Journal of South America Earth Science*, **52**:1–20.

Glikson, A.Y., 1971. Primitive Archean element distribution patterns: chemical evidence and geotectonic significance. *Earth and Planetary Science Letters* 12, 309–320.

Guimarães, J. T. 2005. Projeto Ibitiara-Rio de Contas, Estado da Bahia, Escala 1:200.000. Serviço Geológico do Brasil, CPRM, 217p.

Greene, A. R., S. M. DeBari, P. B. Kelemen, J. Blusztajn, and P. D. Clift (2006), A detailed geochemical study of island arc crust: The Talkeetna Arc section, south-central Alaska, *J. Petrol.*, 47, 1051–1093.

Griffin, W.L., Wang, X., Jackson, S.E., Pearson, N.J., O'Reilly, S.Y., Xu, X.S., Zhou, X.M., 2002. Zircon chemistry and magma mixing, SE China: in-situ analysis of Hf isotopes, Tonglu and Pingtan igneous complexes. *Lithos*, **61**:237–269.

Grochowski, J., Kuchenbecker, M., Barbuena, D., Novo, T.A. 2019. Os plútôns Felício e Mercês: registros da orogênese riaciana-orosiriana no Bloco Guanhães. In: IV Simpósio do Cráton São Francisco (SCSF), Aracaju. *Anais*, p. 42.

Guimarães, J.T., Teixeira, L.R., Silva, M.G., Martins, A.A.M., Filho, E.L.A., Loureiro, H.S.C., Arcanjo, J.B., Dalton de Souza, J., Neves, J.P., Mascarenhas, J.F., Melo, R.C., Bento, R.V., 2005. Datações U/Pb em rochas magmáticas intrusivas no Complexo Paramirim e no Rifte Espinhaço: Uma contribuição ao estudo da Evolução Geocronológica da Chapada Diamantina. In: SBG/BA-SE, Simpósio do Cráton do São Francisco, Salvador, Anais de Resumos Expandidos, pp.159e161.

Hacker, B.R., Mehl, L., Kelemen, P.B., Rioux, M., Behn, M.D., Luffi, P., 2008. Reconstruction of the Talkeetna intra-oceanic arc of Alaska through thermobarometry. *J. Geophys. Res.* 113.

Heilbron M., Tupinambá M., Almeida J.C.H., Valeriano C.M., Valladares C.S., Duarte B.P. 1998. New constraints on the tectonic organization and structural styles related to the Brasiliano collage of the central segment of the Ribeira belt, SE Brazil. In: Abstracts of the International Conference on Precambrian and Craton Tectonics/ International Conference on Basement Tectonics. Ouro Preto, Brasil, *Extended Abstracts*, v. 14, p.15-17.

Heilbron M., Pedrosa-Soares A.C., Campos Neto M., Silva L.C., Trouw R.A.J., Janasi V.C. 2004a. A Província Mantiqueira In: Mantesso-Neto V., Bartorelli A., Carneiro C.D.R., Brito-Neves B.B. (eds.). *O desvendar de um continente: a moderna geologia da América do Sul e o legado da obra de Fernando Flávio Marques de Almeida*, pp. 203–234.

Heilbron M., Duarte B.P., Valeriano C.M., Simonetti A., Machado N., Nogueira J.R. 2010. Evolution of reworked Paleoproterozoic basement rocks within the Ribeira belt (Neoproterozoic), SE-Brazil, based on U/Pb geochronology: Implications for paleogeographic reconstructions of the São Francisco-Congo paleocontinent. *Precambrian Research*, **178**:136–148.

- Hunter, D.R., 1970. The Ancient gneiss complex in Swaziland. *Transactions of the Geological Society of South Africa* 73, 107–150.
- Hurley, P.M., Almeida de, F.F.M., Melcher, G.C., Cordani, U.G., Rand, J.R., Kawashita, K., Vandoros, P., Pinson, W.H., Fairbairn Jr., H.W., 1967. Test of continental drift by comparison of radiometric ages. A pre-drift reconstruction shows matching geologic age provinces in West Africa and Northern Brazil. *Science*, **157**:495–500.
- Jackson, S.E., Pearson, N.J., Griffin, W.L., Belousova, E.A., 2004. The application of laser ablation-inductively coupled plasma-mass spectrometry to in-situ U-Pb zircon geochronology. *Chem. Geo.*, **211**: 47–69.
- Kuribara Y., Tsunogae T, Takamura Y, Santosh M, Costa A, Rosiére C. 2019. Eoarchean to Neoproterozoic crustal evolution of the Mantiqueira and the Juiz de Fora Complexes, SE Brazil: Petrology, geochemistry, zircon U-Pb geochronology and Lu-Hf isotopes. *Precambrian Research*, **323**:82-101.
- Lana, C., Farina, F., Gerdes, A., Alkmim, A., Gonçalves, G.O., Jardim, A., 2017. Characterization of zircon reference materials via high precision U-Pb LA-MC-ICPMS. *J. Anal. At. Spectrom.* **32**: 2011–2023.
- Lana, C., Alkmim, F.F., Armstrong, R., Scholz, R., Romano, R., Nalini, H.A. 2013. The ancestry and magmatic evolution of Archaean TTG rocks of the Quadrilátero Ferrífero province, southeast Brazil. *Precambrian Research*, **230**:1–30.
- Laurent, O., Martin H., Moyen J.F., Doucelance R. 2014 The diversity and evolution of late Archean granitoids: evidence for the onset of ‘modern-style’ plate tectonics between 3.0 and 2.5 Ga. *Lithos*, **205**: 208–235.
- Ledru, P., Johan, V., Milési, J.P., Tegyey, M., 1994. Makers of the last stage of the Paleoproterozoic collision: evidence for 2 Ga continent involving circum-South Atlantic provinces. *Precambrian Research*, **69**:169–191.
- Lerouge, C., Cocherie A., Toteu, S.F., Penaye, J., Milesi, J.-P., Tchameni, R., Nsifa, E.N., Fanning, C.M., Deloule, E. 2006. Shrimp U–Pb zircon age evidence for Paleoproterozoic sedimentation and 2.05 Ga syntectonic plutonism in the Nyong Group, South-Western Cameroon: consequences for the Eburnean-Transamazonian belt of NE Brazil and Central Africa. *Journal of African Earth Sciences*, **44**:413–427.
- Ludwig, K.R., 2011. Isoplot/Ex Version 4: A Geochronological Toolkit for Microsoft Excel: Geochronology Center. Berkeley, California, USA.
- Machado N., Valladares C., Heilbron M., Valeriano C.M. 1996. U-Pb geochronology of the central Ribeira Belt (Brazil) and implications for the evolution of the Brazilian Orogeny. *Precambrian Research*, **79**:347-361.
- Marshak, S., Tinkham, D., Alkmim, F.F., Brueckner, H.K., Bornhorst, T., 1997. Dome and keel provinces formed during Paleoproterozoic orogenic collapse-Diapir clusters or core complexes? Examples from the Quadrilátero Ferrífero (Brazil) and the Penokean Orogen (USA). *Geology*, **25**: 415-418.

- Martin, H. 1986. Effect of steeper Archean geothermal gradient on geochemistry of subduction-zone magmas. *Geology*, **14**: 753– 756.
- Maurin, J. C., Mpemba-Boni, J., Pin, C. and Vicat, J. P. 1990. La granodiorite de Les Saras un témoin de magmatisme éburnéen (2 Ga) au sein de la chaîne ouest-congolaise: conséquences géodynamiques. *C. R. Acad. ScL*, Paris 310, 571-575.
- McGregor, V.R., 1973. The early Precambrian gneisses of the Godthab district, West Greenland. *Philosophical Transactions of Royal Society of London A273*, 343–358.
- McMillan, N.J., Harmon, R.S., Moorbath, S., Lopez-Escobar, L., Strong, D.F., 1989. Crustal sources involved in continental arc magmatism: a case study of volcano MochoChoshuenco, southern Chile. *Geology*, **17**: 1152–1156.
- Medeiros, E.L., 2013. Geologia e geocronologia do complexo Santa Izabel na região de Urandi, Bahia. Universidade Federal da Bahia, p. 203. Dissertação de Mestrado.
- Mello, E. F., Xavier, R. P., McNaughton, N. J., Hagemann, S. G., Fletcher, I. & Snee, L. 2006. Age constraints on felsic intrusions, metamorphism and gold mineralization in the Paleoproterozoic Rio Itapicuru greenstone belt, NE Bahia State, Brazil. *Mineralium Deposita*, **40**: 849–866.
- Moyen, J.F., Martin, H., 2012. Forty years of TTG research. *Lithos*, 148: 312–336.
- Noce C., Pedrosa-Soares A.C., Silva L.C., Armstrong R., Piuzana D. 2007. Evolution of polycyclic basement complexes in the Araçuaí Orogen, based on U-Pb SHRIMP data: Implications for Brazil Africa links in Paleoproterozoic time. *Precambrian Research*, **159**: 60–78.
- Novo, T.; Pedrosa-Soares, A.C. ; Noce, C.M. ; Alkmim, F.F. ; Dussin, I. 2010. Rochas charnockíticas do sudeste de Minas Gerais: a raiz granulítica do arco magnético do Orógeno Araçuaí. *Revista Brasileira de Geociências*, v. 40, p. 573-592.
- Oliveira, E. P., Carvalho M. J., McNaughton N. J.. 2004a. Evolução do segmento norte do orógeno Itabuna-Salvador-Curaçá: cronologia da acresção de arcos, colisão continental e escape de terrenos. *Geologia USP, Série científica*, **4** (1):24–39.
- Oliveira E.P., McNaughton N., Armstrong R. 2010. Mesoarchaean to Palaeoproterozoic growth of the northern segment of the Itabuna–Salvador–Curaçá Orogen, São Francisco Craton, Brazil. In: Kusky T, Mingguo Z, Xiao W (eds.) *The Evolving Continents: Understanding Processes of Continental Growth*. Geol Soc London Spec Publ 338: 263–286.
- Oliveira, E. P., Mello, E. F., McNaughton, N. T. 2002. Reconnaissance U-Pb geochronology of early Precambrian quartzites from the Caldeirão belt and their basement, NE São Francisco Craton, Bahia, Brazil: implications for the early evolution of the Palaeoproterozoic Salvador-Curaçá Orogen. *Journal of South American Earth Sciences*, **15**: 349–362.
- Othman, D.B., Polvé, M. and Allègre, C.J., 1984. Nd—Sr isotopic composition of granulites and constraints on the evolution of the lower continental crust. *Nature*, **307**(5951), pp.510-515.

- Pearce, J. A., 1983 Role of the sub-continental lithosphere in magma genesis at active continental margins. In Continental basalts and mantle xenoliths (ed. C. J. Hawkesworth & M. J. Norry), pp. 230-249. Nantwich, Cheshire: Shiva.
- Pearce, J.A. and Norry, M.J., 1979. Petrogenetic implications of Ti, Zr, Y, and Nb variations in volcanic rocks. *Contrib. Mineral. Petrol.*, **69**: 33-47.
- Peccerillo, A. and Taylor, S.R. 1976. Geochemistry of Eocene calc-alkaline volcanic rocks from the Kastamonu area, Northern Turkey. *Contribution to Mineralogy and Petrology*, **58**: 63-81.
- Pedrosa-Soares, A.C., Dussin, I., Nseka, P., Baudet, D., Fernandez-Alonso, M., Tack, L. 2016. Tonian rifting events on the Congo-São Francisco paleocontinent: New evidence from U-Pb and Lu-Hf data from the Shinkakasa plutonic complex (Boma region, West Congo Belt, Democratic Republic of Congo). In: International Geologica Belgica Meeting. Mons, 5., Belgium. Abstract Book..., p. 44.
- Peucat, J. J., Barbosa, J. S. F., Araújo Pinho I. C., Paquette J. L., Martin H., Fanning, C. M., Menezes Leal A. B., Cruz C. P.S., 2011. Geochronology of granulites from the south Itabuna-Salvador-Curaçá Block, São Francisco Craton (Brazil): Nd isotopes and U-Pb zircon ages. *Journal of South American Earth Sciences*, **31**:397–413.
- Pinho, I.C.A.P., Martins, A.A.M., Cruz Filho, B.E., Wosniak, R., A.A.M.M., Oliveira, R.L.M. 2013. Mapa Geológico Folha Brumado (1:100.000). Serviço Geológico do Brasil.
- Porada, H., 1989. Pan-African rifting and orogenesis in southern to equatorial Africa and eastern Brazil. *Precambrian Research*, **44**:103–136.
- Reymer, A., Schubert, G., 1984. Phanerozoic addition rates to the continental crust and crustal growth. *Tectonics* 3 (1), 63–77.
- Rios, C. D.; Davis D. W.; Conceição, H.; Macambira, M. J. B.; Peixoto, A. A.; Cruz Filho, B. E. da, Oliveira L. L. 2000. Ages of granites of the Serrinha nucleus, Bahia (Brazil): an overview. *Revista Brasileira de Geociências*, **30**: 74–77.
- Rogers, J.J.W., Santosh, M., 2004. Continents and Supercontinents. Oxford University Press, Oxford, pp. 289.
- Rogers, J.J.W., Santosh, M., 2009. Tectonics and surface effects of the supercontinent Columbia. *Gondwana Research*, **15**: 373–380.
- Rosa, M. L. S. 1999. Geologia, geocronologia, mineralogia, litoquímica e petrologia do batólito monzo - sienítico Guanambi – Urandi (SW - Bahia). Unpl. Dr. Thesis. Instituto de Geociências, Universidade Federal da Bahia, Salvador, 186p.
- Santos, M.M., Lana, C., Scholz, R., Buick, I., Schmitz, M.D., Kamo, S.L., Gerdes, A., Corfu, F., Tapster, S., Lancaster, P. and Storey, C.D., 2017. A new appraisal of Sri Lankan BB zircon as a reference material for LA-ICP-MS U-Pb geochronology and Lu-Hf isotope tracing. *Geostandards and Geoanalytical Research*, **41**(3): pp.335-358.

Santosh, M., Maruyama, S., Sato, K., 2009a. Anatomy of a Cambrian suture in Gondwana: pacific-type orogeny in southern India? *Gondwana Research*, **16**: 321–341.

Santos Pinto, M. A., Peucat, J.J., Matin, H., Sabaté, P. 1998. Recycling of the Archaean continental crust: the case study of the Gavião Block, Bahia, Brazil. *Journal of South American Earth Science*, **11**, 487–498.

Shand, S. J., 1943. Eruptive Rocks. Their Genesis, Composition, Classification, and Their Relation to Ore-Deposits with a Chapter on Meteorite. John Wiley & Sons, New York.

Silva, L.C., Pedrosa-Soares, A. C., Armstrong, R., Pinto, C.P., Magalhães, J.T. R., Silva, Pinheiro, M.A.P., Santos, G.G. 2016. Disclosing the Paleoarchean to Ediacaran history of the São Francisco craton basement: The Porteirinha domain (northern Araçuaí orogen, Brazil). *Journal of South American Earth Sciences*, **68**:50-67.

Schmitt RS, Trouw RAJ, Van Schmus WR, Passchier CW. 2008b. Cambrian orogeny in the Ribeira Belt (SE Brazil) and correlations within West Gondwana: ties that bind underwater. In: Pankhurst RJ, Trouw RAJ, Brito Neves BB, de Wit MJ (eds). West Gondwana: Pre-Cenozoic Correlations Across the South Atlantic Region. Spec Publ Geol Soc London, vol 294, pp 279–296.

Schmitt R.S., Trouw R.A.J., Van Schmus W.R., Pimentel M.M. 2004. Late amalgamation in the central part of Western Gondwana: new geochronological data and the characterization of a Cambrian collision orogeny in the Ribeira belt (SE Brazil). *Precambrian Research*, **133**: 29–61.

Schmitt, R.S., 2001. Orogenia Búzios—Um evento tectonometamórfico cambro-ordoviciano caracterizado no Domínio Tectônico de Cabo Frio, Faixa Ribeira—sudeste do Brasil. *Unpublished PhD Thesis*.

Seixas, L. A. R., Bardintzeff, J. M., Stevenson, R., Bonin, B., 2013. Petrology of the high-Mg tonalites and dioritic enclaves of the ca. 2130 Ma Alto Maranhão suite: Evidence for a major juvenile crustal addition event during the Rhyacian orogenesis, Mineiro Belt, southeast Brazil. *Precambrian Research*, **238**:18–41.

Seixas, L.A.R., David, J., Stevenson, R., 2012. Geochemistry, Nd isotopes and U–Pb geochronology of a 2350 Ma TTG suite, Minas Gerais, Brazil: implications for the crustal evolution of the southern São Francisco craton. *Precambrian Research*, **196**:61–80.

Silva, L. C.; Armstrong, R.; Noce, C. M.; Carneiro, M. A.; Pimentel, M.; Pedrosa Soares, A. C.; Leite, C. A.; Vieira, V. S.; Silva, M. A. da; Paes, J. de. C.; Cardoso Filho, J. M. 2002. Reavaliação da evolução geológica em terrenos pré - cambrianos brasileiros com base em novos dados U-Pb SHRIMP, Parte II: orógeno Araçuaí, cinturão mineiro e Cráton do São Francisco meridional. *Revista Brasileira de Geociências*, **32**, 513–528.

Silva L..C., Armstrong R., Delgado I.M., Pimentel M.M., Arcanjo J.B., Melo R.C. de, Teixeira L.R., Jost H., Cardoso Filho J.M., Pereira L.H.M. 2002. Reavaliação da evolução geológica em terrenos Pré-Cambrianos Brasileiros com base em novos dados U-Pb SHRIMP, Parte I: Limite centro-oriental do Craton do São Francisco na Bahia. *Revista Brasileira de Geociências*, **32**:161–172.

- Silva, L.C., 2006. Geocronologia aplicada ao mapeamento regional, com ênfase na técnica U-Pb SHRIMP. Serviço Geológico do Brasil, Publicações Especiais 1, 132.
- Sláma, J., Košler, J., Condon, D.J., Crowley, J.L., Gerdes, A., Hanchar, J.M., Horstwood, M.S., Morris, G.A., Nasdala, L., Norberg, N., Schaltegger, U., 2008. Plešovice zircon- a new natural reference material for U-Pb and Hf isotopic microanalysis. *Chem. Geol.*, **249**: 1–35.
- Stern R. J., Scholl D. W. (2010) Yin and yang of continental crust creation and destruction by plate tectonic processes. *International Geology Review*, **52**:1–31.
- Stowe, C.W., 1973. The older tonalite gneiss complex in the Selukwe area, Rhodesia. In: Lister, L. (Ed.), Symposium on Granites, Gneisses and Related Rocks, 3. Geological Society of South Africa Special Publication, pp. 85–95.
- Sun, S.-S., 1980, Lead isotope study of young volcanic rocks from mid-ocean ridges, ocean islands and island arcs: Royal Society of London Philosophical Transactions, ser. A, v. 297, p. 409-445.
- Sun S.-S. and McDonough W. F. 1989. Chemical and isotopic systematics of oceanic basalts: Implications for mantle composition and processes. In Magmatism in the Ocean Basins(ed. A. D. Saunders and M. J. Norry), pp. 313–345. Geol. Soc. Spec. Publ. 42.
- Tack, L., Wingate, M.T.D., Liégeois, J.-P., Fernandez-Alonso, M., Deblond, A., 2001. Early Neoproterozoic magmatism (1000–910 Ma) of the Zadinian and Mayumbian groups (Bas-Congo): onset of Rodinia rifting at the western edge of the Congo craton. *Precambrian Research*, **110**:227–306.
- Tarney J. & Jones C.E. C.E. 1994. Trace element geochemistry of orogenic igneous rocks and crustal growth models. *Geological Society of London Journal*, **151**, 855–868.
- Taylor, S.R., McLennan, S.M., 1985. The Continental Crust: Its Composition and Evolution. Blackwell, Oxford.
- Teixeira, W., Ávila, C.A., Nunes, L.C., 2008. Nd–Sr isotopic geochemistry and U–Pb geochronology of Fé granitic gneiss and Lajedo granodiorite: implications for Paleoproterozoic evolution of the Mineiro belt, southern São Francisco Craton. *Geologia USP Série Científica*, **8**:53–73.
- Teixeira W., Ávila [C.A.](#), [Dussin](#) I.A., Corrêa Neto [A.V.](#), [Bongiolo](#) E.M., Santos [J.O.](#), [Barbosa N.S.](#) 2015. Juvenile accretion episode (2.35–2.32 Ga) in the Mineiro belt and its role to the Minas accretionary orogeny: Zircon U–Pb–Hf and geochemical evidences. *Precambrian Research*, **256**:148–169.
- Thiéblemont, D., Callec, Y., Fernandez-Alonso, M., & Chène, F. 2018. A geological and isotopic framework of Precambrian terrains in western Central Africa: An introduction. In S. Siegesmund, M. A. S. Basei, P. Oyhantçabal, & S. Oriolo (Eds.), *Geology of Southwest Gondwana, Regional Geology Reviews* (pp. 107–132). Berlin, Heidelberg: Springer-Verlag.

- Thiéblemont, D., Castaing, C., Billa, M., Bouton, P., Préat, A. 2009. Notice explicative de la Carte géologique et des Ressources minérales de la République gabonaise à 1/1,000,000. DGMG Editions, Ministère des Mines, du Pétrole, des Hydrocarbures, Libreville, p 384.
- Toteu, S.F., Van Schmus, W.R., Penaye, J., Nyobé, J.B. 1994. U–Pb and Sm–Nd evidence for Eburnian and Pan-African high-grade metamorphism in cratonic rocks of southern Cameroon. *Precambrian Research*, 67:321–347.
- Thorpe, R. S., Francis, P. W., & Harmon, R. S. 1981. Andean andesites and crustal growth. *Philosophical Transactions of the Royal Society of London A* 301: 305–320.
- Trompette, R., 1994. Geology of Western Gondwana (2000–500 Ma). Pan-AfricanBrasiliano aggregation of South America and Africa. A.A. Balkema, pp. 350.
- Valladares, C.S., Duarte, B.P., Machado, H.T., Viana, S.M., Figueiredo, P.L.C., 2017. Genesis and evolution of a Paleoproterozoic basement inlier within west Gondwana addressed by Sm/Nd isotopic geochemistry and Zr saturation thermometry. *J. S. Am. Earth Sci.* **80**: 95–106.
- Valladares C.S., Souza S.F., Ragatky C.D. 2002. The Quirino Complex: a Transamazonian Magmatic Arc of the Central Segment of the Brasiliano/Pan-African Ribeira Belt, SE Brazil. *Revista Universidade Rural: Série Ciências Exatas e da Terra, Rio de Janeiro*, **21**(1):49–61.
- Valladares, C.S.; Figueiredo, M.C.; Heilbron, M.; Teixeira, W. 1997. Geochemistry and Geochronology of Paleoproterozoic gneissic rocks of the Paraíba do Sul Complex, Barra Mansa Region, Rio de Janeiro, Brazil. Número Temático: Geoquímica do Pré-cambriano. *Revista Brasileira de Geociências*, **27** (1): 111-120.
- Van Achterbergh, E., Ryan, C.G., Jackson, S.E. and Griffin, W.L., 2001, Data reduction software for LA-ICP-MS: appendix; In Sylvester, P.J. (ed.), Laser Ablation –ICP-Mass Spectrometry in the Earth Sciences: Principles and Applications, Mineralogical Association of Canada Short Course Series, Ottawa, Ontario, Canada. 29, 239-243.
- Veizer, J., Jansen, S.L., 1979. Basement and sedimentary recycling and continental evolution. *Journal of Geology*, **87**: 341–370.
- Villeneuve, M., Chorowicz, J. 2004. Les sillons plissés du Burundien supérieur dans la chaîne Kibarienne d'Afrique centrale. *C R Geosci*, **336**(9):807–814.
- Wang, Q., Xu, J.F., Jian, P., Bao, Z.W., Zhao, Z.H., Li, C.F., Xiong, X.L., Ma, J.L., 2006. Petrogenesis of adakitic porphyries in an extensional tectonic setting, Dexing, South China: implications for the genesis of porphyry copper mineralization. *Journal of Petrology*, **47**:119–144.
- Weber, F., Gauthier-Lafaye, F., Whitechurch, H., Ulrich, M. and El Albani, A., 2016. The 2-Ga Eburnean Orogeny in Gabon and the opening of the Francevillian intracratonic basins: A review. *Comptes Rendus Geoscience*, **348**(8), pp.572-586.

- White, A.J.R., Jakes, P., Christie, D., 1971. Composition of greenstones and the hypothesis of seafloor spreading in the Archaean. Geological Society of Australia Special Publication, 3: 47–56.
- Williams, I.S., 1998. U–Th–Pb geochronology by ion microprobe. In: McKibben, M.A., Shanks, W.C., Ridley, W.I. (Eds.), Applications of Microanalytical Techniques to Understanding Mineralizing Processes. *Reviews in Economic Geology*, 7, pp. 1–35.
- Wilson, M. 1989. *Igneous Petrogenesis*. Unwin Hyman, London. Wilson, J.F., 1973. Granites and gneisses of the area around Mashaba, Rhodesia. Geological Society of South Africa (Special Publication) 3, 79–84.
- Windley, B.F., Bridgwater, D., 1971. The evolution of Archaean low- and high-grade terrains. Geological Society of Australia Special Publication 3: 33–46.
- Wu, Y. and Zheng, Y., 2004. Genesis of zircon and its constraints on interpretation of U–Pb age. *Chinese Science Bulletin*, 49(15), pp.1554–1569.
- Zhao, G., Cawood, P.A., Wilde, S.A., Sun, M., 2002. Review of global 2.1–1.8 Ga orogens: implications for a pre-Rodinia supercontinent. *Earth Science Reviews*, 59 (1): 125–162.
- Zhao, G., Sun, M., Wilde, S.A., Li, S., 2004. A Paleo-Mesoproterozoic supercontinent: assembly, growth and breakup. *Earth Science Reviews*, 67 (1): 91–123.

Supplementary Material 1

Table 1A. Zircon U-Pb (SHRIMP) data for the enderbitic granulite (sample VA-LM-07B). The gray color symbolizes the typology presents oscillatory zonning, whereas the red color represents the rims or metamorphic grains.

Grain.Spot	% $^{206}\text{Pb}_\text{c}$	ppm U	ppm Th	^{232}Th $/^{238}\text{U}$	ppm $^{206}\text{Pb}^*$	(1) ^{206}Pb $/^{238}\text{U}$ Age	(1) ^{207}Pb $/^{206}\text{Pb}$ Age	% Dis- cor- dant	(1) $^{207}\text{Pb}^*$ $/^{206}\text{Pb}^*$	$\pm\%$	(1) $^{207}\text{Pb}^*$ $/^{235}\text{U}$	$\pm\%$	(1) $^{206}\text{Pb}^*$ $/^{238}\text{U}$	$\pm\%$	err corr
11.1	0.75	54	16	0.31	18	2058 ±23	2293 ±31	+12	0.145	1.83	7.5	2.2	0.376	1.28	0.6
8.1	0.51	70	21	0.31	24	2184 ±22	2205 ±28	+1	0.138	1.63	7.7	2.0	0.403	1.18	0.6
4.1	0.33	160	67	0.43	56	2214 ±18	2425 ±10	+10	0.157	0.56	8.9	1.1	0.410	0.96	0.9
5.2	0.76	70	26	0.37	26	2313 ±23	2443 ±26	+6	0.159	1.54	9.5	1.9	0.432	1.18	0.6
14.1	0.47	109	60	0.57	41	2322 ±20	2428 ±12	+5	0.157	0.69	9.4	1.2	0.434	1.03	0.8
10.1	0.15	297	135	0.47	111	2326 ±17	2431 ±12	+5	0.158	0.73	9.4	1.1	0.434	0.87	0.8
9.1	0.34	147	63	0.44	56	2365 ±19	2433 ±18	+3	0.158	1.05	9.6	1.4	0.443	0.98	0.7
13.1	0.18	263	131	0.52	101	2382 ±25	2463 ±15	+4	0.161	0.91	9.9	1.5	0.447	1.24	0.8
7.1	0.69	79	57	0.74	31	2390 ±23	2460 ±15	+3	0.160	0.91	9.9	1.5	0.449	1.14	0.8
2.1	0.42	84	33	0.40	33	2407 ±24	2435 ±27	+1	0.158	1.62	9.9	2.0	0.453	1.18	0.6
5.1	0.21	260	113	0.45	101	2410 ±18	2447 ±7	+2	0.159	0.40	9.9	1.0	0.453	0.88	0.9
6.1	0.27	177	78	0.45	69	2412 ±19	2436 ±8	+1	0.158	0.50	9.9	1.1	0.454	0.94	0.9
1.1	0.40	96	34	0.37	37	2421 ±22	2453 ±21	+2	0.160	1.27	10.0	1.7	0.456	1.08	0.6
3.1	0.34	167	85	0.53	66	2434 ±19	2448 ±9	+1	0.159	0.54	10.1	1.1	0.459	0.96	0.9
12.1	0.14	237	88	0.38	94	2445 ±18	2463 ±7	+1	0.161	0.40	10.2	1.0	0.461	0.89	0.9

Table 1B. Summary of U-Pb zircon data (SHRIMP) for the coarsed-charnoenderbitic granulite (sample BP-LM-12). The gray color symbolizes the typology presents the prismatic zircon with oscilatory zoning, whereas the red color represents homogeneous bright rims.

Grão.Spot	% $^{206}\text{Pb}_\text{c}$	ppm U	ppm Th	^{232}Th $/^{238}\text{U}$	ppm $^{206}\text{Pb}^*$	(1) Idade ^{206}Pb $/^{238}\text{U}$	(1) Idade ^{207}Pb $/^{206}\text{Pb}$	% Dis- cor- dância	(1) $^{207}\text{Pb}^*$ $/^{206}\text{Pb}^*$	$\pm\%$	(1) $^{207}\text{Pb}^*$ $/^{235}\text{U}$	$\pm\%$	(1) $^{206}\text{Pb}^*$ $/^{238}\text{U}$	$\pm\%$	err corr. (ρ)		
4.1	0.44	192	106	0.57	64	2119	± 17	2172	± 29	+3	0.136	1.66	7.3	1.9	0.389	0.95	0.5
3.1	0.20	303	152	0.52	103	2139	± 16	2180	± 8	+2	0.136	0.46	7.4	1.0	0.393	0.88	0.9
12.1	0.31	259	122	0.49	88	2140	± 16	2199	± 10	+3	0.138	0.58	7.5	1.1	0.394	0.90	0.8
2.1	0.25	251	131	0.54	85	2147	± 16	2194	± 13	+2	0.137	0.74	7.5	1.2	0.395	0.90	0.8
11.1	0.23	334	224	0.69	114	2162	± 16	2185	± 14	+1	0.137	0.82	7.5	1.2	0.399	0.87	0.7
6.1	0.12	484	329	0.70	168	2184	± 15	2190	± 10	+0	0.137	0.59	7.6	1.0	0.403	0.83	0.8
5.1	0.33	270	124	0.48	94	2188	± 17	2203	± 9	+1	0.138	0.53	7.7	1.0	0.404	0.90	0.9
9.1	0.10	544	297	0.57	189	2189	± 15	2218	± 35	+2	0.139	2.01	7.8	2.2	0.404	0.83	0.4
7.1	0.33	221	156	0.73	77	2192	± 17	2201	± 10	+0	0.138	0.57	7.7	1.1	0.405	0.93	0.9
10.1	0.21	293	134	0.47	103	2208	± 16	2202	± 12	-0	0.138	0.68	7.8	1.1	0.409	0.88	0.8
1.1	0.01	429	222	0.53	151	2211	± 16	2201	± 11	-1	0.138	0.61	7.8	1.0	0.409	0.85	0.8
8.1	0.21	367	192	0.54	130	2219	± 16	2210	± 7	-0	0.139	0.41	7.9	1.0	0.411	0.86	0.9
13.1	0.11	437	289	0.68	155	2227	± 16	2200	± 9	-1	0.138	0.52	7.8	1.0	0.413	0.84	0.8
10.2	0.20	242	34	0.15	84	2190	± 20	2177	± 9	-1	0.136	0.50	7.6	1.2	0.404	1.10	0.9
5.2	0.61	37	48	1.33	14	2289	± 30	2288	± 27	-0	0.145	1.59	8.5	2.2	0.426	1.55	0.7

Table 1C. Summary of U-Pb zircon data (SHRIMP) for the foliated charnoenderbitic granulite (sample BP-LM-12). The gray color symbolizes the typology presents the prismatic zircon with oscillatory zoning, whereas the red color represents metamorphic rims. The green color is referred as inherited zircon spots.

Grain.Spot	% $^{206}\text{Pb}_\text{c}$	ppm U	ppm Th	^{232}Th $/^{238}\text{U}$	ppm $^{206}\text{Pb}^*$	(1) ^{206}Pb $/^{238}\text{U}$ Age	(1) ^{207}Pb $/^{206}\text{Pb}$ Age	% Dis- cor- dant	(1) $^{207}\text{Pb}^*$ $/^{206}\text{Pb}^*$	$\pm\%$	(1) $^{207}\text{Pb}^*$ $/^{235}\text{U}$	$\pm\%$	(1) $^{206}\text{Pb}^*$ $/^{238}\text{U}$	$\pm\%$	Err Corr. (ρ)
10.1	2.62	71	52	0.76	6	566 \pm 10	606 \pm 244	+7	0.060	11	0.8	11.4	0.092	1.81	0.2
4.2	1.25	127	68	0.55	10	578 \pm 6	662 \pm 135	+13	0.062	6.30	0.8	6.4	0.094	1.05	0.2
2.2	0.72	221	101	0.47	18	586 \pm 5	581 \pm 70	-1	0.059	3.24	0.8	3.4	0.095	0.92	0.3
9.2	0.91	197	98	0.52	16	592 \pm 5	595 \pm 100	+0	0.060	4.63	0.8	4.7	0.096	0.94	0.2
13.1	1.04	143	62	0.45	15	750 \pm 7	1255 \pm 53	+43	0.082	2.70	1.4	2.9	0.123	1.01	0.4
1.1	0.67	99	62	0.65	21	1424 \pm 18	1941 \pm 24	+30	0.119	1.33	4.1	1.9	0.247	1.40	0.7
6.1	0.62	87	61	0.72	22	1681 \pm 16	2075 \pm 21	+22	0.128	1.18	5.3	1.6	0.298	1.11	0.7
3.1	0.29	257	73	0.29	72	1813 \pm 21	2127 \pm 34	+17	0.132	1.92	5.9	2.4	0.325	1.35	0.6
10.2	0.64	57	32	0.58	17	1921 \pm 21	2147 \pm 39	+12	0.134	2.21	6.4	2.5	0.347	1.26	0.5
4.1	0.55	107	44	0.42	32	1927 \pm 34	2068 \pm 37	+8	0.128	2.09	6.1	2.9	0.348	2.05	0.7
11.1	0.27	241	65	0.28	73	1948 \pm 18	2151 \pm 34	+11	0.134	1.96	6.5	2.2	0.353	1.06	0.5
8.1	0.28	272	100	0.38	85	2001 \pm 18	2162 \pm 9	+9	0.135	0.51	6.8	1.2	0.364	1.04	0.9
9.1	0.29	219	94	0.44	70	2036 \pm 16	2163 \pm 10	+7	0.135	0.55	6.9	1.1	0.371	0.91	0.9
5.1	0.11	264	61	0.24	88	2110 \pm 16	2166 \pm 35	+3	0.135	2.01	7.2	2.2	0.387	0.90	0.4
2.1	0.14	361	85	0.24	123	2151 \pm 34	2165 \pm 11	+1	0.135	0.65	7.4	2.0	0.396	1.84	0.9
14.1	0.40	220	56	0.26	76	2185 \pm 17	2187 \pm 14	+0	0.137	0.80	7.6	1.2	0.403	0.91	0.8
7.1	0.11	294	124	0.44	102	2188 \pm 16	2218 \pm 7	+2	0.139	0.41	7.8	1.0	0.404	0.87	0.9
12.1	0.38	131	91	0.72	45	2162 \pm 58	2388 \pm 41	+11	0.154	2.43	8.4	4.0	0.399	3.16	0.8
12.2	0.20	193	127	0.68	63	2066 \pm 22	2364 \pm 16	+15	0.152	0.93	7.9	1.5	0.378	1.24	0.8

Table 1D. Summary of U-Pb zircon data (SHRIMP) for the protomylonitic charnoenderbitic granulite (sample RP-LM-04). The gray color symbolizes the typology presents the prismatic zircon with oscillatory zoning. The orange color represents the long and rounded typology with planar zoning around ca. 2000 Ma, whereas the red color represents metamorphic grains.

Grain.Spot	% $^{206}\text{Pb}_\text{c}$	ppm U	ppm Th	^{232}Th / ^{238}U	ppm $^{206}\text{Pb}^*$	(1) ^{206}Pb / ^{238}U Age	(1) ^{207}Pb / ^{206}Pb Age	% Dis- cor- dant	(1) $^{207}\text{Pb}^*$ / $^{206}\text{Pb}^*$	±%	(1) $^{207}\text{Pb}^*$ / ^{235}U	±%	(1) $^{206}\text{Pb}^*$ / ^{238}U	±%	Err. corr. (p)
14.2	1.45	211	110	0.54	19	645 ±6	997 ±73	+37	0.072	3.59	1.1	3.7	0.105	0.97	0.3
9.1	0.57	227	218	0.99	36	1104 ±9	1669 ±30	+37	0.102	1.63	2.6	1.9	0.187	0.91	0.5
5.1	0.42	225	48	0.22	53	1572 ±13	1900 ±32	+19	0.116	1.78	4.4	2.0	0.276	0.91	0.5
4.1	0.98	137	36	0.27	38	1798 ±17	1967 ±25	+10	0.121	1.42	5.4	1.8	0.322	1.08	0.6
4.2	0.36	140	91	0.67	42	1933 ±22	2034 ±35	+6	0.125	1.96	6.0	2.4	0.350	1.32	0.6
10.1	0.72	79	116	1.53	24	1950 ±19	2019 ±22	+4	0.124	1.26	6.1	1.7	0.353	1.14	0.7
2.1	1.12	59	116	2.02	19	2025 ±22	2010 ±52	-1	0.124	2.94	6.3	3.2	0.369	1.25	0.4
13.1	0.83	103	165	1.65	30	1883 ±27	1996 ±21	+7	0.123	1.17	5.7	2.0	0.339	1.66	0.8
7.1	1.02	45	60	1.38	13	1889 ±22	2048 ±53	+9	0.126	3.00	5.9	3.3	0.341	1.36	0.4
14.1	0.27	176	71	0.41	49	1819 ±25	2154 ±20	+18	0.134	1.13	6.0	1.9	0.326	1.55	0.8
12.1	0.10	463	258	0.58	136	1900 ±14	2131 ±13	+13	0.133	0.72	6.3	1.1	0.343	0.83	0.8
1.1	0.23	274	122	0.46	85	1978 ±15	2143 ±17	+9	0.133	0.95	6.6	1.3	0.359	0.87	0.7
3.1	0.09	581	252	0.45	182	2002 ±14	2142 ±5	+8	0.133	0.31	6.7	0.9	0.364	0.81	0.9
8.1	0.23	297	173	0.60	96	2056 ±15	2158 ±18	+6	0.135	1.01	7.0	1.3	0.376	0.87	0.7
6.1	0.14	438	237	0.56	142	2061 ±15	2182 ±12	+6	0.136	0.67	7.1	1.1	0.377	0.83	0.8
11.1	0.16	296	164	0.57	99	2112 ±20	2174 ±13	+3	0.136	0.77	7.3	1.4	0.388	1.13	0.8

Tabela 1E. Summary of U-Pb zircon data (SHRIMP) for the mafic granulite (sample BP-CM-151). The gray color symbolizes the typology presents oscillatory zoning. The orange color represents the typology around ca. 2000 Ma, whereas the red color represents metamorphic grains. The green one represents an inherited zircon grain.

Grain.Spot	% $^{206}\text{Pb}_c$	ppm U	ppm Th	^{232}Th $/^{238}\text{U}$	ppm $^{206}\text{Pb}^*$	(1) ^{206}Pb $/^{238}\text{U}$ Age	(1) ^{207}Pb $/^{206}\text{Pb}$ Age	% Dis- cor- dant	(1) $^{207}\text{Pb}^*$ $/^{206}\text{Pb}^*$	$\pm\%$	(1) $^{207}\text{Pb}^*$ $/^{235}\text{U}$	$\pm\%$	(1) $^{206}\text{Pb}^*$ $/^{238}\text{U}$	$\pm\%$	Err. corr. (ρ)
2.1	2.16	66	62	0.97	5	591 \pm 7	588 \pm 225	-1	0.060	10	0.8	10.5	0.096	1.29	0.1
7.2	0.20	294	122	0.43	87	1904 \pm 17	1945 \pm 9	+2	0.119	0.52	5.6	1.2	0.344	1.03	0.9
9.1	0.34	172	19	0.11	53	1962 \pm 16	1971 \pm 13	+0	0.121	0.71	5.9	1.2	0.356	0.94	0.8
7.1	0.11	155	253	1.68	48	1980 \pm 16	1984 \pm 11	+0	0.122	0.62	6.0	1.1	0.360	0.96	0.8
14.1	0.18	317	174	0.57	104	2075 \pm 18	2157 \pm 13	+4	0.134	0.76	7.0	1.3	0.380	1.01	0.8
1.1	1.23	38	6	0.17	13	2130 \pm 26	2155 \pm 46	+1	0.134	2.62	7.2	3.0	0.391	1.42	0.5
16.1	0.12	516	323	0.65	174	2139 \pm 16	2199 \pm 7	+3	0.138	0.39	7.5	1.0	0.394	0.90	0.9
11.2	0.58	93	16	0.18	33	2231 \pm 25	2253 \pm 38	+1	0.142	2.17	8.1	2.5	0.414	1.30	0.5
4.1	0.26	237	107	0.47	85	2246 \pm 17	2450 \pm 7	+10	0.159	0.44	9.2	1.0	0.417	0.89	0.9
11.1	0.06	451	155	0.35	162	2250 \pm 16	2272 \pm 13	+1	0.144	0.73	8.3	1.1	0.418	0.83	0.8
5.1	--	366	164	0.46	132	2260 \pm 16	2217 \pm 11	-2	0.139	0.61	8.1	1.0	0.420	0.84	0.8
17.1	0.30	180	82	0.47	68	2345 \pm 18	2380 \pm 9	+2	0.153	0.52	9.3	1.1	0.439	0.93	0.9
12.1	0.28	196	89	0.47	74	2349 \pm 18	2439 \pm 14	+4	0.158	0.80	9.6	1.2	0.440	0.92	0.8
18.1	0.23	285	160	0.58	112	2432 \pm 23	2428 \pm 11	-0	0.157	0.62	9.9	1.3	0.458	1.15	0.9
13.1	0.18	365	160	0.45	144	2440 \pm 17	2431 \pm 6	-0	0.158	0.34	10.0	0.9	0.460	0.84	0.9
3.1	--	232	139	0.62	92	2447 \pm 22	2406 \pm 6	-2	0.155	0.38	9.9	1.1	0.462	1.07	0.9
10.1	--	177	94	0.55	71	2468 \pm 19	2456 \pm 7	-1	0.160	0.42	10.3	1.0	0.467	0.93	0.9
6.1	0.29	87	50	0.59	36	2526 \pm 23	2525 \pm 17	-0	0.167	1.00	11.0	1.5	0.480	1.09	0.7

Tabela 1F. Summary of U-Pb zircon data (LA-ICPMS) for the mafic granulite (sample BP-CM-151). The green (dark and light) and dark blue color symbolizes inherited zircon grains. The light blue color represents the magmatic crystallization. The orange color represents the metamorphic typology around ca. 2000 Ma, whereas the red color represents metamorphic grains. The errors are 2σ .

Sample	f-206c	Th/U	207Pb/206Pb	2s (%)	207Pb/235U	2s (%)	206Pb/238U	2s (%)	Rho	207Pb/206Pb	2s	206Pb/238U	2s	207Pb/235U	2s	% Disc
29	0.0260	0.26	0.152371	2.51	9.549937	3.52	0.454565	2.47	0.70	2373	29	2416	33	2392	22	-1
56	0.0000	0.54	0.154005	2.92	9.625898	3.82	0.453320	2.46	0.64	2391	34	2410	33	2400	24	0
30	0.0000	0.11	0.153213	2.54	9.576828	3.56	0.453340	2.49	0.70	2382	29	2410	34	2395	22	-1
16	0.0893	0.32	0.152820	2.51	9.449367	3.63	0.448458	2.63	0.72	2378	29	2388	35	2383	22	0
70	0.0000	0.24	0.150175	3.14	9.181610	4.15	0.443426	2.72	0.65	2348	36	2366	36	2356	26	0
39	0.0000	0.19	0.146397	2.98	8.670525	3.91	0.429547	2.53	0.65	2304	35	2304	33	2304	24	0
54	0.0000	0.21	0.145156	2.61	8.648860	3.60	0.432138	2.48	0.69	2290	30	2315	32	2302	22	-1
55	0.0737	0.19	0.144889	2.66	8.610236	3.64	0.431002	2.48	0.68	2286	31	2310	32	2298	22	-1
71	0.0000	0.17	0.137228	2.95	7.819389	3.96	0.413267	2.64	0.67	2193	35	2230	33	2210	24	-1
52	0.0044	0.05	0.136719	2.51	7.783444	3.52	0.412898	2.47	0.70	2186	30	2228	31	2206	21	-1
35	0.1280	0.12	0.138099	2.76	7.812330	3.72	0.410288	2.49	0.67	2204	32	2216	31	2210	22	0
12	0.0065	0.19	0.138032	2.40	7.848341	3.47	0.412380	2.51	0.72	2203	28	2226	32	2214	21	-1
13	0.0010	0.19	0.137397	2.87	7.759228	3.89	0.409580	2.63	0.67	2195	34	2213	33	2203	23	0
73	0.0000	0.13	0.138148	2.97	7.807486	3.95	0.409889	2.60	0.66	2204	35	2214	33	2209	24	0
40	0.0012	0.11	0.138135	2.49	7.838292	3.54	0.411543	2.51	0.71	2204	29	2222	32	2213	21	0
51	0.0000	0.07	0.138469	3.04	7.837992	3.93	0.410537	2.50	0.64	2208	36	2217	31	2213	24	0
47	0.0000	0.19	0.132948	3.40	7.362186	4.45	0.401629	2.87	0.64	2137	40	2177	35	2156	27	-1
15	0.0000	0.05	0.133333	2.65	7.374725	3.59	0.401151	2.43	0.68	2142	31	2174	30	2158	21	-1
59	0.0243	0.05	0.125085	4.49	6.239590	5.29	0.361785	2.80	0.53	2030	54	1991	32	2010	31	1
09	0.0000	0.70	0.124923	2.72	6.328292	3.67	0.367405	2.46	0.67	2028	33	2017	29	2022	21	0
36	0.0000	0.06	0.123510	3.53	5.749078	4.42	0.337594	2.65	0.60	2008	42	1875	29	1939	26	3
49	0.1756	0.07	0.121071	2.98	5.182332	4.00	0.310443	2.67	0.67	1972	36	1743	27	1850	23	6

68	0.0000	0.05	0.119080	3.18	5.756529	4.08	0.350606	2.56	0.63	1942	38	1937	29	1940	24	0
11	0.0000	0.04	0.119316	2.99	5.776104	3.85	0.351104	2.43	0.63	1946	36	1940	27	1943	22	0
60	0.0000	0.05	0.119177	2.67	5.085016	3.66	0.309457	2.51	0.69	1944	32	1738	26	1834	21	5
67	0.0125	0.04	0.116712	2.72	4.963330	3.71	0.308431	2.52	0.68	1906	33	1733	26	1813	21	4
69	0.2715	0.05	0.110604	3.09	4.250965	4.07	0.278749	2.64	0.65	1809	38	1585	25	1684	22	6
07	0.0000	0.25	0.062980	3.31	0.770431	4.20	0.091949	2.58	0.61	708	48	558	9	589	12	5
08	0.0000	0.05	0.059790	2.56	0.703787	3.58	0.088691	2.50	0.70	596	37	539	9	550	10	2
20	0.2139	0.08	0.060480	2.79	0.809879	3.81	0.100418	2.59	0.68	621	40	608	10	611	12	0
48	0.0000	0.06	0.060730	2.91	0.771402	3.87	0.095416	2.55	0.66	630	42	579	9	589	12	2
18	1.0000	0.18	0.101496	4.0502	2.580476	5.02	0.184395	2.96	0.59	1652	51	1091	20	1295	24	16
19	0.0000	0.07	0.152689	25.9636	0.015835	33.02	0.002965	20.41	0.62	2376	299	9	1	31	6	69
74	1.0679	0.05	0.107411	5.0521	1.460228	6.70	0.098599	4.39	0.66	1756	62	606	17	914	27	34
14	1.0000	0.46	0.115492	4.3844	4.705052	5.35	0.295468	3.07	0.57	1888	53	1669	30	1768	30	6
53	1.0000	0.08	0.134824	3.5043	7.030291	4.38	0.378185	2.63	0.60	2162	41	2068	31	2115	26	2
58	1.0000	0.05	0.118117	4.1416	4.884197	5.04	0.299902	2.88	0.57	1928	50	1691	29	1800	28	6
33	0.0000	0.07	0.125072	2.54	5.337604	3.58	0.309517	2.52	0.70	2030	30	1738	26	1875	20	7
27	1.0000	0.18	0.103578	3.9304	3.715408	4.79	0.260157	2.73	0.57	1689	49	1491	24	1575	26	5
10	1.0000	0.03	0.120467	3.5849	5.651791	4.46	0.340264	2.65	0.59	1963	43	1888	29	1924	26	2
72	1.0000	0.04	0.125287	4.5340	6.242996	5.44	0.361397	3.01	0.55	2033	54	1989	35	2010	32	1
17	1.0000	0.31	0.153432	3.3165	9.522844	4.30	0.450142	2.74	0.64	2385	38	2396	37	2390	27	0
28	1.0000	0.35	0.153126	3.2907	9.528058	4.26	0.451287	2.71	0.64	2381	38	2401	36	2390	26	0
37	1.0000	0.23	0.149671	3.6551	9.130269	4.49	0.442430	2.61	0.58	2342	42	2362	35	2351	28	0
38	1.0000	0.13	0.149269	3.3427	9.110436	4.26	0.442659	2.64	0.62	2338	39	2363	35	2349	26	-1

Supplementary Material 2

Tabela 2A. Lu-Hf zircon data for tholeiitic diorite (sample VA-LM-07B).

VA-LM-07B – enderbitic granulite: tholeiitic diorite							
Sample/ Spot	$^{207}\text{Pb}/^{206}\text{Pb}$ Age (Ma)	$^{176}\text{Lu}/^{177}\text{Hf}$	$^{176}\text{Hf}/^{177}\text{Hf}$	$^{176}\text{Hf}/^{177}\text{Hf}_{(t)}$	$\epsilon\text{Hf}(0)$	$\epsilon\text{Hf}_{(t)}$	$T_{\text{DM}}\text{ Hf}$ (Ma)
1.1	2453	0.000370	0.281312	0.281295	-52.1	3.0	2.49
3.1	2448	0.001821	0.281073	0.280987	-60.6	-8.0	3.09
9.1	2433	0.000761	0.281283	0.281247	-53.1	0.8	2.59
12.1	2463	0.001742	0.281187	0.281105	-56.5	-3.5	2.86
14.1	2428	0.001354	0.281189	0.281127	-56.4	-3.6	2.83
6.1	2436	0.001719	0.281232	0.281152	-54.9	-2.5	2.78
5.1	2447	0.001817	0.281332	0.281247	-51.4	1.2	2.59
10.1	2431	0.000920	0.281318	0.281275	-51.9	1.8	2.54

Table 2B. Lu-Hf zircon data for TTG granodiorite (sample BP-LM-12).

BP-LM-12 – foliated charnoenderbitic granulite: TTG granodiorite							
Grain/S pot	$^{207}\text{Pb}/^{206}\text{Pb}$ Age (Ma)	$^{176}\text{Lu}/^{177}\text{Hf}$	$^{176}\text{Hf}/^{177}\text{Hf}$	$^{176}\text{Hf}/^{177}\text{Hf}_{(t)}$	$\epsilon\text{Hf}(0)$	$\epsilon\text{Hf}_{(t)}$	$T_{\text{DM}}\text{ Hf}$ (Ma)
5.1	2166	0.000689	0.281377	0.281349	-49.8	-1.8	2.53
2.1	2165	0.000456	0.281393	0.281374	-49.2	-0.9	2.48
7.1	2218	0.000510	0.281341	0.281320	-51.1	-1.6	2.56
8.1	2162	0.000475	0.281338	0.281319	-51.2	-2.9	2.59
9.1	2163	0.001108	0.281207	0.281161	-55.8	-8.5	2.90
14.1	2187	0.000388	0.281374	0.281358	-49.9	-1.0	2.50

Table 2C. Lu-Hf zircon data for the sanukitoid granodiorite.

BP-LM-13 – coarsed-charnoenderbitic: sanukitoid granodiorite							
Sample /Spot	$^{207}\text{Pb}/^{206}\text{Pb}$ Age (Ma)	$^{176}\text{Lu}/^{177}\text{Hf}$	$^{176}\text{Hf}/^{177}\text{Hf}$	$^{176}\text{Hf}/^{177}\text{Hf}_{(t)}$	$\epsilon\text{Hf}(0)$	$\epsilon\text{Hf}_{(t)}$	$T_{\text{DM}}\text{ Hf}$ (Ma)
1.1	2201	0.00092	0.281188	0.281150	-56.5	-8.0	2.90
8.1	2210	0.00060	0.281165	0.281140	-57.3	-8.2	2.91
2.1	2194	0.00053	0.281169	0.281147	-57.1	-8.3	2.91
7.1	2201	0.00091	0.281084	0.281046	-60.1	-11.7	3.10
5.1	2203	0.00048	0.281121	0.281101	-58.8	-9.7	2.99
10.1	2202	0.00076	0.281153	0.281122	-57.7	-9.0	2.95
13.1	2200	0.00068	0.281166	0.281138	-57.3	-8.5	2.92
11.1	2185	0.00064	0.281133	0.281106	-58.4	-9.9	2.99
12.1	2199	0.00046	0.281158	0.281138	-57.5	-8.5	2.92
6.1	2190	0.00077	0.281130	0.281098	-58.5	-10.1	3.01

Tabela 2D. Lu-Hf zircon data for the protomylonitic charnoenderbitic granulite (sample RP-LM-04).

RP-LM-04 – protomylonitic charnoenderbitic granulite with associated leucosomes							
Grão. Spot	Idade $^{207}\text{Pb}/^{206}\text{Pb}$ (Ma)	$^{176}\text{Lu}/^{177}\text{Hf}$	$^{176}\text{Hf}/^{177}\text{Hf}$	$^{176}\text{Hf}/^{177}\text{Hf}_{(t)}$	$\epsilon\text{Hf}(0)$	$\epsilon\text{Hf}_{(t)}$	$T_{\text{DM}}\text{ Hf}$ (Ma)
8.1	2158	0.000667	0.281249	0.281221	-54.3	-6.5	2.78
12.1	2131	0.000723	0.281176	0.281147	-56.9	-9.7	2.94
1.1	2143	0.000834	0.281186	0.281152	-56.5	-9.3	2.92
14.1	2154	0.000997	0.281267	0.281226	-53.7	-6.4	2.77
11.1	2174	0.001081	0.281509	0.281464	-45.1	+2.5	2.30
3.1	2142	0.001036	0.281060	0.281017	-61.0	-14.1	3.19
6.1	2182	0.000945	0.281210	0.281171	-55.7	-7.7	2.87
13.1	1996	0.000096	0.281181	0.281177	-56.7	-11.8	2.95
7.1	2048	0.000209	0.281159	0.281151	-57.5	-11.5	2.97
2.1	2010	0.000191	0.281133	0.281126	-58.4	-13.3	3.04
10.1	2019	0.000181	0.281179	0.281172	-56.8	-11.4	2.95

Table 2E. Lu-Hf zircon data for tholeiitic gabbro (sample BP-CM-151).

BP-CM-151 – Massive mafic granulite: tholeiitic gabbro							
Sample/S pot	$^{207}\text{Pb}/^{206}\text{Pb}$ Age (Ma)	$^{176}\text{Lu}/^{177}\text{Hf}$	$^{176}\text{Hf}/^{177}\text{Hf}$	$^{176}\text{Hf}/^{177}\text{Hf}_{(t)}$	$\epsilon\text{Hf}(0)$	$\epsilon\text{Hf}_{(t)}$	$T_{\text{DM}}\text{ Hf}$ (Ma)
47.1	2345	0.001113	0.280575	0.280525	-78.2	-26.9	4.04
3.1	2406	0.001232	0.280201	0.280145	-91.4	-39.0	4.73
12.1	2349	0.000695	0.281340	0.281309	-51.1	1.1	2.51
13.1	2431	0.001022	0.280682	0.280635	-74.4	-21.0	3.79
18.1	2428	0.000951	0.281233	0.281189	-54.9	-1.4	2.71
10.1	2456	0.001579	0.280737	0.280663	-72.4	-19.4	3.72
29	2416	0.000820	0.280880	0.280842	-67.4	-13.9	3.40
55	2286	0.001134	0.281088	0.281038	-60.0	-9.9	3.08
5+	2208	0.001236	0.280689	0.280631	-74.1	-26.1	3.89
13	2195	0.000099	0.281360	0.281355	-50.4	-0.8	2.50
71	2193	0.000866	0.281295	0.281259	-52.7	-4.3	2.69
52	2186	0.000970	0.280848	0.280807	-68.5	-20.5	3.58

APÊNDICE C – Tabelas geocronológicas (U-Pb) e geoquímicas isotópicas (Lu-Hf) em zircão do granulito leucocrático representante do magmatismo intraplaca estateriano.

Tabela A1 – Resumo dos dados de U-Pb (SHRIMP) em zircão para o granulito charnockítico leucocrático (RPM-570). A cor cinza das elipses simboliza a tipologia de grãos com zoneamento oscilatório. Já a cor vermelha, bordas metamórficas de cor cinza na imagem CL.

Grão.Spot	% $^{206}\text{Pb}_\text{c}$	ppm U	ppm Th	^{232}Th $/^{238}\text{U}$	ppm $^{206}\text{Pb}^*$	(1) Idade ^{206}Pb $/^{238}\text{U}$	(1) Idade ^{207}Pb $/^{206}\text{Pb}$	% Dis- cor- dância	(1) $^{207}\text{Pb}^*$ $/^{206}\text{Pb}^*$	±%	(1) $^{207}\text{Pb}^*$ $/^{235}\text{U}$	±%	(1) $^{206}\text{Pb}^*$ $/^{238}\text{U}$	±%	Corr. Err. (ρ)		
1.2	0.41	559	60	0.11	42	536	± 5	658	± 30	+19	0.062	1.39	0.7	1.7	0.087	0.91	0.5
2.2	0.18	1925	154	0.08	162	601	± 4	598	± 14	-0	0.060	0.66	0.8	1.0	0.098	0.78	0.8
14.2	0.12	1174	67	0.06	100	608	± 5	612	± 21	+1	0.060	0.99	0.8	1.3	0.099	0.78	0.6
2.1	0.15	690	298	0.45	106	1059	± 8	1445	± 11	+29	0.091	0.59	2.2	1.0	0.178	0.81	0.8
13.1	0.27	440	208	0.49	81	1254	± 11	1559	± 12	+22	0.097	0.66	2.9	1.2	0.215	0.98	0.8
12.1	0.18	643	354	0.57	150	1547	± 12	1692	± 8	+10	0.104	0.44	3.9	1.0	0.271	0.90	0.9
9.1	0.13	418	348	0.86	105	1650	± 12	1753	± 9	+7	0.107	0.48	4.3	1.0	0.292	0.84	0.9
1.1	0.13	565	489	0.89	150	1733	± 12	1743	± 7	+1	0.107	0.39	4.5	0.9	0.308	0.81	0.9
14.1	0.22	352	370	1.09	94	1740	± 13	1753	± 10	+1	0.107	0.56	4.6	1.0	0.310	0.86	0.8
7.1	0.14	335	227	0.70	91	1773	± 13	1768	± 9	-0	0.108	0.48	4.7	1.0	0.317	0.85	0.9
11.1	--	593	464	0.81	162	1778	± 13	1761	± 6	-1	0.108	0.34	4.7	0.9	0.318	0.82	0.9
3.1	0.02	122	105	0.89	33	1782	± 16	1765	± 13	-1	0.108	0.69	4.7	1.2	0.318	1.00	0.8
15.1	0.19	253	164	0.67	70	1790	± 14	1777	± 18	-1	0.109	0.96	4.8	1.3	0.320	0.90	0.7
6.1	0.02	272	284	1.08	75	1803	± 17	1787	± 8	-1	0.109	0.47	4.9	1.2	0.323	1.06	0.9
10.1	--	315	315	1.03	87	1804	± 14	1779	± 8	-2	0.109	0.46	4.8	1.0	0.323	0.87	0.9
5.1	0.01	247	213	0.89	68	1804	± 14	1800	± 9	-0	0.110	0.49	4.9	1.0	0.323	0.88	0.9
8.1	--	492	697	1.46	137	1809	± 13	1787	± 12	-1	0.109	0.66	4.9	1.1	0.324	0.83	0.8
4.1	--	750	893	1.23	209	1810	± 13	1772	± 5	-2	0.108	0.28	4.8	0.8	0.324	0.80	0.9

Fonte: O autor, 2020.

Tabela A2 – Análises isotópicas do sistema Lu-Hf em zircão do granulito leucocrático (amostra RPM-570).

RPM-570 – granulito leucocrático de alto K							
Grão/ Spot	idade $^{207}\text{Pb}/^{206}\text{Pb}$ (Ma)	$^{176}\text{Lu}/^{177}\text{Hf}$	$^{176}\text{Hf}/^{177}\text{Hf}$	$^{176}\text{Hf}/^{177}\text{Hf}_{(\text{t})}$	$\varepsilon\text{Hf}(0)$	$\varepsilon\text{Hf}_{(\text{t})}$	$T_{\text{DM}} \text{ Hf}$ (Ma)
6.1	1787	0.000826	0.281417	0.281389	-48.4	-9.1	2.63
7.1	1768	0.000836	0.281544	0.281516	-43.9	-5.0	2.40
8.1	1787	0.001180	0.281422	0.281382	-48.2	-9.3	2.65
15.1	1777	0.000607	0.281335	0.281314	-51.3	-12.0	2.78
5.1	1800	0.000902	0.281403	0.281372	-48.9	-9.4	2.66
4.1	1772	0.001075	0.281529	0.281493	-44.4	-5.7	2.44
10.1	1779	0.000928	0.281377	0.281346	-49.8	-10.8	2.72
3.1	1765	0.000522	0.281386	0.281368	-49.5	-10.3	2.69
11.1	1761	0.000755	0.281296	0.281270	-52.7	-13.9	2.88

Fonte: O autor, 2020.